

労災疾病研究事業費補助金

脊椎インストゥルメンテーション患者に

アフターケアは本当に必要か？

全国労災病院と産業医科大学を含む多施設大規模調査

平成 2 8 年度総括研究報告書

研究代表者 須田 浩太

平成 2 9 年 3 月

目 次

I． 総括研究報告

脊椎インストゥルメンテーション患者にアフターケアは本当に必要か？	
全国労災病院と産業医科大学を含む多施設大規模調査	．．．．． 1
独立行政法人労働者健康安全機構	
北海道せき損センター 須田 浩太	

II． 関連他研究の一覧表

．．．．． 9

III． 関連他研究の刊行物

．．．．． 11

労災疾病臨床研究事業費補助金
平成28年度総括研究報告書

脊椎インストゥルメンテーション患者にアフターケアは本当に必要か？
全国労災病院と産業医科大学を含む多施設大規模調査

研究代表者 須田浩太 独立行政法人労働者健康安全機構
北海道せき損センター

研究要旨

脊椎インストゥルメンテーション技術の大幅な進歩に伴い、治療成績は向上したものの、長期にわたる治療が必須な症例も少なくない。

アフターケアの「適応基準」を定め、その際に生じる「医療コスト」を予測する取組を3年計画で包括的に推進することとした。初年度の検討結果は以下である。

1) 労災患者における脊椎インストゥルメンテーション症例のデータ集積

全労災病院（全国に34）と産業医科大学の過去5年を目処に労災患者における脊椎インストゥルメンテーション症例のデータを集積する。

2) 労災患者以外の脊椎インストゥルメンテーション症例のデータ集積

労災患者以外の脊椎インストゥルメンテーション症例のデータを集積し、同様の手法で中央集約管理を行う。

3) データの解析

集積したデータを基にアフターケアの該当基準や頻度を解析する。

〈研究分担者〉

（独）労働者健康安全機構
北海道せき損センター
病院長 三浪 明男

（独）労働者健康安全機構
総合せき損センター
病院長 芝 啓一郎

（独）労働者健康安全機構
北海道せき損センター
部長 松本 聡子

（独）労働者健康安全機構
総合せき損センター
副院長 植田 尊善

（独）労働者健康安全機構
北海道せき損センター
部長 小松 幹

（独）労働者健康安全機構
総合せき損センター
部長 前田 健

(独) 労働者健康安全機構

総合せき損センター

部長 坂井 宏旭

独協医科大学医学部医学科

整形外科

講師 森平 泰

(独) 労働者健康安全機構

吉備高原リハビリテーションセンター

病院長 徳弘 昭博

平成 28 年度は昨年度に引き続きデータ集積が主であり、報告書の内容に著変はない。

(独) 労働者健康安全機構

吉備高原リハビリテーションセンター

副院長 古澤 一成

A. 研究目的

脊椎インストゥルメンテーション技術の大幅な進歩に伴い、従来は不可能であった大規模な脊椎再建術が平常に行われるようになった。治療成績は飛躍的に向上し、後遺症が減ったものの、中には長期にわたる経過観察や治療が必須な症例も少なくない。そこで、脊椎インストゥルメンテーションを行った症例に関して、1) 症状固定後に如何なる症状が生じるか？ 2) 如何なる措置がどの程度の期間必要か？ 3) どの程度の症例数が見込まれるのか？を明らかにすることを目的とする。

産業医科大学整形外科教室

教授 酒井 昭典

限りある財源の有効活用、効率的分配は労災補償行政において重要課題である。脊椎インストゥルメンテーションにおいてアフターケアが必要な症例は極めて少ないと予想するが皆無ではない。どのような症例が該当するのか、どの程度の頻度で存在するのか把握することが第一義である。「適応基準」を定め、その際に生じる「医療コスト」を予測することが労災補償行政に必須である。

産業医科大学整形外科教室

准教授 中村 英一郎

北海道大学大学院医学研究科

機能再生医学講座整形外科分野

教授 岩崎 倫政

本研究には大きな特色が 3 つある。

北海道大学大学院医学研究科

機能再生医学講座整形外科分野

准教授 高畑 雅彦

① 労災医療における国内最大組織（全労災病院＋産業医科大学）による国内最大規模調査

北海道大学大学院医学研究科

社会医学講座医学統計学分野

准教授 伊藤 陽一

② 労働者健康安全機構が持つ職業調査データベース

独協医科大学医学部医学科

整形外科

主任教授 種市 洋

③ 複数の大学・施設・診療科の集学的協力体制

独協医科大学医学部医学科

整形外科

准教授 稲見 聡

全国には 34 労災病院があり（総合せき損センター及び吉備高原医療リハビリテーションセンター含む）、総数 13,000 以上のベッド、約

15,000 人のスタッフを有し、最高水準の労災医療を提供している。また、産業医科大学は産業医学の中核であることは言うまでもない。両施設は我が国における労災医療の中心であり、両施設の共同体がスケールメリットを生かして全国調査を行う意義は非常に大きい。労災医療の調査としては国内最大のスケールとなる。また、労働者健康安全機構が持つ巨大な職業調査データベースから職業別の要因なども解析可能である。更に特殊症例の検討を目的として北海道大学と獨協医科大学の協力を得たこと、社会医学、統計解析のスペシャリストにも協力を得たことも大きな利点である。

1) 症状固定後に如何なる症状の動揺を来すおそれがあるのか、また、2) 如何なる措置がどの程度の期間必要とされるか、さらには、3) どの程度の症例数が見込まれるのかといった、といった疑問全てに回答すべく研究体制を整備した。

日本国内における脊椎インストゥルメンテーション手術は年間 6 万件と目されている。そのうち、麻痺のない労災患者を 2% と仮定すると年間症例数は 1200 例。アフターケアにかかる費用は当院平均で年間 30 万円なので、全例を 20 年間アフターケアとすれば 72 億円を要す。しかし、脊椎インストゥルメンテーションを行った症例全てがアフターケアを要するとは考えづらく、ごく限られた特殊な症例が該当するであろうと予測している。症状固定後に後遺症状に動揺をきたす症例、後遺障害に付随する疾病を発症させる症例はどのような条件が揃えば生じえるのか解析し、アフターケアの適応条件を定めることができれば労災補償行政に資するところ大である。

- ① どのような症例が対象か？
- ② その程度の期間が必要か？
- ③ その頻度や症例数は？
- ④ 追加で必要な医療コストは？

アフターケアを導入する際の適応基準となりえるもので、労災補償行政の施策上、必須のデータになる。また、アフターケアを導入した場合の医療コストを予想することが可能となる。適正なアフターケアの適応基準を定めれば 5% 以下の症例しか該当しないであろうと予想され、年間 72 億円を 3 億程度まで圧縮する科学的根拠となるであろう。アフターケアが「真に必要な症例」、「本来は不要な症例」を見定めることこそ、限りある労災補償財源の適正分配につながる。

B. 研究計画、方法

(1) 労災患者における脊椎インストゥルメンテーション症例のデータ集積 (2 年間)

北海道せき損センター、総合せき損センター、吉備高原医療リハビリテーションセンター、産業医科大学をコアとして全労災病院 (全国に 34) と産業医科大学の過去 5 年を目処に労災患者における脊椎インストゥルメンテーション症例のデータを集積する。

対象施設は以下の 35 施設。

1. 北海道中央労災病院、2. 北海道せき損センター、3. 釧路労災病院、4. 青森労災病院、5. 東北労災病院、6. 秋田労災病院、7. 福島労災病院、8. 鹿島労災病院、9. 千葉労災病院、10. 東京労災病院、11. 関東労災病院、12. 横浜労災病院、13. 燕労災病院、14. 新潟労災病院、15. 富山労災病院、16. 浜松労災病院、17. 中部労災病院、18. 旭労災病院、19. 大阪労災病院、20. 関西労災病院、21. 神戸労災病院、22. 和歌山労災病院、23. 山陰労災病院、24. 岡山労災病院、25. 中国労災病院、26. 山口労災病院、27. 香川労災病院、28. 愛媛労災病院、29. 九州労災病院、30. 九州労災病院門司メディカルセンター、31. 長崎労災病院、32. 熊本労災病院、33. 吉備高原医療リハビリテーションセンター、34. 総合せき損センター、35. 産業医科大学

協力医師

油川修一、池田天史、岡崎裕司、奥山幸一郎、加治浩三、川添泰弘、日下部 隆、楠瀬浩一、武田宏史、千葉光穂、信田進吾、馬場秀夫、放生憲博、山縣正庸、渡邊健一、舘田聡、伊藤圭吾、岩崎幹希、岡部 聡、笠原孝一、河本正昭、菊地 廉、傳田博司、花林昭裕、平野典和、三上容司、三好光太、湯川泰紹、安藤宗治、大園健二、大西英生、大和田哲雄、岡野 徹、城戸研二、木戸健司、楠城誉朗、國司善彦、佐々木俊二、笹重善朗、壺内 貢、富永俊克、生熊久敬、前原 孝、原田良昭

実務担当：須田浩太（北海道せき損センター；以下道せき損）、三浪明男（道せき損）、松本聡子（道せき損）、小松 幹（道せき損）、芝 啓一郎（総合せき損センター；以下総合せき損）、植田尊善（総合せき損）、前田 健（総合せき損）、坂井宏旭（総合せき損）、徳弘昭博（吉備高原医療リハビリテーションセンター；以下吉備リハ）、古澤一成（吉備リハ）、酒井昭典（産業医科大学；以下産業医大）、中村英一郎（産業医大）

（２）労災患者以外の脊椎インストゥルメンテーション症例のデータ集積（３年間）

労災患者以外の脊椎インストゥルメンテーション症例のデータを集積し、同様の手法で中央集約管理を行う。

対象施設は以下の５施設。

1.北海道せき損センター、2.総合せき損センター、3.産業医科大学、4.北海道大学、5.獨協医科大学
担当：須田浩太（道せき損）、三浪明男（道せき損）、松本聡子（道せき損）、小松 幹（道せき損）、芝 啓一郎（総合せき損）、植田尊善（総合せき損）、前田 健（総合せき損）、坂井宏旭（総合せき損）、酒井昭典（産業医大）、中村英一郎（産業医大）、岩崎倫政（北海道大学；以下

北大）、高畑雅彦（北大）、種市 洋（獨協医科大学；以下獨協医大）、稲見 聡（獨協医大）、森平 泰（獨協医大）

（３）データの解析（２年間）

集積したデータを基に下記の７点につき明らかにする。

- 1.労災患者での脊椎固定頻度
- 2.手術内容
- 3.治癒までの期間
- 4.治癒後の加療要否
- 5.麻痺患者との比較
- 6.アフターケアの適応基準
- 7.医療コスト

担当：伊藤陽一（北大）、須田浩太（道せき損）、坂井宏旭（総合せき損）、中村英一郎（産業医大）、高畑雅彦（北大）、森平 泰（獨協医大）

予定通りに「労災患者における脊椎インストゥルメンテーション症例のデータ集積（２年間）」を行い完了した。

2009年１月からの５年間に全国労災病院にて入院加療を行った労災保険患者 18,371 名、総手術 16093 件、うち脊椎インストゥルメンテーション手術 348 件を対象として疾患、年齢、性別、術前・術後レントゲン画像、固定範囲、術後合併症、治療内容、診療報酬内訳、アフターケアの有無などを収集した。多くの労災病院にてアフターケアへの移行がゼロであったため、アフターケアが申請されなかった理由や経緯を再調査中である。また、2009年１月からの５年間に産業医科大学、北海道大学、獨協医科大学にて施行された脊椎インストゥルメンテーション多椎間固定例を対象に、疾患、年齢、性別、固定範囲、固定アライメント、合併症、隣接椎間変性や骨折、術後の加療要否についてデータを収集している。これにより脊椎インストゥルメンテーション手術による隣接椎間変性や骨折など

の頻度につき解明を目指す。また、脊椎インストゥルメンテーション手術による隣接椎間障害の頻度や治療成績のエビデンスを得るためメタ解析を追加実施する。

C.研究結果

全国 34 労災病院（約 13,000 床、約 15,000 人スタッフ）よりデータを収集している。2009 年 1 月から 2014 年 12 月までの 5 年間を対象とした調査を行った。当該機関に全国の労災病院にて入院加療を行った労災保険患者は 18371 名であった。うち労災保険適応の手術は 16093 件あり、このうち、脊椎手術を受けた患者は 514 名、脊椎手術総件数は 594 件であった。その中で脊椎インストゥルメンテーション手術は 348 件であることが判明した。現在、これらの患者を対象に疾患名、術式、固定部位、固定椎間数、矯正の有無、アウターケアの有無、アフターケアの内容、医療費などの調査を開始したところである。各病院の症例数内訳は、北海道中央労災病院：1、北海道せき損センター：65、釧路労災病院：8、青森労災病院：2、東北労災病院：3、秋田労災病院：4、福島労災病院：2、鹿島労災病院：2、千葉労災病院：14、東京労災病院：4、関東労災病院：17、横浜労災病院：10、新潟労災病院：3、富山労災病院：6、浜松労災病院：3、中部労災病院：26、旭労災病院：1、大阪労災病院：3、関西労災病院：8、神戸労災病院：3、和歌山労災病院：2、山陰労災病院：8、岡山労災病院：4、中国労災病院：6、山口労災病院：9、香川労災病院：14、愛媛労災病院：2、九州労災病院：6、長崎労災病院：26、熊本労災病院：12、総合せき損センター：29 であった。

関連する他研究の調査：脊椎インストゥルメンテーションに起因する隣接椎間障害についての検討

頸椎インストゥルメンテーション 外傷

小島孝太らは中下位頸椎損傷に対して PS と LMS を施行した 4 例(男性 3 例、女性 1 例、手術時年齢 25-52 歳)、CF 型 3 例(C4/5 脱臼 1 例、C4/5 脱臼骨折 1 例、C5/6 脱臼骨折 1 例)、VC 型 1 例(C6 圧迫骨折)を調査し 1 例で隣接椎間障害を認めた。すなわち外傷では隣接椎間障害は少なかった。

慢性関節リウマチ

一方で、林 協司らは慢性関節リウマチ（以下 RA）性中下位頸椎病変 19 例(男 2 例、女 17 例、平均 62 歳).Steinbrocker 分類では stage III が 2 例、IV が 17 例で、術式は椎弓形成術 8 例(A 群)、椎弓切除+後方固定術 8 例(B 群)、前方除圧固定術 3 例(C 群)を術後 14～55 ヶ月まで調査した。A 群では Ranawat の疼痛スコアで 1 段階改善が 5 例、2 段階改善が 3 例であった。脊髄症スコアでも術直後は全例 1 段階改善したが、1 例で彎曲異常が増強し、除圧術を追加した。C 群では疼痛スコアが 1 段階改善 2 例、2 段階改善 1 例であったが、脊髄症スコアは全例改善を認めなかった。X 線所見は、A 群では 1 例にのみ不安定性の増強が認められ、C 群も全例骨癒合は得られたが、移植骨の圧潰を認め、2 例に隣接椎間の新たなすべり、不安定性が出現していた。納田真也らは同様に RA 環軸椎亜脱臼に対する環軸椎固定術の手術成績を調査し、軸椎下亜脱臼(SAS)の発生と進行が手術成績に及ぼす影響を調査した。術後 18 ヶ月以上経過した 10 症例とした。神経症状が悪化した 4 例中 3 例では、SAS の出現あるいは進行時期に一致して神経症状が悪化しており、新たな SAS の発生または SAS の進行が術後の神経症状に影響していた。最終調査時に SAS を認めた 7 例中 5 例はムチランス型であり、SAS 発生と進行の要因としてムチランス型の自然経過が最も大きいと考えられ

た。7 例で骨癒合が後頭骨や第 3 頸椎まで多椎間に及んでいたことから、上位頸椎の多椎間に及ぶ骨癒合によって下位頸椎の負担が増大したために生ずる隣接椎間障害も、SAS の要因となり得ると考えられムチランス型に対しては、全頸椎固定を考慮する必要を示唆した。

透析

透析に関しては土屋邦喜らが頸椎後方固定術を施行した血液透析(HD)患者 24 例を検討している。椎弓根スクリュー(PS)が最も多く 13 例に使用されていた。脊髄症の平均改善率は 30.6%であった。骨癒合は 21 例で獲得され、骨癒合率は 87%であった。インプラントの折損を 2 例に認めた。隣接椎間障害が 5 例に認められた。スクリューを用いた後方固定術は長期 HD 患者に対して適した方法と考えられるが隣接椎間障害に関しては十分な注意が必要であると結論した。宮崎幸政らは透析患者で上位頸椎病変を含む手術を施行した 7 例(男性 4 例、女性 3 例)を検討した。平均年齢は 65.1 歳、平均透析歴 23.4 年、病態は、歯突起偽腫瘍 2 例、環軸関節亜脱臼 2 例、DSA に伴う固定術後の隣接椎間障害 2 例、C2 椎体内骨嚢胞を伴う脊髄症 1 例であった。Magerl スクリューを用いた 1 例で骨癒合不全、隣接椎間障害の 2 例でインプラントの破損を認めた。岸田俊一らは後頭胸椎固定術を 4 例(男 2 例・女 2 例)に施行した。平均年齢は 64.5 歳、平均透析期間は 23 年であった。病態は歯突起偽腫瘍と下位頸椎 DSA の合併、環軸関節亜脱臼と下位頸椎 DSA の合併、後頭胸椎固定術後の implant failure、固定術後の隣接椎間障害であり、3 例に多数回手術を行っていた。1 例にロッド折損による再手術を施行したが、最終的には全例骨癒合が得られ、おおむね ADL は保たれた。術後の平均経過観察期間は 5.9 年であり、期間中に 3 例が死亡したと報告した。平野 徹らは透析性脊椎症の頸椎病変に対する手術例 29 例(男

20 例、女 9 例、手術時平均年齢 59 歳)の術後経過を調査した。術式は前方固定術 7 例、後方除圧固定術 8 例、椎弓形成術 14 例であり、周術期合併症として、大量出血、血腫、instrumentation 脱転、早期隣接椎間障害、せん妄などを認めた。日本整形外科学会頸髄症判定基準は術前平均 6.4 点から術後 9.9 点と改善した(改善率 47%)が、最終時 8.9 点であった。3 例に術後平均 4 年で頸椎隣接椎間障害を生じ、9 例に術後平均 3 年で腰椎病変の出現/悪化を生じた。重度脊髄障害の透析患者を作らないためには、患者啓発および実地透析医に施行可能なスクリーニング導入による早期診断と、脊椎手術を受けた透析患者に対する専門医の継続的観察が重要である。以上より、透析患者においては周術期管理が厳重である必要があるとともに、隣接椎間障害の発生が多い。これは脊椎インストゥルメンテーションによるものと言うより、透析性変化と判断できる。

脳性麻痺

三原久範らはアテトーゼ型脳性麻痺に伴う頸椎症性脊髄症に対する手術 89 例中 27 例の再手術例を経験した。術後 6 ヶ月以内の早期再手術例は 6 例あり、固定術後の内固定材の破綻が 4 例(80 例中)、椎弓形成術後の症状悪化が 2 例(4 例中)で、いずれもわれわれのアテトーゼ強度分類で Grade 4(徒手矯正不能な強度)以上の症例であった。一方、術後 6 ヶ月以上経過後の再手術は 21 例あり、抜釘を除くと隣接椎間障害(5 例)と頭蓋頸椎移行部不安定症(2 例)が原因であった。下川 宣幸らは手術治療を行ったアテトーゼ頸髄症患者 7 例(男性 4 例、女性 3 例、平均 59.7 歳)を対象に、術前の画像評価、三原らのアテトーゼ強度分類で「アテトーゼ強度」を評価して術式を選択した。観察期間は平均 23.7 ヶ月であった。アテトーゼ強度が軽度(grade 1、2)で 20 度以上の局所後彎がなければ椎弓形成術を行い、

20 度以上の局所後彎合併例に後彎矯正固定術を併用し、椎間孔狭窄に後方椎間孔開放術を行った。アテトーゼ強度が中等度(grade 3)には A 型ボツリヌス毒素製剤を過緊張筋に術前投与し、後方徐圧固定術を行った。アテトーゼ強度が重度(grade 4、5)には過緊張の選択的筋解離術を併用して後方徐圧固定術を行った。平均 JOA スコアは術前 7.7 点→最終時 10.6 点、平均改善率は 31.2%であった。術後に固定に伴う嚥下障害、隣接椎間障害、頭蓋頸椎移行部の不安定性出現は認めず、後方徐圧例で術後に後彎変形が出現して神経症状を呈する症例も認めなかった。上記 2 論文からは適切な治療選択により隣接椎間障害や再手術は軽減できるものの、限界があることが示され、原因は脊椎インストゥルメンテーションではなくアテトーゼ型脳性麻痺といえる。

腰椎インストゥルメンテーション

英文、和文の関連論文を用いて Meta analysis を腰椎インストゥルメンテーションに関して行った。まとめを別添資料とした。

広範囲インストゥルメンテーション

清水敬親らは骨粗鬆性脊柱矢状面配列異常に対して、上中位胸椎(Th3～7)～骨盤(仙骨又は腸骨)に至る広範囲固定を施行した 22 症例(手術時 54～80 歳・平均 70 歳、術後経過観察期間 1.5～8 年・3.1 年)の臨床像・治療結果について検討し固定頭側端は T3:8 例・T4:3 例・T5:9 例・T6:1 例・T7:1 例、固定尾側端は S1:3 例・S2:14 例・腸骨:5 例であった。術後固定頭側の隣接椎間障害は全例で認めず、フックやスクリューの脱転やワイヤーのカットアウトは認めなかったが、ロッド折損を 2 例で認め、1 例は偽関節であったと報告している。隣接椎間障害は予想以上に少ないと感がある。

D.考察

本調査では労災保険が適応されて脊椎インストゥルメンテーション手術を受けた患者の大半が脊椎損傷であり、大部分が脊髄損傷や馬尾損傷などの神経損傷を伴っていた。神経損傷によって引き起こされる麻痺は後遺症として残存しやすい。上肢、下肢、体幹に留まらず排尿障害や排便障害も引き起こすため永続的な治療を要す。すなわち、これがアフターケアの根拠となっている。麻痺がない患者で脊椎インストゥルメンテーション手術を受けた場合のアフターケアの要否は不明のままであるが、脊椎インストゥルメンテーション手術に関連する他研究から後遺症、隣接椎間障害など長期にわたり治療を要する病態は乏しいと推察できる。

E.結論

労災患者以外のコントロールとして脊椎インストゥルメンテーション手術を受けた労災保険以外の患者データを 1.北海道せき損センター、2.総合せき損センター、3.産業医科大学、4.北海道大学、5.獨協医科大学にて分担して調査している。2 年間はデータの集積業務が主となるため解析作業は行っていないが、次年度から以下の解析を行う予定である。

- 1.労災患者での脊椎固定頻度
- 2.手術内容
- 3.治癒までの期間
- 4.治癒後の加療要否
- 5.麻痺患者との比較
- 6.アフターケアの適応基準
- 7.医療コスト

F.健康危険情報

該当なし

G.研究発表

- 1.論文発表
データ集積および解析後に予定
- 2.学会発表
データ集積および解析後に予定

H.知的財産権の出願・登録状況（予定を含む）

1.特許取得

なし

2.実用新案登録

なし

3.その他

1.論文(英文)

(独)労働者健康安全機構 北海道せき損センター

Komatsu M, Suda K, Takahata M, Matsumoto S, Ushiku C, Yamada K, Yamane J, Endo T, Iwasaki N, Minami A	Delayed bilateral vertebral artery occlusion after cervical spine injury: a case report	Spinal Cord Ser Cases. 2016 Nov 24;2:1631.
Ushiku C, Suda K, Matsumoto S, Komatsu M, Takahata M, Iwasaki N, Minami A	Dural penetration caused by a vertebral bone fragment in a lumbar burst fracture: a case report	Spinal Cord Ser Cases. 2017 Jan 12;3:1640.
Yukawa Y, Kato F, Suda K, Yamagata M, Ueta T, Yoshida M	Normative data for parameters of sagittal spinal alignment in healthy subjects: an analysis of gender specific differences and changes with aging in 626 asymptomatic individuals.	Eur Spine J. 22 Oct 2016

(独)労働者健康安全機構 総合せき損センター

Yugué I, Okada S, Masuda M, Ueta T, Maeda T, Shiba K.	Risk factors for adjacent segment pathology requiring additional surgery after single-level spinal fusion: impact of pre-existing spinal stenosis demonstrated by preoperative myelography.	Eur Spine J. 2016 May;25(5):1542-1549.
Tanaka J, Yugué I, Shiba K, Maeyama A, Naito M.	A Study of Risk Factors for Tracheostomy in Patients With a Cervical Spinal Cord Injury.	Spine (Phila Pa1976). 2016 May;41(9):764-71.
Takao T, Okada S, Morishita Y, aeda T, Kubota K, Ideta R, Mori E, Yugué I, Kawano O, Sakai H, Ueta T, Shiba K.	Clinical Influence of Cervical Spinal Canal Stenosis on Neurological Outcome after Traumatic Cervical Spinal Cord Injury without Major Fracture or Dislocation.	Asian Spine J. 2016 Jun;10(3):536-42.
Yugué I, Okada S, Masuda M, Ueta T, Maeda T, Shiba K.	"Knee-up test" for easy detection of postoperative motor deficits following spinal surgery.	Spine J. 2016 Dec;16(12):1437-1444.
Morishita Y, Masuda M, Maeda T, Ueta T, Shiba K.	Morphologic Evaluation of Lumbosacral Nerve Roots in the Vertebral Foramen: Measurement of Local Pressure of the Intervertebral Foramen.	Clin Spine Surg. 2016 Sep 16.
Desroches A, Morishita Y, Yugué I, Maeda T, Flouzat-Lachaniette CH, Hernigou P, Shiba K.	Kinematic Effects of Cervical Laminoplasty for Cervical Spondylotic Myelopathy on the Occipitoatlantoaxial Junction.	Clin Spine Surg. 2016 Oct 6.
Saito T, Yokota K, Kobayakawa K, Hara M, Kubota K, Harimaya K, Kawaguchi K, Hayashida M, Matsumoto Y, Doi T, Shiba K, Nakashima Y, Okada S.	Experimental Mouse Model of Lumbar Ligamentum Flavum Hypertrophy.	PLoS One. 2017 Jan 6;12(1):e0169717.

北海道大学大学院医学研究院 社会医学分野 医学統計学教室

Kokabu, T., Sudo, H., Abe, Y., Ito, M., Ito, Y. M., & Iwasaki, N.	Effects of Multilevel Facetectomy and Screw Density on Postoperative Changes in Spinal Rod Contour in Thoracic Adolescent Idiopathic Scoliosis Surgery.	PLoS One, 11(8), e0161906. doi:10.1371/journal.pone.0161906
Ohnishi, T., Sudo, H., Iwasaki, K., Tsujimoto, T., Ito, Y. M., & Iwasaki, N.	In Vivo Mouse Intervertebral Disc Degeneration Model Based on a New Histological Classification.	PLoS One, 11(8), e0160486. doi:10.1371/journal.pone.0160486
Sudo, H., Abe, Y., Kokabu, T., Ito, M., Abumi, K., Ito, Y. M., & Iwasaki, N.	Correlation analysis between change in thoracic kyphosis and multilevel facetectomy and screw density in main thoracic adolescent idiopathic scoliosis surgery.	Spine J, 16(9), 1049-1054. doi:10.1016/j.spinee.2016.04.014

2.論文(和文)

(独)労働者健康安全機構 北海道せき損センター

小松 幹、須田浩太	最小侵襲脊椎安定術(MIST)の現状と課題 ～mini-pone TLIFの臨床成績から～	北海道整形災害外科学会雑誌(1343-3873)58巻1号Page51-54(2016.10)
木田博朗、須田浩太、松本聡子、小松幹、牛久智加良、山根淳一、遠藤 努、東條泰明、神谷行宣、三浪明男	手術困難のために遅発性麻痺を生じたびまん性特発性骨増殖症(DISH)脊椎骨折の1例	北海道整形災害外科学会雑誌(1343-3873)58巻1号Page61-64(2016.10)
須田浩太、小松 幹、牛久智加良、校條祐輔、松本聡子	頸椎脱臼骨折の初期治療 私の治療戦略	整形外科Surgical Technique(2185-7733)7巻1号Page16-22(2017.1)
福井隆史、須田浩太、遠藤 努、松本聡子、小松 幹、牛久智加良、山根淳一、東條泰明、神谷行宣、三浪明男、高畑雅彦、岩崎倫政	迅速な整復固定の重要性を示唆した頸椎脱臼骨折の1例「例え運動完全麻痺であっても超早期手術により下肢筋力は完全回復する可能性がある」	北海道整形災害外科学会雑誌(1343-3873)58巻2号Page203-206(2017.3)

ARTICLE PREVIEW

[view full access options ►](#)

SPINAL CORD SERIES AND CASES | CASE REPORT

Delayed bilateral vertebral artery occlusion after cervical spine injury: a case report

Miki Komatsu, Kota Suda, Masahiko Takahata, Satoko Matsumoto, Chikara Ushiku, Katsuhisa Yamada, Junichi Yamane, Tsutomu Endo, Norimasa Iwasaki & Akio Minami

Spinal Cord Series and Cases 2, Article number: 16031 (2016) | doi:10.1038/scsandc.2016.31

Received 12 May 2016 | Accepted 19 July 2016 | Published online 24 November 2016

Abstract

Introduction:

There are considerable risks for the secondary spinal cord injury and the initial and/or delayed vertebral artery occlusion in cases of cervical fracture dislocation.

Case Presentation:

An 86-year-old man was injured in a car accident and was diagnosed with no fracture or dislocation of the cervical spine by the emergency physician. However, he was transferred to our hospital 3 days later because he had motor weakness that was evaluated to be 32 points (out of 50 points) on the upper limb American Spinal Injury Association (ASIA) motor score and was diagnosed with spontaneously reduced fracture dislocation at C5/6. Magnetic resonance images revealed that the bilateral vertebral arteries were occluded, and there were some microinfarction lesions in the brain. On the first visit to his previous doctor, he was found to have a flow void in the right vertebral artery. This indicated that it was occluded during the waiting period at his previous doctor. On the day of his arrival at our hospital, the patient underwent a C5/6 posterior spinal fusion. Three months after surgery, he recovered to 46 points on the upper extremity ASIA motor score, and blood flow in the left vertebral artery was resumed.

Discussion:

Early reduction and stabilization are necessary for cervical spine fracture dislocation; however, it is important not only for the prevention of the secondary injury but also for the reduction of the risk of vertebral artery occlusion.

Subject terms: Spinal cord diseases • Trauma

Read the full article

<p>Subscribe to <i>Spinal Cord Series and Cases</i> for full access:</p> <p>Subscribe</p>	<p>ReadCube Access*: *printing and sharing restrictions apply</p> <p>\$3.99 rent \$9.99 buy</p> <p>Buy/Rent now</p>	<p>Purchase article full text and PDF:</p> <p>\$32</p> <p>Buy now</p>
<p>Additional access options: Already a subscriber? Log in now or Register for online access. Login via Athens Use a document delivery service Purchase a site license</p>		

References

1. Taneichi H, Suda K, Kajino T, Kaneda K. Traumatically induced vertebral artery occlusion associated with cervical spine injuries: prospective study using magnetic resonance angiography. *Spine* 2005; **30**: 1955–1962.
2. Willis BK, Greiner F, Orrison WW, Benzel EC. The incidence of vertebral artery injury after midcervical spine fracture or subluxation. *Neurosurgery* 1994; **34**: 435–441.
3. Nakao Y, Terai H. Distal embolic brain infarction due to recanalization of asymptomatic vertebral artery occlusion resulting from cervical spine injury: a case report. *J Chiropr Med* 2014; **13**: 266–272.

4. Ashley WW Jr, Rivet D, Cross DT 3rd, Santiago P. Development of a giant cervical vertebral artery pseudoaneurysm after a traumatic C1 fracture: case illustration. *Surg Neurol* 2006; **66**: 80–81.
5. Atar E, Griton I, Bachar GN, Bartal G, Kluger Y, Belenky A. Embolization of transected vertebral arteries in unstable trauma patients. *Emerg Radiol* 2005; **11**: 291–294.
6. Cohen JE, Rajz G, Itshayek E, Umansky F, Gomori JM. Endovascular management of exsanguinating vertebral artery transection. *Surg Neurol* 2005; **64**: 331–334.
7. Fassett DR, Dailey AT, Vaccaro AR. Vertebral artery injuries associated with cervical spine injuries: a review of the literature. *J Spinal Disord Tech* 2008; **21**: 252–258.
8. Eftekhari B, Dadmehr M, Ansari S, Ghodsi M, Nazparvar B, Ketabchi E. Are the distributions of variations of circle of Willis different in different populations? Results of an anatomical study and review of literature. *BMC Neurol* 2006; **6**: 22.
9. Hoksbergen AW, Fulesdi B, Legemate DA, Csiba L. Collateral configuration of the circle of Willis: transcranial color-coded duplex ultrasonography and comparison with postmortem anatomy. *Stroke* 2000; **31**: 1346–1351.
10. Macchi C, Molino Lova R, Miniati B, Zito A, Catini C, Gulisano M *et al.* Collateral circulation in internal carotid artery occlusion. A study by duplex scan and magnetic resonance angiography. *Minerva Cardioangiol* 2002; **50**: 695–700.
11. Nagahama K, Sudo H, Abumi K, Ito M, Takahata M, Hiratsuka S *et al.* Anomalous vertebral and posterior communicating arteries as a risk factor in instrumentation of the posterior cervical spine. *Bone Joint J* 2014; **96-B**: 535–540.

Author information

Affiliations

Department of Orthopaedic Surgery, Hokkaido Chuo Rosai Hospital Spinal Cord Injury Center, Bibai, Japan

Miki Komatsu, Kota Suda, Satoko Matsumoto, Chikara Ushiku, Katsuhisa Yamada, Junichi Yamane, Tsutomu Endo & Akio Minami

Department of Orthopaedic Surgery, Hokkaido University Graduate School of Medicine,
Sapporo, Japan

Masahiko Takahata & Norimasa Iwasaki

Competing interests

The authors declare no conflict of interest.

Corresponding author

Correspondence to Miki Komatsu.



This journal is a member of and subscribes to the principles of the Committee on Publication Ethics.

Spinal Cord Series and Cases ISSN 2058-6124 (online) © 2017 International Spinal Cord Society

© 2017 Macmillan Publishers Limited, part of Springer Nature. All rights reserved.

partner of AGORA, HINARI, OARE, INASP, ORCID, CrossRef and COUNTER

Recommended



Bizarre Parosteal Osteochondromatous Proliferation
(Nora's Lesion) of the Sesamoid: a Case Report

Harty, J.A.... Stephens, M.M.

Foot & Ankle International (2017)

ARTICLE PREVIEW

[view full access options ►](#)**SPINAL CORD SERIES AND CASES | CASE REPORT**

Dural penetration caused by a vertebral bone fragment in a lumbar burst fracture: a case report

Chikara Ushiku, Kota Suda, Satoko Matsumoto, Miki Komatsu, Masahiko Takahata, Norimasa Iwasaki & Akio Minami

Spinal Cord Series and Cases 3, Article number: 16040 (2017) | doi:10.1038/scsandc.2016.40

Received 08 May 2016 | Revised 24 October 2016 | Accepted 11 December 2016 | Published online 12 January 2017

Abstract

Introduction:

This case report describes an unusual case of lumbar burst fracture in which a bone fragment from the vertebral body penetrated into the dorsal dura through the ventral dura mater, requiring bone fragment extraction via an intradural approach.

Case Presentation:

A 23-year-old male involved in a motor vehicle accident was admitted to our hospital complaining of right leg paresis and bladder-bowel disorder. Computed tomography (CT) revealed an L5 burst fracture of type B by the Denis classification scheme, with a bone fragment from the vertebral body that had perforated the ventral aspect of the dura mater and penetrated dorsally. We abandoned attempts to extract the bone fragment via an epidural approach and instead resected the fragment via an intradural approach with a dorsal dural incision. We corrected L4/5 kyphosis as possible and performed L4/5 posterolateral fusion. The patient's leg paralysis and bladder-bowel disorder were relieved, and he was discharged 2 months after the surgery with the ability to walk without crutches.

Discussion:

When bone fragments penetrate the dura mater, their extraction must be performed with particular care. For cases in which the dura mater cannot be pulled apart, the removal of bone fragments using an intradural approach is appropriate.

Subject terms: Fracture repair • Trauma

Read the full article

<p>Subscribe to <i>Spinal Cord Series and Cases</i> for full access:</p> <p>Subscribe</p>	<p>ReadCube Access*: *printing and sharing restrictions apply</p> <p>\$4.99 rent \$9.99 buy</p> <p>Buy/Rent now</p>	<p>Purchase article full text and PDF:</p> <p>\$32</p> <p>Buy now</p>
<p>Additional access options: Already a subscriber? Log in now or Register for online access. Login via Athens Use a document delivery service Purchase a site license</p>		

References

1. Keenen TL, Antony J, Benson DR. Dural tears associated with lumbar burst fractures. *J Orthop Trauma* 1990; 4: 243–245.
2. Ozturk C, Ersozlu S, Aydinri U. Importance of greenstick lamina fractures in low lumbar burst fractures. *Int Orthop* 2006; 30: 295–298.
3. Luszczuk MJ, Blaisdell GY, Wiater BP, Bellabarba C, Chapman JR, Agel JA *et al.* Traumatic dural tears: what do we know and are they a problem? *Spine J* 2014; 14: 49–56.
4. Carl AL, Matsumoto M, Whalen JT. Anterior dural laceration caused by thoracolumbar and lumbar burst fractures. *J Spinal Disord* 2000; 5: 399–403.
5. Amano K, Hori T, Kawamata T, Okada Y. Repair and prevention of cerebrospinal fluid leakage in transsphenoidal surgery: a sphenoid sinus mucosa technique. *Neurosurg Rev* 2016; 39: 123–131.

6. McCormack T, Karaikovic E, Gaines RW. The load sharing classification of spine fractures. *Spine* 1994; **19**: 1741–1744.
7. Hitchon P, Torner J, Haddad S, Follett K. Management options in thoracolumbar burst fractures. *Surg Neurol* 1998; **49**: 619–27.
8. Gertzbein SD. Scoliosis Research Society. multicenter spine fracture study. *Spine* 1992; **17**: 528–540.

Author information

Affiliations

Department of Orthopaedic Surgery, Hokkaido Chuo Rosai Hospital Spinal Cord Injury Center, Hokkaido, Japan

Chikara Ushiku, Kota Suda, Satoko Matsumoto, Miki Komatsu & Akio Minami

Department of Orthopaedic Surgery, Hokkaido University Graduate School of Medicine, Hokkaido, Japan

Masahiko Takahata & Norimasa Iwasaki

Competing interests

The authors declare no conflict of interest.

Corresponding author

Correspondence to Chikara Ushiku.



Recommended

This journal is a member of and subscribes to the principles of the Committee on Publication Ethics.




Spinal Cord Series and Cases **Nerve Lesion: Case Report and Literature Review of a Bizarre Parosteal Osteochondromatous Proliferation of a...**

© 2017 Macmillan Publishers Limited, part of Springer Nature. All rights reserved.

partner of AGORA, HINARI, OARE, INASP, CrossRef, and the International Council of Scientific Journals (ICJS) (2017)

Normative data for parameters of sagittal spinal alignment in healthy subjects: an analysis of gender specific differences and changes with aging in 626 asymptomatic individuals

Yasutsugu Yukawa^{1,2}  · Fumihiko Kato² · Kota Suda³ · Masatsune Yamagata⁴ · Takayoshi Ueta⁵ · Munehito Yoshida¹

Received: 19 May 2016 / Revised: 5 September 2016 / Accepted: 3 October 2016
© Springer-Verlag Berlin Heidelberg 2016

Abstract

Purpose This study aims to establish normative data for parameters of spino-pelvic and spinal sagittal alignment, gender related differences and age-related changes in asymptomatic subjects.

Methods A total of 626 asymptomatic volunteers from Japanese population were enrolled in this study, including 50 subjects at least for each gender and each decade from 3rd to 8th. Full length, free-standing spine radiographs were obtained. Cervical lordosis (CL; C3–7), thoracic kyphosis (TK; T1–12), lumbar lordosis (LL; T12–S1), pelvic incidence (PI), pelvic tilt (PT), sacral slope (SS) and sagittal vertical axis (SVA) were measured.

Results The average values (degrees) are 4.1 ± 11.7 for CL, 36.0 ± 10.1 for TK, 49.7 ± 11.2 for LL, 53.7 ± 10.9 for PI, 14.5 ± 8.4 for PT, and 39.4 ± 8.0 for SS. Mean SVA is 3.1 ± 12.6 mm. Advancing age caused an increase in CL, PT and SVA, and a decrease in LL and SS. There was a significant gender difference in CL, TK, LL, PI, PT and SVA. From 7th decade to 8th decade, remarkable

decrease of LL & TK and increase of PT were seen. A large increase of SVA was also seen between 60' and 70'. **Conclusion** Standard values of spino-pelvic sagittal alignment were established in each gender and each decade from 20' to 70'. A remarkable change of spino-pelvic sagittal alignment was seen from 7th decade to 8th decade in asymptomatic subjects.

Keywords Standard value · Spine radiograph · Spinopelvic sagittal alignment · Gender difference · Age-related change

Introduction

The prevalence of adult spinal deformity (ASD) has been reported to be as high as 60 % in the elderly population [1]. For many years, the diagnosis and treatment of ASD was based upon coronal plane radiograph analysis using Cobb angle measurements. However, recent research has shown that sagittal spino-pelvic alignment among patients with ASD plays a critical role in pain and disability and is a primary determinant of health related quality of life (HRQOL) measures [2–5]. One of them concluded that restoration of “a more normal sagittal balance” is the critical goal for any reconstructive spine surgery. However, the definition of what constitutes normal and pathologic alignment in the spine has not been established [3].

Standard values of sagittal alignment and range of motion of the cervical spine in 1230 asymptomatic volunteers were reported in a previous study. This study revealed that cervical lordosis in the neutral position increases with age, particularly in the sixth decade and to a greater degree in females [6]. However, the total range of motion decreased linearly with age, particularly in extension and males. As

✉ Yasutsugu Yukawa
yukawa@wakayama-med.ac.jp

¹ Department of Orthopedic Surgery, Wakayama Medical University, 811-1 Kimiidera, Wakayama 641-8509, Japan

² Department of Orthopedic Surgery, Chubu Rosai Hospital, Nagoya, Japan

³ Department of Orthopedic Surgery, Hokkaido Chuo Rosai Hospital Sekison Center, Bibai, Japan

⁴ Department of Orthopedic Surgery, Chiba Rosai Hospital, Ichihara, Japan

⁵ Department of Orthopedic Surgery, Spinal Injuries Center, Iizuka, Japan

apparent aging and gender changes were seen in cervical alignment, it should be presumed that spino-pelvic sagittal alignment is affected by age and gender.

In recent years, many authors emphasized the importance of spinal sagittal balance and investigated those parameters in healthy subjects [2, 5, 7–21]. However, there have been few studies using a large cohort with an even age and gender distribution. Accordingly, the objective of the current study was to investigate normal spinal and spino-pelvic sagittal alignment in asymptomatic volunteers of each sex and in each decade of life between the 3rd (20's) and 8th (70's), and attempt to elucidate gender related differences and age-related changes using data from radiographs of over 600 healthy subjects.

Materials and method

After obtaining institutional review board approval, healthy Japanese volunteers were sought after the purpose of this study was officially announced. The exclusion criteria included a history of brain or spinal surgery, comorbid neurologic disease such as cerebral infarction or neuropathy, symptoms related to sensory or motor disorders (numbness, clumsiness, motor weakness, and gait disturbances) or having severe low back pain. Pregnant women and individuals who received worker's compensation or presented with symptoms after a motor vehicle accident were also excluded. If radiographs measurements of sagittal parameters were difficult to assess due to lumbosacral transitional anomalies or spinal malformation, the subjects were also excluded. Finally 626 asymptomatic subjects with appropriate images were enrolled in the present study including 50 subjects at least in each gender and each decade from 3rd to 8th (Table 1).

Full length, free-standing spine radiographs with fists on clavicles were obtained in all subjects. All images were transferred to a computer as Digital Imaging and Communications in Medicine (DICOM) data. Cervical lordosis (C3–7, CL), thoracic kyphosis (T1–12, TK), lumbar lordosis (T12–S1, LL), pelvic incidence (PI), pelvic tilt (PT), sacral slope (SS) and sagittal vertical axis (SVA) were measured

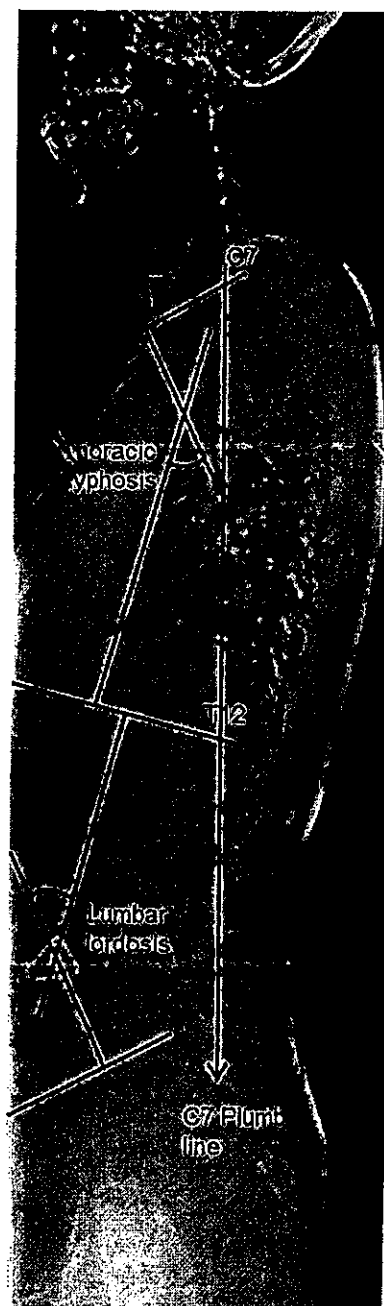


Fig. 1 Methods of measurement of spinal parameters; thoracic kyphosis (TK), lumbar lordosis (LL) and sagittal vertical axis (SVA)

using measurement software (Figs. 1, 2). Each parameter was measured by experienced radiation technologists using imaging software (Osiris4; Icestar Media Ltd, Essex, UK).

Table 1 Materials; age and gender distribution

Age	Men	Women	
20–29	48	53	101
30–39	51	50	101
40–49	50	57	107
50–59	56	51	107
60–69	50	60	110
70–79	50	50	100
Total	305	321	626

Statistical analysis

The data were analyzed using the SPSS version 13.0 software (SPSS Inc., Chicago, IL). Descriptive statistics were calculated for all subjects and separately for males and females in the form of mean value and standard

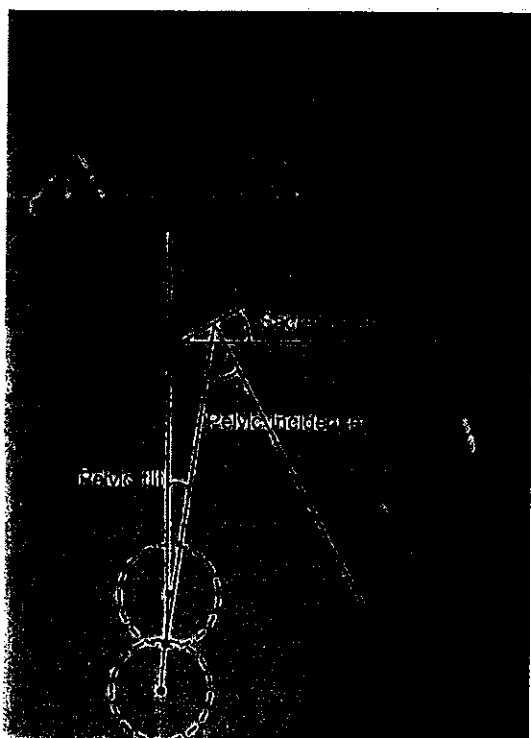


Fig. 2 Methods of measurement of spinal parameters; pelvic incidence (PI), sacral slope (SS) and pelvic tilt (PT)

deviation. Comparison between the male and the female was carried out by un-paired Student *t* tests. Statistical significance was set at a level of $P < 0.05$.

Results

Average height and weight [mean \pm standard deviation (SD)] of all male and female subjects was 169.1 ± 6.5 cm/ 66.7 ± 10.3 kg and 156.2 ± 6.0 cm/ 52.9 ± 8.0 kg, respectively.

The average values (degrees) are 4.1 ± 11.7 of CL, 36.0 ± 10.1 of TK and 49.7 ± 11.2 of LL (Tables 2, 3, 4; Figs. 3, 4, 5). The average values of pelvic morphologic angles are 53.7 ± 10.9 for PI, 14.5 ± 8.4 for PT and 39.4 ± 8.0 for SS (Tables 5, 6, 7; Figs. 6, 7, 8). The mean SVA is 3.1 ± 12.6 mm (Table 8; Fig. 9). CL is greater in males than in females in any decade. CL is increased with age, especially after 60' (Fig. 3; Table 2). Regarding TK and LL, remarkable changes were not seen from 20' to 60'. However, a sudden decrease was detected for both TK and LL in 70' (Figs. 4, 5; Tables 3, 4). PI was higher by several degrees in females with age greater than 40 years, than that in 20' or 30', females or males (Fig. 6; Table 5). PT increased with age and the change was stressed in females (Fig. 7; Table 6). SS was almost similar between males and females, and showed a gradual decrease with aging

Table 2 Cervical lordosis (CL; C3–7)

Decade	Male	Female	P value
20–29	3.3 ± 11.6	-6.0 ± 9.7	<0.001
30–39	4.5 ± 12.7	-3.4 ± 10.7	<0.001
40–49	4.4 ± 8.6	2.4 ± 11.4	NS
50–59	5.3 ± 8.3	0.1 ± 11.1	<0.001
60–69	13.5 ± 11.4	4.7 ± 8.5	<0.001
70–79	13.2 ± 12.4	8.5 ± 12.7	0.059
All	7.3 ± 11.6	1.1 ± 11.6	<0.001
Total	4.1 ± 11.7		

NS indicates not significant

Table 3 Thoracic kyphosis (TK; T1–12)

Decade	Male	Female	P value
20–29	34.9 ± 8.1	33.9 ± 9.1	NS
30–39	37.3 ± 9.1	33.4 ± 9.0	<0.05
40–49	35.9 ± 8.5	35.9 ± 10.4	NS
50–59	39.4 ± 10.5	35.9 ± 10.7	0.088
60–69	39.7 ± 10.0	36.0 ± 11.7	0.074
70–79	35.0 ± 11.8	34.8 ± 11.6	NS
All	37.1 ± 9.9	35.0 ± 10.5	<0.05
Total	36.0 ± 10.1		

NS indicates not significant

Table 4 Lumbar lordosis (LL; T12–S)

Decade	Male	Female	P value
20–29	49.4 ± 8.6	52.4 ± 13.1	NS
30–39	48.5 ± 11.2	52.7 ± 10.3	0.057
40–49	47.6 ± 10.8	54.1 ± 10.3	<0.01
50–59	50.5 ± 9.1	51.5 ± 10.2	NS
60–69	48.5 ± 13.1	52.2 ± 10.9	NS
70–79	42.2 ± 14.8	46.7 ± 13.3	NS
All	47.8 ± 11.6	51.6 ± 11.6	<0.001
Total	49.7 ± 11.2		

NS indicates not significant

(Fig. 8; Table 7) A negative value for the SVA was identified only in males in the 20' as well as in females in the 20' and 30'. SVA increased gradually with age from 3rd decade and 7th decade, and showed apparent increase in the 8th decade (Fig. 9; Table 8).

Discussion

This study represents the large cross-sectional analysis of spinal and spino-pelvic alignment with homogenous age and sex distribution, in 626 healthy subjects as studied on

Table 5 Pelvic incidence (PI)

Decade	Male	Female	P value
20–29	54.4 ± 10.1	51.8 ± 11.7	NS
30–39	52.9 ± 10.2	51.2 ± 9.5	NS
40–49	50.8 ± 7.8	57.0 ± 10.8	<0.001
50–59	53.0 ± 11.3	56.2 ± 11.3	NS
60–69	52.0 ± 10.9	56.0 ± 12.7	NS
70–79	52.0 ± 10.3	57.4 ± 9.5	<0.01
All	52.6 ± 10.4	54.9 ± 11.4	<0.01
Total	53.7 ± 10.9		

NS indicates not significant

Table 6 Pelvic tilt (PT)

Decade	Male	Female	P value
20–29	12.9 ± 8.1	11.4 ± 6.6	NS
30–39	13.1 ± 7.7	12.0 ± 6.7	NS
40–49	11.5 ± 5.8	16.2 ± 8.4	<0.001
50–59	13.3 ± 9.8	15.1 ± 7.5	NS
60–69	13.7 ± 7.1	18.4 ± 9.2	<0.01
70–79	15.3 ± 7.4	21.0 ± 7.8	<0.001
All	13.2 ± 7.7	15.8 ± 8.6	<0.001
Total	14.5 ± 8.4		

NS indicates not significant

Table 7 Sacral slope (SS)

Decade	Male	Female	P value
20–29	41.6 ± 7.4	40.3 ± 9.1	NS
30–39	40.0 ± 7.1	39.7 ± 6.5	NS
40–49	39.8 ± 6.9	41.1 ± 7.8	NS
50–59	40.1 ± 8.9	41.0 ± 7.6	NS
60–69	38.2 ± 8.7	37.5 ± 8.0	NS
70–79	37.2 ± 10.5	36.7 ± 9.1	NS
All	39.6 ± 8.3	39.3 ± 8.1	NS
Total	39.4 ± 8.0		

NS indicates not significant

full spine standing radiographs. Based on our findings, normative data for cervical lordosis (C3–7, CL), thoracic kyphosis (T1–12, TK), lumbar lordosis (T12–S1, LL), pelvic incidence (PI), pelvic tilt (PT), sacral slope (SS) and sagittal vertical axis (SVA) were established for each gender and each decade from 3rd to 8th. Notably, gender differences and age-related changes from the 3rd to the 8th decade were also elucidated. Remarkable changes of spinal and spino-pelvic sagittal alignment, a sudden decrease of TK and LL and a large increase of SVA, were seen from 7th decade to 8th decade.

Table 8 Sagittal vertical axis (SVA)

Decade	Male	Female	P value
20–29	−2.1 ± 8.2	−4.6 ± 13.5	NS
30–39	3.0 ± 9.2	−4.1 ± 13.0	<0.01
40–49	5.0 ± 13.7	0.9 ± 9.0	0.070
50–59	4.5 ± 11.8	3.4 ± 11.1	NS
60–69	5.5 ± 14.0	4.6 ± 10.4	NS
70–79	10.3 ± 14.4	10.7 ± 15.2	NS
All	4.5 ± 11.9	1.8 ± 13.1	<0.01
Total	3.1 ± 12.6		

NS indicates not significant

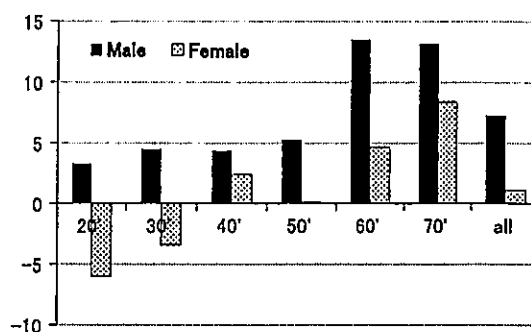


Fig. 3 Cervical lordosis (CL; C3–7)

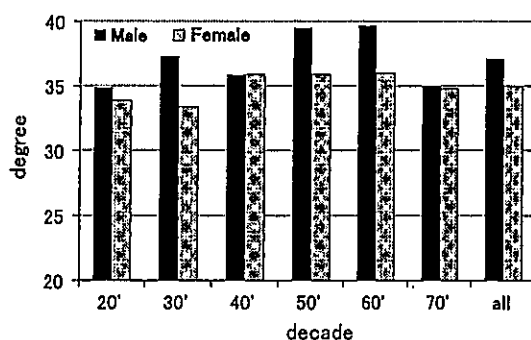


Fig. 4 Thoracic kyphosis (TK; T1–12)

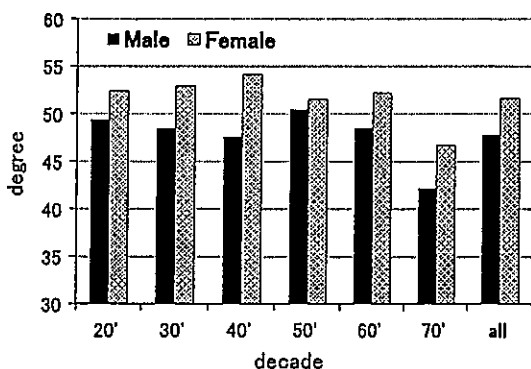


Fig. 5 Lumbar lordosis (LL; T12–S1)

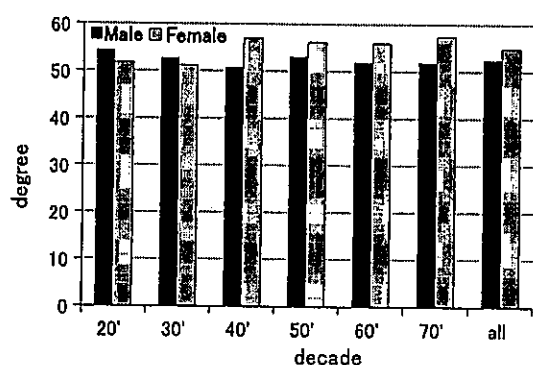


Fig. 6 Pelvic incidence (PI)

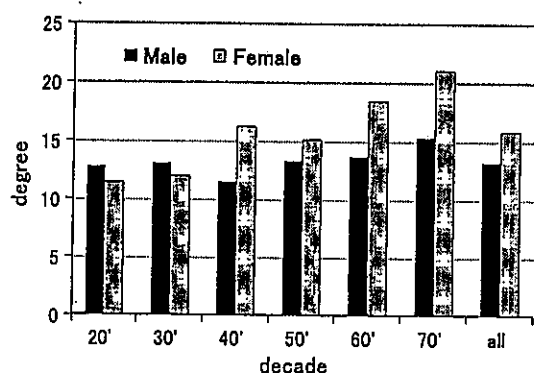


Fig. 7 Pelvic tilt (PT)

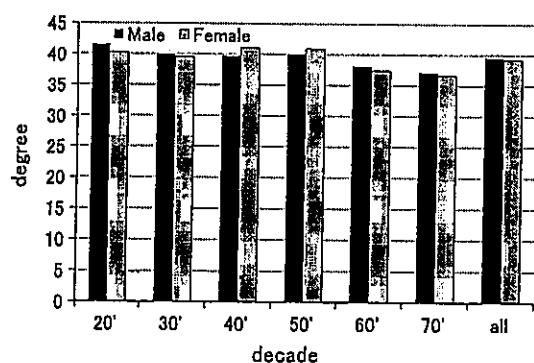


Fig. 8 Sacral slope (SS)

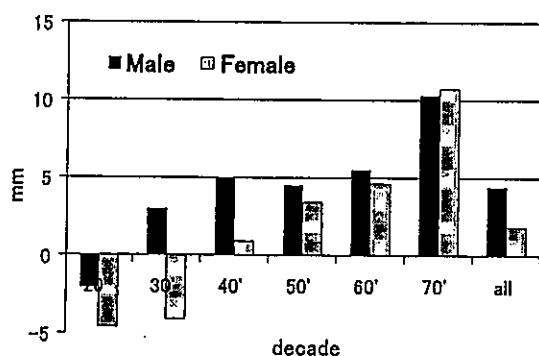


Fig. 9 Sagittal vertical axis (SVA)

Dubousset described the theory known as the “cone of economy”. In this understanding, the head center of gravity is maintained over the pelvis to achieve an energy efficient mechanism for ambulation and upright posture [22]. The body adapts to changes in this balance to regulate the center of gravity over as narrow a perimeter as possible. Various compensation mechanisms would work to maintain sagittal balance to achieve an energy efficient mechanism.

In the cervical spine, Yukawa et al. reported sagittal alignment and range of motion in 1230 asymptomatic volunteers [6]. They revealed gender differences and age-related changes from 3rd decade to 8th decade in the parameters of cervical alignment. Cervical lordosis in the neutral position increased with age, particularly in the sixth decade and to a greater degree in females. However, the total range of motion decreased linearly with age, particularly in extension and males.

With the increasing evidence gathered for the clinical importance of sagittal spinal alignment, we sought to better understand neutral upright sagittal spinal alignment in asymptomatic adults in whom demographic features were similar to those in patients. Therefore, we conducted this large-scale study including more than 600 asymptomatic volunteers, to establish standard values of sagittal spinal and spino-pelvic parameters and to elucidate those gender differences and age-related changes.

Several authors have investigated upon age-related spinal alignment changes among healthy volunteers. Gelb et al. reported that increasing age corresponded to a more anterior sagittal vertical axis with a loss of lumbar lordosis, comparing asymptomatic middle- and old-aged volunteers [7]. Hammerberg and Wood demonstrated that aging induced an anterior shift of C7 plumb line and a decrease of lumbar lordosis [12]. In our data, advancing age led to an increase in CL, PT and SVA, and a decrease in LL and SS. A sudden decrease was seen from 60' to 70' in TK and LL. In response to a LL decrease, a decrease of TK and increase of PT might occur as a compensatory mechanics to maintain global for sagittal balance [23]. A large increase of SVA was also seen between 60' and 70', indicating that the compensation mechanisms for the concurrent LL decrease were not sufficient.

Regarding gender related differences among parameters of sagittal spinal and spino-pelvic alignment, Vialle et al. showed that female subjects had higher values in lumbar lordosis and PI [13]. On the other hand, Mac-Thiong reported that there was no difference in PI, SS and PT between males and females [19]. The current study demonstrated that there was a relatively large gender difference in CL, LL and PT. In females, groups

with age >40 years had higher PI than that of 20' and 30'. The pelvic incidence is considered to be an inherent value for each individual unaffected by body posture. However, some gap of the value of PI was seen between young females and elder females in this study. Although we did not investigate civil status and birth experience, we may speculate that the birth experience is one of the reasons of higher PI in females aged over 40.

There were several limitations in the present study. First, the survey was limited to the Japanese population, so racial differences were not taken into account. Second, only asymptomatic subjects were enrolled in this study. This could have led to a selection bias in favor of relatively healthy participants.

Natural history of sagittal spino-pelvic alignment is gaining importance more than ever, as the number of reconstructive surgeries for adult spinal deformity increases. To detect the real natural history of sagittal alignment changes over time, a long-term follow up study is suitable. However, it seems very difficult to observe aging changes of spinal alignment over a whole life. Therefore, large-scale of cross-sectional observational study could be used as a substitute for longitudinal analysis. In this study we recruited more than 600 asymptomatic volunteers including at least 50 subjects in each gender and each decade from 3rd to 8th decade. This is the one of the largest cohort study of spinal alignment and the sex/sex ratio is almost 50:50. We believe that larger number of subjects and balanced sexual and age distribution should improve reliability of cohort study.

Conclusion

Full length, free-standing spine radiographs were obtained in 626 healthy subjects. Standard values and deviations of spino-pelvic sagittal alignment were established in each gender and each decade from 20' to 70'. A remarkable change of spino-pelvic sagittal alignment, decrease of TK & LL and increase of SVA, was seen from 7th decade to 8th decade.

Acknowledgments This study was supported by institutional funds and by grant research funds, which are intended for promoting hospital functions, of the Japan Labor Health and Welfare Organization (Kawasaki, Japan). No benefits in any form have been or will be received from a commercial party related directly or indirectly to the subject of this manuscript.

Compliance with ethical standards

Conflict of interest None of the authors has any potential conflict of interest.

References

- Schwab F, Dubey A, Gamez L et al (2005) Adult scoliosis: prevalence, SF-36, and nutritional parameters in an elderly volunteer population. *Spine* 30(9):1082–1085
- Jackson RP, McManus AC (1994) Radiographic analysis of sagittal plane alignment and balance in standing volunteers and patients with low back pain matched for age, sex, and size. A prospective controlled clinical study. *Spine* 19(14):1611–1618
- Glassman SD, Berven S, Bridwell K et al (2005) Correlation of radiographic parameters and clinical symptoms in adult scoliosis. *Spine* 30(6):682–688
- Schwab FJ, Blondel B, Bess S et al (2013) Radiographical spinopelvic parameters and disability in the setting of adult spinal deformity: a prospective multicenter analysis. *Spine* 38(13):E803–E812
- Yoshida G, Yasuda T, Togawa D et al (2014) Craniopelvic alignment in elderly asymptomatic individuals: analysis of 671 cranial centers of gravity. *Spine* 39(14):1121–1127
- Yukawa Y, Kato F, Suda K et al (2012) Age-related changes in osseous anatomy, alignment, and range of motion of the cervical spine—Part I, Radiographic data from over 1200 asymptomatic subjects. *Eur Spine J* 21(8):1492–1498
- Gelb DE, Lenke LG, Bridwell KH et al (1995) An analysis of sagittal spinal alignment in 100 asymptomatic middle and older aged volunteers. *Spine* 20(12):1351–1358
- Hardacker JW, Shuford RF, Capicotto PN et al (1997) Radiographic standing cervical segmental alignment in adult volunteers without neck symptoms. *Spine* 22(13):1472–1480 (discussion 1480)
- Vedantam R, Lenke LG, Keeney JA et al (1998) Comparison of standing sagittal spinal alignment in asymptomatic adolescents and adults. *Spine* 23(2):211–215
- Legaye J, Duval-Beaupère G, Hecquet J et al (1998) Pelvic incidence: a fundamental pelvic parameter for three-dimensional regulation of spinal sagittal curves. *Eur Spine J* 7(2):99–103
- Korovessis PG, Stamatakis MV, Baikousis AG (1998) Reciprocal angulation of vertebral bodies in the sagittal plane in an asymptomatic Greek population. *Spine* 23(6):700–704 (discussion 704–5)
- Hammerberg EM, Wood KB (2003) Sagittal profile of the elderly. *J Spinal Disord Tech* 16(1):44–50
- Vialle R, Levassor N, Rillardon L et al (2005) Radiographic analysis of the sagittal alignment and balance of the spine in asymptomatic subjects. *J Bone Joint Surg Am* 87(2):260–267
- Boulay C, Tardieu C, Hecquet J et al (2006) Sagittal alignment of spine and pelvis regulated by pelvic incidence: standard values and prediction of lordosis. *Eur Spine J* 15(4):415–422 Epub 2005 Sep 23
- Roussouly P, Gollogly S, Nosedà O et al (2006) The vertical projection of the sum of the ground reactive forces of a standing patient is not the same as the C7 plumb line: a radiographic study of the sagittal alignment of 153 asymptomatic volunteers. *Spine* 31(11):E320–E325
- Schwab F, Lafage V, Boyce R et al (2006) Gravity line analysis in adult volunteers: age-related correlation with spinal parameters, pelvic parameters, and foot position. *Spine* 31(25):E959–E967
- Kuntz C 4th, Levin LS, Ondra SL et al (2007) Neutral upright sagittal spinal alignment from the occiput to the pelvis in asymptomatic adults: a review and resynthesis of the literature. *J Neurosurg Spine* 6(2):104–112
- Lafage V, Schwab F, Skalli W, Hawkinson N, Gagey PM, Ondra S, Farcy JP (2008) Standing balance and sagittal plane spinal

- deformity: analysis of spinopelvic and gravity line parameters. *Spine* 33(14):1572–1578
19. Mac-Thiong JM, Roussouly P, Berthonnaud E et al (2011) Age- and sex-related variations in sagittal sacropelvic morphology and balance in asymptomatic adults. *Eur Spine J* 20(Suppl 5):572–577
20. Miyakoshi N, Hongo M, Kobayashi T, Abe T, Abe E, Shimada Y (2015) Improvement of spinal alignment and quality of life after corrective surgery for spinal kyphosis in patients with osteoporosis: a comparative study with non-operated patients. *Osteoporos Int* 26(11):2657–2664
21. Hasegawa K, Okamoto M, Hatsushikano S, Shimoda H, Ono M, Watanabe K. (2016) Normative values of spino-pelvic sagittal alignment, balance, age, and health-related quality of life in a cohort of healthy adult subjects. *Eur Spine J*. [Epub ahead of print]
22. Dubousset J (1994) Three-dimensional analysis of the scoliotic deformity. In: Weinstein SL (ed) *The pediatric spine: principles and practice*. Raven Press, New York, pp 480–481
23. Barrey C, Roussouly P, Le Huec JC et al (2013) Compensatory mechanisms contributing to keep the sagittal balance of the spine. *Eur Spine J* 22(Suppl 6):S834–S841

**Itaru Yugué, Seiji Okada, Muneaki
Masuda, Takayoshi Ueta, Takeshi Maeda
& Keiichiro Shiba**

DOI 10.1007/s00586-015-4185-6



Your article is protected by copyright and all rights are held exclusively by Springer-Verlag Berlin Heidelberg. This e-offprint is for personal use only and shall not be self-archived in electronic repositories. If you wish to self-archive your article, please use the accepted manuscript version for posting on your own website. You may further deposit the accepted manuscript version in any repository, provided it is only made publicly available 12 months after official publication or later and provided acknowledgement is given to the original source of publication and a link is inserted to the published article on Springer's website. The link must be accompanied by the following text: "The final publication is available at link.springer.com".

Risk factors for adjacent segment pathology requiring additional surgery after single-level spinal fusion: impact of pre-existing spinal stenosis demonstrated by preoperative myelography

Itaru Yugué¹ · Seiji Okada² · Muneaki Masuda¹ · Takayoshi Ueta¹ · Takeshi Maeda¹ · Keiichiro Shiba¹

Received: 5 June 2015 / Revised: 5 August 2015 / Accepted: 6 August 2015 / Published online: 14 August 2015
© Springer-Verlag Berlin Heidelberg 2015

Abstract

Purpose We determined the incidence of and risk factors for clinical adjacent segment pathology (C-ASP) requiring additional surgeries among patients previously treated with one-segment lumbar decompression and fusion surgery.

Methods We retrospectively analysed 161 consecutive patients who underwent one-segment lumbar decompression and fusion surgery for L4 degenerative spondylolisthesis. Patient age, sex, body mass index (BMI), facet orientation and tropism, laminar inclination angle, spinal canal stenosis ratio [on myelography and magnetic resonance imaging (MRI)], preoperative adjacent segment instability, arthrodesis type, pseudarthrosis, segmental lordosis at L4–5, and the present L4 slip were evaluated by a log-rank test using the Kaplan–Meier method. A multivariate Cox proportional-hazards model was used to analyse all factors found significant by the log-rank test.

Results Of 161 patients, 22 patients (13.7 %) had additional surgeries at cranial segments located adjacent to the index surgery's location. Pre-existing canal stenosis ≥ 47 % at the adjacent segment on myelography, greater facet tropism, and high BMI were significant risk factors for C-ASP. The estimated incidences at 10 years postoperatively for each of these factors were 51.3, 39.6, and

32.5 %, and the risks for C-ASP were 4.9, 3.7, and, 3.1 times higher than their counterparts, respectively. Notably, spinal canal stenosis on myelography, but not on MRI, was found to be a significant risk factor for C-ASP (log-rank test $P < 0.0001$ and 0.299, respectively).

Conclusions Pre-existing spinal stenosis, greater facet tropism, and higher BMI significantly increased C-ASP risk. Myelography is a more accurate method for detecting latent spinal canal stenosis as a risk factor for C-ASP.

Keywords Degenerative spondylolisthesis · Adjacent segment pathology · Pre-existing spinal stenosis · Body mass index · Facet tropism

Introduction

During the past few decades, spinal arthrodesis has become a common treatment component for a variety of spinal disorders. However, it alters the biomechanical and kinematic properties of the lumbar spine [1, 2]. Pathological development at mobile segments above or below the site of spinal fusion is known as adjacent segment pathology (ASP). ASP is considered a potential late complication of spinal arthrodesis that requires further surgical treatment. The clinical failure rate of adjacent segments at 5 years after the index spinal fusion surgery has been reported to range from 3 to 32.3 % [3–7].

Several risk factors for ASP have been reported, such as age [4, 5, 7], sex [4], multilevel arthrodesis [3–5], sagittal imbalance [8], the type of arthrodesis [7], facet tropism [9], and laminar inclination [9]. However, few studies have focused on asymptomatic pre-existing spinal stenosis as a risk factor for clinical ASP (C-ASP) that requires additional surgery at an adjacent segment [10]. In fact, when

The manuscript does not contain information about medical device(s)/drug(s).

✉ Itaru Yugué
iyugue@orange.ocn.ne.jp

¹ Department of Orthopaedic Surgery, Japan Labour Health and Welfare Organization Spinal Injuries Center, 550-4 Igisu, Iizuka, Fukuoka, Japan

² Department of Orthopaedic Surgery, Kyushu University, Fukuoka, Japan

patients demonstrate asymptomatic spinal stenosis adjacent to the fusion segment, there is often controversy as to whether the segment should be included within the surgical site or not.

This study analysed the preoperative prognostic risk factors for C-ASP, and we calculated the survival times of the patients with significant risk factors.

Materials and methods

From January 2000 to December 2006, 204 L4 degenerative spondylolisthesis (DS) patients with radicular pain and/or neurological claudication after unsuccessful conservative treatment underwent either instrumented posterolateral fusion (PLF) or posterior lumbar inter-body fusion (PLIF) at the single level of L4–5. All surgeries were performed using the same procedures at a single institution. Patients with an acute fracture, dislocation, or malignancy were excluded. Informed consent was obtained from all patients. Medical records of all patients were reviewed, and this study was approved by our local ethics committee. Forty-three patients were excluded because of a short follow-up (<2 years) or a lack of preoperative magnetic resonance imaging (MRI) and/or myelography data. The remaining 161 patients with a follow-up period of longer than 2 years were finally selected.

PLF had been performed in 137 patients (85 %) and PLIF in 24 patients (15 %). In all patients undergoing PLF, autogenous cancellous iliac bone was used as a graft. PLIF was performed using a rectangular ceramic cage with morselised local bone from neural decompression in all patients. When patients had spinal stenosis on myelography or MRI at the L3–4 segment, as well as neurological findings (including the presence of patellar tendon reflex and no sensory and motor disturbance associated with the L4 nerve root) and negative findings of L4 nerve root infiltration, we did not include the L3–4 segment in the operation site.

Radiographic evaluation

In all patients, computed tomography (CT), myelography, and MRI were performed within 2 weeks before the index fusion surgery. In this series, no patients required additional surgery at the L5–S1 segment during follow-up, so radiographic evaluations were performed at the L3–4 and L4–5 segments. Standard biplanar anteroposterior, lateral radiography with the lumbosacral spine in neutral, flexion, and extension positions was performed preoperatively, at 24 months after surgery, and at the final follow-up.

The anteroposterior vertebral slip and intervertebral disc angle were measured on lateral radiographs of the L3–4 and L4–5 taken in the neutral, flexion, and extension

positions. To minimise the errors due to different magnifications, the vertebral slip was expressed as a percentage of the caudal vertebral body width (% slip). The ranges of motion (ROM) of the L3–4 and L4–5 segments were defined as the sum of the intervertebral disc angles in the flexion/extension view (Fig. 1). Pseudarthrosis was present if there was no continuity in the PLF fusion mass between the cephalad and caudad transverse processes, no continuity between graft bone and vertebra in PLIF fusion, or if lateral flexion–extension radiographs demonstrated >2° of angular motion or >2 mm of sagittal motion at L4–5 [11].

The criteria for adjacent segment instability were well-defined spondylolisthesis or dynamic instability with slip-page >4 mm and/or an ROM >10° [12]. The laminar inclination angle at L3 was measured as previously described [9] on lateral radiographs (Fig. 2a). Facet orientation and tropism were determined by CT images that were coplanar with the disc and transected the facet joints, as described previously [9]. The sum of the right and left facet angles and the difference between the right and left facet angles were defined as the facet orientation and tropism, respectively (Fig. 2b).

Myelography measurements

After lumbar puncture and injection of radiographic contrast material into the dural sac under fluoroscopic guidance, the physician moved the patient's lower back to maximum flexion and extension in the left lateral decubitus position and obtained lateral radiographs in the neutral, flexion, and extension positions under fluoroscopy. The narrowest anteroposterior dural sac diameter at L3–4 was measured on lateral myelography in the neutral, flexion, and extension positions and on the sagittal view of T2-weighted MRI. The dural sac diameter at the midpoint of the L2 vertebral body was also measured. The spinal canal stenosis ratio (SCSR) was calculated as $x/y \times 100$ (Fig. 3).

All measurements were performed twice by two independent observers blinded to the patient name and clinical findings using an electronic digitiser (MicroAnalyzer; Japan Poladigital Corp., Tokyo, Japan) with an accuracy of 0.01 mm: measurements were averaged. The inter-observer correlation of all measurement was evaluated by the Pearson's correlation coefficient test. The kappa statistic was used to assess inter-observer agreement of pseudarthrosis and preoperative instability at L3–4.

Statistical analysis

The final follow-up examination was defined as the last visit. In patients undergoing re-operation at L3–4, the survival period was defined as the interval from the index operation to the second operation due to C-ASP. C-ASP

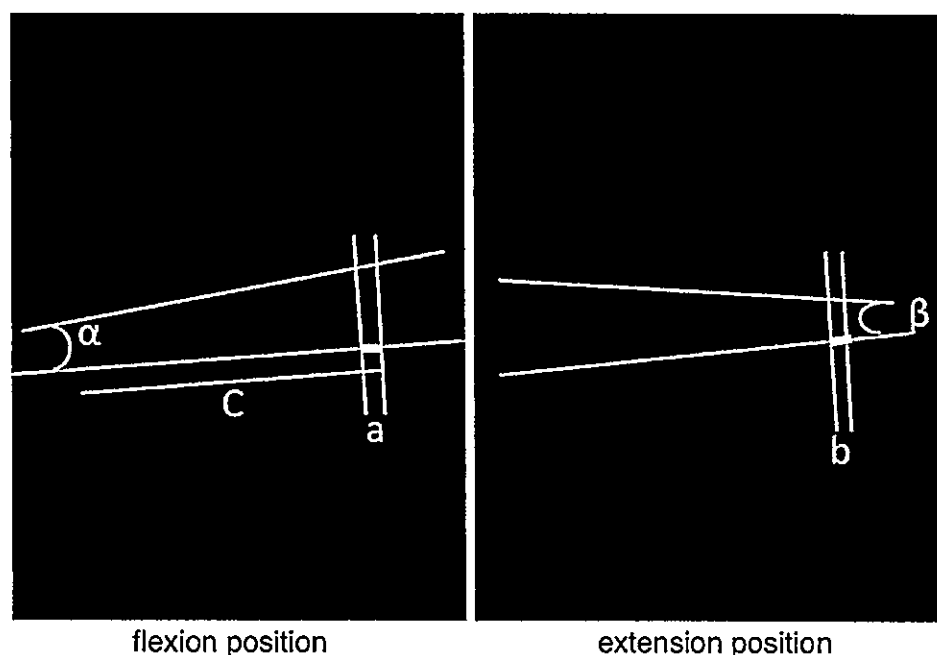


Fig. 1 Plain radiography measurement. *a* Anterior slip in the flexion position, *b* posterior slip in the extension position, *c* vertebral body width. The total percent slip is $(a + b)/c \times 100$. α Intervertebral disc

angle in flexion position, β intervertebral disc angle in the extension position. The range of motion is $\alpha + \beta$ in degrees

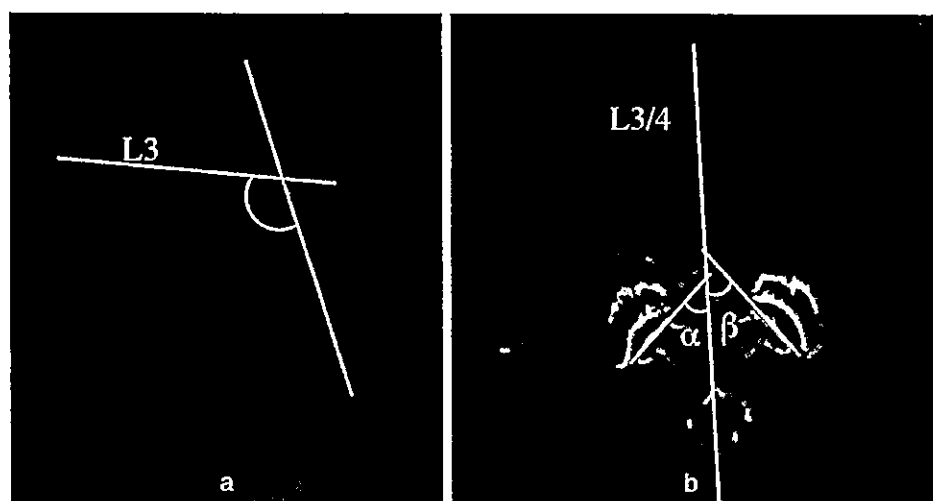


Fig. 2 *a* The laminar inclination angle at L3 was defined as the angle formed by a *straight line* connecting the base of the superior facet with the base of the inferior facet, and a *straight line* connecting the midpoints of the anterior and posterior L3 vertebral cortices on lateral radiographs. *b* Facet orientation and tropism were determined by

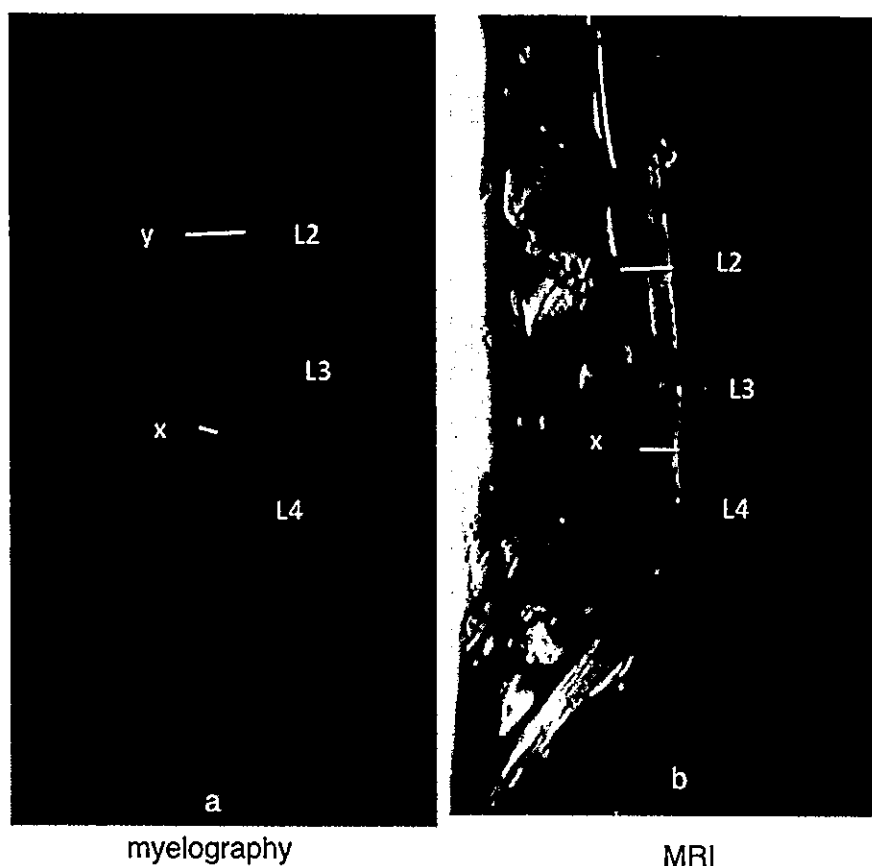
computed tomography images that were coplanar with the disc and transected the facet joints. The sum of the right and left facet angles and the difference between the right and left facet angles were defined as the facet orientation and tropism, respectively

was defined as a condition where an additional surgery at L3–4 was required to treat symptomatic neurological deterioration.

The following prognostic risk factors were examined: age, sex, body mass index (BMI), facet orientation, facet tropism, laminar inclination angle, SCSR by myelography

and MRI, preoperative adjacent segment instability, type of fusion, presence of pseudarthrosis, segmental lordosis at L4–5, and the %slip of L4–5 after 2 years postoperatively. Continuous variables were dichotomised to increase the statistical power using the Youden index from the receiver operating characteristic curve (ROC).

Fig. 3 The narrowest anteroposterior dural sac diameter at L3–4 (x) was measured on lateral myelographs taken in the extension position (a) and on MRI (b) in the same patient. The dural sac diameter at the midpoint of the L2 vertebral body (y) was also measured. The spinal canal stenosis ratio (SCSR) was calculated as $x/y \times 100$



A log-rank test was used for univariate analyses using the Kaplan–Meier method, and survival curves for all patients with significant risk factors were constructed to calculate the survival time. A multivariate Cox proportional-hazards model was used to assess all factors demonstrated to be significant by the log-rank test to adjust for confounding factors.

Statistical analyses were performed using the JMP 10 statistical software package (SAS Institute Inc. Cary, NC). A value of $P < 0.05$ was considered to be statistically significant.

Results

There were 56 males and 105 females. The mean age at index surgery was 65.4 years (range 40–87 years). The average follow-up period was 77.3 months (range 24–183 months). The follow-up rate was 78.9 %. Among the 161 patients, 22 (13.7 %) underwent subsequent procedures at cranial segments adjacent to the L4–5 segment; five patients underwent decompression surgery with arthrodesis and 17 underwent decompression surgery alone. After the additional surgery, all patients show

improved neurological symptoms. The mean duration between the index surgery and the additional surgery was 75.9 months (range 24–141 months).

The inter-observer correlation is shown in Table 1. The kappa coefficient for pseudarthrosis rated between observers was 0.82 ($P < 0.0001$) and that of preoperative instability at L3–4 was 0.89 ($P < 0.0001$).

Patients with a BMI $\geq 25 \text{ kg/m}^2$ had a significantly lower survival rate than their counterparts in a univariate analysis (log-rank test: $P = 0.0497$). The incidence of C-ASP in patients with a BMI $\geq 25 \text{ kg/m}^2$ was estimated to be 32.5 % at 10 years. Conversely, the incidence of C-ASP in patients with a BMI $< 25 \text{ kg/m}^2$ was lower, at 21.1 % at 10 years. The median survival time for patients with a BMI $\geq 25 \text{ kg/m}^2$ was 141 months (Fig. 4).

Patients with facet tropism $\geq 11^\circ$ demonstrated a lower survival rate than their counterparts (log-rank test: $P = 0.0178$). The incidence of C-ASP among patients with facet tropism $\geq 11^\circ$ was 39.6 %, while for facet tropism $< 11^\circ$ it was 19.4 % at 10 years after the initial operation (Fig. 5).

Regarding SCSR, patients with an SCSR $\geq 47\%$ on myelography in the extension position showed a significantly lower survival rate than their counterparts

Table 1 Inter-observer correlations for study parameters

Parameters	P value	Pearson correlation coefficient
Facet orientation	<0.001	0.91
Facet tropism	<0.001	0.92
Laminar inclination angle	<0.001	0.86
Segmental lordosis at L4–5	<0.001	0.87
%Slip of L4	<0.001	0.89
SCSR of MRI	<0.001	0.91
SCSR of myelography (neutral position)	<0.001	0.88
SCSR of myelography(flexion position)	<0.001	0.87
SCSR of myelography(extension position)	<0.001	0.89

Significance was set at $P < 0.05$

SCSR spinal canal stenosis ratio, MRI magnetic resonance imaging

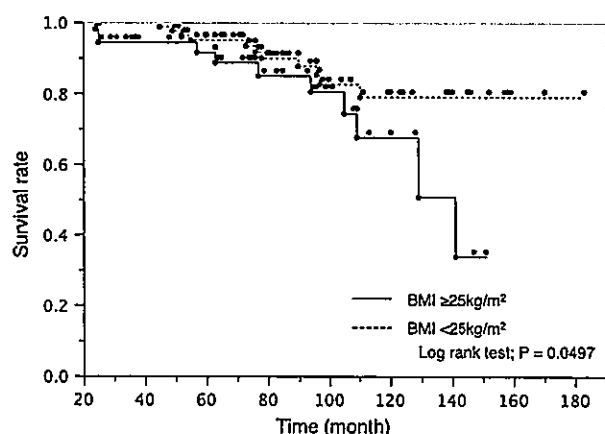


Fig. 4 The Kaplan–Meier survivorship curve of patients with BMI ≥ 25 kg/m² versus those with BMI < 25 kg/m²

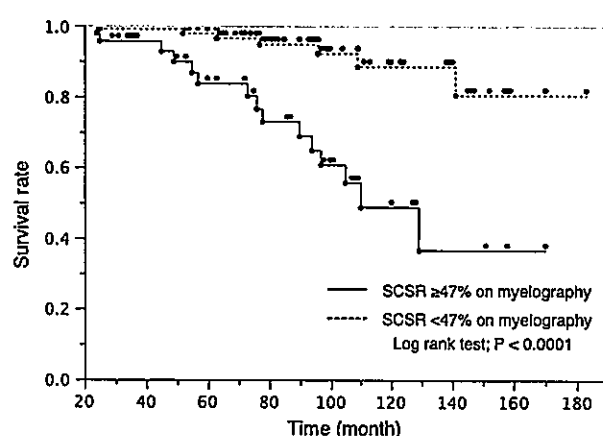


Fig. 6 The Kaplan–Meier survivorship curve of patients with an SCSR ≥ 47 % versus those with an SCSR < 47 % on myelography. SCSR spinal canal stenosis ratio

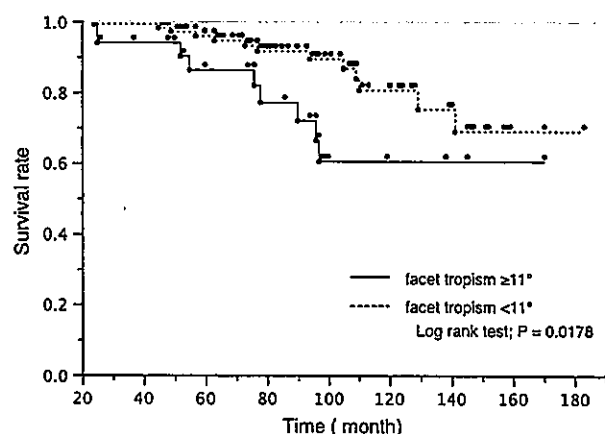


Fig. 5 The Kaplan–Meier survivorship curve of patients with facet tropism $\geq 11^\circ$ versus those with facet tropism $< 11^\circ$

($P < 0.0001$). In these patients, the prevalence of C-ASP requiring reoperation was 51.3 % at 10 years, whereas it was 11.4 % in patients with an SCSR < 47 %. The median

survival time for patients with an SCSR ≥ 47 % was 110 months (Fig. 6).

Interestingly, SCSR determined by MRI was not a significant risk factor (log-rank test: $P = 0.2990$). Since a factor with a higher discrimination ability makes an ROC curve closer to the top left corner, the area under the ROC curve (AUC) is used to indicate the sensitivity and specificity of each factor. We compared the AUC values of MRI and myelography in the extension positions. In this analysis, the AUC of the SCSR determined by myelography was significantly higher than that of the SCSR determined by MRI (Fig. 7). In fact, 13.2 % of patients who exhibited SCSR on MRI < 50 % had an SCSR ≥ 50 % on myelography in the extension position.

Other potential risk factors, such as age, sex, facet orientation, laminar inclination angle, preoperative adjacent segment instability, type of fusion, pseudarthrosis, segmental lordosis, the %slip, and SCSR on myelography in the neutral and flexion positions, were not statistically significant (Table 2). A multivariate Cox proportional-

Fig. 7 Receiver operating characteristic curves of the SCSR on myelography at extension and the SCSR on MRI. *AUC* area under the ROC curve, *SCSR* spinal canal stenosis ratio

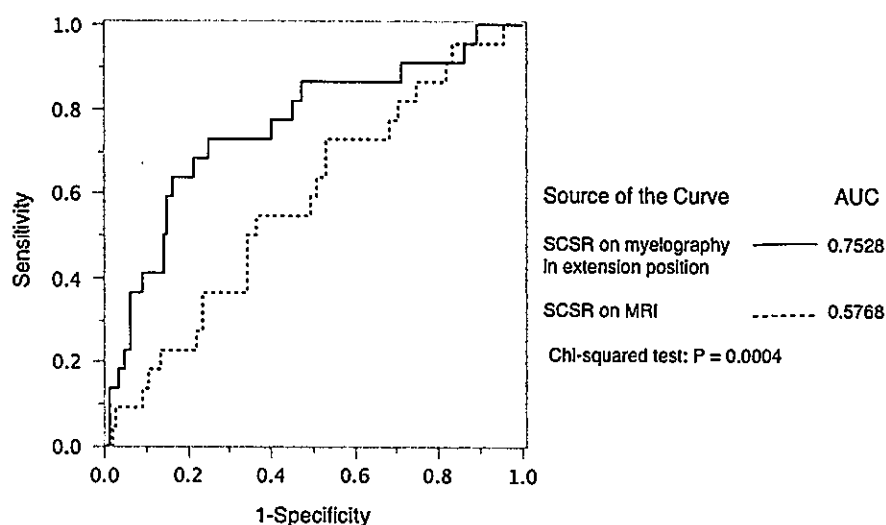


Table 2 Potential risk factors for clinical adjacent segment pathology after lumbar spinal fusion based on the log-rank test

Risk factor	<i>P</i> value
Sex (female)	0.3530
Age ≥ 68 years	0.3989
BMI ≥ 25 kg/m ²	0.0497*
Facet orientation $\geq 65^\circ$	0.2272
Facet tropism $\geq 11^\circ$	0.0178*
Laminar inclination $\geq 120^\circ$	0.6325
SCSR on MRI $\geq 35\%$	0.2990
SCSR on myelography in extension $\geq 47\%$	$<0.0001^*$
SCSR on myelography in neutral $\geq 33\%$	0.0757
SCSR on myelography in flexion $\geq 18\%$	0.1467
Preoperative instability	0.6902
Type of fusion	0.4737
Pseudarthrosis	0.2086
Segmental lordosis at L4–5 $\geq 6.3^\circ$	0.2278
%Slip of L4 $\geq 13.4\%$	0.1465

Significance was set at $P < 0.05^*$

BMI body mass index, *SCSR* spinal canal stenosis ratio, *MRI* magnetic resonance imaging

hazards model revealed a BMI ≥ 25 kg/m², facet tropism $\geq 11^\circ$, and SCSR $\geq 47\%$ on myelography to be significant risk factors, and patients with these factors had 3.1-, 3.7-,

and 4.9-fold higher risks of adjacent segment reoperation than their counterparts, respectively (Table 3).

Discussion

The definition of C-ASP has often been reported as adjacent segment pathology, manifesting radiculopathy, neurogenic intermittent claudication, back pain, or a combination of any of these [13], and the need for additional surgeries [3–5, 8–10] on the index fusion segments. Park et al. [3] reported the incidence of C-ASP to range from 5.2 to 18.5 %. The term ‘degeneration’ itself suggests a time-dependent phenomenon. Therefore, the survival function estimated by the Kaplan–Meier method and the multivariate Cox regression model are good ways to analyse the development of ASP as a late complication of spinal arthrodesis.

Regardless of the use of spinal arthrodesis, the clinical course of patients with severe spinal stenosis often deteriorates over time during conservative treatments [14]. This indicates that pre-existing spinal stenosis in itself may be a significant risk factor for C-ASP. Cho et al. [10] reported a significant relationship between pre-existing spinal stenosis and C-ASP. However, they did not indicate a cutoff point for spinal stenosis that may increase the likelihood of C-ASP. In the current study, patients with an SCSR $\geq 47\%$

Table 3 Risk factors for clinical adjacent segment pathology after lumbar spinal fusion

Risk factor	<i>P</i> value	Hazard ratio	95 % confidence interval
BMI ≥ 25 kg/m ²	0.0212*	3.12	1.18–8.49
Facet tropism $\geq 11^\circ$	0.0114*	3.74	1.35–10.30
SCSR in myelography $\geq 47\%$	0.0003*	4.87	2.05–12.78

Significance was set at $P < 0.05^*$

BMI body mass index, *SCSR* spinal canal stenosis ratio

on myelography in the extension position exhibited a 4.87-fold higher risk of adjacent segment reoperation than their counterparts. Interestingly, spinal stenosis demonstrated by MRI was not a significant factor. We attempted to change the cutoff point for SCSR on MRI from 35 to 60 %; however, the MRI findings were not a significant factor. Moreover, the AUC of SCSR on myelography in the extension position (0.7528) was significantly larger than that on MRI (0.5768) (Chi squared; $P = 0.0004$). These results suggest that myelography has a significantly higher sensitivity and specificity to detect not only latent spinal canal stenosis, but also the risk of ASP requiring additional surgery.

While these results indicate that pre-existing severe stenosis can be a significant risk factor for C-ASP, this does not lead directly to a recommendation for performing laminectomy during the index surgery, since performing laminectomy adjacent to a fusion segment demonstrated a significant association with ASP [5, 15–17]. Imagama et al. [15] recommended that the adjacent segment with asymptomatic spinal stenosis should not be subjected to a concomitant decompression from the viewpoint of preventing ASP. We therefore recommend that surgeons should have thorough discussions with patients to determine whether a concomitant operation at adjacent segments with asymptomatic stenosis should be performed.

Facet tropism is defined as asymmetry in the facet joint that causes an abnormal rotation of the spinal segment, which increases the mechanical stress on the disc and could lead to lumbar degeneration or disc herniation [18, 19]. Several studies have reported greater facet tropism to have a significant relationship with C-ASP [9]. In the current study, patients with facet tropism $\geq 11^\circ$ had a 3.74-fold higher risk of adjacent segment reoperation compared to their counterparts. We hypothesised that facet tropism may affect the rotational stability, which accelerates the thickening of the ligamentum flavum, thus resulting in spinal canal stenosis. However, some authors have reported no association between facet tropism and the occurrence of C-ASP [10]. Further studies are required to clarify this issue.

It remains controversial as to whether an association exists between BMI and ASP. Some studies reported no association between BMI and radiographic ASP [20]; however, Cho et al. [10] reported BMI to be a significant risk factor for C-ASP, and Liuke et al. [21] reported that a BMI $\geq 25 \text{ kg/m}^2$ increased the risk of lumbar disc degeneration on MRI. It is assumed that being overweight might cause disc degeneration [22], resulting in earlier ASP over the long term. In this series, a BMI $\geq 25 \text{ kg/m}^2$ was identified as a significant risk factor for C-ASP, and patients with this factor had a 3.12-fold higher risk of needing adjacent segment reoperation than their

counterparts. Patients with high BMI appear to have a higher risk of C-ASP; however, a large prospective study is needed to confirm this finding.

In this study, other factors were not significant risk factors for C-ASP. The association between the conditions of fused segments and the occurrence of ASP also remains controversial. Since almost all past studies were retrospective analyses that contained potential bias, a randomised prospective study will be necessary to resolve these issues.

There are several possible limitations associated with this study. First, it was a retrospective study. Second, the predictors derived were not prospectively validated in an independent population. Third, the sample size was relatively small. Finally, whole spinal radiographs were not routinely taken for DS patients who underwent one-segment spinal fusion and decompression and, therefore, a whole spinal radiographic analysis was not possible in this study. Despite these limitations, the factors identified in this study may assist both surgeons and patients when making decisions about whether or not to include an adjacent segment at the time of index fusion surgery.

In conclusion, a BMI $\geq 25 \text{ kg/m}^2$, facet tropism $\geq 11^\circ$, and pre-existing stenosis $\geq 47\%$ demonstrated on myelography in the extension position were found to be important risk factors for C-ASP requiring a second operation. Careful consideration of the type and extent of surgery is therefore necessary when these risk factors are present.

Compliance with ethical standards

Conflict of interest No funds were received in support of this work. No benefits in any form have been or will be received from a commercial party related directly or indirectly to the subject of this manuscript.

Ethical standards The study was approved by the local ethics committee.

References

1. Axelsson P, Johnsson R, Strömqvist B (1997) The spondylolytic vertebra and its adjacent segment. Mobility measured before and after posterolateral fusion. *Spine (Phila Pa 1976)* 22(4):414–417
2. Bastian L, Lange U, Knop C et al (2001) Evaluation of the mobility of adjacent segments after posterior thoracolumbar fixation: a biomechanical study. *Eur Spine J* 10(4):295–300
3. Ghiselli G, Wang JC, Bhatia NN et al (2004) Adjacent segment degeneration in the lumbar spine. *J Bone Joint Surg Am* 86-A(7):1497–1503
4. Ahn DK, Park HS, Choi DJ et al (2010) Survival and prognostic analysis of adjacent segments after spinal fusion. *Clin Orthop Surg* 2(3):140–147
5. Sears WR, Sergides IG, Kazemi N et al (2011) Incidence and prevalence of surgery at segments adjacent to a previous posterior lumbar arthrodesis. *Spine J* 11(1):11–20

6. Celestre PC, Montgomery SR, Kupperman AI et al (2014) Lumbar clinical adjacent segment pathology: predilection for proximal levels. *Spine (Phila Pa 1976)* 39(2):172–176
7. Lee JC, Kim Y, Soh JW, Shin BJ (2014) Risk factors of adjacent segment disease requiring surgery after lumbar spinal fusion: comparison of posterior lumbar interbody fusion and posterolateral fusion. *Spine (Phila Pa 1976)* 39(5):E339–E445
8. Kumar MN, Baklanov A, Chopin D (2001) Correlation between sagittal plane changes and adjacent segment degeneration following lumbar spine fusion. *Eur Spine J* 10(4):314–319
9. Okuda S, Oda T, Miyauchi A et al (2008) Lamina horizontalization and facet tropism as the risk factors for adjacent segment degeneration after PLIF. *Spine (Phila Pa 1976)* 33(25):2754–2758
10. Cho TK, Lim JH, Kim SH et al (2013) Preoperative Predictable Factors for the Occurrence of Adjacent Segment Degeneration Requiring Second Operation after Spinal Fusion at Isolated L4–L5 Level. *J Neurol Surg A Cent Eur Neurosurg* [Epub ahead of print]
11. Kornblum MB, Fischgrund JS, Herkowitz HN et al (2004) Degenerative lumbar spondylolisthesis with spinal stenosis: a prospective long-term study comparing fusion and pseudarthrosis. *Spine (Phila Pa 1976)* 29(7):726–733
12. Chen WJ, Lai PL, Niu CC et al (2001) Surgical treatment of adjacent instability after lumbar spine fusion. *Spine (Phila Pa 1976)* 26(22):E519–E524
13. Liao JC, Chen WJ, Chen LH et al (2011) Surgical outcomes of degenerative spondylolisthesis with L5–S1 disc degeneration: comparison between lumbar floating fusion and lumbosacral fusion at a minimum 5-year follow-up. *Spine (Phila Pa 1976)* 36(19):1600–1607
14. Minamide A, Yoshida M, Maio K (2013) The natural clinical course of lumbar spinal stenosis: a longitudinal cohort study over a minimum of 10 years. *J Orthop Sci* 18(5):693–698
15. Imagama S, Kawakami N, Kanemura T et al (2013) Radiographic adjacent segment degeneration at five years after L4/5 posterior lumbar interbody fusion with pedicle screw instrumentation: evaluation by computed tomography and annual screening with magnetic resonance imaging. *J Spinal Disord Tech* [Epub ahead of print]
16. Miyagi M, Ikeda O, Ohtori S et al (2013) Additional decompression at adjacent segments leads to adjacent segment degeneration after PLIF. *Eur Spine J* 22(8):1877–1883
17. Lai PL, Chen LH, Niu CC et al (2004) Relation between laminectomy and development of adjacent segment instability after lumbar fusion with pedicle fixation. *Spine (Phila Pa 1976)* 29(22):2527–2532
18. Noren R, Trafimow J, Andersson GB et al (1991) The role of facet joint tropism and facet angle in disc degeneration. *Spine (Phila Pa 1976)* 16(5):530–532
19. Karacan I, Aydin T, Sahin Z et al (2004) Facet angles in lumbar disc herniation: their relation to anthropometric features. *Spine (Phila Pa 1976)* 29(10):1132–1136
20. Ha KY, Son JM, Im JH et al (2013) Risk factors for adjacent segment degeneration after surgical correction of degenerative lumbar scoliosis. *Indian J Orthop* 47(4):346–351
21. Liuke M, Solovieva S, Lamminen A et al (2005) Disc degeneration of the lumbar spine in relation to overweight. *Int J Obes (Lond)* 29(8):903–908
22. Weiler C, Lopez-Ramos M, Mayer HM et al (2011) Histological analysis of surgical lumbar intervertebral disc tissue provides evidence for an association between disc degeneration and increased body mass index. *BMC Res Notes* 4:497

CLINICAL CASE SERIES

A Study of Risk Factors for Tracheostomy in Patients With a Cervical Spinal Cord Injury

Jun Tanaka, MD,* Itaru Yugue, MD, PhD,[†] Keiichiro Shiba, MD, PhD,[†] Akira Maeyama, MD, PhD,* and Masatoshi Naito, MD, PhD*

Study Design. A retrospective, consecutive case series.

Objective. To determine the risk factors for a tracheostomy in patients with a cervical spinal cord injury.

Summary and Background Data. Respiratory status cannot be stabilized in patients with a cervical spinal cord injury (CSCI) for various reasons, so a number of these patients require long-term respiratory care and a tracheostomy. Various studies have described risk factors for a tracheostomy, but none have indicated a relationship between imaging assessment and the need for a tracheostomy. The current study used imaging assessment and other approaches to assess and examine the risk factors for a tracheostomy in patients with a CSCI.

Methods. Subjects were 199 patients who were treated at the Spinal Injuries Center within 72 hours of a CSCI over 8-year period. Risk factors for a tracheostomy were retrospectively studied. Patients were assessed in terms of 10 items: age, sex, the presence of a vertebral fracture or dislocation, ASIA Impairment Scale, the neurological level of injury (NLI), PaO₂, PaCO₂, the level of injury on magnetic resonance imaging (MRI), the presence of hematoma-like changes (a hypointense core surrounded by a hyperintense rim in T2-weighted images) on MRI, and the Injury Severity Score.

Items were analyzed multivariate logistic regression, and $P < 0.05$ was considered to indicate a significant difference.

Results. Twenty-three of the 199 patients required a tracheostomy, accounting for 11.6% of patients with a CSCI. Univariate analyses of the risk factors for tracheostomy revealed significant differences for six items: age, Injury Severity Score, presence of

fracture or dislocation, ASIA Impairment Scale A, NLI C4 or above, and MRI scans revealing hematoma-like changes. Multivariate logistic regression analyses revealed significant differences in terms of two items: NLI C4 or above and MRI scans revealing hematoma-like changes. Thirty patients had both an NLI C4 or above and MRI scans revealing hematoma-like changes. Of these, 17 (56.7%) required a tracheostomy.

Conclusion. Patients with an NLI C4 or above and MRI scans revealing hematoma-like changes were likely to require a tracheostomy. An early tracheostomy should be considered for patients with both of these characteristics.

Key words: arterial blood gases, ASIA impairment scale, cervical spinal cord injury, hematoma-like changes on magnetic resonance imaging, imaging assessment, injury severity score, neurological level of injury, risk factors, tracheostomy, vertebral fracture or dislocation.

Level of Evidence: 3

Spine 2016;41:764–771

Respiratory status cannot be stabilized in patients with a cervical spinal cord injury (CSCI) for various reasons, so a number of these patients require long-term respiratory care and a tracheostomy. Numerous studies have reported that respiratory dysfunction is closely associated with morbidity and mortality in CSCI,^{1–3} and respiratory dysfunction leads to massive financial expenses.³ The cause of death for patients with a CSCI is often a urinary complication or a respiratory complication.^{4,5} A recent study from abroad has reported that respiratory complications represent the leading cause of death in patients with a CSCI,⁵ and the same is true in Japan.⁴

In the acute phase of CSCI, spinal shock can have an effect and the patient's respiratory status might be unstable, so temporary ventilator management is often required.^{6–16} If the patient's respiratory status fails to improve with temporary ventilator management and long-term intubation is required, a tracheostomy is often performed. Performing a tracheostomy early on is known to be useful in reducing respiratory complications, as various studies have reported^{6,9,16–18}; however, unnecessary intubation and unnecessary tracheostomies are known to increase

From the *Faculty of Medicine, Department of Orthopaedic Surgery, Fukuoka University; and [†]Department of Orthopaedic Surgery, Spinal Injuries Center, Iizuka city, Fukuoka, Japan.

Acknowledgment date: July 10, 2015. First revision date: October 5, 2015. Acceptance date: October 19, 2015.

The manuscript submitted does not contain information about medical device(s)/drug(s).

No funds were received in support of this work.

No relevant financial activities outside the submitted work.

Address correspondence and reprint requests to Jun Tanaka, MD, Faculty of Medicine, Department of Orthopaedic Surgery, Fukuoka University, 7–45–1 Nanakuma, Jonan-ku, Fukuoka 814–0180, Japan; E-mail: jt0120jt@gmail.com

DOI: 10.1097/BRS.0000000000001317

764 www.spinejournal.com

May 2016

Copyright © 2016 Wolters Kluwer Health, Inc. Unauthorized reproduction of this article is prohibited.

the risk of complications in both the short and long term.⁹ Exaggerating the usefulness of an early tracheostomy can result in unnecessary tracheal intubation or an unnecessary tracheostomy. Thus, predicting true risk factors for intubation or a tracheostomy in patients with a CSCI is important.

Various studies have described risk factors for a tracheostomy in patients with a CSCI. These include advanced age,^{7,12} complete paralysis,^{1,6–8,14,17,19–22,23} a high level of neurological paralysis,^{6,12,14,21} the patient's general condition prior to the injury and a prior history of lung disease,^{1,8,12} a high injury severity score (ISS),^{8,17} a history of smoking,¹⁹ and a low forced vital capacity upon admission.^{7,9}

Nevertheless, no previous studies have indicated a relationship between imaging assessment (radiographs, computed tomography, or magnetic resonance imaging [MRI]) and the need for a tracheostomy. The current study used imaging assessment and other approaches to assess and examine the risk factors for a tracheostomy in patients with a CSCI.

METHODS

Subjects were 199 patients who were treated by the Department of Orthopedic Surgery of the Spinal Injuries Center within 72 hours of a CSCI over 8-year period from January 1, 2005 to December 31, 2012. Patients consisted of 165 males and 34 females ranging in age from 14 to 91 years with a mean age of 61.9 years.

All patients were examined by two or more physicians and a physical therapist upon admission, and patients were assessed neurologically. In addition, the presence or absence of a vertebral fracture or dislocation was assessed using X-ray films or computed tomography scans and the presence or absence of cord damage was assessed using MRI scans in all patients upon admission. Surgery (anterior spine fusion, posterior spine fusion, or anterior spine fusion and posterior spine fusion) was performed on patients with apparent spinal instability. Arterial blood gases were measured in all patients upon admission. If patients had apnea or ventilatory failure prior to initial admission and they needed assistance breathing, a tracheostomy was performed on the day of admission. If, however, a patient's respiratory status gradually worsened after admission, intubation was performed at the discretion of the patient's primary physician in accordance with the patient's respiratory status. When long-term ventilator management was considered necessary, a tracheostomy was performed. This Center has not formulated definite standards for intubation and tracheostomy, although blood gas results of PaO₂ 70 mm Hg or less and PaCO₂ at least 50 mm Hg serve as somewhat of a guide, regardless of whether O₂ is administered.

Medical records, the patient's discharge summary, and imaging findings upon admission and discharge were retrospectively studied.

The following items were studied retrospectively: age, sex, the presence or absence of a vertebral fracture or dislocation at the level of injury, the American Spinal Association (ASIA) Impairment Scale (AIS), the neurological

level of injury (NLI), PaO₂ according to a blood gas analysis, PaCO₂ according to a blood gas analysis, the level of injury on MRI, hematoma-like changes on MRI (presence or absence of a hypointense core surrounded by a hyperintense rim in T2-weighted images), and the ISS.

Statistical analyses were done using the Jump11 statistical software package from SAS Institute Inc. (Cary, NC).

In instances wherein there was no avulsion fracture of the anterior aspect of the vertebral body or a spinous process fracture in conjunction with a hyperextension injury, no bone injury on MRI scans, and no need for surgery due to the lack of spinal instability, bone injury or dislocation was deemed to be absent. In addition, the NLI was the most caudal segment wherein normal motor and sensory function were intact. If hematoma-like changes were present, the level of those changes served as the level of injury on MRI. If those changes were absent, the segment wherein the center of a wider ranging hyperintensity was located on T2-weighted images served as the level of injury on MRI (Figure 1A, B).

Age, PaO₂, PaCO₂, and the ISS were assessed as continuous variables. To increase statistic power, the AIS, the NLI, and the level of injury on MRI were dichotomized as an AIS A or not, an NLI C4 or above or not, and a level of injury on MRI C3/4 or less or not.

RESULTS

A total of 199 patients with a cervical spinal cord injury were treated at this center over 8-year period. Patients consisted of 165 males and 34 females ranging in age from 14 to 91 years with a mean age of 61.9 years. All of the patients had suffered blunt trauma. Sixty patients (30.1%) had a vertebral fracture or dislocation.

The extent of paralysis upon admission was AIS A in 66 patients (33.2%), AIS B in 38 (19.1%), AIS C in 51 (25.6%), and AIS D in 44 (22.1%). The NLI upon admission was C2 in 1 patient (0.5%), C3 in 10 (5.0%), C4 in 90 (45.2%), C5 in 62 (31.2%), C6 in 19 (9.6%), C7 in 6 (3.0%), C8 in 1 (0.5%), and T1 in 10 (5.0%) (Table 1).

All of the patients underwent an MRI upon admission, and hyper-intensity changes on T2-weighted images were noted in all of the patients. The level of injury on MRI was C2/3 in 5 patients (2.5%), C3 in 2 (1.0%), C3/4 in 70 (35.2%), C4 in 4 (2.0%), C4/5 in 49 (24.6%), C5 in 10 (5.0%), C5/6 in 29 (14.6%), C6 in 4 (2.0%), C6/7 in 24 (12.1%), C7 in 1 (0.5%), and C7/T1 in 1 (0.5%). Hematoma-like changes were noted in 46 patients (23.1%) and such changes were not noted in 153 (76.9%) (Table 2).

Twenty-three of the 199 patients required a tracheostomy, accounting for 11.6% of patients with a cervical spinal cord injury. The average time from injury until a tracheostomy was performed was 4.69 days (day of injury–13 days later). Details on the 23 patients who underwent a tracheostomy are indicated below (Table 3).

Eleven patients had a vertebral fracture or dislocation; a bone injury was not noted in 12 patients. Seventeen patients had an AIS A, 4 had AIS B, and 2 had AIS C. The NLI was C2



Figure 1. "Hematoma-like changes" and the level of injury on MRI. A, MRI findings of a hypointense core surrounded by a hyperintense rim in a T2-weighted image. We described these changes as "hematoma-like changes." When these changes were present, the level of the changes served as the level of injury on MRI. This patient's level of injury on MRI was "C3/4". B, When hematoma-like changes were absent, the segment containing the center of a wider-ranging hyperintensity area served as the level of injury on MRI. This patient's level of injury on MRI was "C5/6." MRI indicates magnetic resonance imaging.

in 1 patient, C3 in 5, C4 in 15, C5 in 1 and T1 in 1. The level of injury on MRI scans was at C2/3 in 1 patient, at C3/4 in 9, at C4/5 in 7, at C5/6 in 5, and at C6/7 in 1. Hematoma-like changes were noted on MRI images of 17 patients.

The final outcome (state at final follow-up) was death for one patient and permanent ventilator management for seven. The respiratory status of 15 patients stabilized, and they were weaned from the ventilator.

TABLE 1. Patients Demographic Data

Mean \pm SD	Overall (n = 199)	Tracheostomy (n = 23)	No Tracheostomy (n = 176)
Age (yrs)	61.9 \pm 17.7	69.1 \pm 15.8	60.9 \pm 17.8
Sex			
Male	165 (82.9%)	17 (73.9%)	148 (84.1%)
Female	34 (17.1%)	6 (26.1%)	28 (15.9%)
Fracture or dislocation			
+	60 (30.1%)	11 (43.5%)	49 (27.8%)
-	139 (69.9%)	12 (56.5%)	127 (72.2%)
Initial AIS			
A	66 (33.2%)	17 (73.9%)	49 (27.8%)
B	38 (19.1%)	4 (17.4%)	34 (19.4%)
C	51 (25.6%)	2 (8.7%)	49 (27.8%)
D	44 (22.1%)	0	44 (25.0%)
Initial NLI			
C2	1 (0.5%)	1 (4.4%)	0
C3	10 (5.0%)	5 (21.7%)	5 (2.8%)
C4	90 (45.2%)	15 (65.3%)	75 (42.6%)
C5	62 (31.2%)	1 (4.4%)	61 (34.7%)
C6	19 (9.6%)	0	19 (10.9%)
C7	6 (3.0%)	0	6 (3.4%)
C8	1 (0.5%)	0	1 (0.5%)
T1	10 (5.0%)	1 (4.4%)	9 (5.1%)
Arterial blood gases			
PO ₂ (mm Hg)	91.9 \pm 40.7	104.1 \pm 71.2	90.3 \pm 34.9
PCO ₂ (mm Hg)	38.3 \pm 5.1	39.9 \pm 5.4	38.1 \pm 5.0
ISS	21.4 \pm 10.6	31.7 \pm 18.9	20.1 \pm 8.2

AIS indicates American Spinal Association impairment scale; ISS, injury severity score; NLI, neurological level of injury; SD, standard deviation.

TABLE 2. Level of Spinal Cord Injury and Hematoma-Like Changes on MRI

	Overall (n = 199)	Tracheostomy (n = 23)	No tracheostomy (n = 176)
Level of spinal cord injury on MRI			
C2/3	5 (2.5%)	1 (4.4%)	4 (2.3%)
C3	2 (1.0%)	0	2 (1.1%)
C3/4	70 (35.2%)	9 (39.1%)	61 (34.7%)
C4	4 (2.0%)	0	4 (2.3%)
C4/5	49 (24.6%)	7 (30.4%)	42 (23.9%)
C5	10 (5.0%)	0	10 (5.7%)
C5/6	29 (14.6%)	5 (21.7%)	24 (13.6%)
C6	4 (2.0%)	0	4 (2.3%)
C6/7	24 (12.1%)	1 (4.4%)	23 (13.1%)
C7	1 (0.5%)	0	1 (0.5%)
C7/T1	1 (0.5%)	0	1 (0.5%)
Hematoma-like changes on MRI			
+	46 (23.1%)	17 (73.9%)	29 (16.5%)
-	153 (76.9%)	6 (26.1%)	147 (83.5%)

MRI indicates magnetic resonance imaging; SD, standard deviation.

Univariate analyses of the risk factors for tracheostomy revealed significant differences for six items: age ($P=0.0422$, odds ratio [OR]=1.035), ISS ($P=0.0002$, OR=1.065), presence of fracture or dislocation ($P=0.0209$, OR=2.827), AIS A ($P<0.0001$, OR=7.344), NLI C4 or above ($P=0.0008$, OR=12.599), and MRI scans revealing hematoma-like changes ($P<0.0001$, OR=9.504) (Table 4).

The aforementioned items with significant differences in the univariate analyses were further analyzed using multivariate logistic regression. The results revealed significant differences for two items: NLI C4 or above ($P=0.0058$, OR=9.681) and MRI scans revealing hematoma-like changes ($P=0.0212$, OR=3.941) (Table 5).

In addition, 17 of 30 patients (56.7%) who had both an NLI C4 or above and MRI scans revealing hematoma-like

TABLE 3. Demographic Data of Tracheostomy Patients

Case No.	Age	Sex	Type of Fracture	AIS	NLI	T2 High Level	Hematoma-like changes on MRI	PO2 on Admission (mm Hg)	PCO2 on Admission (mm Hg)	Final Form
1	80	F	C6 fracture dislocation	A	C4	C6/7	+	74.73	45.2	Trach collar
2	47	M	C3 tear drop fracture T4 fracture dislocation	A	T1	C3/4	-	80.9	36	Closed
3	49	M	C5 burst fracture	A	C4	C5/6	+	66.7	41.8	Closed
4	64	M	C4 fracture dislocation	A	C4	C4/5	+	72.1	36.5	Trach collar
5	82	F	C3 fracture dislocation	C	C4	C3/4	+	145.7	45.1	Closed
6	84	M	C4 fracture dislocation	A	C3	C4/5	+	74.5	34.4	Mechanical ventilation
7	75	M	C5 fracture (post ASF)	C	C3	C4/5	-	45.8	46.6	Closed
8	61	F	C5 fracture dislocation	A	C4	C5/6	+	116.9	37.4	Closed
9	80	F	C3 burst fracture	B	C4	C3/4	+	59.0	40.0	Closed
10	76	M	C5 fracture dislocation	A	C4	C5/6	+	161.0	33.0	Trach collar
11	70	M	C3 fracture dislocation	A	C3	C3/4	+	166.0	46.7	Mechanical ventilation
12	51	M	No fracture	A	C3	C5/6	-	97.0	49.0	Mechanical ventilation
13	77	M	No fracture	A	C4	C4/5	+	48.6	47.6	Mechanical ventilation
14	22	M	No fracture	A	C3	C2/3	+	392 (intubated)	40.7 (intubated)	Closed
15	63	M	No fracture	B	C4	C3/4	-	63.4	33.8	Closed
16	89	M	No fracture	A	C4	C4/5	+	93.6	34.8	Died
17	72	M	No fracture	B	C4	C3/4	-	86.5	33.4	Closed
18	69	F	No fracture	A	C4	C3/4	+	123	43.9	Closed
19	61	M	No fracture	B	C2	C3/4	+	127	35.7	Mechanical ventilation
20	85	F	No fracture	A	C4	C4/5	+	69.5	43.1	Closed
21	83	M	No fracture	A	C5	C5/6	-	72.5	37.2	Closed
22	66	M	No fracture	A	C4	C4/5	+	72.7	31.6	Mechanical ventilation
23	84	M	No fracture	A	C4	C3/4	+	86.2	43.9	Mechanical ventilation

AIS indicates American Spinal Association impairment scale; ASF, anterior spine fusion; MRI, magnetic resonance imaging; NLI, neurological level of injury.

TABLE 4. Results of the Simple Logistic Regression Model

	<i>P</i>	OR	95% Confidence Interval
Age	0.0422	1.035	1.004–1.074*
ISS	0.0002	1.065	1.032–1.106*
PO ₂ on admission	0.1445	1.006	0.997–1.014
PCO ₂ on admission	0.1055	1.076	0.986–1.183
Sex	0.2284	1.866	0.629–4.939
Fracture or dislocation (+)	0.0209	2.827	1.166–6.931*
AIS A	<0.0001	7.344	2.870–21.353*
NLI ≥ C4	0.0008	12.599	3.550–80.260*
Injury level on MRI ≥ C3/4	0.6169	1.251	0.508–3.004
Hematoma-like changes on MRI	<0.0001	9.504	3.780–25.604*

Age, ISS, PO₂, and PCO₂ were calculated by the continuous variable function unit odds ratio.

AIS indicates American Spinal Association impairment scale; ISS, injury severity score; MRI, magnetic resonance imaging; NLI, neurological level of injury; OR, odds ratio.

**P* < 0.05.

changes required a tracheostomy, whereas 15 of 40 patients (37.5%) who had both an NLI C4 or above and AIS A on admission required a tracheostomy.

DISCUSSION

Various complications can occur after a CSCI, although the most frequent are respiratory complications.^{1–5} Typical complications include atelectasis, pneumonia, and ventilatory failure. These complications often occur in the acute phase within 5 days of injury.¹³

The diaphragm is innervated by nerves originating from C3–C5 (primarily from C4), and damage to the spinal cord at a higher level will immediately necessitate ventilator management. Sputum is expelled and coughing is accomplished primarily with the intercostal muscles and abdominal muscles. Even if the injury occurred at a lower level and the diaphragm still functioned, paralysis of these muscles causes sputum to pool, thereby facilitating atelectasis and pneumonia.^{10,16} In the acute phase of injury, the sympathetic nerves are interrupted and the vagus nerve predominates. Furthermore, tracheobronchial secretions increase and the airway constricts. The amount of sputum increases and the sputum cannot be readily expelled. This phenomenon is one reason for why respiratory complications are so frequent.

In the first week after injury, a patient's vital capacity will decrease by 30% or more. About 5 weeks after injury, vital capacity will begin to recover, and 3 months after injury the vital capacity will double.^{11,16} If the period of an unstable respiratory status in the acute-subacute phase of injury can be weathered, then the respiratory status will subsequently stabilize for the most part. Thus, predicting risk factors for intubation or tracheostomy in patients with a CSCI is important.

Studies cite widely differing figures for the percentage of patients requiring a tracheostomy after CSCI. These figures range from 15.2% to 81%, and recent studies have noted that a relatively high percentage of those patients require a tracheostomy.^{6–9,12,17,19,21,24} Numerous studies have reported that performing a tracheostomy early on is useful in reducing respiratory complications.^{6,9,16–18} This might be the reason for the substantial difference in the percentage of patients with a tracheostomy. That said, one possibility is that intubation or tracheostomy is performed unnecessarily, and such situations should be avoided.

The current study found that 11.6% of patients with a CSCI require a tracheostomy, and this is lower than the percentages described in other studies. This Center is a dedicated facility with a Department of Orthopedic Surgery and in principle this facility does not accept patients in the

TABLE 5. Results of the Multiple Logistic Regression Model

	<i>P</i>	OR	95% Confidence Interval
Age	0.0782	1.031	0.999–1.071
ISS	0.2784	1.025	0.983–1.077
Fracture or Dislocation (+)	0.2477	2.049	0.597–6.970
AIS A	0.2180	2.329	0.600–9.154
NLI ≥ C4	0.0058	9.681	2.362–66.748*
Hematoma-like changes on MRI	0.0212	3.941	1.243–13.131*

Age and ISS were calculated by the continuous variable function unit odds ratio.

AIS indicates American Spinal Association impairment scale; ISS, injury severity score; MRI, magnetic resonance imaging; NLI, neurological level of injury; OR, odds ratio.

**P* < 0.05.

acute phase of multiple trauma. This Center sees a small proportion of patients with complications such as a brain contusion, multiple rib fractures, a hemopneumothorax, or injuries to the abdominal viscera, which might explain why so few of the current patients required a tracheostomy. The aforementioned reasons are also presumably the reason why tracheal intubation or a tracheostomy is so often indicated for a simple CSCI seen at this Center. In this study, univariate analyses and multivariate analyses yielded significant differences in terms of two items: an NLI C4 or above and MRI scans revealing hematoma-like changes. The aforementioned reasons are presumably why these two items were predictors for a tracheostomy, in a true sense, in patients with a CSCI.

Numerous studies have reported that complete paralysis is a risk factor for intubation or a tracheostomy.^{1,6-8,14,17,19-22,23} In the current study, univariate analyses indicated that AIS A was a risk factor for tracheostomy, whereas multivariate analyses revealed no significant differences in AIS A.

This might be because complete paralysis means that the intercostal muscles and abdominal muscles are paralyzed, regardless of the level of the CSCI; however, Yague *et al*⁷ reported that 18.8% of patients who were AIS A upon admission had an improved level of paralysis (a grade other than A) at final follow-up. Similarly, 66 patients in the current study were AIS A upon admission, although eight (12.1%) had improvement at final follow-up. The period of spinal shock might have been included in the 72 hours after injury. Given this possibility, improvement in the level of paralysis needs to be assessed.

The ISS was similarly found to be a risk factor for tracheostomy according to univariate analyses. ISS is a score for the severity of multiple trauma. Several studies have reported that a high ISS is a predictor for tracheostomy in patients with a CSCI^{8,21}; however, Velmahos *et al*²¹ stated that assessment of the ISS is difficult in the acute phase of trauma, and they recommended that the ISS not be used as a predictor of tracheostomy.

No studies have indicated the relationship between imaging assessment and the need for a tracheostomy. The current study is the first to do so. In the acute phase of injury,

blurred hyperintensity on T2-weighted MRI indicates spinal cord contusion or edema.²⁵⁻²⁷ This imaging finding suggests injury to the spinal cord. If cord damage is severe and hematomyelia is present, hypointensities will be found inside hyperintensities in T2-weighted images. This finding mostly suggests severe spinal cord injury,^{28,29} and we described those change as "hematoma-like changes." Bozzo *et al*²⁹ reported that 93% of patients with MRI scans revealing a hypointense core surrounded by a hyperintense rim in T2-weighted images (hematoma-like changes) were AIS A upon admission. Of these, 95% were AIS A at final follow-up. In the current study, 82.6% of patients who were found to have hematoma-like changes were AIS A upon admission. All of the patients were AIS A at final follow-up, and this grade might be correlated with severe paralysis.

In the current study, univariate analyses and multivariate analyses revealed significant differences in MRI scans revealing hematoma-like changes. The AIS grade might change over time because of its relationship to spinal shock. Consequently, the ISS might change as well. Thus, these indicators change. In contrast, MRI images revealing hematoma-like changes do not change with spinal shock, making these MRI findings an independent indicator.

Of course, MRI was performed within a few hours after the injury. Therefore, there was a possibility that hematoma-like changes (hypointense core surrounded by a hyperintense rim) did not appear on T2-weighted images, even if a hematomyelia occurred, reflecting the intracellular oxyhemoglobin³⁰; however, if hypointensity changes were revealed on T2-weighted image within 72 hours after the injury, they reflected deoxyhemoglobin, suggesting that a hemorrhage had occurred in the spinal cord and that the damage was severe.

In addition, significant differences in the level of injury on MRI scans were not noted, although an NLI C4 or above was a risk factor for tracheostomy.

The level of injury on MRI and the NLI did not necessarily coincide. Results suggested that the NLI is important because of its greater clinical significance.

Several studies have reported that an NLI at a high level is a predictor for tracheotomy.^{6,12,14,21} Nerves innervating the diaphragm originate at levels C3–C5. The diaphragm is

TABLE 6. Results of the Multiple Logistic Regression Model in CSCI Patients Who Had NLI \geq C4 on Admission

	P	OR	95% Confidence Interval
Age	0.1383	1.031	0.993–1.078
ISS	0.4848	1.016	0.974–1.066
Fracture or dislocation (+)	0.1476	2.617	0.101–1.411
AIS A	0.2180	1.705	0.386–7.369
Hematoma-like changes on MRI	0.0049	6.101	1.779–22.842*

Age and ISS were calculated by the continuous variable function unit odds ratio.

AIS indicates American Spinal Association impairment scale; CSCI, cervical spinal cord injury; ISS, injury severity score; MRI, magnetic resonance imaging; NLI, neurological level of injury; OR, odds ratio.

* $P < 0.05$.

involved in about 65% of breathing. The current study yielded significant differences at C4 or above. Paralysis due to an injury at C4 or above causes motor paralysis of the diaphragm, which is likely to result in the patient's respiratory status worsening.

Several studies have reported that the risk of tracheostomy is related to age^{7,12}; however, multivariate analyses revealed no significant differences in patient age. In addition, this study found no significant differences in patient sex.

Studies have reported that the forced vital capacity upon admission is correlated with the risk of tracheostomy,^{7,9} although this characteristic might present problems for facilities that do not have a simple spirometer on hand. Blood gas analysis is simple and convenient, and the results might serve as an indicator in place of forced vital capacity. In actuality, however, significant differences in blood gas results were not evident.

An extensive search yielded no studies indicating a relationship between bone injury or dislocation and the risk of tracheostomy. The current study noted no significant differences in terms of the presence or absence of a vertebral fracture or dislocation in multivariate analyses. This is probably because the damage to the spinal cord is a more important factor than the presence or absence of a vertebral fracture or dislocation.

In the current study, multivariate analyses revealed significant differences in terms of two items: an NLI C4 or above and MRI scans revealing hematoma-like changes.

Multivariate analyses revealed significant differences in terms of two items in 30 patients. Of these patients, 17 (57%) required a tracheostomy, suggesting that patients with both of the aforementioned characteristics are likely to require a tracheostomy.

In addition, we examined the risk factors for a tracheostomy in a total of 101 CSCI patients who had NLI C4 or above on admission. As a result, hematoma-like changes on MRI only showed a significant difference in the multivariate logistic regression model ($P = 0.0049$, $OR = 6.101$) (Table 6). This finding raises the possibility that hematoma-like changes on MRI are an optimal indicator of the risk for tracheostomy in patients with a CSCI.

The current study had several limitations. One is that this study was a retrospective study that studied a relatively small sample over an 8-year period. In addition, this study was conducted at a single special facility, that is, the Spinal Injuries Center, and not at other facilities. In addition, definite eligibility criteria for a tracheostomy have yet to be formulated at this facility, and the final decision is left to the discretion of the patient's primary physician. In addition, there is a possibility that hematoma-like changes did not appear on T2-weighted images, when MRI was performed within a few hours after the injury. Moreover, this study did not examine aspects such as patient history, original respiratory status, or whether or not the patient smoked.

Despite these limitations, however, the current study identified significant differences in terms of the two

items: an NLI C4 or above and MRI scans revealing hematoma-like changes. These two items are statistically independent risk factors. If patients have both of these characteristics, they are extremely likely to have respiratory failure even if they had a satisfactory respiratory status upon admission. These characteristics can serve as important indices with which to study early tracheal intubation and early tracheostomy.

➤ Key Points

- ❑ The current study used imaging assessment and other approaches to assess and examine the risk factors for a tracheostomy in patients with a CSCI.
- ❑ Univariate analyses of the risk factors for tracheostomy revealed significant differences for six items: age, ISS, presence of fracture or dislocation, AIS A, NLI C4 or above, and MRI scans revealing hematoma-like changes.
- ❑ Multivariate logistic regression analyses of the risk factors for tracheostomy revealed significant differences in terms of two items: NLI C4 or above and MRI images revealing hematoma-like changes.
- ❑ Spinal shock has an effect in the acute phase of injury, hampering assessment of the AIS. In contrast, MRI scans revealing hematoma-like changes do not change with spinal shock, making these MRI findings an independent indicator.
- ❑ Patients with an NLI C4 or above and MRI scans revealing hematoma-like changes were likely to require a tracheostomy.

References

1. Ellen MH, Stein AL, Tiina R, et al. Mortality after traumatic spinal cord injury: 50 years of follow-up. *J Neurol Neurosurg Psychiatry* 2010;81:368–73.
2. Reines David H, Harris Robert C. Pulmonary complications of acute spinal cord injuries. *Neurosurgery* 1987;21:193–6.
3. Winslow C, Rozovsky J. Effect of spinal cord injury on the respiratory system. *Am J Phys Med Rehabil* 2003;82:803–14.
4. Nakajima A, Honda S, Yoshimura S, et al. The disease pattern and causes of death of spinal cord injured patients in Japan. *Paraplegia* 1989;27:163–71.
5. Sekhon LH, Fehlings MG. Epidemiology, demographics, and pathophysiology of acute spinal cord injury. *Spine* 2001;26:2–12.
6. Como JJ, Sutton ER, McCunn M, et al. Characterizing the need for mechanical ventilation following cervical spinal cord injury with neurologic deficit. *J Trauma* 2005;59:912–6.
7. Yague I, Okada S, Ueta T, et al. Analysis of the risk factors for tracheostomy in traumatic cervical spinal cord injury. *Spine* 2012;37:E1633–8.
8. Branco BC, Plurad D, Green DJ, et al. Incidence and clinical predictors for tracheostomy after cervical spinal cord injury: a national trauma databank review. *J Trauma* 2011;70:111–5.
9. Berney SC, Gordon IR, Opdam HI, et al. A classification and regression tree to assist clinical making in airway management for patients with cervical spinal cord injury. *Spinal Cord* 2011;49:244–50.

10. McMichan JC, Michel L, Westbrook PR. Pulmonary dysfunction following traumatic quadriplegia. *JAMA* 1980;243:528–31.
11. Ledsome JR, Sharp JM. Pulmonary function in acute cervical cord injury. *Am Rev Respir Dis* 1981;124:41–4.
12. Harrop LS, Sharan AD, Scheid EH Jr, et al. Tracheostomy placement in patients with complete cervical spinal cord injuries: American Spinal Injury Association Grade A. *J Neurosurg* 2004;100:20–3.
13. Berly M, Shem K. Respiratory management during the first five days after spinal cord injury. *J Spinal Cord Medicine* 2007;30:309–18.
14. Berney S, Bragge P, Granger C, et al. The acute respiratory management of cervical spinal cord injury in the first 6 weeks after injury: a systematic review. *Spinal Cord* 2011;49:17–29.
15. Biering-Sorensen M, Biering-Sorensen F. Tracheostomy in spinal cord injured: frequency and follow up. *Paraplegia* 1992;30:656–60.
16. Perry AB. Critical care of spinal cord injury. *Spine* 2001;26: S27–30.
17. Leelapattana P, Fleming JC, Gurr KR, et al. Predicting the need for tracheostomy in patients with cervical spinal cord injury. *J Trauma Acute Care Surg* 2012;73:880–4.
18. Romero J, Vari A, Gambarrutta C, et al. Tracheostomy timing in traumatic spinal cord injury. *Eur Spine J* 2009;18:1452–7.
19. Nakashima H, Yukawa Y, Imagama S, et al. Characterizing the need for tracheostomy placement and decannulation after cervical spinal cord injury. *Eur Spine J* 2013;22:1526–32.
20. Hassid VJ, Schinco MA, Tepas JJ, et al. Definitive establishment of airway control is critical for optimal outcome in lower cervical spinal cord injury. *J Trauma* 2008;65:1328–32.
21. Velmahos GC, Toutouzas K, Chan L, et al. Intubation after cervical spinal cord injury: to be done selectively or routinely? *Am Surg* 2003;69:892–4.
22. Call MS, Kutcher ME, Izenberg RA, et al. Spinal cord injury: outcomes of ventilator weaning and extubation. *J Trauma* 2011;71:1673–9.
23. Menaker J, Kufera JA, Glaser J, et al. Admission ASIA motor score predicting the need for tracheostomy after cervical spinal cord injury. *J Trauma Acute Care Surg* 2013;75:629–34.
24. Lemons VR, Wagner FV Jr. Respiratory complications after cervical spinal cord injury. *Spine* 1994;15:2315–20.
25. Fujii H, Yone K, Sakou T. Magnetic resonance imaging study of experimental acute spinal cord injury. *Spine* 1993;18:2030–4.
26. Ohshio I, Hatayama A, Kaneda K, et al. Correlation between histopathologic features and magnetic resonance images of spinal cord lesions. *Spine* 1993;18:1140–9.
27. Machino M, Yukawa Y, Ito K, et al. Can magnetic resonance imaging reflect the prognosis in patients of cervical spinal cord injury without radiographic abnormality? *Spine* 2011;36: E1568–72.
28. Schaefer DM, Flanders AE, Osterholm JL, et al. Prognostic significance of magnetic resonance imaging in the acute phase of cervical spine injury. *J Neurosurg* 1992;76:218–23.
29. Bozzo A, Marcoux J, Radhakrishna M, et al. The role of magnetic resonance imaging in the management of acute spinal cord injury. *J Neurotrauma* 2011;28:1401–11.
30. Bradley WG Jr. MR appearance of hemorrhage in the brain. *Radiology* 1993;189:15–26.

Clinical Influence of Cervical Spinal Canal Stenosis on Neurological Outcome after Traumatic Cervical Spinal Cord Injury without Major Fracture or Dislocation

Tsuneaki Takao¹, Seiji Okada², Yuichiro Morishita¹, Takeshi Maeda¹, Kensuke Kubota², Ryosuke Ideta³, Eiji Mori¹, Itaru Yugue¹, Osamu Kawano¹, Hiroaki Sakai¹, Takayoshi Ueta¹, Keiichiro Shiba¹

¹Department of Orthopaedic Surgery, Spinal Injuries Center, Iizuka, Japan

²Department of Orthopaedic Surgery, Kyushu University, Fukuoka, Japan

³Department of Rehabilitation Medicine, Spinal Injuries Center, Iizuka, Japan

Study Design: Retrospective case series.

Purpose: To clarify the influence of cervical spinal canal stenosis (CSCS) on neurological functional recovery after traumatic cervical spinal cord injury (CSCI) without major fracture or dislocation

Overview of Literature: The biomechanical etiology of traumatic CSCI remains under discussion and its relationship with CSCS is one of the most controversial issues in the clinical management of traumatic CSCI.

Methods: To obtain a relatively uniform background, patients non-surgically treated for an acute C3–4 level CSCI without major fracture or dislocation were selected. We analyzed 58 subjects with traumatic CSCI using T2-weighted mid-sagittal magnetic resonance imaging. The sagittal diameter of the cerebrospinal fluid (CSF) column, degree of canal stenosis, and neurologic outcomes in motor function, including improvement rate, were assessed.

Results: There were no significant relationships between sagittal diameter of the CSF column at the C3–4 segment and their American Spinal Injury Association motor scores at both admission and discharge. Moreover, no significant relationships were observed between the sagittal diameter of the CSF column at the C3–4 segment and their neurological recovery during the following period.

Conclusions: No relationships between pre-existing CSCS and neurological outcomes were evident after traumatic CSCI. These results suggest that decompression surgery might not be recommended for traumatic CSCI without major fracture or dislocation despite pre-existing CSCS.

Keywords: Cervical spinal canal stenosis; Cervical spinal cord injury without major fracture or dislocation; Magnetic resonance imaging; Neurological outcome

Introduction

Numerous previous studies have been published concern-

ing adult traumatic cervical spinal cord injuries (CSCI) without major bony injury or dislocation, using various nomenclature, such as hyperextension dislocation [1],

Received Sep 13, 2015; Revised Oct 25, 2015; Accepted Oct 26, 2015

Corresponding author: Tsuneaki Takao

Department of Orthopaedic Surgery, Spinal Injuries Center, 550-4 Igisu, Iizuka 820-8508, Japan

Tel: +81-948-24-7500, Fax: +81-948-29-1065, E-mail: tsuneaki@iris.ocn.ne.jp

ASJ

Copyright © 2016 by Korean Society of Spine Surgery

This is an Open Access article distributed under the terms of the Creative Commons Attribution Non-Commercial License (<http://creativecommons.org/licenses/by-nc/3.0/>) which permits unrestricted non-commercial use, distribution, and reproduction in any medium, provided the original work is properly cited.

Asian Spine Journal • pISSN 1976-1902 eISSN 1976-7846 • www.asianspinejournal.org

Table 1. Neurological status (ASIA impairment score) at admission and discharge

On admission	No.	On discharge				
		A	B	C	D	E
A	10	2	1	6	1	-
B	11	-	1	6	4	-
C	31	-	-	1	30	-
D	6	-	-	-	5	1

ASIA, American Spinal Injuries Association.

spinal cord injury (SCI) without radiographical abnormality in adults (SCIWORA) [2-6], SCI without radiographical evidence of trauma (SCIWORET) [7-9], and CSCI without bony injury [10-11]. Most patients are elderly and may present with tetraplegia caused by a hyperextension injury, predominantly at the C3-4 segment, with cord compression as a result of a stenotic spondylotic canal [3,7,12-14]. However, the influence of cervical spinal canal stenosis (CSCS) on neurological recovery after CSCI remains unclear.

The broad definition of SCIWORA/SCIWORET includes disc injury, anterior vertebral body tip or spinous process fracture, or other ligamentous injury. We defined CSCI with or without those injuries but without spinal canal bony injury as traumatic CSCI without major fracture or dislocation. Traumatic CSCI can occur with or without CSCS and cervical cord compression. The biomechanical etiology of traumatic CSCI without major fracture or dislocation remains under discussion, and its relationship with CSCS is one of the most controversial issues in the clinical management of traumatic CSCI.

The aims of the current study were to clarify the influence of spinal canal stenosis on neurological functional recovery after traumatic CSCI without major fracture or dislocation.

Materials and Methods

1. Study population

A total of 101 subjects with traumatic CSCI without major fracture or dislocation were treated conservatively in our facility from 2010 to 2013. All patients underwent functional plain radiographs including flexion and extension, computed tomography (CT), magnetic resonance imaging (MRI), and neurologic examination by a senior

spine surgeon at the time of admission. All patients wore a Philadelphia collar for 4 weeks and started their rehabilitation from sitting exercise immediately without causing any discomfort if their general conditions were stable. Of these patients, 58 had the injury at C3-4 (57.4%); 1 at C2-3 (1.0%); 26 at C4-5 (25.7%); 12 at C5-6 (11.9%); and 4 at C6-7 (4.0%). In the study, we focused on the subjects with responsible injured segment at the C3-4 segment who were admitted to our facility within 48 hours following trauma and had evidence of cervical cord injury with cervical cord intensity change on T2-weighted MRI at the C3-4 segment. A total of 58 subjects (52 men, 6 women; average age, 63.8 years [range, 42-89 years]) were included in the study. Of the 58 patients, 34 showed central cord syndrome, 20 showed transverse, 2 showed anterior cord syndrome, and 2 showed Brown-Sequard syndrome. The average period of hospitalization was 258 days (range, 61 to 550). The neurologic status of the patients at the time of admission and discharge are summarized in Table 1. Patients with the following conditions were excluded from the study: multiple segmental cervical cord injury, cervical myelopathy before trauma, apparent herniated disc at the injured segment, severe instability on functional radiographs as defined by White et al. [15] (dynamic translation >3.5 mm or 11° greater angulation than that in the adjacent segment) or indication of spontaneous reduction of dislocation at C3-4 segment, or ankylosing spondylitis.

Institutional Review Board approval was granted and informed consent was obtained from all patients included in the study.

2. Measurement of sagittal diameter of the CSF column

We used a T2-weighted mid-sagittal MRI scan obtained at the time of admission to measure the sagittal diameters of the cerebrospinal fluid (CSF) column at the C3-4

intervertebral disc level and C3 pedicle level. The rate of spinal canal stenosis was calculated using the following equation: $(A-B)/A \times 100$ (Fig. 1).

3. Neurological status (ASIA motor score)

The American Spinal Injuries Association (ASIA) motor

score (range, 0 to 100) was documented at the time of admission and discharge for each patient. Neurological recovery was evaluated as an improvement rate (%) calculated as $(\text{motor score at discharge} - \text{motor score at admission}) / (100 - \text{motor score at admission}) \times 100$.

4. Statistical analysis

Statistical analysis was performed using the Spearman rank-correlation coefficient to evaluate the relationships between neurological status and CSCI. $p < 0.05$ was considered statistically significant.

Results

The average value of the sagittal diameters of the CSF columns at the C3–4 intervertebral disc and C3 pedicle level was 6.5 mm and 8.9 mm, respectively. The average period of hospitalization was 258 days (range, 61 to 550 days). The average value of ASIA motor score at the time of admission and discharge was 28.5 and 67.7, respectively, and the improvement rate was 61.1%. The average value of the spinal canal stenosis ratio was 25.7%.

Fig. 2 shows the relationships between the sagittal diameter of the cervical CSF column at the C3–4 intervertebral disc level and ASIA motor score, which reflects neurological status at the time of admission and discharge. There were no significant relationships between the sagittal diameter of the cervical CSF column and ASIA motor scores both at the time of admission ($p = 0.773$) and discharge ($p = 0.138$) for the subjects with traumatic CSCI.

Fig. 3 shows the relationship between the sagittal diam-



Fig. 1. T2-weighted midsagittal magnetic resonance imaging. A is the diameter of the cervical cord at the non-compression level and B is the diameter of the cervical cord at the injured level.

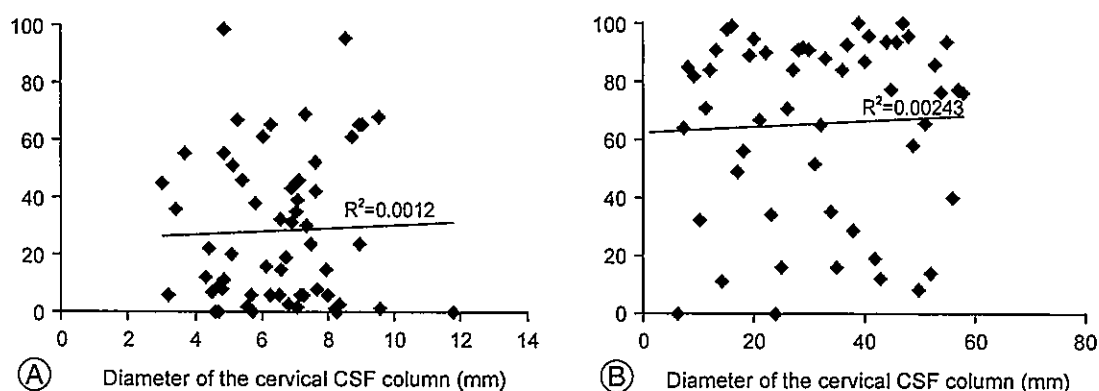


Fig. 2. The sagittal diameter of the cervical cerebrospinal fluid (CSF) column and American Spinal Injuries Association motor score (A) at admission and (B) at discharge.

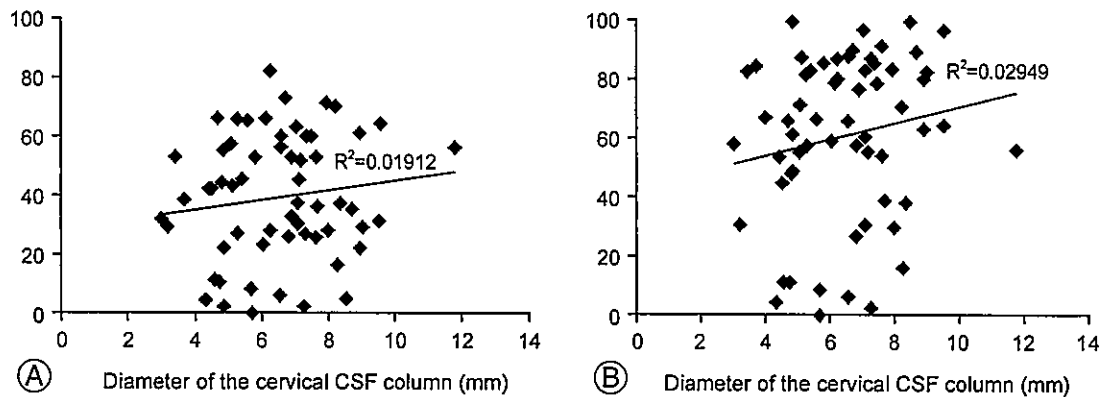


Fig. 3. Sagittal diameter of the cervical cerebrospinal fluid (CSF) column and the improvement rate according to the (A) subtraction score and (B) improvement rate (%).

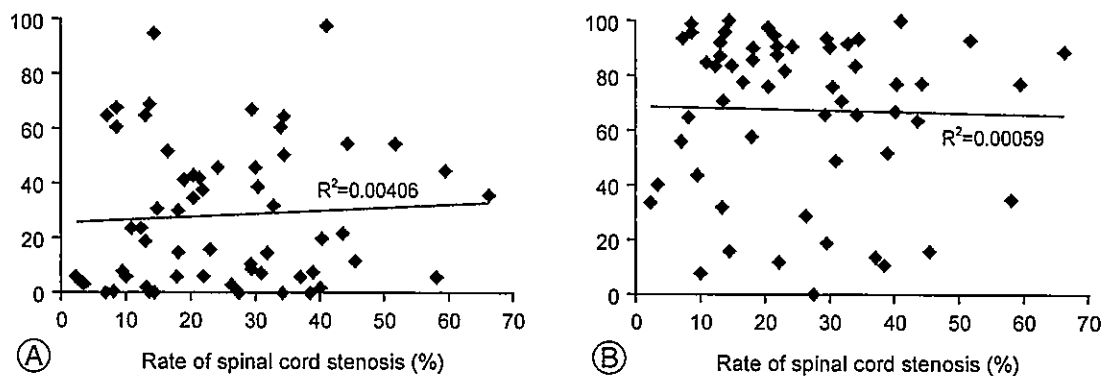


Fig. 4. The rate of spinal cord stenosis and American Spinal Injuries Association motor score (A) at admission and (B) at discharge.

eter of the cervical CSF column at the C3–4 intervertebral disc level and the improvement rate, which reflects neurological recovery at the time of discharge. We defined the subtraction score as (motor score on discharge)–(motor score on admission). There was no significant relationship between the sagittal diameter of the cervical CSF column and neurological recovery at the time of discharge (subtraction score; $p=0.155$, improvement rate; $p=0.111$).

Fig. 4 shows the relationships between the rate of spinal canal stenosis and ASIA motor scores. There were no significant relationships between the rate of spinal canal stenosis and ASIA motor scores both at the time of admission ($p=0.897$) and discharge ($p=0.315$).

Fig. 5 shows the relationship between the rate of spinal canal stenosis and improvement rate. There was also no significant relationship between the rate of spinal canal stenosis and neurological recovery at the time of discharge

(subtraction score; $p=0.441$, improvement rate; $p=0.277$).

Discussion

The number of CSCI without major fracture or dislocation has been increasing as the population ages [16]. However, the clinical management of traumatic CSCI is contentious.

Some authors recommend surgery for patients with pre-existing canal stenosis, as persistent cord compression may hinder neurological improvement [17–19]. La Rosa et al. [17] reported that early decompression surgery within 24 hours after trauma had a significantly better outcome compared with late surgical management. Chen et al. [18] recommended surgical treatment to achieve rapid neurological recovery and shorter hospitalization despite the level of functional recovery in the surgical and conserva-

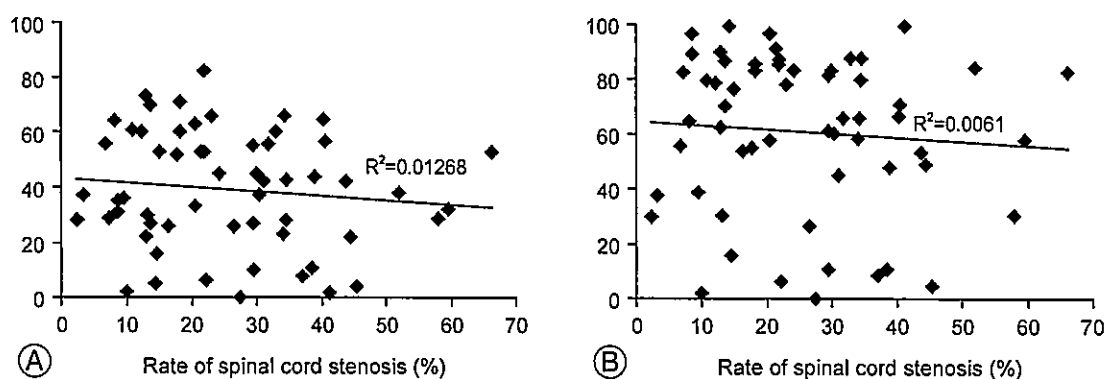


Fig. 5. The rate of spinal cord stenosis and the improvement rate according to the (A) subtraction score and (B) improvement rate (%).

tive treatment groups. Yamazaki et al. [19] reported that the canal diameter was a reliable predictor of recovery and recommended early decompression surgery. However, these studies were retrospective comparisons with small data sets and so likely had an inherent selection bias for surgical management.

In contrast, other researchers have reported no additional benefit with surgery compared to conservative treatment [20-22]. For example, Itoh et al. [20] reported no significant difference in neurological improvement between surgical and conservative management of CSCI without major bony injury; a higher frequency of postoperative complications was observed in subjects who were treated surgically. Kawano et al. [21] reported that surgical treatment was not superior to conservative treatment for CSCI without major bony injury with spinal cord compression in the acute phase. Although this study is not a comparison of conservative and operative treatment, our results propound prudence for surgical decompression until unequivocal evidence demonstrating improved neurological recovery or the prevention of delayed deterioration through surgery is presented.

In our facility, CSCI patients without major fracture or dislocation have consistently been treated conservatively and rehabilitated as early as possible, thus providing an appropriate study cohort to examine whether cervical canal stenosis is a risk factor for a deteriorative neurological course. We focused on the subjects with CSCI injured at C3-4 segment because of its high frequency (57.4%). Several studies have reported the frequent incidence of traumatic CSCI at the level of C3-4 segment. However, under the circumstances, this remains a matter of debate. In the study, there were no significant relationships between

sagittal C3-4 cord diameters and ASIA motor scores both at the time of admission and discharge. Moreover, no significant relationship between CSCS and neurological recovery was seen in CSCI subjects. These results appear to be unreasonable, since pathophysiology is closely related with stenotic factors, especially in degenerative cervical myelopathy [23,24]. Yet, careful consideration of the mechanism of traumatic SCI could provide accountable interpretations. At the moment of traumatic injury, the unphysiological and instantaneous dynamic stenosis would most significantly affect the neurological outcomes [16]. In the present study, what we consider to be most important finding is that canal stenosis on radiographs is a different condition from the unphysiological stenosis at the moment of injury. For this reason, the neurological outcome varies greatly, even among patients with the same canal diameter. Our data are consistent with those of earlier studies that showed that motor deficit severity does not statistically correlate with spinal canal stenosis degree [16,25,26]. Our results suggest that decompression surgery might not be necessary for CSCI without major fracture or dislocation with asymptomatic pre-existing stenosis in the acute phase.

Nevertheless, some questions remain unanswered even after the current study and so this study can only serve as a pilot study for further research using larger populations, which may help resolve several issues not addressed in this study and further clarify the clinical management of traumatic CSCI without major fracture or dislocation.

Conclusions

Our results showed no relationships between pre-existing

CSCS and neurological outcomes after traumatic CSCI. These results suggested that decompression surgery might not be recommended for traumatic CSCI without major fracture or dislocation despite pre-existing CSCS.

Conflict of Interest

No potential conflict of interest relevant to this article was reported.

References

- Harris JH, Yeakley JW. Hyperextension-dislocation of the cervical spine: ligament injuries demonstrated by magnetic resonance imaging. *J Bone Joint Surg Br* 1992;74:567-70.
- Hendey GW, Wolfson AB, Mower WR, Hoffman JR; National Emergency X-Radiography Utilization Study Group. Spinal cord injury without radiographic abnormality: results of the National Emergency X-Radiography Utilization Study in blunt cervical trauma. *J Trauma* 2002;53:1-4.
- Tewari MK, Gifti DS, Singh P, et al. Diagnosis and prognostication of adult spinal cord injury without radiographic abnormality using magnetic resonance imaging: analysis of 40 patients. *Surg Neurol* 2005;63:204-9.
- Kothari P, Freeman B, Grevitt M, Kerslake R. Injury to the spinal cord without radiological abnormality (SCIWORA) in adults. *J Bone Joint Surg Br* 2000; 82:1034-7.
- Yucesoy K, Yuksel KZ. SCIWORA in MRI era. *Clin Neurol Neurosurg* 2008;110:429-33.
- Machino M, Yukawa Y, Ito K, et al. Can magnetic resonance imaging reflect the prognosis in patients of cervical spinal cord injury without radiographic abnormality? *Spine (Phila Pa 1976)* 2011;36:E1568-72.
- Koyanagi I, Iwasaki Y, Hida K, Akino M, Imamura H, Abe H. Acute cervical cord injury without fracture or dislocation of the spinal column. *J Neurosurg* 2000; 93(1 Suppl):15-20.
- Tator CH. Clinical manifestations of acute spinal cord injury. In: Benzel EC, Tator CH; Aans Publications Committee, editors. *Contemporary management of spinal cord injury*. Park Ridge: American Association of Neurological Surgeons; 1995. p.15-26.
- Saruhashi Y, Hukuda S, Katsuura A, Asajima S, Omura K. Clinical outcomes of cervical spinal cord injuries without radiographic evidence of trauma. *Spinal Cord* 1998;36:567-73.
- Hardy AG. Cervical spinal cord injury without bony injury. *Paraplegia* 1977;14:296-305.
- Shimada K, Tokioka T. Sequential MRI studies in patients with cervical cord injury but without bony injury. *Paraplegia* 1995;33:573-8.
- Harrop JS, Sharan A, Ratliff J. Central cord injury: pathophysiology, management, and outcomes. *Spine J* 2006;6(6 Suppl):198S-206S.
- Takahashi M, Harada Y, Inoue H, Shimada K. Traumatic cervical cord injury at C3-4 without radiographic abnormalities: correlation of magnetic resonance findings with clinical features and outcome. *J Orthop Surg (Hong Kong)* 2002;10:129-35.
- Regenbogen VS, Rogers LF, Atlas SW, Kim KS. Cervical spinal cord injuries in patients with cervical spondylosis. *AJR Am J Roentgenol* 1986;146:277-84.
- White AA 3rd, Johnson RM, Panjabi MM, Southwick WO. Biomechanical analysis of clinical stability in the cervical spine. *Clin Orthop Relat Res* 1975;(109):85-96.
- Okada S, Maeda T, Ohkawa Y, et al. Does ossification of the posterior longitudinal ligament affect the neurological outcome after traumatic cervical cord injury? *Spine (Phila Pa 1976)* 2009;34:1148-52.
- La Rosa G, Conti A, Cardali S, Cacciola F, Tomasello F. Does early decompression improve neurological outcome of spinal cord injured patients? Appraisal of the literature using a meta-analytical approach. *Spinal Cord* 2004;42:503-12.
- Chen TY, Dickman CA, Eleraky M, Sonntag VK. The role of decompression for acute incomplete cervical spinal cord injury in cervical spondylosis. *Spine (Phila Pa 1976)* 1998;23:2398-403.
- Yamazaki T, Yanaka K, Fujita K, Kamezaki T, Uemura K, Nose T. Traumatic central cord syndrome: analysis of factors affecting the outcome. *Surg Neurol* 2005; 63:95-9.
- Itoh Y, Mazaki T, Koshimune K, Morita T, Mizuno S. Randomized controlled study of treatment for acute cervical cord injury with spinal canal stenosis but without radiographic evidence of trauma (SCIWORET): operative or conservative treatment. *J Spine Res* 2011;2:965-7.

21. Kawano O, Ueta T, Shiba K, Iwamoto Y. Outcome of decompression surgery for cervical spinal cord injury without bone and disc injury in patients with spinal cord compression: a multicenter prospective study. *Spinal Cord* 2010;48:548-53.
22. Takao T, Morishita Y, Okada S, et al. Clinical relationship between cervical spinal canal stenosis and traumatic cervical spinal cord injury without major fracture or dislocation. *Eur Spine J* 2013;22:2228-31.
23. Morishita Y, Naito M, Wang JC. Cervical spinal canal stenosis: the differences between stenosis at the lower cervical and multiple segment levels. *Int Orthop* 2011;35:1517-22.
24. Morishita Y, Naito M, Hymanson H, Miyazaki M, Wu G, Wang JC. The relationship between the cervical spinal canal diameter and the pathological changes in the cervical spine. *Eur Spine J* 2009;18:877-83.
25. Katoh S, el Masry WS, Jaffray D, et al. Neurologic outcome in conservatively treated patients with incomplete closed traumatic cervical spinal cord injuries. *Spine (Phila Pa 1976)* 1996;21:2345-51.
26. Ishida Y, Tominaga T. Predictors of neurologic recovery in acute central cervical cord injury with only upper extremity impairment. *Spine (Phila Pa 1976)* 2002;27:1652-8.

Clinical Study

“Knee-up test” for easy detection of postoperative motor deficits following spinal surgery

Itaru Yugué, MD, PhD^{a,*}, Seiji Okada, MD, PhD^b, Muneaki Masuda, MD^a,
Takayoshi Ueta, MD, PhD^a, Takeshi Maeda, MD, PhD^a, Keiichiro Shiba, MD, PhD^a

^aDepartment of Orthopedic Surgery, Spinal Injuries Center, 550-4 Igisu, Izuka 820-8508, Fukuoka, Japan

^bDepartment of Orthopedic Surgery, Kyushu University, 3-1-1 Maedashi, Higashi-ku 812-8582, Fukuoka, Japan

Received 8 September 2015; revised 2 June 2016; accepted 2 August 2016

Abstract

BACKGROUND CONTEXT: Neurologic motor deficit is a serious complication of spinal surgery. Early diagnosis of complications by neurologic examination immediately after spinal surgery is mandatory. However, patients cannot always cooperate with the physician in the very early stages of recovery. **PURPOSE:** The aim of the present study is to prospectively investigate the usefulness of the “knee-up test” for easy detection of postoperative motor deficits.

STUDY DESIGN: A prospective clinical study was carried out.

PATIENT SAMPLE: Patients with spinal disorder operated upon at a single institute were administered the knee-up test after an anesthesiologist had judged that endotracheal extubation was possible.

OUTCOME MEASURES: The outcome measures were preoperative and postoperative Manual Muscle Testing.

METHODS: A simple yet reliable method known as the “knee-up test” was developed to easily assess postoperative deficits before endotracheal extubation. When the patient’s knee is passively lifted up and the patient is able to maintain this position in both legs, the result is negative, whereas when the patient is unable to maintain the knee in an upright position for one or both legs, the result is positive. The presently accepted criterion for a new-onset postoperative neurologic motor deficit is motor weakness leading to a decrease in function of at least two grades in more than one muscle function within 12 hours of spinal surgery, as evaluated by the Manual Muscle Testing. The association between the presence of new-onset motor deficits and the results of the knee-up test was prospectively investigated.

RESULTS: Seventeen patients exhibited positive results when evaluated using the knee-up test, whereas 521 patients exhibited negative results. Sixteen of the patients with positive results were determined to have new-onset motor deficits, whereas no new-onset motor deficits were observed in the remaining patient. Of the 521 patients with negative knee-up test results, only 2 were determined to have new-onset motor deficits, whereas no new-onset motor deficits were observed in the remaining 519 patients. The sensitivity, specificity, positive predictive value, and negative predictive value were 88.9, 99.8, 94.1, and 99.6, respectively.

CONCLUSIONS: The knee-up test may allow for early and easy detection of postoperative motor deficits with high probability in very early stages. © 2016 Elsevier Inc. All rights reserved.

Keywords:

Clinical evaluation; Diagnosis method; Neurologic deficits; Postoperative complication; Spinal Injuries Center test; Spinal surgery

FDA device/drug status: Not applicable.

Author disclosures: *IY*: Nothing to disclose. *SO*: Nothing to disclose. *MM*: Nothing to disclose. *TU*: Nothing to disclose. *TM*: Nothing to disclose. *KS*: Nothing to disclose.

Itaru Yugué had full access to all the data in the study and takes responsibility for the integrity of the data and the accuracy of the data analysis as well as the decision to submit for publication.

Conflict of interest and sources of funding: None declared.

The study was approved by the local ethics committee.

* Corresponding author. Department of Orthopaedic Surgery, Spinal Injuries Center, 550-4 Igisu Izuka 820-8508, Fukuoka, Japan. Tel.: 81-948-24-7500; fax: 81-948-29-1065.

E-mail address: iyugue@orange.ocn.ne.jp (I. Yugué)

Introduction

Neurologic complications immediately after spinal surgery present a serious problem for both patients and spinal surgeons [1]. Previous studies have reported that the incidence of significant perioperative spinal cord or cauda equina injury ranges from approximately 0% to 15% but is usually less than 2% [2–19]. Early diagnosis of neurologic complications immediately after spinal surgery is very important for preventing the development of permanent neurologic deficits; surgeons must promptly investigate the etiologies of complications with imaging methods such as magnetic resonance imaging (MRI) and computed tomography (CT) scans [12,20] to determine whether re-operation is required [2]. However, just after operation, patients cannot always cooperate with physicians in undergoing a neurologic examination, especially before airway extubation.

In a previous study, the present authors developed a simple and reliable test for hysterical paralysis known as the Spinal Injuries Center (SIC) test [21]. This test showed that patients with severe organic paralysis were unable to keep the knee in a lifted position. Notably, the greatest merit of the test lies in not requiring the patient's cooperation. The purpose of the present study is to prospectively investigate the usefulness of the knee-up test for easy identification of postoperative motor deficits in the very early stages of recovery using a modified version of the Spinal Injuries Center test (ie, the knee-up test) to assess potential deficits following spinal surgery.

Materials and methods

Study sample

The present study enrolled 544 consecutive patients with spinal disorder who had been operated upon by a single surgeon (IY) in the same institution between May 1, 2006 and May 31, 2015. The knee-up test was administered to patients after an anesthesiologist had determined that endotracheal extubation was possible. Informed consent was obtained from all patients before enrollment in the study, and the study was approved by our local ethics committee. A precondition to performing the "knee-up test" is that the knee can be lifted up preoperatively on both sides; patients whose knees could not be lifted preoperatively because of severe motor deficits in the lower extremity were excluded from the study. However, patients who could not bend the knee more than 100 degrees because of hip- or knee-joint osteoarthritis (OA) were not excluded from this study. Six of the 544 patients were excluded because of preoperative inability to sustain the lifted position as a result of severe paralysis. The remaining 538 patients (324 men, 214 women) were selected for inclusion in the final sample (Fig. 1). The mean patient age was 63.9 years (range 16–89 years). The operated spinal region was broadly categorized as cervical (145 patients), thoracic (38 patients), or lumbar or sacral (355 patients). The preoperative disease

EVIDENCE & METHODS

Context

Postoperative motor deficits can portend serious complications and adversely impact outcomes following surgery. Early and effective detection are of paramount importance to maximize the potential for intervention and reversal. However, patients are not always able to participate in examination during the immediate postsurgical period. To address this concern, the authors describe a novel and simple "knee-up test" for detection of postoperative motor deficits.

Contribution

The authors evaluated 537 patients at a single center using this postsurgical test. The sensitivity, specificity, positive predictive value and negative predictive value were determined to be 88.9, 99.8, 94.1, and 99.6, respectively.

Implications

The authors' study provides metrics for a useful postoperative test that may be applied to the clinical setting. Given that this study was conducted in the center where the test was devised, there may be differences in its performance in the hands of other practitioners. As the authors recognize, the number of postsurgical defects was small and the sample may be clinically heterogeneous. As a result, the accuracy of this test has not been completely described and remains to be determined through further study. In light of this fact, the current study presents Level II evidence.

—The Editors

process was broadly categorized as degenerative, traumatic, neoplastic, infectious, or other (Fig. 2).

Experimental test procedure

The knee-up test is performed as follows. The patient is placed on a bed in the supine position, and the surgeon flexes the patient's hip to near 90 degrees while the knee is maximally flexed with the foot of the flexed leg on the table. The surgeon then gradually releases without any intention of keeping the knee in its lifted position (Fig. 3A and B). When the patient is unable to maintain one or both knees in an upright position, then the result is considered positive (Fig. 3C). When the patient is able to maintain both knees in the upright position, then the result is considered negative (Fig. 3D). In the present study, this test was performed twice, once by each of two independent observers (IY and MM) who were blinded to the results obtained by the other observer. When the results obtained by two observers disagreed, the result was classified as negative. It is better to examine the right and left sides separately with this test because administering this test to both legs at the same time risks twisting the waist (Fig. 3E). The

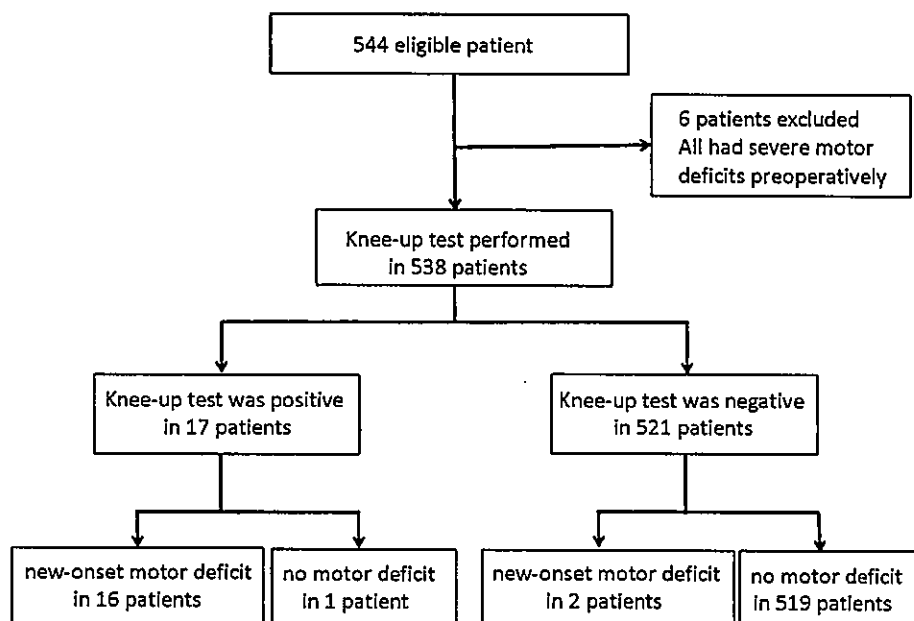


Fig. 1. Flow chart of the study.

knee-up test is performed just before the time of endotracheal extubation, which is determined by an expert anesthesiologist. The criteria for extubation are that the patient can maintain a patent airway and generate adequate spontaneous ventilation. Generally, this requires the patient to possess adequate level of the following: central inspiratory drive, cough strength to clear secretions, laryngeal function, consciousness (awake and oriented), stability of hemodynamic function, clearance of sedative and neuromuscular blocking effects, and respiratory muscle strength. The latter is defined as respiratory rate <35 breaths per minute during spontaneous breathing, vital capacity >10 mL/kg of ideal body weight, and spontaneous exhaled minute ventilation <10 L/min [22].

The muscle function test procedure

Preoperative and postoperative Manual Muscle Testing was performed by the attending surgeon, who was blinded to the results of the knee-up test. The functional strength of each muscle was graded on a six-point scale as follows: 0=total paralysis; 1=palpable or visible contraction; 2=active movement with full range of motion (ROM), provided that gravity is eliminated; 3=active movement with full ROM against gravity; 4=active movement with full ROM against moderate resistance; and 5=(normal) active movement with full ROM against gravity and sufficient resistance [23]. For patients with cervical-region disease, the following muscles were exam-

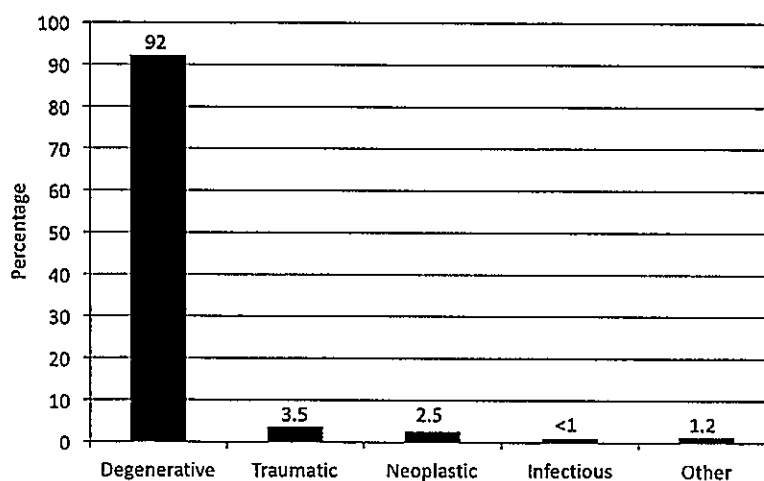


Fig. 2. Bar graph showing distribution of preoperative disease processes for spinal operations. Numbers above the bars indicate the percentage of 544 patients undergoing spinal operations.

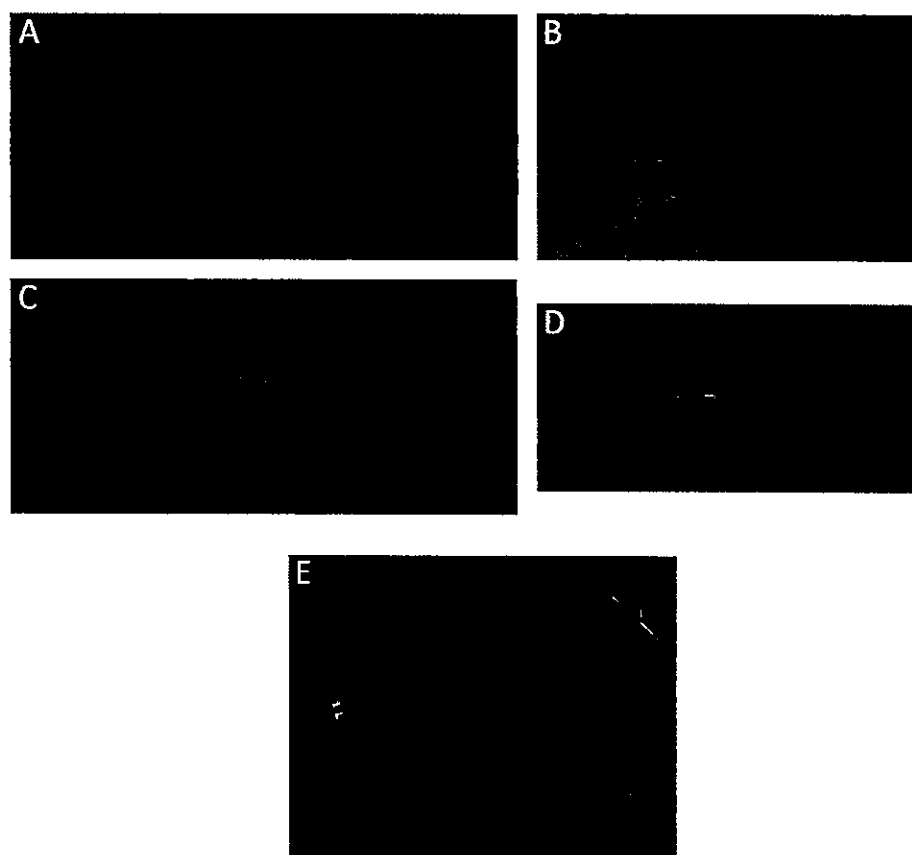


Fig. 3. (A) The “knee-up test” placing the patient in a supine position. (B) The patient’s knee is raised passively on the bed. Then, the knee is released gently. A key point of this test is to lift the knee until it is in maximally flexed. (C) When the patient is unable to maintain the knee upright, the knee-up test is positive. Usually, the positive patient’s leg comes to rest with the hip joint in an externally rotated position and the knee joint in a slightly extended position. (D) When the patient is able to maintain the knee upright in both sides, the knee-up test is negative. (E) Applying the knee-up test to both legs at the same time for a bilaterally positive patient may risk twisting the waist.

ined bilaterally and graded using the aforementioned scale: shoulder abductors, elbow flexors, wrist extensors, finger flexors, small-finger abductors, hip flexors, hip adductors, hip abductors, knee extensors, ankle dorsiflexors, long-toe extensors, and ankle plantar flexors. For patients with thoracic or lumbar or sacral-region disease, the following muscles were examined bilaterally and graded as above: hip flexors, hip adductors, hip abductors, knee extensors, ankle dorsiflexors, long-toe extensors, and ankle plantar flexors. The Manual Muscle Testing criteria for new-onset neurologic motor deficit after spinal surgery consisted of motor weakness leading to a decrease in score of at least two points compared with the preoperative score in more than one muscle within 12 hours after spinal surgery.

Methods of statistical comparison

The association between the presence of a new-onset motor deficit and the results of the knee-up test was investigated. We used Fisher exact test for categorical comparisons of the data and a logistic regression analysis to calculate both the odds ratio

and the 95% confidence interval. The sensitivity, specificity, positive predictive value (PPV), and negative predictive value (NPV) were also calculated. The kappa statistic was used to assess the inter-observer agreement on the knee-up test. Statistical analyses were performed using the JMP 11 statistical software package (SAS Institute Inc, Cary, NC, USA). A value of $p < .05$ was considered to be statistically significant.

Results

Seventeen patients exhibited positive results when evaluated using the knee-up test, whereas 521 patients exhibited negative results. Sixteen of the patients with positive results were determined to have new-onset motor deficits, whereas no new-onset motor deficits were observed in the remaining patient. Of the 521 patients with negative knee-up test results, only 2 were determined to have new-onset motor deficits, whereas no new-onset motor deficits were observed in the remaining 519 patients (Fisher exact $p < .0001$; odds ratio, 4152; 95% confidence interval, 357.8–48185.4) (Table 1). The sensitivity, specificity, PPV, and NPV of this test for all cases were 88.89,

Table 1
Relationship between the presence of postoperative new onset motor deficit and knee-up test findings

	The presence of postoperative new onset motor deficit		
	Yes	No	Total
Knee-up test positive	16 patients	1 patient	17 patients
Knee-up test negative	2 patients	519 patients	521 patients
Total	18 patients	520 patients	538 patients

Fisher exact $p < .0001$; odds ratio, 4152; 95% confidence interval, 357.8–48185.4. The sensitivity, specificity, positive predictive value, and negative predictive value of this test were 88.89, 99.81, 94.12, and 99.62, respectively.

99.81, 94.12, and 99.62, respectively. The kappa coefficient for the knee-up test between observers was 0.91 ($p < .0001$).

Of the 18 patients with new-onset motor deficits, 16 exhibited positive knee-up test results (Table 2). Interestingly, patients whose lesions were below the L3–L4 level exhibited positive knee-up test results when hip abductor function had decreased by two points or fewer. However, two patients with normal hip abductor function exhibited negative knee-up test results.

Patients with positive knee-up test results underwent detailed neurologic examination immediately following extubation, and MRI and CT scans were performed if deemed necessary. The causative factors leading to the motor deficits were as follows: damage caused by intraoperative manipulation of neural tissue in 11 cases, epidural hematoma in 3 cases, insufficient decompression in 2 cases, bony fragment in 1 case, and unknown cause in 1 case. All case of epidural hematoma and one of insufficient decompression required immediate re-operation, following which neurologic deteriorations fully recovered.

One patient with intramedullary thoracic spinal cord tumor exhibited a false-positive result on the knee-up test. This patient had completely lost position sensation after tumor resection but had no postoperative motor weakness.

Discussion

Many patients with new-onset major neurologic deficit require further surgical procedures [2,3,5–7,11,12]. Early diagnosis of such deficits following spinal surgery may allow enough time for MRI and CT evaluation and prompt decisions regarding re-operation [5,9].

The use of electrophysiological monitoring for neurologic safety during spinal surgery has become widespread. Efficacy requires multimodal monitoring, associating somatosensory evoked potentials to motor potentials evoked by transcranial stimulation [8,17,24]. Despite the usefulness of multimodal monitoring, it is not applied to all cases of spinal surgery. Hamilton et al. [18] reported that neuromonitoring was used in 65% of 108,419 operative cases from 2004 to 2007. However, the sensitivity and PPV for neuromonitoring with regard to new-onset neurologic complication were surprisingly low (sensitivity, 0.43; PPV, 0.21).

In any case, neurologic examination upon awakening is mandatory for detecting new-onset neurologic motor deficit. However, some patients may not be able to cooperate with the physician in performing the neurologic examination because of age, language barriers, or mental status [17]. The absence of deep tendon reflexes secondary to spinal shock provides good indication for the onset of new motor deficits. However, 46% ($n=247$) of the 538 patients included in the present study exhibited preoperative areflexia, so evaluation of postoperative areflexia is not always useful for detecting new-onset motor deficits. Moreover, three patients with incomplete spinal cord damage exhibited no signs of areflexia.

What are the key muscles for keeping the knee in its lifted position? We re-analyzed the 96 legs of the 48 patients reported in our previous article confirmed to have myelomalacia [21]. All legs were evaluated on their ability to maintain the knee in an upright position, and the relationship of this result with the strength of each leg muscle was analyzed using a multiple logistic regression model. According to these results, hip flexors, hip adductors, and hip abductors were the statistically significant muscles for keeping the knee in its lifted position (Table 3). Anatomically, the hip flexors are innervated by the L1–L4 nerve roots, whereas the hip adductors are innervated by the L2–L4 nerve roots, and the hip abductors are innervated by the L4–S2 nerve roots [25], indicating that results of the knee-up test may be influenced by dysfunction of nerve roots L1–S2. Because of the aforementioned anatomical features, it may be possible to identify severe new-onset motor deficits below the level of L3–L4. However, when the patient had motor weakness in muscles unrelated to these hip functions, the knee-up test could not detect new-onset motor deficit. This is a limitation of the knee-up test. A second limitation is that patients with severe joint OA who cannot lift the knee into an upright position will seem to have difficulty maintaining the knee-up position. Disagreement over the results occurred in two patients with severe knee OA; thus, it is necessary to evaluate the results of the test carefully. A third limitation is that the knee-up test is not applicable to patients with severe paralysis who are unable to preoperatively lift both knees—a precondition for performing the knee-up test.

Although the knee-up test presents an easy method for detecting new-onset postoperative motor deficits without the patient's cooperation, the exact time frame for performing the test is of little importance. Garreau de Loubresse [24] emphasizes the importance of repetition of the neurologic examination by a co-medical care staff who should be alerted in case of any change in motor parameters. For the co-medical staff, the knee-up test upon awakening is not only very easy to perform without the patient's cooperation but is also easy to evaluate.

There are several possible limitations associated with this study. First, the sample size was relatively small. Second, the knee-up test was performed at a single institution. Finally, despite the fact that this test was performed

Table 2
Details of new-onset motor deficits observed in study participants

Case	Preoperative diagnosis	Operation	Knee-up test	Motor deficits	Cause of deficits	Progress of case
1	Intradural-extradural spinal tumor	Extirpation of tumor at T2–T4	Left side positive	Left HAB decreased from 5 to 2, ADF from 5 to 3, LE from 5 to 3, and AF from 5 to 4.	Damage caused by intraoperative manipulation of neural tissue (tumor resection)	Re-operation was not required. Leg motor function fully improved within 2 mo of operation.
2	Intradural-extradural spinal tumor	Extirpation of tumor at T4–T7	Left side positive	Left HAB decreased from 4 to 2, ADF from 5 to 3, and LE from 5 to 4.	Damage caused by intraoperative manipulation of neural tissue (tumor resection)	Re-operation was not required. Leg motor function fully improved within 1 y of operation.
3	Intradural-extradural spinal tumor	Extirpation of tumor at T9–T12	Right side positive	Right HAB decreased from 4 to 2 and KE from 5 to 3.	Damage caused by intraoperative manipulation of neural tissue (tumor resection)	Re-operation was not required. Leg motor function fully improved within 1 y of operation.
4	Intradural spinal tumor	Extirpation of tumor at C1–C2	Right side positive	Right FF decreased from 4 to 3, SFA from 3 to 2, HAB from 4 to 2, ADF from 4 to 2, and LE from 4 to 2.	Damage caused by intraoperative manipulation of neural tissue (tumor resection)	Re-operation was not required. Leg motor function fully improved and upper limb function partially improved within 1 y of operation.
5	Intradural spinal tumor	Extirpation of tumor at C4–C5	Right side positive	Right EF decreased from 5 to 4, WE from 5 to 2, EE from 5 to 2, FF from 5 to 3, SFA from 4 to 2, HF from 5 to 3, HAD from 5 to 3, HAB from 5 to 2, ADF from 5 to 3, LE from 5 to 3, and AF from 5 to 3.	Damage caused by intraoperative manipulation of neural tissue (tumor resection)	Re-operation was not required. All motor function except FF and SFA fully improved within 1 y of operation.
6	Intradural spinal tumor	Extirpation of tumor at C3–C4	Both sides positive	AIS deteriorated from D to B.	Damage caused by intraoperative manipulation of neural tissue (tumor resection)	Re-operation was not required. AIS improved from B to D within 1 y of operation.
7	OPLL	Posterior decompression and fusion at T9–T11	Both sides positive	AIS deteriorated from D to C.	Damage caused by intraoperative manipulation of neural tissue (ossification resection)	Re-operation was not required. Leg motor function fully improved within 1 y of operation.
8	OPLL	Posterior decompression and fusion at T7–T9	Both sides positive	AIS deteriorated from D to B.	Damage caused by intraoperative manipulation of neural tissue (ossification resection)	Re-operation was not required. AIS improved from B to C within 1 y of operation.
9	OPLL	Laminoplasty at C3–C7	Negative	Both EE decreased from 4 to 2.	Unknown (probably root tethering)	Re-operation was not required. Both EE improved from 2 to 3 within 1 y of operation.
10	Arachnoid cyst	Removal of cyst at T5–T11	Left side positive	Left HAB decreased from 4 to 2, ADF from 5 to 3, and AF from 5 to 3.	Damage caused by intraoperative manipulation of neural tissue (cyst resection)	Re-operation was not required. Left HAB improved from 2 to 5, AF from 3 to 5 within 1 y of operation.
11	Lumbar disc herniation	Discectomy at L3–L4	Left side positive	Left HAB decreased from 5 to 2 and ADF from 4 to 2.	Damage caused by intraoperative manipulation of neural tissue (nerve root neurolysis)	Re-operation was not required. Left HAB improved from 2 to 5, ADF from 2 to 3 within 1 y of operation.
12	Lumbar degenerative spondylolisthesis	Posterior decompression and fusion at L4–L5	Negative	Left ADF decreased from 5 to 4 and LE from 5 to 3.	Damage caused by intraoperative manipulation of neural tissue (nerve root neurolysis)	Re-operation was not required. Leg motor function fully improved within 8 mo of operation.

(Continued)

Table 2
(Continued)

Case	Preoperative diagnosis	Operation	Knee-up test	Motor deficits	Cause of deficits	Progress of case
13	Osteoporotic burst fracture	Posterior fixation at T11–L1 with vertebroplasty at T12	Right side positive	Right HAB decreased from 5 to 4, and AF from 4 to 3.	Leaked bony fragment from posterior vertebral wall.	Motor weakness gradually improved day by day so re-operation was not required. Right HAB improved from 2 to 4, KE from 4 to 5, and AF from 3 to 5 within 6 mo of operation.
14	Lumbar canal stenosis	Laminectomy at L3–L5	Both sides positive	Both of HAB decreased from 4 to 2, right ADF from 5 to 4, left ADF from 5 to 1, right LE from 5 to 3, left LE from 5 to 1, and right AF from 5 to 4.	Insufficient decompression and possible operative manipulation (dural tear)	Dural tear was sutured in the 1st operation; however, cauda equina syndrome developed. Patient received rehabilitation, but the paralysis gradually progressed. Myelography showed complete block at L2–L3. Posterior decompression and fusion was performed 1 mo later; however, patient had no improvement. Myelography showed complete block at T9–T10 after 1st operation.
15	Vertebral fracture with OLF at T9–T10	Posterior fixation at T1–L5	Both sides positive	AIS deteriorated from D to B.	OLF (insufficient decompression)	Laminectomy was performed and 1 y later, AIS improved from B to D. MRI showed epidural hematoma. Re-operation was performed and motor weakness fully improved within 2 d. MRI showed epidural hematoma. Re-operation was performed and motor weakness fully improved the next day. MRI showed epidural hematoma. Re-operation was performed and motor weakness fully improved within 3 mo of operation.
16	OLF	Laminectomy at T1–T2	Both sides positive	AIS deteriorated from D to C.	Epidural hematoma	
17	Idiopathic epidural hematoma	Removal of hematoma at C3–T1	Both sides positive	AIS deteriorated from D to C.	Epidural hematoma	
18	Lumbar degenerative spondylolisthesis	Posterior decompression and fusion at L4–L5	Right side positive	Right HAB decreased from 5 to 2, ADF from 4 to 3, and LE from 3 to 0.	Epidural hematoma	

SA, shoulder abductors; EF, elbow flexors; WE, wrist extensors; EE, elbow extensors; FF, finger flexors; SFA, small-finger abductors; HF, hip flexors; HAD, hip adductors; HAB, hip abductors; KE, knee extensors; ADF, ankle dorsiflexors; LE, long-toe extensors; AF, ankle plantar flexors; AIS, ASIA Impairment Scale; OLF, ossification of the ligamentum flavum; OPLL, ossification of posterior longitudinal ligament.

Table 3

Multiple logistic regression by combined muscle functions for keeping the knee in its lifted position in organic paralysis patients

Combined muscle functions	p	Odds ratio	95% Confidence interval
Hip flexors	0.0359*	28.4	1.18–162506
Hip adductors	0.0168*	375.4	1.75–37852
Hip abductors	0.0424*	43.2	1.08–11666191
Knee extensors	0.6078	0.53	0.001–4.98
Ankle dorsiflexors	0.3550	0.36	0.0009–2.56
Ankle plantar flexors	0.1383	0.01	0.0001–2.06

* p<.005.

after an anesthesiologist had judged that endotracheal extubation was possible, peripheral nerve stimulators with train-of-four ratio were not routinely used for confirmation of complete disappearance of neuromuscular block at the time of examination. Despite these limitations, we have established that the knee-up test is very easy to perform and can alert the surgeon or physician to the outbreak of postoperative motor deficits with high statistical power at very early stages. In addition, this test is useful for evaluating patients with impaired hearing or advanced age, who may find it difficult to voluntarily coordinate their movements with instructions from the physician.

In conclusion, the sensitivity, specificity, PPV, and NPV of the knee-up test were 88.89, 99.81, 94.12, and 99.62, respectively. When patients cannot maintain the knee in a lifted-up position upon awakening, the surgeon must correct their neurologic condition after the operation. On the other hand, when patients can maintain the knee-up position, in over 99% of cases, they have no severe motor deficit.

References

- [1] Winter RB. Neurologic safety in spinal deformity surgery. *Spine* 1997;22:1527–33.
- [2] Cramer DE1, Maher PC, Pettigrew DB, et al. Major neurologic deficit immediately after adult spinal surgery: incidence and etiology over 10 years at a single training institution. *J Spinal Disord Tech* 2009;22:565–70.
- [3] Yonenobu K, Okada K, Fuji T, Fujiwara K, et al. Causes of neurologic deterioration following surgical treatment of cervical myelopathy. *Spine* 1986;11:818–23.
- [4] Matsuzaki H, Tokuhashi Y, Matsumoto F, et al. Problems and solutions of pedicle screw plate fixation of lumbar spine. *Spine* 1990;15:1159–65.
- [5] Yonenobu K1, Hosono N, Iwasaki M, et al. Neurologic complications of surgery for cervical compression myelopathy. *Spine* 1991;16:1277–82.
- [6] West JL 3rd, Ogilvie JW, Bradford DS. Complications of the variable screw plate pedicle screw fixation. *Spine* 1991;16:576–9.
- [7] Esses SI, Sachs BL, Dreyzin V. Complications associated with the technique of pedicle screw fixation. A selected survey of ABS members. *Spine* 1993;18:2231–8, discussion 2238–9.
- [8] Padberg AM, Wilson-Holden TJ, Lenke LG, et al. Somatosensory- and motor-evoked potential monitoring without a wake-up test during idiopathic scoliosis surgery. An accepted standard of care. *Spine* 1998;23:1392–400.
- [9] Bridwell KH, Lenke LG, Baldus C, et al. Major intraoperative neurologic deficits in pediatric and adult spinal deformity patients. Incidence and etiology at one institution. *Spine* 1998;23:324–31.
- [10] Suk SI, Kim WJ, Lee SM, et al. Thoracic pedicle screw fixation in spinal deformities: are they really safe? *Spine* 2001;26:2049–57.
- [11] Bridwell KH, Lewis SJ, Edwards C, et al. Complications and outcomes of pedicle subtraction osteotomies for fixed sagittal imbalance. *Spine* 2003;28:2093–101.
- [12] Nohara Y, Taneichi H, Ueyama K, et al. Nationwide survey on complications of spine surgery in Japan. *J Orthop Sci* 2004;9:424–33.
- [13] Sallhan F, Golligly S, Roussouly P. The radiographic results and neurologic complications of instrumented reduction and fusion of high-grade spondylolisthesis without decompression of the neural elements: a retrospective review of 44 patients. *Spine* 2006;31:161–9, discussion 170.
- [14] Cho KJ, Suk SI, Park SR, et al. Complications in posterior fusion and instrumentation for degenerative lumbar scoliosis. *Spine* 2007;32:2232–7.
- [15] Kalanithi PS, Patil CG, Boakye M. National complication rates and disposition after posterior lumbar fusion for acquired spondylolisthesis. *Spine* 2009;34:1963–9.
- [16] Rodgers WB, Gerber EJ, Patterson J. Intraoperative and early postoperative complications in extreme lateral interbody fusion: an analysis of 600 cases. *Spine* 2011;36:26–32.
- [17] Pastorelli F, Di Silvestre M, Plasmati R, et al. The prevention of neural complications in the surgical treatment of scoliosis: the role of the neurophysiological intraoperative monitoring. *Eur Spine J* 2011;20(Suppl. 1):S105–14.
- [18] Hamilton DK, Smith JS, Sansur CA, et al. Rates of new neurological deficit associated with spine surgery based on 108,419 procedures: a report of the Scoliosis Research Society morbidity and mortality committee. *Spine* 2011;36:1218–28.
- [19] Imajo Y, Taguchi T, Yone K, et al. Japanese 2011 nationwide survey on complications from spine surgery. *J Orthop Sci* 2015;20:38–54.
- [20] Ogilvie JW. Complications in spondylolisthesis surgery. *Spine* 2005;30(6 Suppl.):S97–101.
- [21] Yugué I, Shiba K, Ueta T, et al. A new clinical evaluation for hysterical paralysis. *Spine* 2004;29:1910–13, discussion 1913.
- [22] AARC. AARC Clinical practice guideline removal of the endotracheal tube—2007 revision & update. *Respir Care* 2007;52:81–93.
- [23] Kirshblum SC, Burns SP, Biering-Sorensen F, et al. International standards for neurological classification of spinal cord injury (revised 2011). *J Spinal Cord Med* 2011;34:535–46.
- [24] Garreau de Loubresse C. Neurological risks in scheduled spinal surgery. *Orthop Traumatol Surg Res* 2014;100(1 Suppl.):S85–90.
- [25] Platzer W. Color atlas of human anatomy, locomotor system, vol. 1. New York: Thieme; 2004.

Morphologic Evaluation of Lumbosacral Nerve Roots in the Vertebral Foramen

Measurement of Local Pressure of the Intervertebral Foramen

Yuichiro Morishita, MD, PhD, Muneaki Masuda, MD, Takeshi Maeda, MD, PhD, Takayoshi Ueta, MD, PhD, and Keiichiro Shiba, MD, PhD

Study Design: The prospective cohort study.

Objective of the Study: The objective was to evaluate the relationships between local pressure changes of the intervertebral foramen during lumbar spine extension and lumbar foraminal morphology.

Summary of Background Data: The physiological states of lumbosacral nerve roots in the vertebral foramen remain controversial.

Methods: We evaluated 56 lumbosacral vertebral foramina in 21 patients with L4-degenerative spondylolisthesis. All patients underwent L4-5 posterolateral fusion (PLF). The local pressure of the intervertebral foramen was measured intraoperatively, and measurement was performed before and after L4-5 PLF. We defined the changes in the ratio of local pressure between lumbar flexion to extension as percent pressure. The sagittal angular motion, distance between the inferior cortex of the cranial pedicle and superior cortex of the caudal pedicle, posterolateral margin of the superior vertebral body and superior articular facet, posterolateral edge of the superior vertebral body and inferior articular facet, and the intervertebral disc height were measured using preoperative functional plain radiographs and CT images.

Results: The average local pressure of the intervertebral foramen significantly increased during lumbar extension. However, the L4-5 vertebral foraminal pressure after PLF were nearly identical. There was no significant correlation between percent pressure and lumbar range of motion. Furthermore, there were no significant correlations between percent pressure and each morphologic parameter of the lumbar foramen.

Conclusions: There were no significant relationships between the lumbar foraminal morphology and intervertebral foraminal pressure changes during lumbar extension, and L4-5 vertebral foraminal pressure was not affected by the lumbar posture after L4-5 posterior fusion. On the basis of the results, the external

dynamic stresses on the nerve roots in the vertebral foramen might be improved by lumbar posterior fusion using instrumentation without direct decompression of the vertebral foramen.

Key Words: local pressure of the intervertebral foramen, percent pressure, morphology of lumbar foramen, lumbar range of motion, intervertebral disc height, posterolateral fusion, lumbosacral nerve root, L4-degenerative spondylolisthesis, vertebral foramen, foraminal stenosis

(*Clin Spine Surg* 2016;00:000-000)

The anatomic boundaries of the intervertebral foramen consist of the adjacent vertebral pedicles superiorly and inferiorly, posterolateral margin of the superior vertebral body, the intervertebral disc, the posterolateral vertebral notch of the inferior vertebral body anteriorly, and the ligamentum flavum and superior and inferior articular facets posteriorly.¹ In addition, transforaminal or intraforaminal ligaments are present in the inferior aspect of the foramen.^{2,3} The geometry of the lumbar foramen has been described as an oval, round, or inverted teardrop-shaped window in the lateral aspect of the lumbar spine.⁴

The lumbosacral nerve roots traverse through the lateral canal after originating from the thecal sac. The existing nerve root and dorsal root ganglion (DRG), often located in the superior and anterior region of the foramen or subpedicular notch, are surrounded by fat and radicular vessels. The location of the DRG can vary; it can be intraforaminal or intraspinal in the lumbosacral spine.^{5,6} The S1 DRG, found in a more cephalad or intraspinal location, is larger than the lumbar DRG. The L4 and L5 DRG are more commonly located intraforaminally.^{5,6} The spatial relation of the DRG in the lumbar foramen is a clinically important concept to understand because of its association with lumbar symptomatology.

There are numerous studies regarding the anatomic or morphologic evaluation of the lumbar foramen. However, to the best of our knowledge, the physiological state of lumbosacral nerve roots in the vertebral foramen has been described in only a few reports. We previously

Received for publication September 17, 2015; accepted July 21, 2016.
From the Department of Orthopedic Surgery, Spinal Injuries Center, Iizuka, Japan.

The authors declare no conflict of interest.

Reprints: Yuichiro Morishita, MD, PhD, 550-4, Igisu, Iizuka 820-0053, Japan (e-mail: uchiro1968@mac.com).

Copyright © 2016 Wolters Kluwer Health, Inc. All rights reserved.

reported that the local pressure of the intervertebral foramen significantly increased during lumbar spine extension.⁷⁻⁹ Furthermore, the electrophysiological values of the L5 nerve roots, as evaluated from the compound muscle activation potentials from the tibialis anterior muscle after L5 nerve root stimulation, deteriorated with the increasing local pressure of the L5-S1 intervertebral foramen.^{8,9} The local pressure of the intervertebral foramen reflected the electrophysiological values of the spinal nerve roots in the vertebral foramen. The objective of this current study was to determine the relationships between local pressure changes of the intervertebral foramen during lumbar spine extension and lumbar foraminal morphology.

MATERIALS AND METHODS

Measurement of the Local Pressure of the Intervertebral Foramen⁷⁻⁹

A total of 21 L4-degenerative spondylolisthesis patients with lumbar spinal canal stenosis at the L4-5 and/or L3-4 segments (8 men and 13 women; average age, 66.0 y; age range, 47–79 y) were included in the study. The following subjects were excluded from the study: patients diagnosed as having isthmic spondylolisthesis, obvious foraminal stenosis on magnetic resonance imaging or responsible lesion in the intravertebral or extravertebral foramen, or Meyerding¹⁰ grade of degenerative spondylolisthesis > II. Fifty-six lumbosacral vertebral foramina, including 26 L4-5 and 30 L5-S1 vertebral foramina, were finally evaluated.

All patients underwent L4-5 and/or L3-4 bilateral laminotomy with L4-5 posterolateral fusion (PLF) using instrumentation. The operation was performed with the patients under general anesthesia and placed in the prone position with both hip joints in flexion.

A micro-tip 5F flexible catheter transducer (MPC-500, Millar Instruments Inc., TX) was used as a pressure transducer. Before measuring the pressure, the tip of the catheter transducer was placed in saline at a constant temperature of 37°C for 30 minutes. Zero balancing of the transducer was performed after a few minutes after temperature equilibrium was reached. Before recording, the output signals of the pressure measurement equipment were calibrated.

Intraoperatively, after L4-5 and/or L3-4 bilateral laminotomy, the pedicle screws were inserted into L4 and L5 pedicles bilaterally. For the subjects treated with laminotomy at both L4-5 and L3-4 segments, the L4-5 and L5-S1 vertebral foraminal pressures were measured. Although for the subjects treated with laminotomy at only L4-5 segment, the L5-S1 vertebral foraminal pressure was measured. The catheter transducer was inserted from the decompressed segments (L3-4 or L4-5) into the caudal vertebral foramen (L4-5 or L5-S1), and the tip of the catheter transducer was placed just below the pedicle in the vertebral foramen (pedicle zone in the vertebral foramen) dorsal to the spinal nerve root. The local pressure was continuously measured while the lumbar spine



FIGURE 1. The vertical and sagittal dimensions of the lumbar foramen. (1) The distance between inferior cortex of the cranial pedicle and superior cortex of the caudal pedicle. (2) The distance between posterior margin of the superior vertebral body and superior articular facet. (3) The distance between posterior edge of the superior vertebral body and inferior articular facet. (4) The distance between posterior margins of the disc height.

postures were changed. Two different postures, include lumbar spine flexion and extension, were studied, and each posture was maintained for 10 seconds. The measurements were performed before and after L4-5 internal fixation. The pressure levels showed a waveform with respiratory pulsation and we estimated the average values to be the intermediate value of the wave. The changes in the ratio of the local pressure of the intervertebral foramen between lumbar spine flexion and extension was calculated as a percent pressure (%) = $\{(\text{local pressure with extension} - \text{local pressure with neutral}) / (\text{local pressure with neutral})\} \times 100$.

Institutional Review Board approval was granted and informed consent was obtained from all patients.

TABLE 1. The Average Values of Local Pressure of L4-5 Vertebral Foramen

	Neutral		Extension	% Pressure
Before fixation	33.82 ± 15.85	***	56.07 ± 23	79.66 ± 69.18
After fixation	40.37 ± 19.21	NS	42.32 ± 18.72	7.07 ± 10.2

NS indicates not significant.

*** $P < 0.001$.

TABLE 2. The Average Values of Local Pressure of L5-S Vertebral Foramen

	Neutral		Extension	% Pressure
Before fixation	25.41 ± 17.8	***	49.73 ± 28.05	138.05 ± 159.34
After fixation	25.07 ± 16.83	***	54.96 ± 34.24	153.82 ± 205.5

NS indicates not significant.
*** $P < 0.001$.

Lumbar Spine Range of Motion (ROM)

Using functional plain radiographs in the sagittal plane, the sagittal angular motion from lumbar spine flexion to extension was measured with the Cobb technique (angle between superior and inferior vertebral endplate) at the L4-5 or L5-S segment.

Morphometric Measurement of the Lumbar Foramen

The vertical and sagittal dimensions of the lumbar foramen were measured with the preoperative parasagittal CT images at the middle of the pedicle. We conducted the following 4 measurement: the distance between the (1) inferior cortex of the cranial pedicle and superior cortex of the caudal pedicle, (2) posterosuperior margin of the superior vertebral body and superior articular facet, and (3) posteroinferior edge of the superior vertebral body and inferior articular facet; and the (4) intervertebral disc height at the posterior margin of the disc height (Fig. 1).

Statistical Analysis

The Mann-Whitney U test and Pearson correlation coefficient were used for statistical analyses. A P -value of < 0.05 was considered statistically significant.

RESULTS

Local Pressure of the Intervertebral Foramen

The average local pressures of the intervertebral foramen ($n = 56$; including 26 L4-5 and 30 L5-S foramina) with lumbar spine flexion and extension before L4-5 PLF were 29.31 ± 17.3 mm Hg and 53.68 ± 25.8 mm Hg, respectively. The average local pressure significantly increased during lumbar spine extension ($P < 0.001$). The percent pressure was $110.94\% \pm 128.16\%$.

The average local pressures of the intervertebral foramen at the L4-5 segment are shown in Table 1. The local pressures of the intervertebral foramen significantly increased during lumbar spine extension before L4-5 PLF, but were nearly identical after PLF. The percent pressure before and after L4-5 PLF was significantly different.

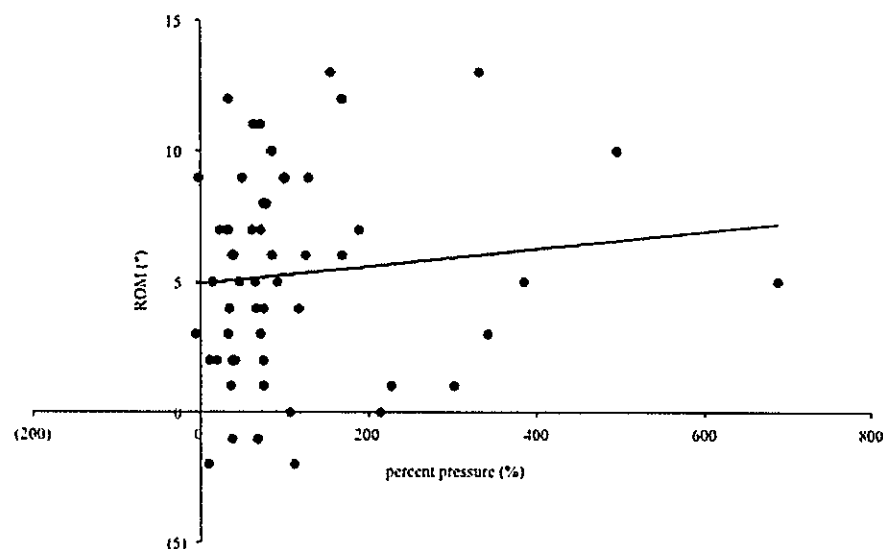
The average local pressures of the intervertebral foramen at the L5-S segment are shown in Table 2. The local pressures of the intervertebral foramen, both before and after L4-5 PLF, significantly increased during lumbar spine extension. The percent pressure was not significantly different between before and after L4-5 PLF; however, the percent pressure after PLF tended to be higher than that obtained before PLF.

Lumbar Spine ROM

The average value of the sagittal angular motion from lumbar spine flexion to extension was 5.17 ± 4.11 degrees. There was no significant correlation between the percent pressure and lumbar ROM ($P = 0.42$, $r = 0.11$; Fig. 2).

Morphometric Analysis of the Lumbar Foramen

The average distance between the inferior cortex of the cranial pedicle and superior cortex of the caudal

**FIGURE 2.** No significant correlation was observed between the percent pressure and lumbar range of motion. [full color online](#)

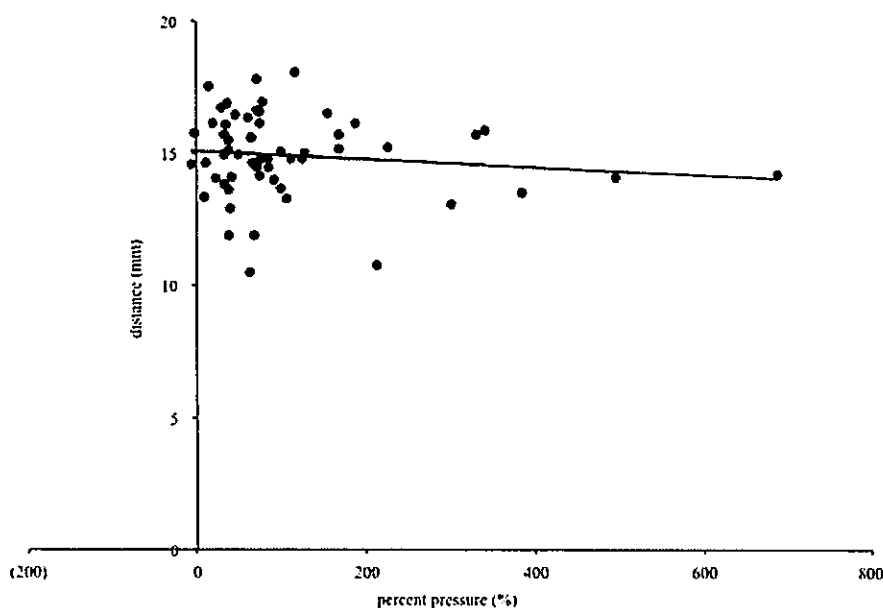


FIGURE 3. No significant correlation was observed between the percent pressure and the distance between inferior cortex of the cranial pedicle and superior cortex of the caudal pedicle. [full color online](#)

pedicle, posterosuperior margin of the superior vertebral body and superior articular facet, and posteroinferior edge of the superior vertebral body and inferior articular facet were 8.62 ± 1.89 , 14.91 ± 1.59 , and 7.98 ± 2.86 mm, respectively. The average value of intervertebral disc height was 3.84 ± 1.49 mm. There were no significant correlations between the percent pressure and each mor-

phologic parameter of the lumbar foramen ($P = 0.2$, $r = -0.17$; $P = 0.36$, $r = -0.13$; $P = 0.14$, $r = -0.2$; $P = 0.24$, $r = -0.16$; respectively; Figs. 3–6).

DISCUSSION

The foraminal height and width varies from 15.9 to 18.0 mm and from 5.0 to 7.2 mm, respectively,¹¹ and the

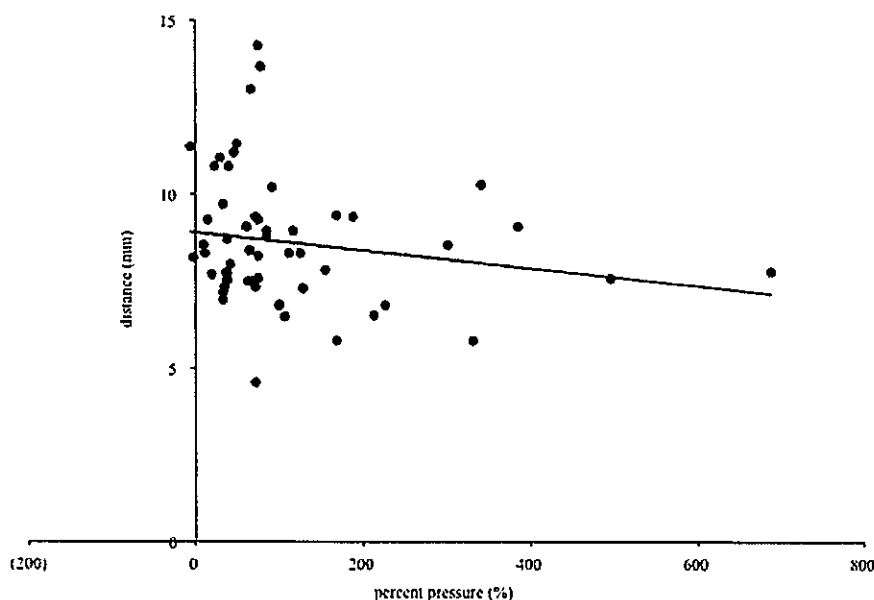


FIGURE 4. No significant correlation was observed between the percent pressure and the distance between posterior margin of the superior vertebral body and superior articular facet. [full color online](#)

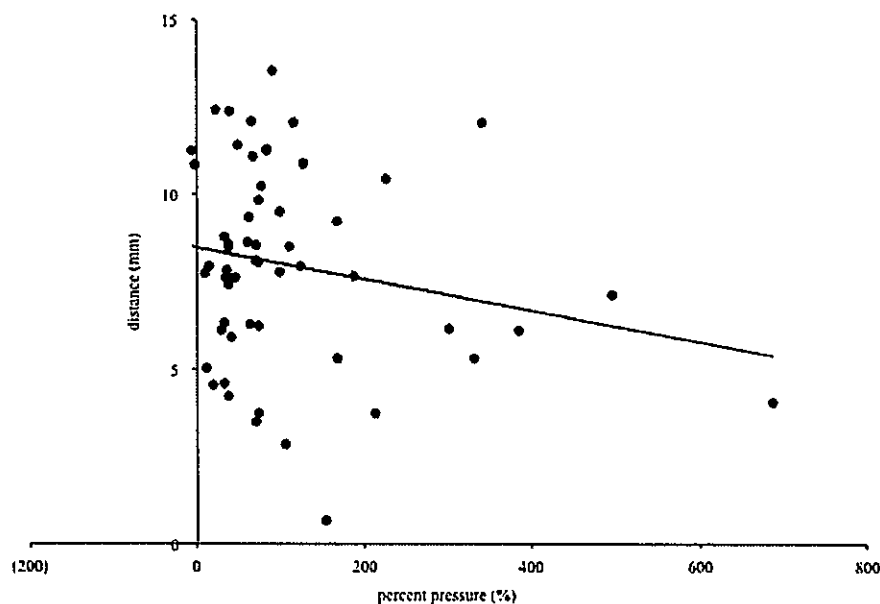


FIGURE 5. No significant correlation was observed between the percent pressure and the distance between posterior edge of the superior vertebral body and inferior articular facet. [full color online](#)

cross-sectional area vary from 40 to 160 mm².⁴ The development of foraminal stenosis is related to the process of lumbar spondylosis. Hasegawa et al¹² reported that critical dimensions of foraminal stenosis are 4 mm or less for the posterior disc height and 15 mm or less for the foraminal height. However, in our results, posterior disc height was 3.84 ± 1.49 mm and foraminal height (distance between the inferior cortex of the cranial pedicle and superior cortex of the caudal pedicle) was 8.62 ± 1.89 mm; none of the subjects showed obvious

foraminal stenosis on the images or responsible lesion in the intravertebral or extravertebral foramen. We presume that the bony foraminal stenosis on the images may not directly reflect the clinical symptomatology.

Mayoux-Benhamou et al¹³ reported that all diameters of the lumbar vertebral foramina decreased as the spine moved from flexion to extension. Inufusa et al¹⁴ also showed that the cross-sectional area of the vertebral foramen increased by 12% during flexion and decreased by 15% during extension. The lumbosacral nerve roots

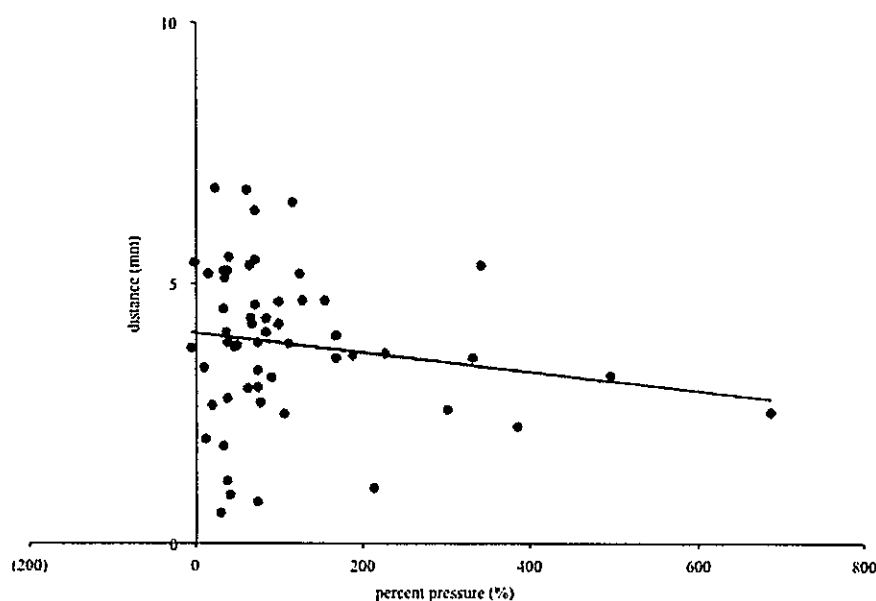


FIGURE 6. No significant correlation was observed between the percent pressure and the disc height. [full color online](#)

normally occupy ~30% of the available foraminal area.¹⁵ According to our findings, the local pressure of the intervertebral foramen significantly increased during lumbar spine extension. Moreover, the local pressure of the intervertebral foramen reflected the electrophysiological values of the spinal nerve roots in the vertebral foramen in our previous published study.^{8,9} According to these results, the spatial volume of the spinal nerve root in the vertebral foramen may increase relatively to the decreasing the capacity of the vertebral foramen during lumbar spine extension, and the external dynamic stresses on the spinal nerve root in the vertebral foramen may increase during lumbar spine extension.

The genesis of neurological intermittent claudication in lumbar spinal canal stenosis might be greatly affected by dynamic changes in the local pressure of the intervertebral foramen due to lumbar motion, rather than the static local pressure with each lumbar posture.⁹ According to the current results, there were no significant relationships between the morphology of lumbar foramen and local pressure changes of the intervertebral foramen between lumbar spine flexion and extension, and the L4-5 vertebral foraminal pressure was not affected by the lumbar posture after L4-5 posterior fusion. Although the lumbar interbody fusion (posterior or transforaminal) may have advantages in postoperative bony union or certain decompression, abundant intraoperative or postoperative hemorrhage and postoperative infection may be suspected due to curettage of the intervertebral discs and insert the foreign substance in the intervertebral disc space. On the basis of the results, the external dynamic stresses on the nerve roots in the vertebral foramen might be improved by lumbar posterior fusion using instrumentation without direct decompression of the vertebral foramen.

Some issues remain unaddressed in the current study. Subjects with obvious foraminal stenosis based on the images or clinical symptoms were not discussed in the study. Therefore, the current investigation can be considered as a pilot study, and further research using a larger patient population may help to resolve several unclear issues in this study. Moreover, the physiological states of the pathologic condition of the lumbosacral

nerve roots in the vertebral foramen should be clarified in more detail.

REFERENCES

1. Gilchrist RV, Slipman CW, Bhagia SM. Anatomy of the intervertebral foramen. *Pain Physician*. 2002;5:372-378.
2. Hasegawa T, An H, Haughton V. Imaging anatomy of the lateral lumbar spinal canal. *Semin Ultrasound CT MRI*. 1993;14:404-413.
3. Nowicki B, Haughton V. Neural foraminal ligaments of the lumbar spine: appearance at CT and MR imaging. *Radiology*. 1992;183:257-264.
4. Stephens MM, Evans JH, O'Brien JP. Lumbar intervertebral foramina. An *in vitro* study of their shape in relation to intervertebral disc pathology. *Spine*. 1991;16:525-529.
5. Hasegawa T, Mikawa Y, Watanabe R, et al. Morphometric analysis of the lumbosacral nerve roots and dorsal root ganglia by magnetic resonance imaging. *Spine*. 1996;21:1005-1009.
6. Kikuchi S, Sato K, Konno S, et al. Anatomic, radiographic study of dorsal root ganglia. *Spine*. 1994;19:6-11.
7. Morishita Y, Maeda T, Ueta T, et al. Pathophysiological effects of lumbar instrumentation surgery on lumbosacral nerve roots in the vertebral foramen: measurement of local pressure of intervertebral foramen. *Spine*. 2014;39:E1256-E1260.
8. Morishita Y, Hida S, Naito M, et al. Measurement of the local pressure of the intervertebral foramen and the electrophysiologic values of the spinal nerve roots in the vertebral foramen. *Spine*. 2006;31:3076-3080.
9. Morishita Y, Hida S, Naito M, et al. Neurogenic intermittent claudication in lumbar spinal canal stenosis: the clinical relationship between the local pressure of the intervertebral foramen and the clinical findings in lumbar spinal canal stenosis. *J Spinal Disord Tech*. 2009;22:130-134.
10. Meyerding HW. Spondylolisthesis. *J Bone Joint Surg Am*. 1931;13:39-48.
11. Senoo I, Espinoza Orias AA, An HS, et al. *In vivo* 3-dimensional morphometric analysis of the lumbar foramen in healthy subjects. *Spine*. 2014;39:E929-E935.
12. Hasegawa T, An HS, Haughton VM, et al. Lumbar foraminal stenosis: Critical height of the intervertebral discs and foramina. A cryomicrotome study in cadaver. *J Bone Joint Surg Am*. 1995;77:32-38.
13. Mayoux-Benhamou MA, Revel M, Aaron C, et al. A morphometric study of the lumbar foramen: influence of flexion-extension movements and of isolated disc collapse. *Surg Radiol Anat*. 1989;11:97-102.
14. Inufusa A, An HS, Lim TH, et al. Anatomic changes of the spinal canal and intervertebral foramen associated with flexion-extension movement. *Spine*. 1996;21:2412-2420.
15. Hasue M, Kunogi J, Konno S, et al. Classification by position of dorsal root ganglia in the lumbosacral region. *Spine*. 1989;14:1261-1264.

Kinematic Effects of Cervical Laminoplasty for Cervical Spondylotic Myelopathy on the Occipitoatlantoaxial Junction

Asuka Desroches, MD,* Yuichiro Morishita, MD, PhD,† Itaru Yague, MD, PhD,†
Takeshi Maeda, MD, PhD,† Charles-Henri Flouzat-Lachaniette, MD,*
Philippe Hernigou, MD, PhD,* and Keiichiro Shiba, MD, PhD†

Study Design: A retrospective evaluation of sagittal angular motion from cervical spinal flexion to extension.

Objective: To evaluate the kinematic effects of cervical laminoplasty for cervical spondylotic myelopathy (CSM) on the occipitoatlantoaxial junction.

Summary of Background Data: The kinematic effects of cervical laminoplasty for CSM on the occipitoatlantoaxial junction remain controversial.

Methods: A total of 65 CSM patients who were treated with cervical laminoplasty ranging from the C3 to C7 vertebrae were included in the study. After surgery, all patients wore a Philadelphia collar for the first week and began cervical range of motion exercises as soon as possible. Functional plain radiographs were obtained preoperatively and at 1 and 3 years postoperatively. Sagittal angular motion from cervical spinal flexion to extension was measured using the Cobb technique at 7 cervical segments (Oc-C1, C1-C2, C2-C3, C3-C4, C4-C5, C5-C6, and C6-C7). We defined the contribution of each segment's mobility to the total angular mobility of the cervical spine as percent segmental mobility.

Results: Total cervical angular mobility significantly decreased after cervical laminoplasty. There were no significant differences in Oc-C2 angular mobility; however, C2-C7 angular mobility had significantly decreased by 3 years postoperatively. No significant differences in percent segmental mobility were observed at 1 year postoperatively except at the C3-C4 segment. By 3 years postoperatively, percent mobility at the Oc-C1 and C1-C2 segments had significantly increased, whereas that at the C3-C4 and C5-C6 segments had significantly decreased.

Conclusions: Our results suggest that, although the contribution of occipitoatlantoaxial junctional mobility to total cervical

mobility increases, dynamic mechanical stress to the occipitoatlantoaxial junction does not increase following laminoplasty, and no adjacent segmental disorder at the occipitoatlantoaxial junction was observed within 3 years postoperatively. We hypothesized that early removal of the cervical collar and early cervical range of motion exercises may contribute to these kinematic changes.

Key Words: cervical spondylotic myelopathy, cervical laminoplasty, cervical spine, occipitoatlantoaxial junction, sagittal angular motion, percent segmental mobility, functional plain radiographs, kinematic evaluation, Oc-C2, C2-C7

(*Clin Spine Surg* 2016;00:000-000)

Cervical spondylotic myelopathy (CSM) is the development of long-tract signs secondary to degenerative changes in the cervical spinal column. CSM is the most common cause of myelopathy in patients older than 50 years of age. A careful evaluation of the patient's history and physical examination allow early diagnosis and treatment and can prevent neurological deterioration, leading to optimal clinical outcomes.

There are many surgical procedures for addressing multilevel cervical compressive myelopathy. Posterior cervical decompression with laminectomy effectively decompresses the spinal cord in patients with multilevel spondylosis, ossification of the posterior longitudinal ligament, or developmental canal stenosis. However, complications of laminectomy, including postoperative segmental instability, progressive kyphotic deformity, formation of a postlaminectomy membrane, perineural adhesions, and late neurological deterioration have been identified.¹⁻⁶ Cervical laminoplasty is considered to be an alternative to laminectomy and is intended to decompress the spinal cord while preserving the posterior elements of the vertebra.

Numerous experimental studies have reported the kinematic effects of cervical laminoplasty.^{4,7-13} However, to the best of our knowledge, few reports have thus far referred to the kinematic effects of cervical laminoplasty on the occipitoatlantoaxial junction. In the current study, we evaluated the kinematic changes in cervical mobility

Received for publication September 12, 2015; accepted July 21, 2016.
From the *Department of Orthopedic Surgery, Paris East University, Henri Mondor Hospital, Créteil, France; and †Department of Orthopedic Surgery, Spinal Injuries Center, Iizuka, Japan.
The authors declare no conflict of interest.
Reprints: Yuichiro Morishita, MD, PhD, Department of Orthopedic Surgery, Spinal Injuries Center, 550-4, Iigisu, Iizuka 820-0053, Japan (e-mail: uchihiro1968@mac.com).
Copyright © 2016 Wolters Kluwer Health, Inc. All rights reserved.

following cervical laminoplasty at 1 and 3 years postoperatively. The purpose of this retrospective clinical study was to elucidate the kinematic effects of cervical laminoplasty on the occipitoatlantoaxial junction.

MATERIALS AND METHODS

Study Population

From January 2007 to December 2011, a total of 394 patients with CSM (266 males and 128 females) with an average age of 76.0 years (range, 34–89 y) underwent surgical posterior decompression by senior spine surgeons. All patients showed cervical cord intramedullary intensity changes on magnetic resonance T2-weighted images and demonstrated long-tract signs, such as finger fine motion disturbance, gait disturbance, and hyperreflexia of the deep tendons in the lower limbs. Exclusion criteria included the following: continuous ossification of the posterior longitudinal ligament at multiple segments, history of rheumatoid arthritis or cerebral palsy, and history of cervical surgery before or after the cervical laminoplasty. After exclusion, 65 patients (47 males and 18 females) with an average age of 69.2 years (range, 38–89 y) who were treated by means of cervical laminoplasty ranging from the C3 to the C7 vertebrae (including C7 dome osteotomy) were included in this study and were radiologically followed for 3 years postoperatively.

The study was approved by our Institutional Review Board, and informed consent was obtained from all patients.

Surgical Treatment: Cervical Laminoplasty and Postoperative Therapy

All patients underwent French-door cervical laminoplasty at the C3–C7 level.¹⁴ The semispinalis cervicis muscles were preserved without detachment from the axis. A threadwire saw was used to perform the sagittal split in the spinous process, and hydroxyapatite blocks were placed as struts to maintain the patency of the hinged hemilaminae (Fig. 1).¹⁵

After surgery, all patients wore a Philadelphia collar for 1 week. Cervical range of motion (ROM) exercises were performed immediately after collar removal without causing any discomfort.

Measurement of Cervical Kinematics

For all patients, functional plain sagittal radiographs were obtained preoperatively and at 1 and 3 years postoperatively. Sagittal angular motion from cervical spinal flexion to extension was measured with the Cobb technique for each segment at 7 cervical segments: Oc–C1, the angle between the line from the basion to the opisthion (Oc) and the line from the anterior to the posterior tubercle of the inferior margin of C1 (C1); C1–C2, the angle between C1 and the inferior C2 endplate; and C2–C3, C3–C4, C4–C5, C5–C6, and C6–C7, the angle between the inferior vertebral endplate of the superior vertebral body and the superior vertebral endplate of the

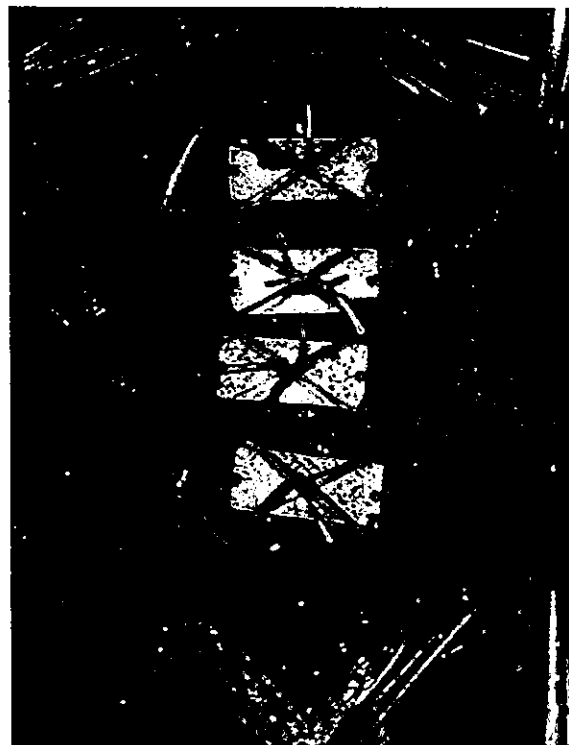


FIGURE 1. French-door cervical laminoplasty at C3–C6 and C7 dome osteotomy. The hydroxyapatite blocks were placed as a strut to maintain the patency of the hinged hemilaminae.

inferior vertebral body (Fig. 2). We defined the total sagittal motion of the cervical spine as the absolute total of the individual sagittal angular motions (Oc–C1 + C1–C2 + C2–C3 + C3–C4 + C4–C5 + C5–C6 + C6–C7) in degrees, and the contribution of each segment's mobility to the total angular mobility of the cervical spine was defined as the percent segmental mobility (%) [(sagittal angular motion of each segment in degrees)/(total sagittal angular motion in degrees) × 100].

Statistical Analysis

The Mann-Whitney *U* test was used for all statistical analyses. A *P*-value of <0.05 was considered statistically significant.

RESULTS

Table 1 shows the mean total (Oc–C7), Oc–C2, and C2–C7 cervical angular mobility preoperatively and at 1 and 3 years postoperatively. The total cervical angular mobility significantly decreased after cervical laminoplasty. With respect to Oc–C2 angular mobility, there were no significant differences at 3 years postoperatively. In contrast, with respect to C2–C7 angular mobility, significant decreases were seen at 3 years postoperatively.

Table 2 shows the mean percent segmental mobility for each segment preoperatively and at 1 and 3 years postoperatively. There were no significant differences between preoperative values and those observed 1 year

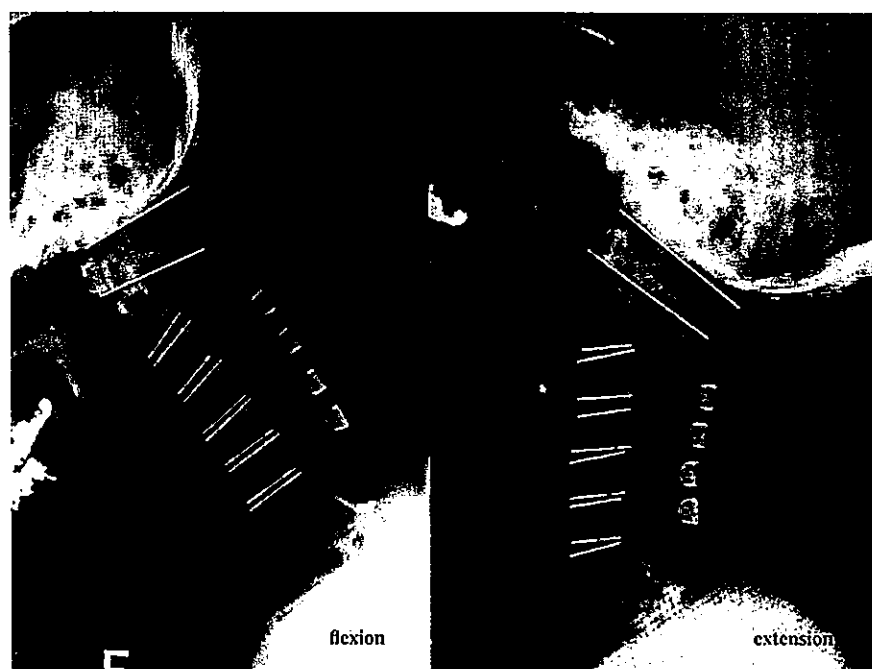


FIGURE 2. The sagittal angular motion through cervical spine flexion to extension was measured with the Cobb technique for each segment at seven cervical segments.

postoperatively, except for percent mobility at the C3–C4 segment. In a comparison of preoperative values and those at 3 years postoperatively, percent mobility at the Oc–C1 and C1–C2 segments significantly increased, whereas percent mobility at the C3–C4 and C5–C6 segments significantly decreased.

DISCUSSION

Cervical laminoplasty has been widely performed with good results in patients with multilevel cervical myeloradiculopathy.^{7,16–18} Cervical laminoplasty ideally avoids postoperative instability or the need for fusion at multiple levels. Commonly used types of laminoplasty include the expansive open-door technique,^{19,20} in which the arch is opened on one side and hinged on the contralateral side, and the French-door technique,¹⁴ in which the laminae are opened in the midline and bilaterally hinged.

Several studies have described a reduction of cervical (C2–C7) sagittal mobility after cervical laminoplasty.^{7–9,11} Loss of lordosis occurs after laminoplasty in 10%–50% of patients, and cervical ROM usually continues to diminish up to 18 months postoperatively.²¹ Some authors have reported a relationship between cervical ROM and cervical posterior deep nuchal muscle atrophy after laminoplasty.^{22–24} Fujishima and Nishi²² reported that the volume of postoperative posterior deep nuchal muscle decreased to $\leq 60\%$ of the preoperative muscle volume evaluated with computed tomography. Seichi et al⁷ and Chiba et al⁸ reported that the patients wore a cervical collar for 8–20 weeks after surgery, and postoperative cervical mobility at C2–C7 after laminoplasty was restricted to 22%–32% of preoperative cervical mobility. We believe that there is no absolute necessity of postoperative external fixation after cervical laminoplasty. We used cervical collar mainly for the

TABLE 1. The Average Values of Cervical Angular Mobility at Preoperatively, 1 Year, and 3 Years Postoperatively

	Angular Mobility (deg.)		
	Total	Oc–C2	C2–C7
Preoperative†	49.75 ± 10.57*	19.85 ± 7.05 (NS)	31.19 ± 9.84*
Postoperative 1 y‡	45.43 ± 11.5**	19.66 ± 7.25 (NS)	25.49 ± 10.09***
Postoperative 3 y	44.08 ± 12.17	21.37 ± 6.73	22.62 ± 11.26

†The Mann-Whitney *U* test.

**P* < 0.05.

***P* < 0.01.

****P* < 0.001.

†Compared with preoperative and postoperative 1 year.

‡Compared with preoperative and postoperative 3 years.

TABLE 2. The Average Values of Percent Segmental Mobility at Preoperatively, 1 Year, and 3 years Postoperatively

	Percent Segmental Mobility (%)						
	%Oc-C1	%C1-C2	%C2-C3	%C3-C4	%C4-C5	%C5-C6	%C6-C7
Preoperative†	22.46 ± 12.21 (NS)	17.5 ± 8.8 (NS)	10.77 ± 6.23 (NS)	14.99 ± 6.82*	11.67 ± 6.86 (NS)	12.23 ± 7.31 (NS)	10.38 ± 8.63 (NS)
Postoperative 1 y‡	24.4 ± 13.11**	19.65 ± 10.59*	10.05 ± 7.52 (NS)	12.08 ± 8.47***	13.43 ± 8.2 (NS)	10.08 ± 7.34**	10.31 ± 8.81 (NS)
Postoperative 3 y	28.74 ± 12.44	21.86 ± 10.25	11.07 ± 7.95	10.58 ± 8.01	10.19 ± 7.72	9.06 ± 7.95	8.5 ± 8.56

The Mann-Whitney U test.

* $P < 0.05$.** $P < 0.01$.*** $P < 0.001$.

†Compared with preoperative and postoperative 1 year.

‡Compared with preoperative and postoperative 3 years.

management of postoperative neck pain for 1 week after surgery. In our study, the C2–C7 sagittal angular mobility significantly decreased within 3 years postoperatively; however, >70% of the preoperative cervical mobility was preserved during the first 3 years postoperatively, and most patients did not complain of a limitation in activities of daily living accompanying reduced cervical mobility. We presume that early removal of the cervical collar and early cervical ROM exercises prevented contraction of the facet joint and postoperative atrophy and dysfunction of the extensor musculature of the cervical spine.

With respect to postoperative Oc–C2 mobility, Chiba et al⁸ reported that the average sagittal mobility slightly increased from 22 to 28 degrees in patients with CSM. They discussed that the severe reduction (32%) of C2–C7 sagittal mobility due to laminar fusions were compensated to some degree by the increase in sagittal mobility of the upper cervical spine, resulting in only minor disturbances in activities of daily living. Hayashi et al²⁵ demonstrated that the Oc–C1 segment of the upper cervical spine plays an important role in compensating for decreased sagittal subaxial cervical spinal motion. In our study, preoperative Oc–C2 angular mobility was 19.85 degrees, which remained almost identical over the first 3 years postoperatively. We hypothesized that due to the relatively preserved C2–C7 sagittal mobility, compensatory mobility changes may not have occurred at the upper cervical spine.

The cervical angular mobility for each segment is unreliable for evaluating a patient's cervical kinematics because these values depend on the patient's condition, that is, axial pain, or a radiologist. Therefore, we believe that the contribution of each cervical segment's mobility to the total mobility of the cervical spine is the most reliable method for evaluating the patient's cervical kinematics. In our results, only percent segmental mobility at the C3–C4 segment significantly decreased during the first postoperative year. Cervical kinematics were not affected by cervical laminoplasty at 1 year postoperatively. However, at 3 years postoperatively, percent segmental mobility at the C3–C4 and C5–C6 segments had significantly decreased, and that at the Oc–C1 and C1–C2 segments had significantly increased. Therefore, there may be no compensatory mobility changes but rather compensatory kinematic changes that occur at the occipitoatlantoaxial junction. Our results suggest that although the contribution of occipitoatlantoaxial junctional mobility to total cervical mobility increases, dynamic mechanical stresses to the occipitoatlantoaxial junction do not increase, and no adjacent segmental disorder at the occipitoatlantoaxial junction was observed within 3 years postoperatively. We hypothesized that early removal of the cervical collar and early cervical ROM exercise may have contributed to these kinematic changes.

Certain issues remain unaddressed in the current study. Our study only addressed the radiographic factors during a mid-term postoperative period and did not address clinical symptoms. Therefore, using the current investigation as a pilot study, further research using a larger

patient population and longer-term follow-up may resolve several remaining unclear issues. Moreover, the kinematic effects of cervical laminoplasty on the occipitotatlantoaxial junction need to be clarified in greater detail.

REFERENCES

1. Albert TJ, Vacarro A. Postlaminectomy kyphosis. *Spine*. 1998;23:2738–2745.
2. Baisden J, Voo LM, Cusick JF, et al. Evaluation of cervical laminectomy and laminoplasty. A longitudinal study in the goat model. *Spine*. 1999;13:1283–1289.
3. Guigui P, Benoist M, Deburge A. Spinal deformity and instability after multilevel cervical laminectomy for spondylotic myelopathy. *Spine*. 1998;23:440–447.
4. Kode S, Gandhi AA, Fredericks DC, et al. Effect of multilevel open-door laminoplasty and laminectomy on flexibility of the cervical spine. An experimental investigation. *Spine*. 2012;37:E1165–E1170.
5. Matsunaga S, Sakou T, Nakanishi K. Analysis of the cervical spine alignment following laminoplasty and laminectomy. *Spinal Cord*. 1999;37:20–24.
6. Mikawa Y, Shikata J, Yamamuro T. Spinal deformity and instability after multilevel cervical laminectomy. *Spine*. 1987;12:6–11.
7. Seichi A, Takeshita K, Ohishi I, et al. Long-term results of double-door laminoplasty for cervical stenotic myelopathy. *Spine*. 2001;26:479–487.
8. Chiba K, Ogawa Y, Ishii K, et al. Long-term results of expansive open-door laminoplasty for cervical myelopathy—average 14-year follow-up study. *Spine*. 2006;31:2998–3005.
9. Hyun S, Rhim S, Roh S, et al. The time course of range of motion loss after cervical myelopathy: a prospective study with minimum two-year follow-up. *Spine*. 2009;34:1134–1139.
10. Ohashi M, Yamazaki A, Watanabe K, et al. Two-year clinical and radiological outcomes of open-door cervical laminoplasty with prophylactic bilateral C4-5 foraminotomy in a prospective study. *Spine*. 2014;39:721–727.
11. Machino M, Yukawa Y, Hida T, et al. Cervical alignment and range of motion after laminoplasty: radiographic data from more than 500 cases with cervical spondylotic myelopathy and a review of the literature. *Spine*. 2012;37:E1243–E1250.
12. Nakashima H, Kato F, Yukawa Y, et al. Comparative effectiveness of open-door laminoplasty versus French-door laminoplasty in cervical compressive myelopathy. *Spine*. 2014;39:642–647.
13. Suk K, Kim K, Lee J, et al. Sagittal alignment of the cervical spine after the laminoplasty. *Spine*. 2007;32:E656–E660.
14. Kurokawa T, Tsuyama N, Tanaka H, et al. Enlargement of spinal canal by the sagittal splitting of the spinous process. *Bessatsu Seikei Geka*. 1982;2:234–240.
15. Tomita K, Kawahara N, Toribatake Y, et al. Expansive midline T-saw laminoplasty (modified spinous process-splitting) for the management of cervical myelopathy. *Spine*. 1998;23:32–37.
16. Heller JG, Edward CC II, Murakami H, et al. Laminoplasty versus laminectomy and fusion for multilevel cervical myelopathy: an independent matched cohort analysis. *Spine*. 2001;26:1330–1336.
17. Ogawa Y, Toyama Y, Chiba K, et al. Long-term results of expansive open-door laminoplasty for ossification of the posterior longitudinal ligament of the cervical spine. *J Neurosurg Spine*. 2004;1:168–174.
18. Satomi K, Nishu Y, Kohno T, et al. Long-term follow-up studies of open door expansive laminoplasty for cervical stenotic myelopathy. *Spine*. 1994;19:507–510.
19. Hirabayashi K, Satomi K. Operative procedure and results of expansive open-door laminoplasty. *Spine*. 1988;13:870.
20. Hirabayashi K, Watanabe K, Wakano K, et al. Expansive open-door laminoplasty for cervical spinal stenotic myelopathy. *Spine*. 1983;8:693–699.
21. Cason GW, Anderson ER III, Herkowitz HN. The evaluation and treatment of cervical radiculopathy and myelopathy. *Orthop Knowl Updat*. 2012;5:293–304.
22. Fujishima Y, Nishi Y. Atrophy of the nuchal muscle and change in cervical curvature after expansive open-door laminoplasty. *Arch Orthop Trauma Surg*. 1996;115:203–205.
23. Roselli R, Pompucci A, Formica F, et al. Open-door laminoplasty for cervical stenotic myelopathy: surgical technique and neurophysiological monitoring. *J Neurosurg*. 2000;92:38–43.
24. Takeuchi K, Yokoyama T, Ono A, et al. Limitation of activities of daily living accompanying reduced neck mobility after laminoplasty preserving or reattaching the semispinalis cervicis into axis. *Eur Spine J*. 2008;17:415–420.
25. Hayashi T, Daubs MD, Suzuki A, et al. The compensatory relationship of upper and subaxial cervical motion in the presence of cervical spondylosis. *Clin Spine Surg*. 2016;29:E196–E200.

RESEARCH ARTICLE

Experimental Mouse Model of Lumbar Ligamentum Flavum Hypertrophy

Takeyuki Saito^{1,2}, Kazuya Yokota³, Kazu Kobayakawa², Masamitsu Hara^{1,2}, Kensuke Kubota³, Katsumi Harimaya², Kenichi Kawaguchi², Mitsumasa Hayashida², Yoshihiro Matsumoto², Toshio Doi⁴, Keiichi Shiba³, Yasuharu Nakashima², Seiji Okada^{1,2*}

1 Department of Advanced Medical Initiatives, Graduate School of Medical Sciences, Kyushu University, Fukuoka, Japan, **2** Department of Orthopaedic Surgery, Graduate School of Medical Sciences, Kyushu University, Fukuoka, Japan, **3** Department of Orthopaedic Surgery, Spinal Injuries Center, Fukuoka, Japan, **4** Department of Orthopaedic Surgery, Kyushu University Beppu Hospital, Oita, Japan

* Current address: Departments of Advanced Medical Initiatives and Orthopaedic Surgery, Graduate School of Medical Sciences, Kyushu University, Maidashi, Higashi-ku, Fukuoka, Japan

* seokada@ortho.med.kyushu-u.ac.jp



OPEN ACCESS

Citation: Saito T, Yokota K, Kobayakawa K, Hara M, Kubota K, Harimaya K, et al. (2017) Experimental Mouse Model of Lumbar Ligamentum Flavum Hypertrophy. PLoS ONE 12(1): e0169717. doi:10.1371/journal.pone.0169717

Editor: Alejandro A. Espinoza Orias, Rush University Medical Center, UNITED STATES

Received: September 26, 2016

Accepted: December 20, 2016

Published: January 6, 2017

Copyright: © 2017 Saito et al. This is an open access article distributed under the terms of the Creative Commons Attribution License, which permits unrestricted use, distribution, and reproduction in any medium, provided the original author and source are credited.

Data Availability Statement: All relevant data are within the paper.

Funding: Grant funds were received in support of this work from a Grant-in-Aid for Scientific Research (16H05450) from the Ministry of Education, Science, Sports and Culture of Japan, and Research foundations from the general insurance association of Japan.

Competing Interests: There are no conflicts of interest concerning this manuscript.

Abstract

Lumbar spinal canal stenosis (LSCS) is one of the most common spinal disorders in elderly people, with the number of LSCS patients increasing due to the aging of the population. The ligamentum flavum (LF) is a spinal ligament located in the interior of the vertebral canal, and hypertrophy of the LF, which causes the direct compression of the nerve roots and/or cauda equine, is a major cause of LSCS. Although there have been previous studies on LF hypertrophy, its pathomechanism remains unclear. The purpose of this study is to establish a relevant mouse model of LF hypertrophy and to examine disease-related factors. First, we focused on mechanical stress and developed a loading device for applying consecutive mechanical flexion-extension stress to the mouse LF. After 12 weeks of mechanical stress loading, we found that the LF thickness in the stress group was significantly increased in comparison to the control group. In addition, there were significant increases in the area of collagen fibers, the number of LF cells, and the gene expression of several fibrosis-related factors. However, in this mechanical stress model, there was no macrophage infiltration, angiogenesis, or increase in the expression of transforming growth factor- β 1 (TGF- β 1), which are characteristic features of LF hypertrophy in LSCS patients. We therefore examined the influence of infiltrating macrophages on LF hypertrophy. After inducing macrophage infiltration by micro-injury to the mouse LF, we found excessive collagen synthesis in the injured site with the increased TGF- β 1 expression at 2 weeks after injury, and further confirmed LF hypertrophy at 6 weeks after injury. Our findings demonstrate that mechanical stress is a causative factor for LF hypertrophy and strongly suggest the importance of macrophage infiltration in the progression of LF hypertrophy via the stimulation of collagen production.

Introduction

Lumbar spinal canal stenosis (LSCS) is a common spinal disorder in elder people. There are approximately 250,000 to 500,000 LSCS patients in the United States, with the number increasing due to the aging of the population [1]. LSCS causes lower back pain, leg pain, and claudication, leading to severe disability in the activities of daily living [2]. These symptoms primarily result from the hypertrophy of the ligamentum flavum (LF). The LF is a spinal ligament that covers most of the posterior and lateral parts of the spinal canal. Thus, hypertrophy of LF directly compresses the nerve roots and/or cauda equine, resulting in spinal disorders [3]. Although there have been several studies about LF hypertrophy, its pathomechanism remains unclear.

In previous studies, only human samples have been used due to the lack of a relevant animal model. A limitation of these studies was the difficulty in observing the gradual process of LF hypertrophy because the hypertrophied LF obtained from LSCS patients already showed advanced histological changes; the loss of elastic fibers and an excessive accumulation of collagen fibers [4,5]. Molecular expression changes were also observed in human hypertrophied LF, such as transforming growth factor- β 1 (TGF- β 1) [6], connective-tissue growth factor (CTGF) [7] and platelet-derived growth factor (PDGF) [8], which are related to collagen production [9–11]. However, whether such factors are causative or merely a consequence of LF hypertrophy remains unknown. Therefore, basic research using an experimental animal model is necessary to elucidate its etiology.

Various possible factors for LF hypertrophy have been considered, such as age, activity level, genetic components, and mechanical stress [12–14]. Among them, we focused on mechanical stress, which has been considered an influencing factor in previous studies. Indeed, Fukuyama et al. reported that the LF thickness of lumbar degenerative instability patients was larger than that of non-instability patients [12]. Furthermore, mechanical stretching force was reported to increase collagen synthesis in cultured human LF cells [15]. However, there are no *in vivo* studies directly demonstrating that mechanical stress induces LF hypertrophy.

In this study, we established a LF hypertrophy mouse model using a novel loading device and examined the influence of consecutive mechanical stress on LF hypertrophy. In addition, we induced macrophage infiltration into the mouse LF by applying micro-injury and examined the pathological role of macrophages in LF hypertrophy.

Materials and Methods

Animals

Eight-week-old female C57BL/6 wild-type mice and CAG-EGFP transgenic mice were used in this study (Japan SLC, Shizuoka, Japan). All mice were housed in a temperature- and humidity-controlled environment with a 12 h light–dark cycle. In all animal experiments, the mice were anesthetized intraperitoneally with an anesthetic mixture (medetomidine 0.3 mg/kg, midazolam 4 mg/kg, and butorphanol 5 mg/kg) every hour in consideration of the anesthetic duration [16]. The animal protocol was approved by the Committee of Ethics on Animal Experiment in Faculty of Medicine, Kyushu University (A-27-220-0) in accordance with the Guidelines for Animal Experimentation. All efforts were made to reduce the number of animals used and to minimize their suffering.

Histological analysis

After the mice were transcardially fixed with 4% paraformaldehyde, the lumbar spine was removed and immersed in the same fixative. The spine was decalcified in ethylenediaminetetraacetic acid solution and dehydrated in sucrose solution. The sample was then embedded

into OCT compound, frozen in liquid nitrogen, and cut into 10- μ m sections on a cryostat. The sections were subjected to hematoxylin-eosin (HE) and Elastica-van Gieson (EVG) staining. For immunostaining, the sections were stained with primary antibodies against Iba1 (1:200; macrophage marker; Wako, Osaka, Japan), laminin (1:200; basement membrane marker; Sigma-Aldrich, Saint Louis, MO), collagen type 1 alpha 1 (COL1A1; 1:200; Sigma-Aldrich), and 5-bromo-20-deoxyuridine (BrdU; 1:200; proliferating cell marker; Abcam, Cambridge, UK). Then, the sections were incubated with Alexa Fluor-conjugated secondary antibodies (1:200; Invitrogen, Carlsbad, USA). Nuclear counterstaining was performed using Hoechst 33342 (1:1000; Invitrogen). For BrdU detection, the sections were pre-treated with 2N-HCl for 30 min at 37°C.

Experimental procedures

To examine bone-marrow-derived cell (BMDC) infiltration into the LF under consecutive mechanical stress, 1×10^7 bone-marrow cells prepared from CAG-EGFP mice by flushing the femurs and tibias were transplanted into irradiated wild-type recipient mice as previously described [17]. After confirming the reconstitution of >90% EGFP-bone-marrow cells in the chimeric mice, we applied 12-week mechanical stress.

To quantify the number of proliferating cells by consecutive mechanical stress, BrdU (100 μ g/g body weight) was intraperitoneally administered daily during the loading period in the two groups.

To induce macrophage infiltration, after peeling the lumbar paraspinal muscles and exposing the mouse LF, we applied micro-injury to the LF at the dorsal side with a sharp 30-gauge needle tip. At 1, 2, and 6 weeks after micro-injury, histological and gene expression analyses were performed. Sham surgery was performed on the controls.

Human LF samples

Human LF was obtained at surgery from 20 LSCS patients (mean age 68.6 years, range 65–78 years, as hypertrophied LF) and 10 lumbar disc herniation (LDH) patients (mean age 29.9 years, range 24–34 years, as non-hypertrophied LF). Hypertrophied LF from LSCS patients was then divided into two groups: mild (<4 mm) and severe (>4 mm) hypertrophy ($n = 10$ per group). Human LF sections were subjected to HE and EVG staining. All procedures were approved by the Kyushu University Institutional Review Board (25–126) and the analyses of the sample were performed after obtaining written informed consent from each patient.

Image acquisition and quantification

All radiographs of the mouse spine were scanned with micro-computed tomography (CT) (60 kV, 50 μ m per pixel, Rigaku, Tokyo, Japan). For histological and immunohistochemical analyses, images were obtained using a BZ-9000 digital microscope (Keyence, Osaka, Japan). The thickness of human LF was measured at the facet joint level on axial T1-weighted magnetic resonance imaging (MRI) as previously described [18]. The thickness of the mouse LF with/without mechanical stress (the mechanical stress group and the control group) was also measured at the facet joint level on the axial sections with EVG staining ($n = 5$ per group). To calculate the area of collagen and elastic fibers after EVG staining, we used the ImageJ software program (National Institutes of Health). The area was calculated 3 times and the average value was taken [5]. The number of LF cells in human samples was counted by HE staining of the sagittal sections in 5 random fields at 400 \times magnification as previously described ($n = 10$ per group) [19]. The number of LF cells, BMDCs, and proliferating cells in our mouse model was

quantified by counting Hoechst, EGFP, and BrdU-immunopositive cells in the axial sections at the L5-L6 facet joint level at 200× magnification (n = 5 per group). The algorithms for counting the cells were provided by the measurement software program Dynamic cell count BZ-H1c (Keyence).

Quantitative reverse transcription-polymerase chain reaction (qRT-PCR) Analysis

Total RNA was isolated from LF cells using the RNeasy Mini Kit (Qiagen, Hilden, Germany) and cDNA was synthesized from the total RNA using a PrimeScript reverse transcriptase (TaKaRa, Shiga, Japan) according to the manufacturer's instructions. Quantitative RT-PCR was performed using 20 µl reaction mixture with primers specific to the genes of interest (Table 1) and SYBR Premix Dimmer-Eraser (TaKaRa) [20]. The mRNA levels in each sample were normalized to those of glyceraldehyde-3-phosphate dehydrogenase mRNA (n = 5 per group).

Table 1. Primers used for quantitative reverse transcription polymerase chain reaction.

Gene (Accession Number)		5'- Primer -3'
COL1A1 (NM_007742.3)	Forward	AACCCCTGGAAACAGACGAACAACC
	Reverse	TGGTCACGTTCAAGTTGGTCAAAGG
COL1A2 (NM_007743.2)	Forward	ATCCAACTAAGTCTCCTCCCTTGG
	Reverse	CTCTGTGGAAGATAGTCAGAAGCC
COL3A1 (NM_009930.2)	Forward	TAAAGAAGTCTCTGAAGCTGATGG
	Reverse	ATCTATGATGGGTAGTCTCATTGC
TNF-α (NM_013693.2)	Forward	TTATGGCTCAGGGTCCAACTCTGT
	Reverse	TGGACATTCGAGGCTCCAGTGAAT
IL-1β (NM_013693.2)	Forward	GGGCTGGACTGTTTCTAATGCCTT
	Reverse	CCATCAGAGGCAAGGAGGAAAACA
IL-6 (NM_013693.2)	Forward	GCTCTCCTAACAGATAAGCTGGAG
	Reverse	CCACAGTGAGGAATGTCCACAAC
CTGF (NM_010217.2)	Forward	GGCCATACAAGTAGTCTGTCAACC
	Reverse	CACTCCAAAAGTAGGCACACTGC
PDGF-A (NM_008808.3)	Forward	AGACAGATGTGAGGTGAGATGAGC
	Reverse	ACGGAGGAGAACAAAGACCGCACG
TGF-β1 (NM_011577.1)	Forward	TGGACACACAGTACAGCAAGGTCC
	Reverse	ATCATGTTGGACAACCTGCTCCACC
VEGF-A (NM_001025257.3)	Forward	CGGAGGCAGAGAAAAGAGAAAGTG
	Reverse	GGGAGAGAGAGATTGGAAACACAG
MMP-2 (NM_008610.2)	Forward	CCTGGTGACTTCAGATTTAAGAGG
	Reverse	GATGTTGAAGAACCAGAAGAGTGG
MMP-9 (NM_013599.3)	Forward	CTGGTGATCTCTTCTAGAGACTGG
	Reverse	ATGCATCTGCAACTACAGATAAGC
GAPDH (NM_004503)	Forward	GACTTCAACAGCAACTCCCACTCT
	Reverse	GGTTTCTTACTCCTGGAGGCCAT

COL1A1 indicates collagen type 1 alpha 1; COL1A2, collagen type 1 alpha 2; COL3A1, collagen type 3 alpha 1; TNF-α, tumor necrosis factor-α; IL-1β, interleukin-1β; IL-6, interleukin-6; CTGF, connective tissue growth factor; PDGF-A, platelet-derived growth factor-A; TGF-β1, transforming growth factor-β1; VEGF-A, vascular endothelial cell growth factor-A; MMP-2, matrix metalloproteinase-2; MMP-9, matrix metalloproteinase-9; GAPDH, glyceraldehyde-3-phosphate dehydrogenase.

doi:10.1371/journal.pone.0169717.t001

Statistical analysis

Wilcoxon's rank sum test was used to compare the medians of the data between two groups for the area, width, and thickness of the LF, the area of the collagen and elastic fibers, the qRT-PCR results, and the cell count in the mouse LF. To analyze the differences among three groups in the ratio of elastic fibers to collagen fibers and the cell count in human LF, ANOVA with the Tukey-Kramer post hoc test was performed. Statistical significance was set at $p < 0.05$. The data were presented as the mean \pm SEM. All statistical analyses were carried out using the JMP software program (version 11; SAS Institute, Cary, NC, USA).

Results

Consecutive mechanical stress loading to the mouse LF

First, to evaluate whether the mouse was a feasible experimental animal model for studying LF hypertrophy, we performed histological analyses of the mice lumbar spine. In the axial sections of the spine, HE staining showed that the mouse LF was located between the dural tube and facet joints (Fig 1A). In the sagittal sections, EVG staining demonstrated that the LF ran between adjacent laminae and mostly consisted of black-staining elastic fibers (Fig 1B). These histological features were very similar to those of human LF. Therefore, we decided to use mice to examine the pathomechanism underlying LF hypertrophy.

To establish a LF hypertrophy mouse model, we initially developed a loading device by which the mouse LF was subjected to consecutive mechanical stress for the present experiment (Fig 1C). The device consisted of a moving bed, straps, and motor driver (UNIQUE MEDICAL, Tokyo, Japan) (Fig 1D). During the loading, the limbs were firmly strapped onto the bed under anesthesia. When the upper half of the bed was constantly moving, the spine was bent and extended repeatedly at the rate of 20 cycles per minute by the motor. To determine the appropriate loading, we performed a preliminary experiment with 12 weeks of mechanical stress loading for 1.5, 3, and 4.5 h/day, and then decided on a 12-week loading period because an experimental period exceeding 12 weeks was not practical. During this period, some mice in the 4.5 h/day group showed weight and hair loss, whereas no adverse events were noted in the other groups. We therefore performed 3 h/day loading in subsequent experiments. The controls were under anesthesia alone. To apply mechanical stress consistently at the L5-L6 level, we used the iliac crest line as an anatomical landmark of the level (Fig 1E) and confirmed that mechanical stress was adequately loaded to the mouse LF at the level by CT images (Fig 1F).

Mechanical stress brought about LF hypertrophy

To examine whether mechanical stress indeed induced LF hypertrophy, we compared the axial cross-sectional area of the mouse LF with/without mechanical stress loading (the stress group vs. the control group, respectively). We found the sectional area in the stress group to be about 1.5-fold that in the control group on EVG staining after 12-week mechanical stress (Fig 2A and 2B). Although the width was comparable between the two groups, the thickness of the stress group was significantly higher than that of the control group (Fig 2B). These results indicated the successful establishment of a LF hypertrophy mouse model via mechanical stress.

We then investigated the effect of mechanical stress on the extracellular matrix (ECM). Previous observations in human samples demonstrated that the major ECM component was elastic fibers, while the minor component was collagen fibers in non-hypertrophied LF, whereas the ratio of collagen fibers was markedly increased in hypertrophied LF [4,5]. Similarly, in our mouse model, the area of collagen fibers was considerably higher in the stress group than in

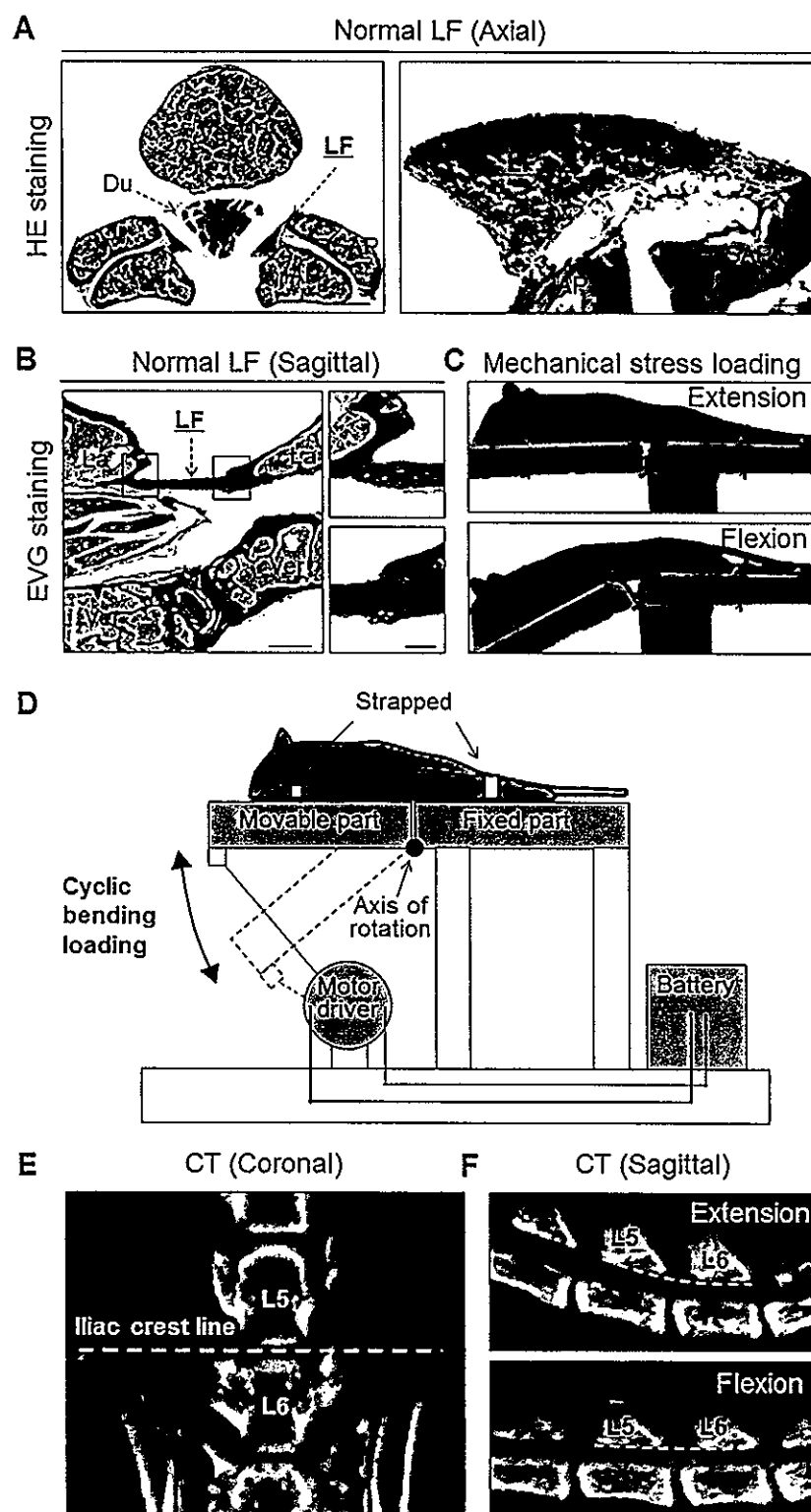


Fig 1. Histological analyses of the mouse lumbar spine and a mechanical stress loading device. The application of mechanical stress to the mouse LF using a novel device. (A) HE and (B) EVG staining of the spine sections. (C) Photographs and (D) schematic illustrations of the device. (E) A coronal CT image showing that the iliac crest line corresponds to the L5-L6 disc level. (F) Sagittal CT images showing that mechanical stress was consistently applied at the L5-L6 level. Scale bars (A): 300 μ m; insets: 50 μ m; (B): 300 μ m; insets: 100 μ m. LF, ligamentum flavum; Ver, vertebral body; Du, dural tube; SAP, superior articular process; IAP, inferior articular process; La, lamina.

doi:10.1371/journal.pone.0169717.g001

the control group (Fig 2C). Although the area of elastic fibers also increased, the density of elastic fibers decreased compared to that of collagen fibers (Fig 2C–2F).

The histological comparison of the mouse and human LF

We next evaluated the severity of LF hypertrophy in the mouse model in comparison to human samples. Non-hypertrophied LF of human showed a dense and regular bundle of elastic fibers, whereas severely hypertrophied LF showed thin, irregular, and fragmented elastic fibers in EVG staining (Fig 3A). Additionally, the elastin-to-collagen ratio decreased in hypertrophied LF compared to non-hypertrophied LF (Fig 3B). In our mouse model, the elastic fibers in the control group were dense and aligned, whereas in the stress group, they were slightly degenerated, and a decreased elastin-to-collagen ratio was observed (Fig 3C and 3D). These results indicated that our mouse model by mechanical stress was histologically identical to mildly hypertrophied LF of human.

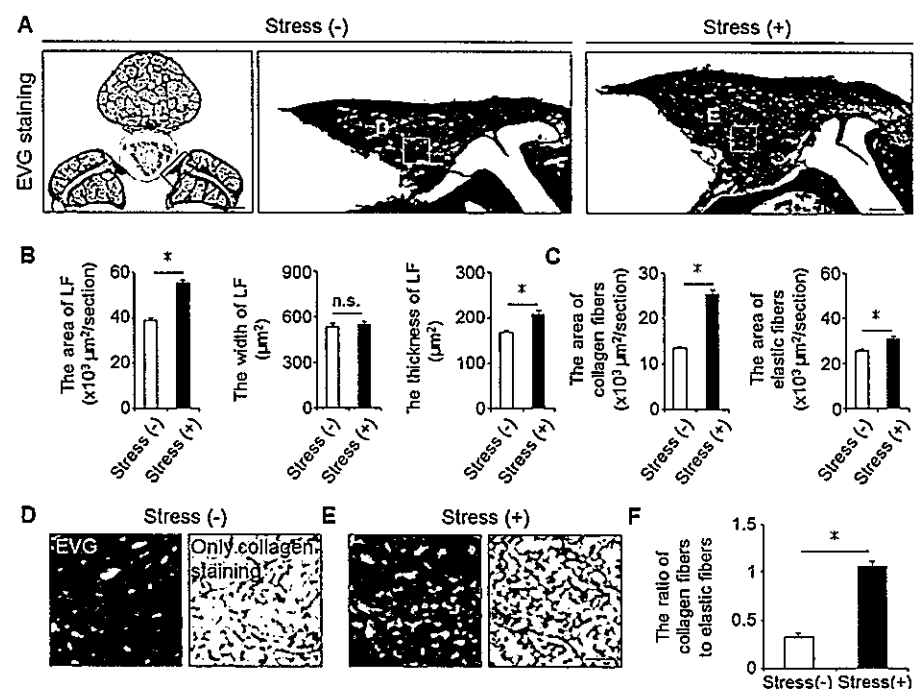


Fig 2. Mechanical stress induced LF hypertrophy. (A) Axial sections of the mouse LF with/without 12-week mechanical stress loading on EVG staining. (B and C) Bar graphs showing the cross-sectional area, width, thickness, and the area of collagen fibers and elastic fibers in the two groups. (D and E) High magnifications of (A). (F) Bar graph showing the ratio of collagen fibers to elastic fibers in the two groups. Scale bars (A): 500 μ m; insets: 50 μ m; (D and E): 10 μ m. * p < 0.05, Wilcoxon's rank sum test, n.s. = not significant (n = 5/group).

doi:10.1371/journal.pone.0169717.g002

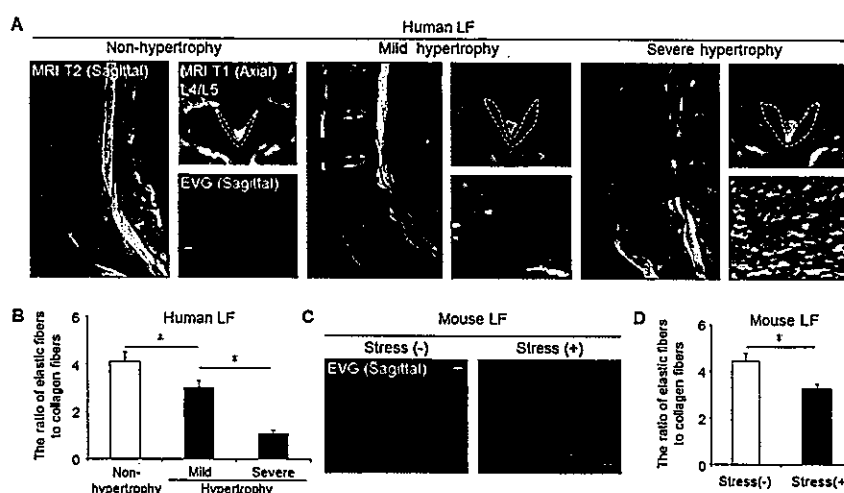


Fig 3. Our mouse model histologically reflected mildly hypertrophied LF in humans. (A) MRI and EVG staining of human samples: non-hypertrophy and mild and severe hypertrophy. The white broken lines indicate outlines of the LF. (B) Bar graph showing the ratio of elastic fibers to collagen fibers in the three groups. * $p < 0.05$, an ANOVA with the Tukey-Kramer post hoc test ($n = 10/\text{group}$). (C) EVG staining of the mouse LF with/without 12-week mechanical stress. (D) Bar graph showing the ratio of elastic fibers to collagen fibers in the two groups. * $p < 0.05$, Wilcoxon's rank sum test ($n = 5/\text{group}$). Scale bars (A): 100 μm ; (C): 50 μm .

doi:10.1371/journal.pone.0169717.g003

Increased number of LF cells by mechanical stress

In addition to these ECM component changes, we examined the cellular distribution changes using human and our mouse samples. There were few cells in human non-hypertrophied LF, whereas a significantly increased number of cells was observed in human hypertrophied LF (Fig 4A and 4B). Also in our mouse model, the number of Hoechst-positive LF cells was significantly higher in the stress group than in the control group (Fig 4C and 4D). Furthermore, the number of BrdU-positive proliferating cells was significantly higher in the stress group (Fig 4E and 4F). We initially expected to observe BMDC infiltration by mechanical stress because macrophage infiltration was reported in human hypertrophied LF [21]. However, no EGFP-positive BMDC infiltration occurred in the bone-marrow-chimeric mouse LF with/without mechanical stress (Fig 4C).

Increased gene expression of fibrosis-related factors by mechanical stress

To examine the influence of mechanical stress on the activation of fibrosis-related factors in LF cells, we evaluated the gene expression of inflammatory cytokines, growth factors, and angiogenesis-related factors in the mouse model. Quantitative RT-PCR demonstrated that the gene expression of collagens, tumor necrosis factor- α , interleukin-1 β , and interleukin-6 were significantly higher in the stress group than in the control group (Fig 5A and 5B). A significant increase in the CTGF and PDGF-A expression was also observed in the stress group (Fig 5C). Although an abundant TGF- β 1 expression and angiogenic factors were reported in severely hypertrophied LF of humans [21], no significant differences were seen in the two mouse groups (Fig 5C and 5D).

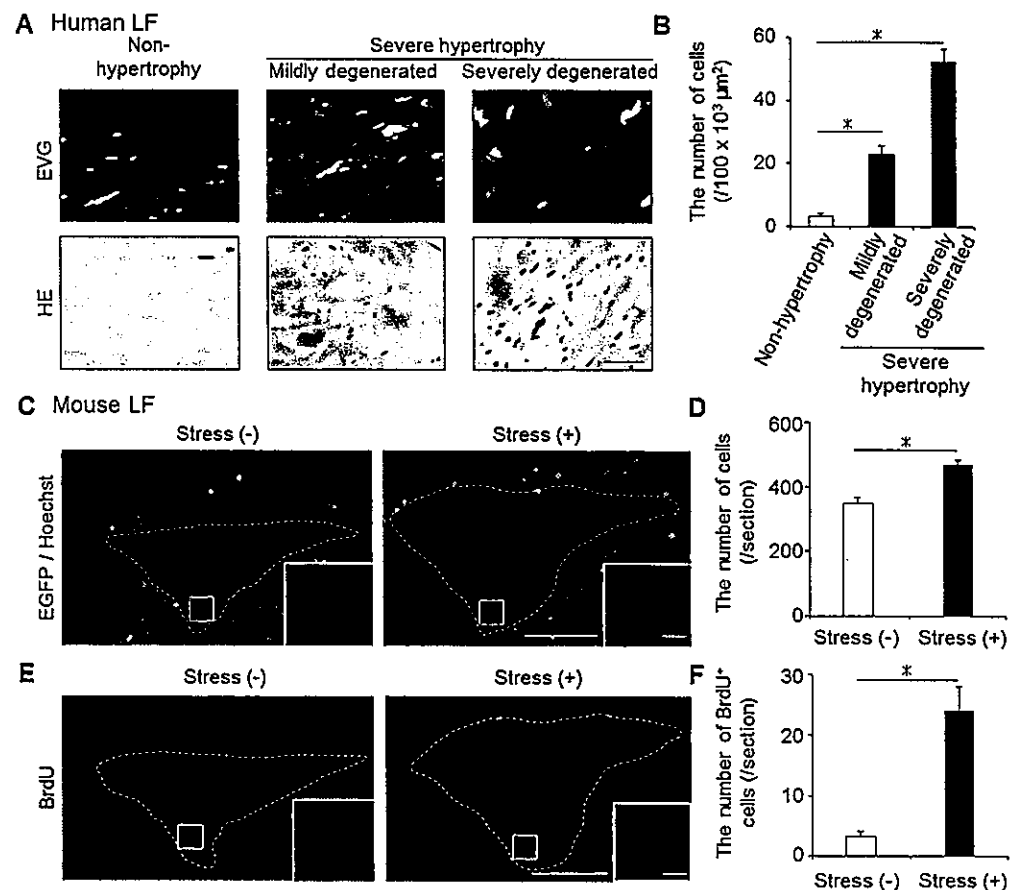


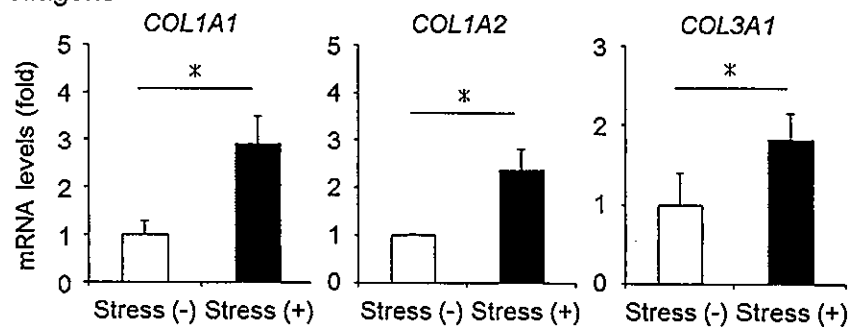
Fig 4. The changes in the cellular distribution in the hypertrophied LF of mice and humans. (A and B) The number of cells significantly increased with LF hypertrophy in humans. $*p < 0.05$, an ANOVA with the Tukey-Kramer post hoc test ($n = 10/\text{group}$). (C-F) The comparison of the number of cells (Hoechst, blue), infiltrating BMDCs (EGFP, green), and proliferating cells (BrdU, red) in the mouse LF with/without 12-week mechanical stress. To detect BMDCs, we generated bone-marrow-chimeric mice by transplanting from CAG-EGFP mice. The white broken lines indicate the outlines of the LF. $*p < 0.05$, Wilcoxon's rank sum test ($n = 5/\text{group}$). Scale bars (A): $100 \mu m$; (C and E): $100 \mu m$; insets: $10 \mu m$.

doi:10.1371/journal.pone.0169717.g004

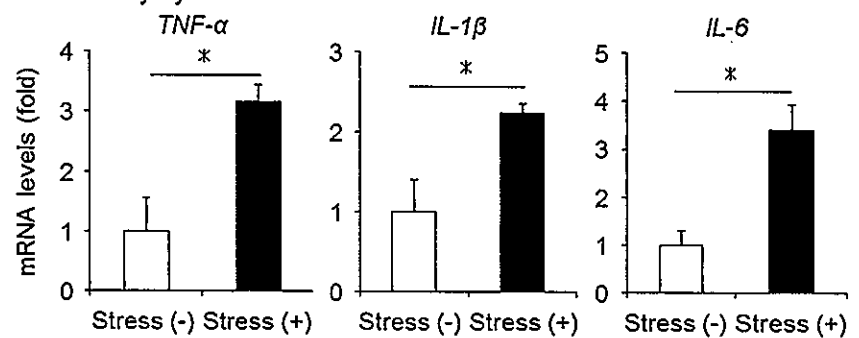
Micro-injury-induced macrophage infiltration and collagen accumulation in the injured area

In contrast to severely hypertrophied LF of LSCS patients, our mouse model by mechanical stress demonstrated no infiltrating macrophages, increase in TGF- $\beta 1$ expression, or angiogenesis (Figs 4C, 5C and 5D). We therefore hypothesized that factors other than mechanical stress were involved in the progression of LF hypertrophy. To examine the pathological role of macrophages in LF hypertrophy, we induced macrophage infiltration by applying micro-injury to the normal mouse LF at the dorsal side. At 1 week after micro-injury, Iba1-positive macrophages had infiltrated around the injured lesion (Fig 6A). Notably, a qRT-PCR analysis revealed the gene expression of collagens and fibrosis-related growth factors, including TGF- $\beta 1$, to be significantly higher in the micro-injured group than in the non-injured group (Fig 6B and 6C). Furthermore, laminin-positive micro-vessels and a significant increase in the levels of angiogenesis-related factors were also observed (Fig 6A and 6D). Indeed, excessive collagen

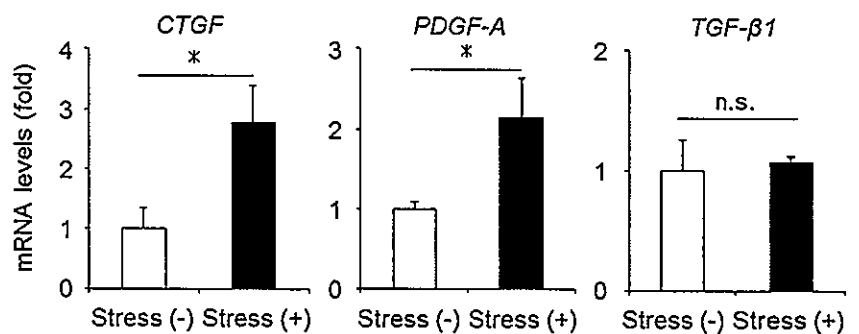
A Collagens



B Inflammatory cytokines



C Growth factors



D Angiogenesis-related factors

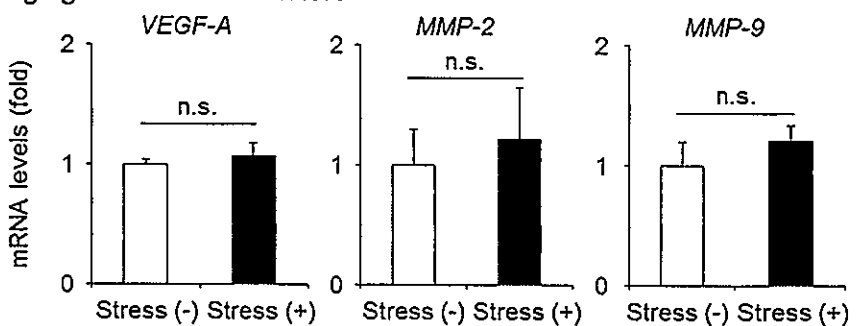


Fig 5. The mRNA expression of fibrosis-related factors in our mechanical stress mouse model. (A-D) The gene expression of collagens, inflammatory cytokines, growth factors, and angiogenesis-related factors evaluated in the mouse LF with/without mechanical stress loading by qRT-PCR ($n = 5/\text{group}$). $*p < 0.05$, Wilcoxon's rank sum test, n.s. = not significant. COL1A1, collagen type 1 alpha 1; TNF- α , tumor necrosis factor- α ; IL, interleukin; CTGF, connective tissue growth factor; PDGF-A, platelet-derived growth factor-A; TGF- β 1, transforming growth factor- β 1; VEGF-A, vascular endothelial cell growth factor-A; MMP, matrix metalloproteinase.

doi:10.1371/journal.pone.0169717.g005

synthesis without elastic fibers was observed in the injured area at 2 weeks after micro-injury (Fig 6E), and LF hypertrophy was detected selectively in the micro-injury area at 6 weeks after injury (Fig 6F). These results strongly suggested that macrophage infiltration was a significant factor involved in the progression of LF hypertrophy by activating collagen production.

Discussion

In this study, by applying consecutive mechanical bending stress to the mouse LF, we demonstrated that mechanical stress was one of the direct causes of LF hypertrophy. In the mouse hypertrophied LF, increased collagen fibers, proliferating cells, and the gene expression of several fibrosis-related factors were found. In addition, macrophage infiltration with angiogenesis was induced by applying micro-injury to the mouse LF. In this macrophage infiltration model, LF hypertrophy was observed along with the excessive expression of collagen and the increased expression of TGF- β 1. These findings suggest that long-term mechanical stress and macrophage infiltration significantly influence the progression of LF hypertrophy.

To date, previous studies have reported the common histological characteristics of human hypertrophied LF as follows: collagen deposition, elastic fiber fragmentation, and calcification [22,23]; inflammatory cell accumulation [21]; and an increased expression of fibrosis-related factors [6–8,24,25]. However, these pathological changes in human samples only indicated the advantaged stage of LF hypertrophy, and determining which factors contribute to the process of LF hypertrophy is difficult. Therefore, we established an experimental animal model to clarify its pathomechanisms. In our mechanical stress model, we confirmed the increases in collagen fibers, cell proliferation, and the fibrosis-related factors expression, in line with human LF pathology.

In fibrotic diseases of several organs, TGF- β 1 has been reported to be an important disease-related factor for collagen production [26,27]. The main source of this cytokine was believed to be infiltrating macrophages in fibrosis [28,29]. For example, the number of infiltrating macrophages correlated with the TGF- β 1 expression and the progression of collagen accumulation in liver fibrosis [28]. In addition, in severely hypertrophied LF of humans, macrophage infiltration was observed in the collagen deposition area with increased TGF- β 1 expression [21]. In the development of a LF hypertrophy mouse model, we hypothesized that consecutive mechanical stress would induce macrophage infiltration and increased TGF- β 1 expression. However, although the increased gene expression of several fibrosis-related factors was observed in our mechanical stress mouse model, there was no BMDC infiltration or increased TGF- β 1 expression (Figs 4C and 5C). Therefore, we additionally induced macrophage infiltration by applying micro-injury, and found that macrophages were associated with the increased expression of collagens and TGF- β 1 (Fig 6A–6C). Indeed, we found excessive collagen synthesis in the injured site at 2 weeks after micro-injury (Fig 6E) and confirmed LF hypertrophy at 6 weeks after micro-injury (Fig 6F). These results suggested that infiltrating macrophages may also play a significant role in the progression of LF hypertrophy via the increased expression of TGF- β 1.

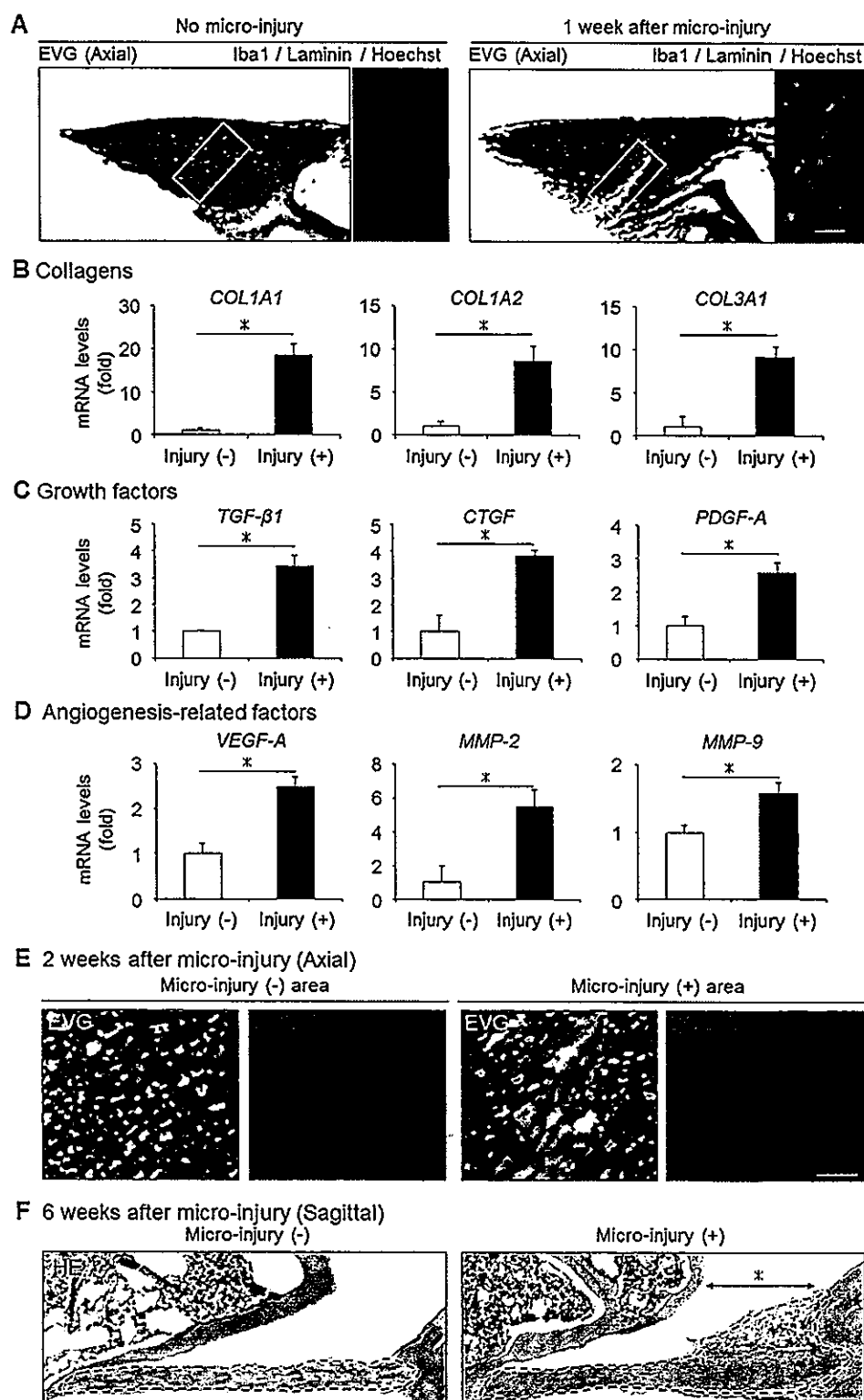


Fig 6. The influence of macrophage infiltration following micro-injury on the mouse LF. (A) The presence of infiltrating macrophages (Iba1, green) and neovascular vessels (laminin, red) in the mouse LF with/without micro-injury. (B-D) Bar graphs showing the gene expression of collagens, fibrosis-related growth factors, and angiogenesis-related factors in the two groups. (E) The collagen synthesis in the injured area (COL1A1, green) at 2 weeks after micro-injury. (F) Sagittal sections of the mouse LF with/without micro-injury on HE staining at 6 weeks after micro-injury. The black broken lines indicate the outlines of the LF. The asterisk indicates the area to which micro-injury was applied. * $p < 0.05$, Wilcoxon's rank sum test ($n = 5$ /group). Scale bars (A): 50 μ m; insets: 20 μ m; (E): 20 μ m; (F) 200 μ m. COL1A1, collagen type 1 alpha 1; TGF- β 1, transforming growth factor- β 1; CTGF, connective tissue growth factor; PDGF-A, platelet-derived growth factor-A; VEGF-A, vascular endothelial cell growth factor-A; MMP, matrix metalloproteinase.

doi:10.1371/journal.pone.0169717.g006

Another characteristic of human hypertrophied LF is angiogenesis. While the normal LF is non-vascularized, marked angiogenesis was observed in the area of collagen accumulation in the severely hypertrophied LF [21]. Several factors such as VEGF and MMPs are considered to be important for angiogenesis, and their actual expression has been mainly observed in fibrotic areas [30]. These angiogenic factors were reported to be derived from infiltrating macrophages, and neovascular vessels further promoted macrophage infiltration, resulting in the excessive expression of TGF- β 1 as well as collagen production [31]. Therefore, the interplay between infiltrating macrophages and angiogenesis may also worsen the fibrotic pathology in LF hypertrophy progression. In our macrophage infiltration model, angiogenesis and the significantly increased expression of angiogenic factors were observed with infiltrating macrophages (Fig 6A and 6D). This macrophage infiltration model may help elucidate the effect of disrupting the cycle of macrophage infiltration and angiogenesis to prevent the progression to severe LF hypertrophy. Indeed, an angiogenesis inhibitor was reported to successfully suppress macrophage infiltration and subsequently prevent fibrotic collagen accumulation in renal fibrosis [32].

There are several limitations associated with the present study. We did not establish a LF hypertrophy mouse model showing advanced histological changes only by mechanical stress. Although we tried to investigate the influence of the combination of mechanical stress and micro-injury on LF hypertrophy, the combination unexpectedly caused an LF tear and the sample could not be analyzed. In addition to this limitation, our mechanical stress mouse model cannot be used to develop an LSCS model because the ratio of the LF to the dural tube was significantly smaller in mice than in humans. Nevertheless, we believe that each model we established in this study showed the pathological characteristics of human hypertrophied LF, at least in part, and is thus useful for a better understanding its pathogenesis.

In conclusion, we demonstrated for the first time that consecutive mechanical stress directly brought about LF hypertrophy in a mouse model. In addition, macrophage infiltration following micro-injury was found to be associated with severe LF hypertrophy by stimulating angiogenesis, collagen synthesis, and increased TGF- β 1 production.

Acknowledgments

We thank Dr. Brian Quinn for his valuable grammatical review of this manuscript.

Author Contributions

Conceptualization: TS SO.

Data curation: TS.

Formal analysis: TS KY K. Kobayakawa M. Hara K. Kubota KH K. Kawaguchi M. Hayashida YM TD KS YN SO.

Funding acquisition: SO.

Investigation: TS SO.

Methodology: TS.

Project administration: SO.

Resources: TS K. Kubota KH K. Kawaguchi M. Hayashida KS SO.

Supervision: SO.

Validation: SO.

Visualization: TS.

Writing – original draft: TS.

Writing – review & editing: SO.

References

1. Kalichman L, Cole R, Kim DH, Li L, Suri P, Guermazi A, et al. Spinal stenosis prevalence and association with symptoms: the Framingham Study. *Spine J.* 2009; 9: 545–50. doi: 10.1016/j.spinee.2009.03.005 PMID: 19398386
2. Szpalski M, Gunzburg R. Lumbar spinal stenosis in the elderly: an overview. *Eur Spine J.* 2003; 12: S170–5. doi: 10.1007/s00586-003-0612-1 PMID: 13680315
3. Towne EB, Reichert FL. Compression of the Lumbosacral Roots of the Spinal Cord by Thickened Ligamenta Flava. *Ann Surg.* 1931; 94: 327–36. PMID: 17866626
4. Okuda T, Baba I, Fujimoto Y, Tanaka N, Sumida T, Manabe H, et al. The pathology of ligamentum flavum in degenerative lumbar disease. *Spine.* 2004; 29: 1689–97. PMID: 15284518
5. Kosaka H, Sairyo K, Biyani A, Leaman D, Yeasting R, Higashino K, et al. Pathomechanism of loss of elasticity and hypertrophy of lumbar ligamentum flavum in elderly patients with lumbar spinal canal stenosis. *Spine.* 2007; 32: 2805–11. doi: 10.1097/BRS.0b013e31815b650f PMID: 18246001
6. Park JB, Chang H, Lee JK. Quantitative analysis of transforming growth factor-beta 1 in ligamentum flavum of lumbar spinal stenosis and disc herniation. *Spine.* 2001; 26: E492–5. PMID: 11679833
7. Zhong ZM, Zha DS, Xiao WD, Wu SH, Wu Q, Zhang Y, et al. Hypertrophy of ligamentum flavum in lumbar spine stenosis associated with the increased expression of connective tissue growth factor. *J Orthop Res.* 2011; 29: 1592–7. doi: 10.1002/jor.21431 PMID: 21484860
8. Zhang Y, Chen J, Zhong ZM, Yang D, Zhu Q. Is platelet-derived growth factor-BB expression proportional to fibrosis in the hypertrophied lumbar ligamentum flavum? *Spine.* 2010; 35: E1479–86. doi: 10.1097/BRS.0b013e3181f3d2df PMID: 21102276
9. Lewindon PJ, Pereira TN, Hoskins AC, Bridle KR, Williamson RM, Shepherd RW, et al. The role of hepatic stellate cells and transforming growth factor-beta(1) in cystic fibrosis liver disease. *Am J Pathol.* 2002; 160: 1705–15. PMID: 12000722
10. Chen MM, Lam A, Abraham JA, Schreiner GF, Joly AH. CTGF expression is induced by TGF-beta in cardiac fibroblasts and cardiac myocytes: a potential role in heart fibrosis. *J Mol Cell Cardiol.* 2000; 32: 1805–19. doi: 10.1006/jmcc.2000.1215 PMID: 11013125
11. Antoniadou HN, Bravo MA, Avila RE, Galanopoulos T, Neville-Golden J, Maxwell M, et al. Platelet-derived growth factor in idiopathic pulmonary fibrosis. *J Clin Invest.* 1990; 86: 1055–64. doi: 10.1172/JCI114808 PMID: 2170444
12. Fukuyama S, Nakamura T, Ikeda T, Takagi K. The effect of mechanical stress on hypertrophy of the lumbar ligamentum flavum. *J Spinal Disord.* 1995; 8: 126–30. PMID: 7606119
13. Sairyo K, Biyani A, Goel V, Leaman D, Booth R Jr, Thomas J, et al. Pathomechanism of ligamentum flavum hypertrophy: a multidisciplinary investigation based on clinical, biomechanical, histologic, and biologic assessments. *Spine.* 2005; 30: 2649–56. PMID: 16319751
14. Kim HN, Min WK, Jeong JH, Kim SG, Kim JR, Kim SY, et al. Combination of Runx2 and BMP2 increases conversion of human ligamentum flavum cells into osteoblastic cells. *BMB Rep.* 2011; 44: 446–51. doi: 10.5483/BMBRep.2011.44.7.446 PMID: 21777514

15. Nakatani T, Marui T, Hitora T, Doita M, Nishida K, Kurosaka M. Mechanical stretching force promotes collagen synthesis by cultured cells from human ligamentum flavum via transforming growth factor-beta1. *J Orthop Res*. 2002; 20: 1380–6. doi: 10.1016/S0736-0266(02)00046-3 PMID: 12472256
16. Kiriha Y, Takechi M, Kurosaki K, Kobayashi Y, Kurosawa T. Anesthetic effects of a mixture of medetomidine, midazolam and butorphanol in two strains of mice. *Exp Anim*. 2013; 62: 173–80. doi: 10.1538/expanim.62.173 PMID: 23903051
17. Oyamada A, Ikebe H, Itsumi M, Saiwai H, Okada S, Shimoda K, et al. Tyrosine kinase 2 plays critical roles in the pathogenic CD4 T cell responses for the development of experimental autoimmune encephalomyelitis. *J Immunol*. 2009; 183: 7539–46. doi: 10.4049/jimmunol.0902740 PMID: 19917699
18. Altinkaya N, Yildirim T, Demir S, Alkan O, Sarica FB. Factors associated with the thickness of the ligamentum flavum: is ligamentum flavum thickening due to hypertrophy or buckling? *Spine*. 2011; 36: E1093–7. doi: 10.1097/BRS.0b013e318203e2b5 PMID: 21343862
19. Shafaq N, Suzuki A, Terai H, Wakitani S, Nakamura H. Cellularity and cartilage matrix increased in hypertrophied ligamentum flavum: histopathological analysis focusing on the mechanical stress and bone morphogenetic protein signaling. *J Spinal Disord Tech*. 2012; 25: 107–15. doi: 10.1097/BSD.0b013e31820bb76e PMID: 21430570
20. Kumamaru H, Saiwai H, Ohkawa Y, Yamada H, Iwamoto Y, Okada S. Age-related differences in cellular and molecular profiles of inflammatory responses after spinal cord injury. *J Cell Physiol*. 2012; 227: 1335–46. doi: 10.1002/jcp.22845 PMID: 21604270
21. Löhr M, Hampl JA, Lee JY, Ernestus RI, Deckert M, Stenzel W. Hypertrophy of the lumbar ligamentum flavum is associated with inflammation-related TGF- β expression. *Acta Neurochir*. 2011; 153: 134–41. doi: 10.1007/s00701-010-0839-7 PMID: 20960015
22. Schröder PK, Grob D, Rahn BA, Cordey J, Dvorak J. Histology of the ligamentum flavum in patients with degenerative lumbar spinal stenosis. *Eur Spine J*. 1999; 8: 323–8. doi: 10.1007/s005860050181 PMID: 10483836
23. Yoshida M, Shima K, Taniguchi Y, Tamaki T, Tanaka T. Hypertrophied ligamentum flavum in lumbar spinal canal stenosis. Pathogenesis and morphologic and immunohistochemical observation. *Spine*. 1992; 17: 1353–60. PMID: 1462211
24. Hur JW, Kim BJ, Park JH, Kim JH, Park YK, Kwon TH, et al. The Mechanism of Ligamentum Flavum Hypertrophy: Introducing Angiogenesis as a Critical Link That Couples Mechanical Stress and Hypertrophy. *Neurosurgery*. 2015; 77: 274–81; discussion 281–2. doi: 10.1227/NEU.0000000000000755 PMID: 25850600
25. Lakemeier S, Schofer MD, Foltz L, Schmid R, Efe T, Rohlf J, et al. Expression of hypoxia-inducible factor-1 α , vascular endothelial growth factor, and matrix metalloproteinases 1, 3, and 9 in hypertrophied ligamentum flavum. *J Spinal Disord Tech*. 2013; 26: 400–6. doi: 10.1097/BSD.0b013e3182495b88 PMID: 2323068
26. Li J, Campanale NV, Liang RJ, Deane JA, Bertram JF, Ricardo SD. Inhibition of p38 mitogen-activated protein kinase and transforming growth factor-beta1/Smad signaling pathways modulates the development of fibrosis in adriamycin-induced nephropathy. *Am J Pathol*. 2006; 169: 1527–40. doi: 10.2353/ajpath.2006.060169 PMID: 17071578
27. Li J, Chen J, Kirsner R. Pathophysiology of acute wound healing. *Clin Dermatol*. 2007; 25: 9–18. doi: 10.1016/j.clindermatol.2006.09.007 PMID: 17276196
28. Chu PS, Nakamoto N, Ebinuma H, Usui S, Saeki K, Matsumoto A, et al. C-C motif chemokine receptor 9 positive macrophages activate hepatic stellate cells and promote liver fibrosis in mice. *Hepatology*. 2013; 58: 337–50. doi: 10.1002/hep.26351 PMID: 23460364
29. Ishida Y, Kimura A, Kondo T, Hayashi T, Ueno M, Takakura N, et al. Essential roles of the CC chemokine ligand 3-CC chemokine receptor 5 axis in bleomycin-induced pulmonary fibrosis through regulation of macrophage and fibrocyte infiltration. *Am J Pathol*. 2007; 170: 843–54. doi: 10.2353/ajpath.2007.051213 PMID: 17322370
30. Nagai T, Sato M, Kutsuna T, Kokubo M, Ebihara G, Ohta N, et al. Intravenous administration of anti-vascular endothelial growth factor humanized monoclonal antibody bevacizumab improves articular cartilage repair. *Arthritis Res Ther*. 2010; 12: R178. doi: 10.1186/ar3142 PMID: 20868495
31. Araújo FA, Rocha MA, Mendes JB, Andrade SP. Atorvastatin inhibits inflammatory angiogenesis in mice through down regulation of VEGF, TNF-alpha and TGF-beta1. *Biomed Pharmacother*. 2010; 64: 29–34. doi: 10.1016/j.biopha.2009.03.003 PMID: 19811885
32. Yoshio Y, Miyazaki M, Abe K, Nishino T, Furusu A, Mizuta Y, et al. TNP-470, an angiogenesis inhibitor, suppresses the progression of peritoneal fibrosis in mouse experimental model. *Kidney Int*. 2004; 66: 1677–85. doi: 10.1111/j.1523-1755.2004.00935.x PMID: 15458466

RESEARCH ARTICLE

Effects of Multilevel Facetectomy and Screw Density on Postoperative Changes in Spinal Rod Contour in Thoracic Adolescent Idiopathic Scoliosis Surgery

Terufumi Kokabu¹, Hideki Sudo^{1*}, Yuichiro Abe², Manabu Ito³, Yoichi M. Ito⁴, Norimasa Iwasaki¹

1 Department of Orthopaedic Surgery, Hokkaido University Hospital, Sapporo, Hokkaido, Japan, **2** Eniwa Hospital, Eniwa, Hokkaido, Japan, **3** Department of Spine and Spinal Cord Disorders, Hokkaido Medical Center, Sapporo, Hokkaido, Japan, **4** Department of Biostatistics, Hokkaido University Graduate School of Medicine, Sapporo, Hokkaido, Japan

* hideki.sudo@yahoo.co.jp



Abstract

Flattening of the preimplantation rod contour in the sagittal plane influences thoracic kyphosis (TK) restoration in adolescent idiopathic scoliosis (AIS) surgery. The effects of multilevel facetectomy and screw density on postoperative changes in spinal rod contour have not been documented. This study aimed to evaluate the effects of multilevel facetectomy and screw density on changes in spinal rod contour from before implantation to after surgical correction of thoracic curves in patients with AIS prospectively. The concave and convex rod shapes from patients with thoracic AIS ($n = 49$) were traced prior to insertion. Postoperative sagittal rod shape was determined by computed tomography. The angle of intersection of the tangents to the rod end points was measured. Multiple stepwise linear regression analysis was used to identify variables independently predictive of change in rod contour ($\Delta\theta$). Average $\Delta\theta$ at the concave and convex side were $13.6^\circ \pm 7.5^\circ$ and $4.3^\circ \pm 4.8^\circ$, respectively. The $\Delta\theta$ at the concave side was significantly greater than that of the convex side ($P < 0.0001$) and significantly correlated with Risser sign ($P = 0.032$), the preoperative main thoracic Cobb angle ($P = 0.031$), the preoperative TK angle ($P = 0.012$), and the number of facetectomy levels ($P = 0.007$). Furthermore, a $\Delta\theta$ at the concave side $\geq 14^\circ$ significantly correlated with the postoperative TK angle ($P = 0.003$), the number of facetectomy levels ($P = 0.021$), and screw density at the concave side ($P = 0.008$). Rod deformation at the concave side suggests that corrective forces acting on that side are greater than on the convex side. Multilevel facetectomy and/or screw density at the concave side have positive effects on reducing the rod deformation that can lead to a loss of TK angle postoperatively.

OPEN ACCESS

Citation: Kokabu T, Sudo H, Abe Y, Ito M, Ito YM, Iwasaki N (2016) Effects of Multilevel Facetectomy and Screw Density on Postoperative Changes in Spinal Rod Contour in Thoracic Adolescent Idiopathic Scoliosis Surgery. PLoS ONE 11(8): e0161906. doi:10.1371/journal.pone.0161906

Editor: Ara Nazarian, Harvard Medical School/BIDMC, UNITED STATES

Received: May 28, 2016

Accepted: August 12, 2016

Published: August 26, 2016

Copyright: © 2016 Kokabu et al. This is an open access article distributed under the terms of the Creative Commons Attribution License, which permits unrestricted use, distribution, and reproduction in any medium, provided the original author and source are credited.

Data Availability Statement: All relevant data are within the paper.

Funding: The authors received no specific funding for this work.

Competing Interests: The authors have declared that no competing interests exist.

Introduction

Restoration and maintenance of the normal sagittal contour as well as coronal correction of the thoracic curve is an important surgical strategy in patients with thoracic adolescent idiopathic scoliosis (AIS), because these patients typically have a hypokyphotic thoracic spine compared with nonscoliosis patients [1]. Currently, posterior segmental pedicle screw (PS) instrumentation and fusion has become one of the most common surgical treatments. However, recent studies have reported that PS constructs to maximize scoliosis correction can cause further lordosis of the thoracic spine [2–4]. These patients exhibit a flat back, leading to progressive decompensation and sagittal imbalance [1,5]. Preservation of thoracic kyphosis (TK) is also critical to maintain lumbar lordosis after surgical treatment of AIS [1].

To overcome these issues, Ito et al. [6] and Sudo et al. [7–9] recently developed a very simple surgical technique called the simultaneous double-rod rotation technique (SDRRT) for correcting AIS. In this technique, two rods are connected to the screw heads and are simply rotated simultaneously to correct the scoliosis, while TK is maintained or improved. Moreover, hypokyphotic rod deformation is prevented with dual-rod derotation instead of single-rod derotation [6–9].

Some studies have investigated the correlation between AIS curve correction and destabilization procedures such as multilevel facetectomy [10] or the number of fixation anchors, such as PS density [11–14]. Implant rod curvature will also influence the postoperative TK. The initial shape of the rod could lead to a certain sagittal outcome. However, it has been recognized that rods bent by surgeons prior to implantation tend to flatten after surgery [15,16]. The postoperative implant rod deformation as a “spring-back” effect can alter the sagittal alignment of the spine and consequently the clinical outcome [17]. Until now, there has been no consensus on what possible factors can alter the shape of the rod. Based on the biomechanical point of view, the comprehensive effects of the surgical strategies on postoperative TK remain unknown. This study aimed to evaluate the effects of multilevel facetectomy and/or screw density on the change in the rod contour and TK in patients with thoracic AIS.

Materials and Methods

Patients

This study was an investigator-initiated observational cohort study conducted at a single medical center and approved by institutional review board of Hokkaido University Hospital (approval number: 014–0370). A written informed consent was obtained from all participants. Data from 49 patients (1 male, 48 female) with Lenke type 1 or type 2 AIS curves who underwent posterior thoracic curve correction between June 2009 and April 2016 were evaluated at our institution. Exclusion criteria included syndromic, neuromuscular, and congenital scoliosis and the presence of other double or triple major AIS curves, as well as thoracolumbar and lumbar AIS curves. The average age and Risser sign at surgery were 15.5 ± 2.2 years (range, 12–20) and 3.9 ± 1.1 (range, 1–5; Table 1), respectively.

Standing long-cassette posteroanterior and lateral radiographs were evaluated for multiple parameters before and at the 2-week follow-up. Coronal and sagittal Cobb angle measurements of the main thoracic (MT) curves were obtained. The end vertebrae levels were determined on preoperative radiographs and measured on subsequent radiographs to maintain consistency for statistical comparisons [7,8]. Sagittal measurements included the TK (T5–T12) angle [7,8]. The number of facetectomy levels was counted, and screw density was expressed as the number of screws per level instrumented for each patient. In this study, the number of hooks in the instrumented level was not counted.

Table 1. Disease characteristics and clinical features of the subjects.

	Mean \pm standard deviation	Range
Body mass index (kg/m ²)	18.8 \pm 2.4	12.4 to 24.2
Risser sign (grade)	3.9 \pm 1.1	1 to 5
Preoperative main thoracic Cobb angle (°)	59.5 \pm 10.2	46 to 88
Postoperative main thoracic Cobb angle (°)	13.3 \pm 7.3	1 to 36
Preoperative thoracic kyphosis angle (°)	11.7 \pm 7.8	-4 to 34
Postoperative thoracic kyphosis angle (°)	21.1 \pm 6.3	7 to 33
Number of vertebrae in fusion (no.)	10.8 \pm 1.6	7 to 14
Number of facetectomy levels (no.)	6.5 \pm 3.4	0 to 12
Screw density at concave side (no. of screws / level instrumented)	0.89 \pm 0.14	0.5 to 1
Screw density at convex side (no. of screws / level instrumented)	0.80 \pm 0.16	0.4 to 1

doi:10.1371/journal.pone.0161906.t001

Surgical Technique

Six-millimeter diameter titanium-alloy implant rods and polyaxial PSs (USS II Polyaxial, DePuy Synthes, Raynham, MA, USA) were used to correct the scoliosis deformity. All rods were prebent only at a single plane. Rods and screws were surgically implanted via the double rod rotation technique [6–9]. In this technique, two implant rods were inserted into the polyaxial screw heads. The polyaxial screw heads remained unfastened until the completion of rod rotation, allowing the rods to rotate and translate freely inside the screw head. A torque was applied to the rod-rotating device to rotate the rods simultaneously, transferring the previous curvature of the rod at the coronal plane to the sagittal plane. Additional in situ bending or other reduction maneuvers were not performed in all cases. All polyaxial screws were carried upward and medially to the concave side of the curve by the rotation of the rods, which did not exert any downward force on the vertebral body [6–9]. Both polyaxial screw heads and simultaneous double-rod rotation were key to the current technique. Frictional force at the screw-rod interface was decreased, and there was little chance of screw cut-out laterally [9]. This technique provided derotation of the apical vertebra as well as restoration of TK, leading to rib hump correction without additional costoplasty [9].

Rod Analysis

The implant rod angle of curvature was used to evaluate implant rod deformation. Prior to implantation, following the intraoperative contouring of the rods, the surgeon traced the rod shapes on paper [15]. The angle between the proximal and distal tangential line was measured as the rod angle before implantation (θ_1) as previously described [15]. Postoperative implant rod geometry was obtained a maximum of 2 weeks after the surgical operation using computed tomography (Aquilion 64 CT scan; Toshiba Medical Systems Corporation, Tokyo, Japan). Digital Imaging and Communications in Medicine (DICOM) data were obtained to reconstruct new images by DICOM viewer software (OsiriX Imaging Software; Pixmeo Labs., Geneva, Switzerland). The reconstructed sagittal images of the implanted rods were obtained, and the angle between the proximal tangential line and the distal tangential line was measured (θ_2) (Fig 1). In cases in which the rod shape had both thoracic and lumbar curvature, the distal tangential line was determined based on the inflection point. The angle of rod deformation ($\Delta\theta$) was defined as the difference between θ_1 and θ_2 ($\theta_1 - \theta_2$). The angles θ_1 , θ_2 , and $\Delta\theta$ were obtained from the rods at both the concave and convex sides.

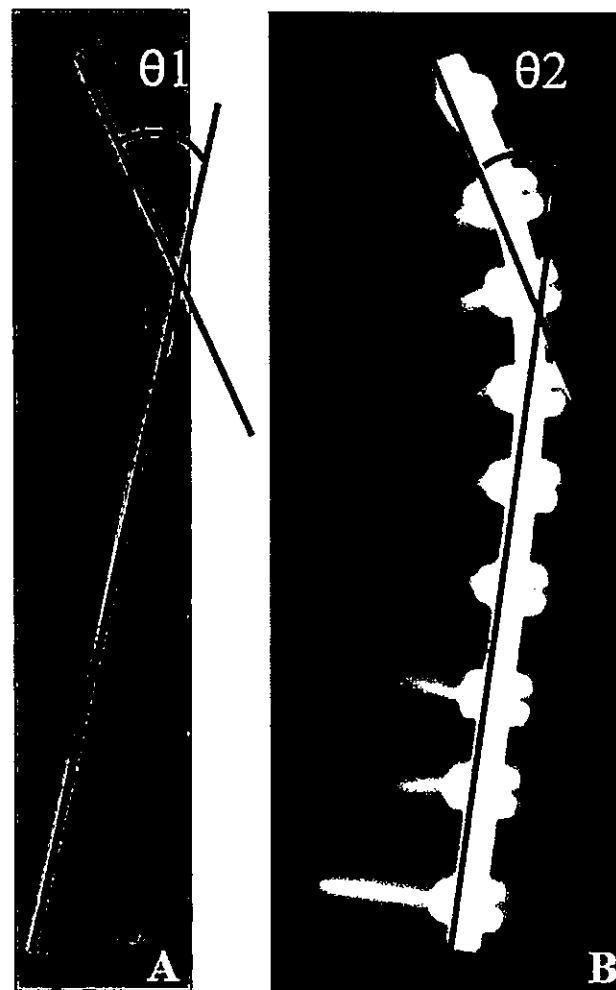


Fig 1. Rod angle before and after implantation. (A) Prior to implantation, the surgeon traced the rod shapes on paper. The angle between the proximal and distal tangential line was measured (θ_1). (B) Postoperative implant rod geometry (θ_2) was obtained after the surgical operation using computed tomography.

doi:10.1371/journal.pone.0161906.g001

Statistical Analysis

Bivariate statistical analysis was performed between the change in TK (postoperative TK–preoperative TK) and the $\Delta\theta$ at the concave or convex side using the Wilcoxon rank sum test. Pearson's correlation coefficient analysis was used to assess relationships between independent variables. Stepwise linear regression analysis was applied to control for possible confounding variables and to identify variables independently predictive of $\Delta\theta$ both at the concave and convex side. Patients' age and disease characteristics were included in the variables: age, body mass index [weight (kg)/height(m)²], Risser sign, preoperative MT Cobb angle, postoperative MT Cobb angle, preoperative TK angle, postoperative TK angle, number of facetectomy levels, and screw density at both the concave and convex side. Significant multivariate predictors are reported with their respective predictive equations, including the intercept and regression coefficients (β). Model fit was assessed by using the goodness-of-fit *F* test and *R*² statistic. Data

analyses were performed using JMP statistical software for Windows (version 12; SAS, Inc., Cary, NC, USA). $P < 0.05$ was considered statistically significant. All data are expressed as mean \pm standard deviation.

Results

Disease characteristics are summarized in Table 1. On average, 10.8 ± 1.6 vertebrae were instrumented in the 49 patients. The average preoperative MT curve was $59.5^\circ \pm 10.2^\circ$. Postoperative radiographs showed an average MT curve of $13.3^\circ \pm 7.3^\circ$. Sagittal plane analysis revealed that the average preoperative TK was $11.7^\circ \pm 7.8^\circ$, which improved significantly to $21.1^\circ \pm 6.3^\circ$ ($P < 0.0001$).

The preoperative θ_1 and postoperative θ_2 implant rod angle of curvatures at the concave and convex sides of the deformity are listed in Table 2.

The θ_2 was significantly lower than the θ_1 at the concave side ($P < 0.001$ at the concave side, $P = 0.019$ at the convex side, respectively). The $\Delta\theta$ at the concave side was significantly greater than that of the convex side ($P < 0.0001$) (Fig 2).

Postoperative TK was significantly correlated with the postoperative θ_2 implant rod angle at both sides, particularly at the concave side (concave: $r = -0.415$, $P = 0.003$; convex: $r = -0.321$, $P = 0.025$, respectively) (Fig 3).

In multiple stepwise linear regression analysis, 4 variables were independent predictive factors for $\Delta\theta$ at the concave side: Risser sign ($P = 0.032$), the preoperative MT Cobb angle ($P = 0.031$), the preoperative TK angle ($P = 0.012$, and the number of facetectomy levels ($P = 0.007$). The model fit the data well (goodness-of-fit F test = 7.05, $R^2 = 0.50$, $P = 0.0001$) (Table 3).

Conversely, for $\Delta\theta$ at the convex side, 3 variables emerged as predictors: the number of vertebrae in fusion (standardized $\beta = -0.596$, $P = 0.0003$), the number of facetectomy levels (standardized $\beta = 0.578$, $P = 0.0006$), and the Risser sign (standardized $\beta = -0.292$, $P = 0.026$). However, R^2 was low (goodness-of-fit F test = 5.67, $R^2 = 0.34$, $P = 0.0009$), indicating that only 34% of the variation in $\Delta\theta$ was explained by these 3 predictors.

Subgroup Analysis

To determine whether $\Delta\theta$ affects postoperative TK, the total cohort was then divided into 2 groups on the basis of the mean $\Delta\theta$ at the concave side. The $\Delta\theta \geq 14^\circ$ group was defined by $\Delta\theta$ above the mean degree ($13.6^\circ \pm 7.5^\circ$) at the concave side and further analyzed. The average age ($n = 23$) were 15.4 ± 2.1 years (range, 12–20). Disease characteristics and rod data in the group of $\geq 14^\circ$ rod deformation are summarized in Table 4.

Pearson's correlation coefficient analysis showed that in the group of $\Delta\theta \geq 14^\circ$, $\Delta\theta$ at the concave side had significant correlation with the postoperative TK angle ($r = -0.590$, $P = 0.003$),

Table 2. Implant rod angle of curvature at the concave and convex side of deformity.

	Mean \pm standard deviation	Range
Preoperative rod angle (θ_1) at concave side ($^\circ$)	41.8 ± 7.1	22.3 to 66.5
Preoperative rod angle (θ_1) at convex side ($^\circ$)	38.4 ± 9.5	19.5 to 69.9
Postoperative rod angle (θ_2) at concave side ($^\circ$)	28.2 ± 9.1	9.2 to 48.5
Postoperative rod angle (θ_2) at convex side ($^\circ$)	34.1 ± 8.2	15.0 to 55.8
Rod deformation ($\Delta\theta$) at concave side ($^\circ$)	13.6 ± 7.5	-0.3 to 36.5
Rod deformation ($\Delta\theta$) at convex side ($^\circ$)	4.3 ± 4.8	-6.8 to 17.8

doi:10.1371/journal.pone.0161906.t002

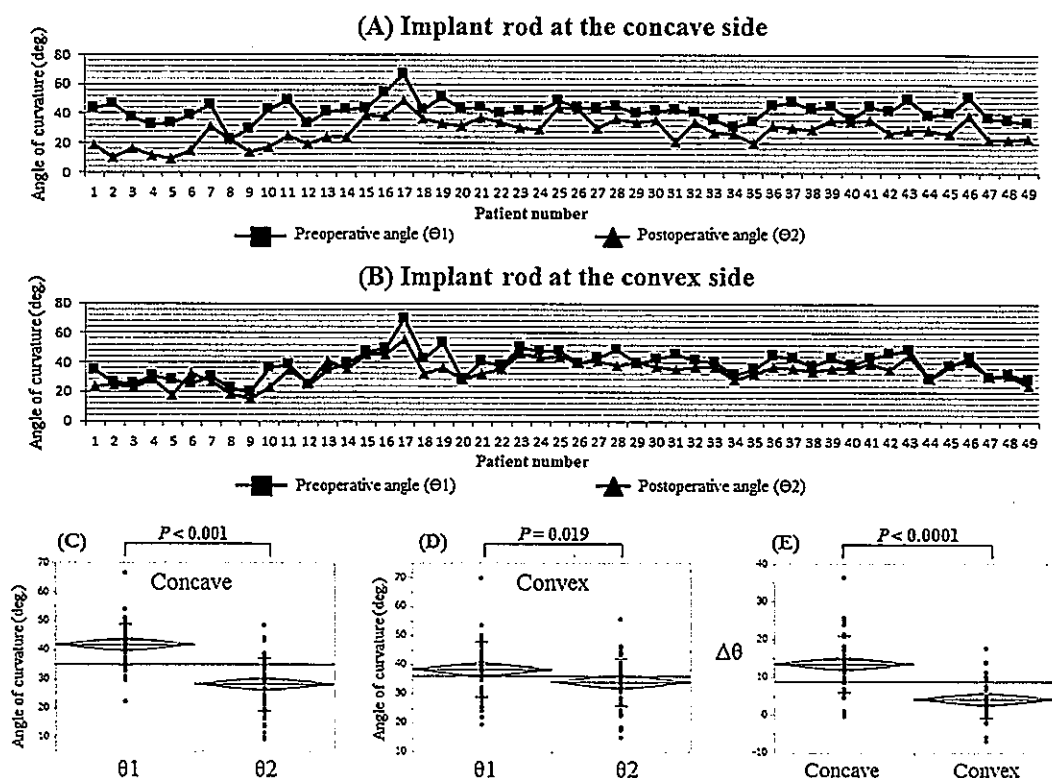


Fig 2. Implant rod angle of curvature at the concave and convex sides of the deformity. (A) θ_1 and θ_2 at the concave side of each patients. (B) θ_1 and θ_2 at the convex side of each patients. (C) Comparison between θ_1 and θ_2 at the concave side. (D) Comparison between θ_1 and θ_2 at the convex side. (E) Comparison between $\Delta\theta$ at the concave side and $\Delta\theta$ at the convex side.

doi:10.1371/journal.pone.0161906.g002

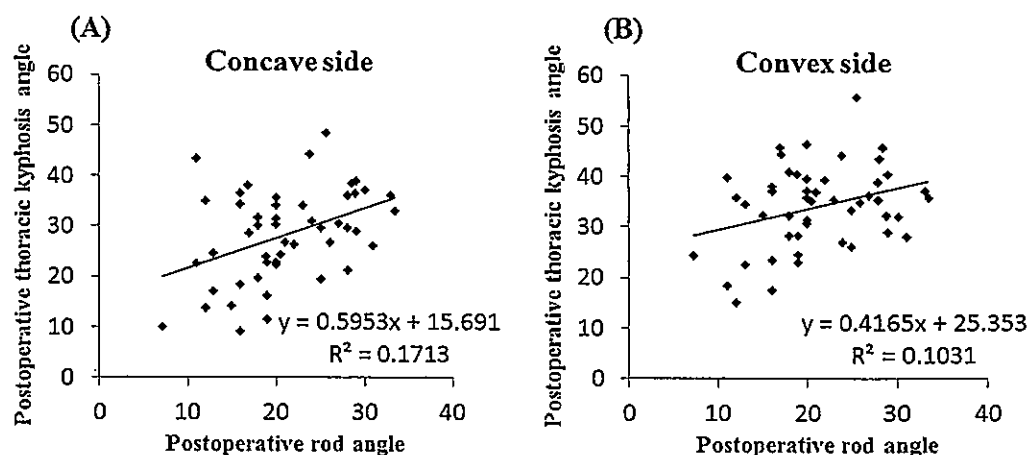


Fig 3. Correlation analysis between the postoperative rod angle and the thoracic kyphosis angle. (A) concave side. (B) convex side.

doi:10.1371/journal.pone.0161906.g003

Table 3. Associations between various factors and rod deformation at the concave side (°) using multiple stepwise linear regression analysis.

	Regression Coefficient	Standard Error	95% Confidence Interval	t	Standardized β	P
Constant	-10.787	8.57	(-28.081, 6.509)	-1.26	-	0.215
Risser sign (grade)	1.668	0.753	(0.148, 3.188)	2.21	0.249	0.032
Preoperative main thoracic Cobb angle (°)	0.265	0.085	(0.095, 0.436)	3.14	0.362	0.031
Preoperative thoracic kyphosis angle (°)	-0.279	0.106	(-0.494, -0.064)	-2.62	-0.292	0.012
Number of facetectomy levels (no.)	-0.716	0.253	(-1.225, -0.206)	-2.83	-0.325	0.007
Screw density at convex side (no. of screws / level instrumented)	10.372	5.205	(-0.133, 20.876)	1.99	0.223	0.053

$P < 0.05$ was considered statistically significant

doi:10.1371/journal.pone.0161906.t003

the number of facetectomy levels ($r = -0.479$, $P = 0.021$), and screw density at the concave side ($r = -0.537$, $P = 0.008$) (Table 5).

Discussion

Careful investigation of the changes in implant rod geometry is important to fully understand the biomechanics of scoliosis correction [16]. However, there have been few studies examining the relationship between rod deformation and sagittal alignment of the thoracic spine [15,16,18]. Cidambi et al. [15] documented that a significant difference was observed between pre- and postoperative rod contour, particularly for concave rods, and that the resulting deformations were likely associated with substantial *in vivo* deforming forces. Similarly, Salmingo et al. [16] reported that implant rods at the concave side were significantly deformed after surgery, whereas rods at the convex side had no significant deformation. Abe et al. [18] suggested that the corrective force during scoliosis surgery was 4 times greater at the concave side than at the convex side. The present study also showed that there was a significant positive relationship between postoperative TK and the postoperative implant rod angle of curvature, indicating

Table 4. Disease characteristics and rod data in the group of $\geq 14^\circ$ rod deformation at the concave side.

	Mean \pm standard deviation	Range
Body mass index (kg/m ²)	18.6 \pm 2.5	13.1 to 23.4
Risser sign (grade)	4.0 \pm 0.9	1 to 5
Preoperative main thoracic Cobb angle (°)	61.7 \pm 11.7	46 to 88
Postoperative main thoracic Cobb angle (°)	14.0 \pm 6.3	1 to 27
Preoperative thoracic kyphosis angle (°)	7.6 \pm 5.5	-4 to 23
Postoperative thoracic kyphosis angle (°)	19.6 \pm 6.0	7 to 33
Number of vertebrae in fusion (no.)	10.5 \pm 1.6	7 to 13
Number of facetectomy levels (no.)	5.6 \pm 3.4	0 to 11
Screw density at concave side (no. of screws / level instrumented)	0.89 \pm 0.15	0.56 to 1
Screw density at convex side (no. of screws / level instrumented)	0.84 \pm 0.15	0.5 to 1
Preoperative rod angle (θ_1) at concave side (°)	43.4 \pm 8.0	29.6 to 66.5
Preoperative rod angle (θ_1) at convex side (°)	37.9 \pm 11.3	19.5 to 69.9
Postoperative rod angle (θ_2) at concave side (°)	23.7 \pm 9.6	9.2 to 48.5
Postoperative rod angle (θ_2) at convex side (°)	32.5 \pm 9.3	15.0 to 55.8
Rod deformation ($\Delta\theta$) at concave side (°)	19.7 \pm 5.3	14.1 to 36.5
Rod deformation ($\Delta\theta$) at convex side (°)	5.5 \pm 6.0	-6.8 to 17.8

doi:10.1371/journal.pone.0161906.t004

Table 5. Correlation analysis between rod deformation and variable in patients with rod deformation $\geq 14^\circ$ at the concave side.

Variable	Pearson's correlation coefficients		
	Correlation coefficient	95% CI	Statistical significance
Age at surgery (yrs)	$r = -0.017$	$(-0.398, 0.427)$	$P = 0.937$
Body mass index (kg/m^2)	$r = -0.207$	$(-0.570, 0.225)$	$P = 0.344$
Risser sign (grade)	$r = -0.084$	$(-0.479, 0.340)$	$P = 0.705$
Preoperative main thoracic Cobb angle ($^\circ$)	$r = 0.142$	$(-0.287, 0.524)$	$P = 0.518$
Postoperative main thoracic Cobb angle ($^\circ$)	$r = 0.396$	$(-0.019, 0.695)$	$P = 0.061$
Preoperative thoracic kyphosis angle ($^\circ$)	$r = -0.286$	$(-0.625, 0.143)$	$P = 0.186$
Postoperative thoracic kyphosis angle ($^\circ$)	$r = -0.590$	$(-0.806, -0.235)$	$P = 0.003$
Number of vertebrae in fusion (no.)	$r = -0.324$	$(-0.649, 0.102)$	$P = 0.132$
Number of facetectomy levels (no.)	$r = -0.479$	$(-0.744, -0.083)$	$P = 0.021$
Screw density at concave side (no. of screws / level instrumented)	$r = -0.537$	$(-0.777, -0.160)$	$P = 0.008$
Screw density at convex side (no. of screws / level instrumented)	$r = 0.350$	$(-0.073, 0.666)$	$P = 0.102$
Rod deformation ($\Delta\theta$) at convex side ($^\circ$)	$r = 0.014$	$(-0.424, 0.400)$	$P = 0.948$

$P < 0.05$ was considered statistically significant

doi:10.1371/journal.pone.0161906.t005

that implant rod curvature influences sagittal curve correction. In addition, rod deformation at the concave side was significantly greater than that of the convex side.

Removing the facets and soft tissues between the posterior elements has been shown to allow greater distraction abilities along the length of the posterior column [1]. Destabilization of the posterior spinal segment by releasing soft tissue or facet joints could be important to prevent implant breakage or pedicle fracture during maneuver in more severe curve corrections [18]. However, it is still unclear whether these posterior releases positively affect the TK, especially with a hypokyphotic thoracic spine [1,9]. Recently, Sudo et al. [9] documented that in patients with a hypokyphotic thoracic spine $< 15^\circ$, a significant correlation was found between the change in TK and the number of facetectomy levels, indicating that multilevel facetectomy is an important factor to restore TK in patients with hypokyphotic thoracic spines. In the present study, there was a significant negative correlation between preoperative TK and rod deformation, indicating that the rod deformation was greater in patients with preoperative hypokyphotic thoracic spines. In addition, the deformation could be decreased by increasing the number of facetectomy levels.

Screw density may be also a possible factor in optimizing restoration of TK. However, the effect of implant density on sagittal plane correction and TK restoration has been reported in only a few studies, and the results have been controversial [12,14,19]. Larson et al. [12] demonstrated that decreased TK was correlated with increased screw density for Lenke type 1 and 2 curves. Conversely, Liu et al. [14] documented that higher screw density provided better TK restoration than low screw density. Recently, Sudo et al. [9] also documented that in patients with preoperative TK $< 15^\circ$, a significant positive correlation was found between the change in TK and screw density, whereas no correlation was found in patients with TK $\geq 15^\circ$, suggesting that screw density had a positive effect on TK restoration in patients with hypokyphotic thoracic spines. Their results indicate that screw density at the concave side has an impact not only on scoliosis correction but also on TK restoration.

In the present study, in patients with rod deformation at the concave side $\geq 14^\circ$, there were significant negative correlations between rod deformation at the concave side and postoperative TK or screw density at the concave side. These results suggest that rod deformation $\geq 14^\circ$ at the concave side significantly decreases postoperative TK. However, this rod deformation

could be decreased by increasing screw density at the concave side. Hence, the current results biomechanically supported the results presented by Sudo et al.[9], documenting that in patients with preoperative hypokyphotic thoracic spines, increasing screw density at the concave side is important for optimizing postoperative TK.

There were limitations to this study. First, we evaluated deformity surgery with the use of titanium rods. The module of elasticity of the titanium alloy is much less than either stainless steel or cobalt chrome implants [16]. Second, we did not analyze the effects of multilevel osteotomy on the *in vivo* flexibility of the thoracic spine. We are now measuring *in vivo* force acting at the vertebrae before and after multilevel osteotomies in order to investigate the biomechanical effects of spinal flexibility provided by multilevel facet osteotomies on rod deformation. Third, resisting forces from the deformed spine might be different between males and females and this would need to be addressed in our predominantly female cohort. However, there were no effects of gender on thoracic hypokyphosis postoperatively (data not shown). Last, the relationships between rod deformation and clinical symptoms remain unclear.

Conclusion

The present study showed that there was a significant relationship between postoperative TK and the postoperative implant rod angle of curvature. In addition, the rod at the concave side was significantly deformed after the surgical treatment. The rod deformation at the concave side suggests that corrective forces acting on that side are greater than on the convex side. Multilevel facetectomy and/or screw density at the concave side have positive effects on reducing the rod deformation that can lead to a loss of TK angle postoperatively.

Author Contributions

Conceptualization: HS.

Data curation: HS YA.

Formal analysis: TK HS YMI.

Investigation: TK HS.

Methodology: TK HS YA.

Project administration: HS.

Resources: HS MI.

Software: TK YMI.

Supervision: HS MI NI.

Validation: TK HS YMI.

Visualization: TK.

Writing – original draft: TK HS.

Writing – review & editing: HS.

References

1. Newton PO, Yaszay B, Upasani VV, Pawelek JB, Bastrom TP, Lenke LG, et al. Preservation of thoracic kyphosis is critical to maintain lumbar lordosis in the surgical treatment of adolescent idiopathic scoliosis. *Spine (Phila Pa 1976)* 2010; 35:1365–70.

2. Lowenstein JE, Matsumoto H, Vitale MG, Weidenbaum M, Gomez JA, Lee FY, et al. Coronal and sagittal plane correction in adolescent idiopathic scoliosis: a comparison between all pedicle screw versus hybrid thoracic hook lumbar screw constructs. *Spine (Phila Pa 1976)* 2007; 32:448–52.
3. Winter RB, Lovell WW, Moe JH. Excessive thoracic lordosis and loss of pulmonary function in patients with idiopathic scoliosis. *J Bone Joint Surg Am* 1975; 57:972–7. PMID: 1184646
4. Kim YJ, Lenke LG, Kim J, Bridwell KH, Cho SK, Cheh G, et al. Comparative analysis of pedicle screw versus hybrid instrumentation in posterior spinal fusion of adolescent idiopathic scoliosis. *Spine (Phila Pa 1976)* 2006; 31:291–8.
5. Roussouly P, Nnadi C. Sagittal plane deformity: an overview of interpretation and management. *Eur Spine J* 2010; 19:1824–36. doi: 10.1007/s00586-010-1476-9 PMID: 20567858
6. Ito M, Abumi K, Kotani Y, Takahata M, Sudo H, Hojo Y, et al. Simultaneous double-rod rotation technique in posterior instrumentation surgery for correction of adolescent idiopathic scoliosis. *J Neurosurg Spine* 2010; 12:293–300. doi: 10.3171/2009.9.SPINE09377 PMID: 20192630
7. Sudo H, Ito M, Abe Y, Abumi K, Takahata M, Nagahama K, et al. Surgical treatment of Lenke 1 thoracic adolescent idiopathic scoliosis with maintenance of kyphosis using the simultaneous double-rod rotation technique. *Spine (Phila Pa 1976)* 2014; 39:1163–9.
8. Sudo H, Abe Y, Abumi K, Iwasaki N, Ito M, et al. Surgical treatment of double thoracic adolescent idiopathic scoliosis with a rigid proximal thoracic curve. *Eur Spine J* 2016; 25:569–77. doi: 10.1007/s00586-015-4139-z PMID: 26195082
9. Sudo H, Abe Y, Kokabu T, Ito M, Abumi K, Ito YM, et al. Correlation analysis between change in thoracic kyphosis and multilevel facetectomy/ screw density in main thoracic adolescent idiopathic scoliosis surgery. *Spine J*, Epub ahead of print.
10. Halanski MA, Cassidy JA. Do multilevel Ponte osteotomies in thoracic idiopathic scoliosis surgery improve curve correction and restore thoracic kyphosis? *J Spinal Disord Tech* 2013; 26:252–5. doi: 10.1097/BSD.0b013e318241e3cf PMID: 22198324
11. Bharucha NJ, Lonner BS, Auerbach JD, Kean KE, Trobisch PD, et al. Low-density versus high-density thoracic pedicle screw constructs in adolescent idiopathic scoliosis: do more screws lead to a better outcome? *Spine J* 2013; 13:375–81. doi: 10.1016/j.spinee.2012.05.029 PMID: 22901787
12. Larson AN, Polly DW Jr, Diamond B, Ledonio C, Richards BS 3rd, Emans JB, et al. Does higher anchor density result in increased curve correction and improved clinical outcomes in adolescent idiopathic scoliosis? *Spine (Phila Pa 1976)* 2014; 39:571–8.
13. Le Navéaux F, Aubin CE, Larson AN, Polly DW Jr, Baghdadi YM, Labelle H. Implant distribution in surgically instrumented Lenke 1 adolescent idiopathic scoliosis: does it affect curve correction? *Spine (Phila Pa 1976)* 2015; 40:462–8.
14. Liu H, Li Z, Li S, Zhang K, Yang H, Wang J, et al. Main thoracic curve adolescent idiopathic scoliosis: association of higher rod stiffness and concave-side pedicle screw density with improvement in sagittal thoracic kyphosis restoration. *J Neurosurg Spine* 2015; 22:259–66. doi: 10.3171/2014.10.SPINE1496 PMID: 25525960
15. Cidambi KR, Glaser DA, Bastrom TP, Nunn TN, Ono T, Newton PO. Postoperative changes in spinal rod contour in adolescent idiopathic scoliosis: an in vivo deformation study. *Spine (Phila Pa 1976)* 2012; 37:1566–72.
16. Salmingo RA, Tadano S, Abe Y, Ito M. Influence of implant rod curvature on sagittal correction of scoliosis deformity. *Spine J* 2014; 14:1432–9. doi: 10.1016/j.spinee.2013.08.042 PMID: 24275616
17. Delorme S, Labelle H, Poitras B, Rivard CH, Coillard C, Dansereau J. Pre-, intra-, and postoperative three-dimensional evaluation of adolescent idiopathic scoliosis. *J Spinal Disord* 2000; 13:93–101. PMID: 10780682
18. Abe Y, Ito M, Abumi K, Sudo H, Salmingo R, Tadano S. Scoliosis corrective force estimation from the implanted rod deformation using 3D-FEM analysis. *Scoliosis* 2015; 10(Suppl 2):S2. doi: 10.1186/1748-7161-10-S2-S2 PMID: 25810754
19. Lonner BS, Lazar-Antman MA, Sponseller PD, Shah SA, Newton PO, Betz R, et al. Multivariate analysis of factors associated with kyphosis maintenance in adolescent idiopathic scoliosis. *Spine (Phila Pa 1976)* 2012; 37:1297–302.

RESEARCH ARTICLE

In Vivo Mouse Intervertebral Disc Degeneration Model Based on a New Histological Classification

Takashi Ohnishi¹, Hideki Sudo^{2*}, Koji Iwasaki¹, Takeru Tsujimoto¹, Yoichi M. Ito³, Norimasa Iwasaki¹

¹ Department of Orthopaedic Surgery, Hokkaido University Graduate School of Medicine, Sapporo, Hokkaido, Japan, ² Department of Advanced Medicine for Spine and Spinal Cord Disorders, Hokkaido University Graduate School of Medicine, Sapporo, Hokkaido, Japan, ³ Department of Biostatistics, Hokkaido University Graduate School of Medicine, Sapporo, Hokkaido, Japan

* hidekisudo@yahoo.co.jp



OPEN ACCESS

Citation: Ohnishi T, Sudo H, Iwasaki K, Tsujimoto T, Ito YM, Iwasaki N (2016) *In Vivo* Mouse Intervertebral Disc Degeneration Model Based on a New Histological Classification. PLoS ONE 11(8): e0160486. doi:10.1371/journal.pone.0160486

Editor: Lachlan J. Smith, University of Pennsylvania, UNITED STATES

Received: April 2, 2016

Accepted: July 19, 2016

Published: August 2, 2016

Copyright: © 2016 Ohnishi et al. This is an open access article distributed under the terms of the Creative Commons Attribution License, which permits unrestricted use, distribution, and reproduction in any medium, provided the original author and source are credited.

Data Availability Statement: All relevant data are within the paper.

Funding: This work was supported partly by the Ministry of Education, Culture, Sports, Science, and Technology of Japan (a Grant-in-Aid for Challenging Exploratory Research, 26670651) (to H. Sudo). The funders had no role in study design, data collection and analysis, decision to publish, or preparation of the manuscript.

Competing Interests: The authors have declared that no competing interests exist.

Abstract

Although human intervertebral disc degeneration can lead to several spinal diseases, its pathogenesis remains unclear. This study aimed to create a new histological classification applicable to an *in vivo* mouse intervertebral disc degeneration model induced by needle puncture. One hundred six mice were operated and the L4/5 intervertebral disc was punctured with a 35- or 33-gauge needle. Micro-computed tomography scanning was performed, and the punctured region was confirmed. Evaluation was performed by using magnetic resonance imaging and histology by employing our classification scoring system. Our histological classification scores correlated well with the findings of magnetic resonance imaging and could detect degenerative progression, irrespective of the punctured region. However, the magnetic resonance imaging analysis revealed that there was no significant degenerative intervertebral disc change between the ventrally punctured and non-punctured control groups. To induce significant degeneration in the lumbar intervertebral discs, the central or dorsal region should be punctured instead of the ventral region.

Introduction

Human intervertebral disc (IVD) degeneration is a common cause of low back pain and it affects the daily activities [1–3]. It is the cause of spinal diseases such as spinal canal stenosis, disc herniation, and spinal deformity. Currently, there is no clinical treatment to prevent the development of IVD degeneration, and the present available therapeutic options for spinal complications, namely analgesics and surgical procedures, do not address the etiology [1].

The research focusing on IVD degeneration, from the gross anatomical to histological studies, has been conducted using various animal models: scalpel incision to annulus fibrosus (AF) in canines [4] and rats [5]; surface incision to AF in sheep [6]; full puncture to IVD using needle in mice [7] and rats [8]; and hemi-AF puncture using needle in mice [9], rats [10], and

rabbits [11–13]. However, because of the animal size and the species-specific physiological variations, the level of IVD degeneration differs [10,14]. To establish an IVD degeneration model induced by needle puncture, a precise size and shape of the device and a detailed procedure for each of the species are necessary. In addition, although the number of reports describing IVD degeneration in terms of the genetic approaches is increasing [1,15–19], there has been no appropriate histological classification applicable to an *in vivo* mouse intervertebral disc degeneration model, which is also applicable to genetically modified mice. The aim of this study was to create a new histological classification applicable to an *in vivo* mouse intervertebral disc degeneration model induced by needle puncture.

Materials and Methods

All animal procedures in this study were conducted with the approval of the Institutional Animal Care and Use Committee of Hokkaido University (approval number: 13–0051). Moreover, all these procedures were carried out in accordance with the approved guidelines. Inbred C57BL/6 mice were obtained from Sankyo Labo Service Corporation (Tokyo, Japan). The mice were bred and housed under specific pathogen-free conditions before surgery, and housed under P2 conditions after surgery at Hokkaido University Creative Research Institution Platform for Research on Biofunctional Molecules. P2 means a level of isolation from natural environment, that keeps the room in sterilized and safe condition. They were kept in cages at room temperature ($23^{\circ}\text{C} \pm 2^{\circ}\text{C}$) and humidity of $50\% \pm 10\%$, under standard laboratory conditions with a 12 h light/dark cycle. They were allowed unrestricted cage activity and ad libitum access to food and water. Standard laboratory diet, Labo MR Stock (Nosan Corporation, Yokohama, Japan) and sterilized tap water were provided as sources of food and water, respectively. All the surgeries were performed under general anesthesia with ketamine 1.9 mg and xylazine 0.2 mg intraperitoneal injection, and all animal suffering was minimized. After surgery, the mice were monitored once in two days. During the experiment, five mice (which are not included in the total of 106 mice) died within one to two days after surgery, presumably with respiratory depression due to anesthesia or hemorrhage due to surgery. The protocol of early euthanasia/humane endpoints for mice that were severely ill or moribund, as indicated by shivering and respiratory distress with disability in walking suggestive of apparent distress, with no recovery expected, was intraperitoneal injection of 5 mg of pentobarbital sodium. However, none was applicable. Except for the five mice that died, all mice exhibited good health and well-being until the end of the experiment. They were euthanized with pentobarbital sodium intraperitoneal injection.

One hundred six C57BL/6 mice (male, 54; female, 52) were operated under general anesthesia. All the mice were 11 weeks old at the time of surgery. The lumbar spine was posterolaterally approached from the right side, and the L4/5 IVD was punctured with a 35-gauge (G) or 33G needle. Micro-CT scanning [3D micro X-ray CT R_mCT 2 (Rigaku, Tokyo, Japan)] was performed, and the punctured region was confirmed through multiplanar reconstruction views (Fig 1a). The regions in IVD were determined in order to identify the position of the needle, which are as follows. First, the mid-sagittal diameter was divided into three parts: a concentric ellipsoid that constituted the central region was described using boundary points. Second, the peripheral region was divided into the ventral and dorsal regions. Third, the ventral, central, and dorsal regions were defined (Fig 1b). The regions were space prescribed by the endplates. The outer layer of AF that bulged from the endplates was not counted as the intervertebral space. When the needle did not get punctured into the intervertebral space, the trial was repeated until the needle hit the intervertebral space. We determined the position of the needle by visually analyzing the multi-slice CT scan images. If the needle penetrated the central

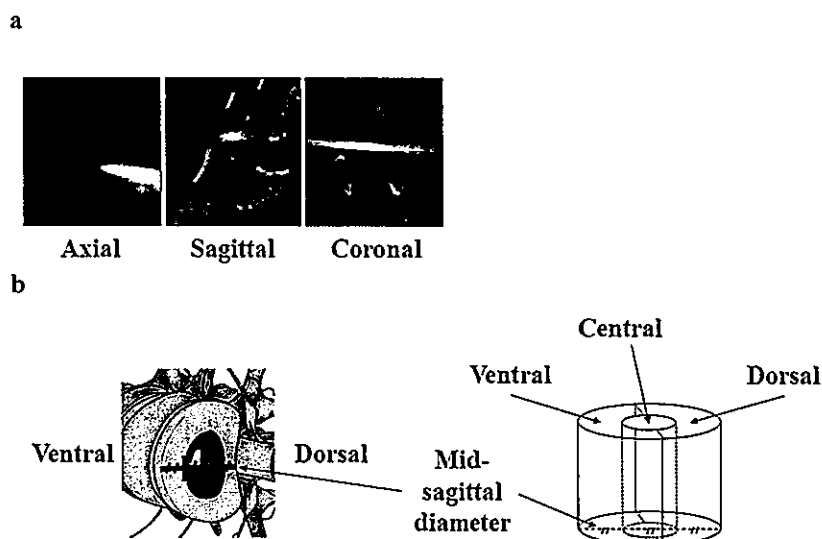














Fig 1. The location of a needle in the intervertebral disc was evaluated using micro-computed tomography scanning. (a) The punctured region was confirmed by multiplanar reconstruction views. (b) The punctured region was defined as the ventral (V), central (C), or dorsal (D) region.

doi:10.1371/journal.pone.0160486.g001

region, we designate the position of the needle as the ‘central region’, and in cases when the needle partially penetrated the dorsal or ventral region, consensus was obtained for the designation of the region. Before closing the wound, the needles were removed and the mice were euthanized one, two, four, eight, or 12 weeks after the surgery.

The mid-sagittal images of the punctured discs were qualitatively analyzed by using MRI to evidence the degenerative changes. More precisely, T2-weighted mid-sagittal images of the punctured discs were qualitatively analyzed by using a 7.0-Tesla MR scanner (Varian Unity Inova; Varian Medical Systems, Palo Alto, CA, USA) [1,17,20]. The degree of IVD was assessed by using the Pfirrmann classification [21]. A quantitative analysis of the sagittal image slices was also performed by using Analyze 10.0 software (AnalyzeDirect, Overland Park, KS, USA), as reported previously [1,17,20]. To quantify the alterations in the NP, the MRI index (the product of the NP area and the average signal intensity) was used [1,17,20]. Data were expressed as percentages of the results obtained when using untreated, non-punctured control discs [1,17,20]. The control was defined for the Pfirrmann grade as the value of L3/4 IVD and for the MRI index as the average value of both L3/4 and L5/6 IVDs. All the image assessments were performed by two independent blind observers, and the quantitative data were presented as means of three evaluations.

After the MRI examinations, each IVD was fixed in 10% neutral buffered formalin solution for 48 h, followed by decalcification with 10% EDTA for 2–4 weeks, and paraffin embedding. Mid-sagittal sections were obtained and stained with safranin O-fast green. For the histological analysis, four types of classification [for rabbits by Masuda et al. [11], for rats by Nishimura et al. [22], for mice by Yang et al. [9], and our group (Fig 2)] were used to evaluate the degeneration. For each classification type, the maximum points represent severe degeneration. The control was defined as the histological score of L3/4 IVD. All the histological assessments were performed by two independent blind observers, and the quantitative data were presented as the mean of three evaluations. Our internal studies of intra-/inter-rater reliability have shown excellent kappa statistics for all measures regarding MRI and histological examinations (0.85–1.0).

Intervertebral disc		Score	Findings				
Annulus fibrosus (AF)	fibrosus	0	Normal	0		1	
		1	Mildly serpentine (not bulge beyond endplate edge)				
		2	Moderately serpentine (slightly bulge beyond endplate edge)	2		3	
		3	Severely serpentine (obviously bulge beyond endplate edge)				
		4	Severely serpentine and ruptured	4		5	
		5	Indistinct				
Nucleus pulposus (NP)	pulposus	0	Normal	0		1	
		1	Condensed				
		2	Existence of chondrocyte-like cells, residual NP matrix	2		3	
		3	Global existence of chondrocyte-like cells				
		4	Mildly replaced by fibrous cartilaginous tissue	4		5	
		5	Moderately or severely replaced by fibrous cartilaginous tissue				

Degeneration score = AF score + NP score

Degeneration score = AF score + NP score.

Fig 2. The novel proposed histological grading score. Arrows indicate the serpentine findings in the annulus fibrosus.

doi:10.1371/journal.pone.0160486.g002

The number of mice for each needle size and time point were as follows; ten for the 1-week, fourteen for the 2-week, eleven for the 4-week, ten for the 8-week, and ten for the 12-week time point for the 35G needle puncture; ten for the 1-week, ten for the 2-week, eleven for the 4-week, ten for the 8-week, and ten for the 12-week time point for the 33G needle puncture. A sham operation was defined as the posterolateral surgical approach without a needle puncture. The number of mice stratified according to sex in each time point of the 35G group were as follows: 1-week: female, 5; male, 5; 2 weeks: female, 10; male, 4; 4 weeks: female, 7; male, 4; 8 weeks: female, 5; male, 5; 12 weeks: female, 5; male, 5; for the 33G group: 1 week: female, 5; male, 5; 2 weeks: female, 1, male, 9; 4 weeks: female, 6; male, 5; 8 weeks: female, 5; male, 5; 12 weeks: female, 3; male, 7. For each time point there were four sham operations (female, 2; male, 2) (Fig 3).

Furthermore, statistical analyses were performed. A correlation analysis was used to evaluate the MRI index relationships with the histological classification scores. The multiple regression analysis was used to determine whether the postoperative time points and the punctured regions were significant variables. Kruskal-Wallis test was used for comparison of each subgroup of region with non-punctured control. Single regression analysis was used to determine whether the postoperative time point is a significant variable for NP score or AF score of punctured IVD. The Tukey HSD test was used for comparison of NP score at each time point. Single regression analysis was used to determine whether the postoperative time point is a significant variable for IVD height and width of punctured IVD. The Kruskal Wallis test was used to compare the 35G and the 33G needle for Pfirrmann grades, MRI indexes, or our histological classification scores.

Results

The comparison of four histological classification scores

We firstly analyzed the score distribution according to four histological classifications. Fig 4 shows the data distributions of the 35G puncture group based on the histological classification

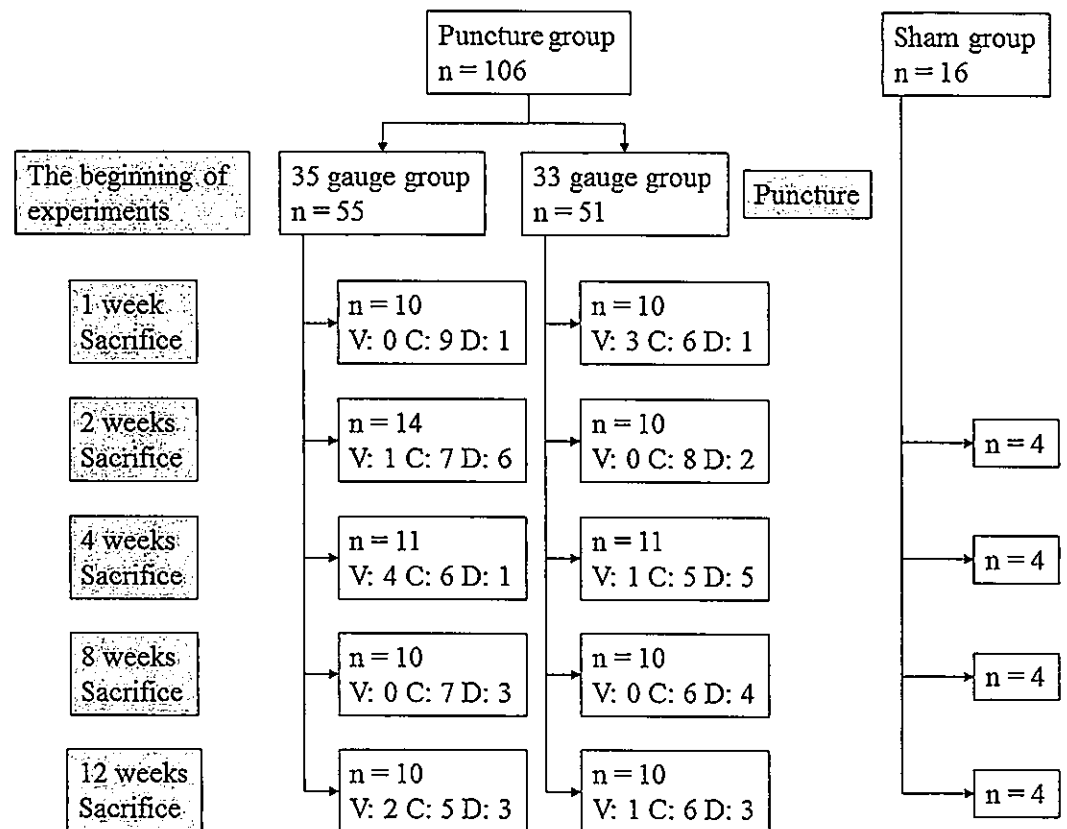


Fig 3. The flowchart of the experiment indicating the time course and the case number. V, ventral region; C, central region; D, dorsal region.

doi:10.1371/journal.pone.0160486.g003

scores. The score distribution of the classification by Masuda et al. [11] did not show normality, with a skewness (Sk) value of -1.27. Additionally, the score showed a ceiling effect, indicating that it was inappropriate for the present mice IVD degeneration model. In contrast, the distribution of the scores by Nishimura et al. [22]'s, Yang et al. [9]'s, and our classifications showed

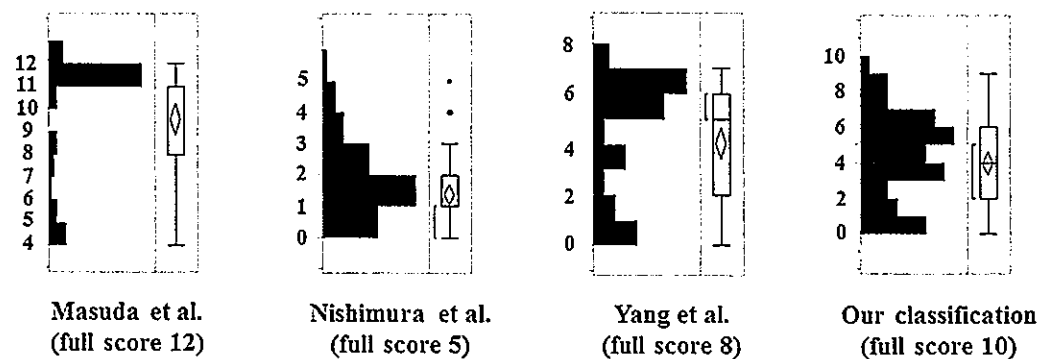


Fig 4. The comparison of the histological classifications. The distribution of scores in each classification. Red brackets indicate the minimum ranges that include 50% of the data. The red and black dots of the classification score of Nishimura et al. [22] indicate the outliers.

doi:10.1371/journal.pone.0160486.g004

normality, given that their Sk and kurtosis (Ku) were less than 1.00 (Sk = 0.97, Ku = 0.66 by Nishimura et al. [22], Sk = -0.69, Ku = -0.96 by Yang et al. [9], and Sk = -0.09, Ku = -0.72 by our classification). However, the Sk of Nishimura et al. [22]'s classification was higher than ours because their score had some outliers. In addition, compared to our classification, the Nishimura et al. [22] score showed a floor effect and the Yang et al. [9] score showed a ceiling effect. These results indicated that our classification could more precisely detect the gradual progression of the degenerative changes (Fig 4).

Correlation analysis relating MRI index

In the correlation and the simple linear regression analysis relating the MRI index with our classification, the results yielded $\rho = -0.66$ and $R^2 = 0.44$, showing that our classification yielded a good correlation and linear fit with the MRI index (Fig 5).

In a scatterplot and probability ellipse analysis, the 50% confidence probability ellipse for each punctured region were thin and well separated, indicating the good linear fit of our score. In addition, our score showed significant correlation with the MRI index in the central and dorsal regions with P values of 0.01 and 0.002, respectively (Fig 5).

Significant variable for inducing degenerative IVDs

Next, to identify the variables most predictive of degenerative IVDs, the following were tested in the multiple regression analysis: punctured region (including ventral, central, and dorsal regions) and time point. The results of the analysis revealed that not the "time point" but the "punctured region" was predictive of the degenerative outcomes (Table 1).

We further analyzed the whole data regarding punctured region. Compared with the non-punctured IVDs, those punctured through the central or the dorsal region showed significantly higher Pfirrmann grade and lower MRI index. Similarly, on using our classification, the IVDs punctured through the central or the dorsal region showed significantly higher histological scores. For the IVDs punctured through the ventral regions, our histological score was

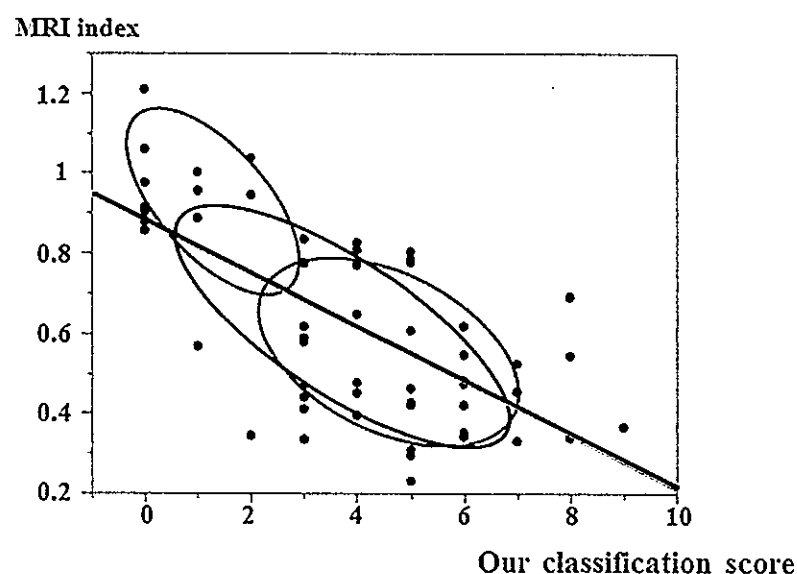


Fig 5. Correlation analysis between our histological score and MRI index. The blue, black, and red dots indicate the ventral, dorsal, and central region cases, respectively. Ovals indicate 50% confidence ellipse with bivariate normal distribution of each region.

doi:10.1371/journal.pone.0160486.g005

Table 1. Multiple regression analysis to identify significant variable for the degenerative intervertebral discs.

	Punctured region	Time point
35G		
Pfirmann grade	< 0.01*	0.99
MRI index	< 0.01*	0.03**
Classification by us	0.04*	0.20
33G		
Pfirmann grade	< 0.01*	0.34
MRI index	< 0.01*	0.13
Classification by us	< 0.01*	0.27

Numerical values indicate p values.

*Statistically significant.

**Not significant as a result of Tukey HSD test.

doi:10.1371/journal.pone.0160486.t001

significantly higher compared with that for the non-punctured IVDs. However, in the MRI analysis, no significant degenerative IVD difference was observed between the ventrally punctured and the non-punctured control groups (Table 2) (Fig 6).

In addition to the total score, AF and NP scores were separately analyzed. The single regression analysis was used to determine whether the postoperative time point was significant variable for NP score or AF score of punctured IVD excluding ventral puncture. For comparisons of NP score of each time point, Tukey HSD test was used. There was no significant change in the AF and NP scores, except that both 8- and 12-week NP scores were significantly higher compared to 1-week NP score in the 33G needle puncture group (data not shown). As for IVD height and width, the single regression analysis was also used to determine whether the postoperative time point is significant variable for IVD height and width of punctured IVD excluding ventral puncture. The L4/5 IVD punctured with either the 35G or the 33G needle showed an approximately 10% decrease in IVD height and approximately 20% (35G) or 30% (33G) increase in IVD width 1 week after the puncture compared to L3/4 non-punctured control IVD. However, there was no significant difference in IVD height and width among each time point (data not shown).

Center of the nucleus pulposus (NP) was deviated dorsally in IVD

From the anatomical point of view, we measured the deviation of the NP center relative to the IVD center in 77 intact mouse lumbar IVDs. To match the results of the punctured regions

Table 2. Punctured region and intervertebral disc degeneration compared to the control.

	Central region	Dorsal region	Ventral region
35G			
Pfirmann grade	> Control*	> Control *	= Control
MRI index	< Control *	< Control *	< Control
Our classification score	> Control *	> Control *	> Control *
33G			
Pfirmann grade	> Control *	> Control *	> Control
MRI index	< Control *	< Control *	< Control
Our classification score	> Control *	> Control *	> Control *

*p < 0.05.

doi:10.1371/journal.pone.0160486.t002

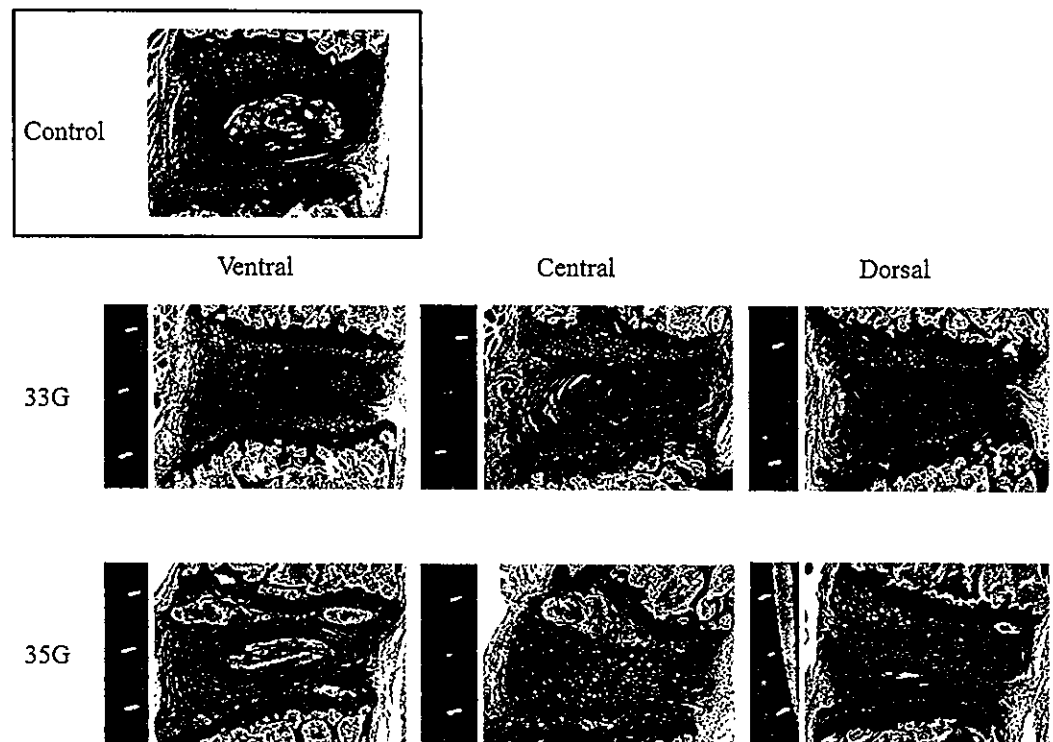


Fig 6. Punctured region and intervertebral disc degeneration. Representative magnetic resonance imaging and histological images at four weeks after puncturing with 35- and 33-gauge needles.

doi:10.1371/journal.pone.0160486.g006

based on the CT scan images and histological evaluations, the AF was measured on the space prescribed by the endplates. After the NP position was determined visually, the measurement was performed using Image J software (National Institutes of Health, Bethesda, Maryland, USA). The width of ventral AF, the dorsal deviation of the NP center relative to the IVD center, and the width of the dorsal AF were calculated as proportion relative to the major axis of the IVD. The average amount of the NP deviation (7%) corresponded to the difference in width between the average ventral (28%) and average dorsal AF (15%); the ventral site of AF is thicker compared to the dorsal site (Fig 7).

Intervertebral disc degeneration and needle size

Based on either the MRI (Table 3) or the histological analysis by our classification (Table 4), the IVD punctured with the 33G needle showed more degenerative changes compared with the IVDs punctured with the 35G needle. Regarding the vascularization and mineralization of the end plate, there was no certain findings in this puncture model (data not shown). In the sham group, both the MRI and histological findings were normal.

Discussion

Although it is ideal to use an age-related IVD degeneration mouse model to investigate the mechanisms of IVD degeneration, some genetically modified mice have short life spans [23,24]. To overcome this limitation, an *in vivo* mouse IVD degeneration model induced by needle puncture is needed. There may be a criticism that the IVD of a quadruped animal was

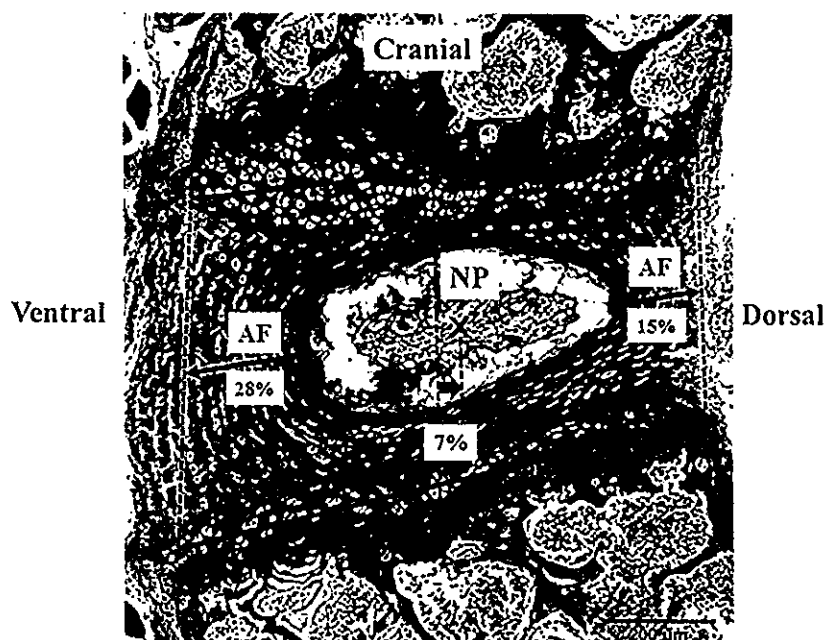


Fig 7. The mid-sagittal slice of the lumbar intervertebral disc (IVD). The nucleus pulposus (NP) center was deviated dorsally relative to the IVD center. In 77 intact mouse lumbar IVDs, the width of ventral annulus fibrosus (AF), the dorsal deviation of the NP center relative to the IVD center, and the width of dorsal AF were calculated as proportion relative to the major axis of the IVD. The average amount of NP deviation (7%) corresponded to the difference in width between the average ventral (28%) and the average dorsal AF (15%); the ventral site of AF is thicker compared to the dorsal site.

doi:10.1371/journal.pone.0160486.g007

used as an alternative to the bipedal human IVD. However, Elliott et al. [25] reported that the mouse discs, when normalized for geometry, they represented well the mechanical properties of the human lumbar spine. Their findings provided strong support for the use of the rodent model in the study of human disc function, disease, and degeneration. In addition, they found

Table 3. Intervertebral disc degeneration and needle size.

	35G	33G	P
Pfirrmann grade			
1-week	2.50 ± 0.71	3.71 ± 1.11	0.03*
2-week	2.54 ± 0.88	4.30 ± 0.82	< 0.01*
4-week	2.43 ± 1.13	4.50 ± 0.53	< 0.01*
8-week	2.50 ± 0.85	4.60 ± 0.70	< 0.01*
12-week	2.50 ± 0.93	4.22 ± 0.83	< 0.01*
MRI index			
1-week	0.71 ± 0.14	0.47 ± 0.11	< 0.01*
2-week	0.54 ± 0.23	0.34 ± 0.09	0.01*
4-week	0.62 ± 0.29	0.34 ± 0.09	0.04*
8-week	0.51 ± 0.17	0.34 ± 0.15	0.02*
12-week	0.49 ± 0.20	0.34 ± 0.10	0.08

Ventral puncture data were removed from groups.

*Statistically significant.

doi:10.1371/journal.pone.0160486.t003

Table 4. Intervertebral disc degeneration and needle size.

	35G	33G	P
Our classification score			
1-week	5.10 ± 1.91	4.86 ± 1.57	0.73
2-week	4.15 ± 1.82	6.30 ± 2.83	0.08
4-week	4.00 ± 3.00	6.70 ± 2.54	0.11
8-week	5.20 ± 2.66	7.30 ± 1.25	0.05*
12-week	2.88 ± 1.73	7.11 ± 1.69	< 0.01*

Ventral puncture data were removed from groups.

*Statistically significant.

doi:10.1371/journal.pone.0160486.t004

that some geometrical and mechanical properties correlated with the animal body weight in the lumbar spine but no parameter correlated in the tail spine, suggesting that the lumbar spine is a more appropriate model of the bipedal human spine than is the tail spine. [25,26] This is because the loading from the animal body weight may be transferred to the rodent lumbar spine.

To our knowledge, there is only one report of mouse lumbar IVD degeneration model induced by needle puncture [27]. However, there were some limitations to that study: short duration of follow-up, small number of cases, and subjective histological evaluation [27]. In addition, they punctured consecutive three discs in one mouse (L4/5, 5/6, 6/S1), and they evaluated the punctured status by using naked eye observation only [27]. In contrast, in our study, the number of mice was greater than 10 for each time point, and the follow-up periods were of up to 12 weeks. In addition, we used four histological classification scores. Only one lumbar IVD per mouse was punctured, and the punctured status was verified by CT scanning.

Masuda et al. [11] were the first to establish a rabbit model of disc degeneration based on puncturing the AF with a needle and evaluating the IVD degeneration by their original grading system for histology. Nishimura et al. [22] also evaluated IVD degeneration by their original grading system for rat IVD. Furthermore, Yang et al. [9] evaluated IVD degeneration by their original grading system for mice IVD. In the present study, the classification by Masuda et al. [11] showed a severe score even at early time points. In their classification, the AF grade received the maximum score when 30% of the AF fibers were serpentine, and the NP grade received the maximum score when NP was moderately condensed. In mice, those findings commonly appeared at the early stage or in mild degeneration. In the sections "border between the AF and NP" and "cellularity of the NP," the same problem appeared. In the classification by Nishimura et al. [22], scores were condensed to 0 to 2 points. In their classification, NP was not evaluated. With reference to the mice, the degenerative changes in NP were drastic even in the early stage, meaning that by excluding the NP from the evaluation of IVD degeneration leads to underestimation. In the classification by Yang et al. [9], scores were condensed to 5 to 6 points, indicating that the classification could not differentiate severe degeneration. Consequently, neither classification could detect the gradual progression of the IVD degeneration. In contrast, our classification could classify precisely the gradual degenerative changes for mouse AF and NP, and combine them as a total degeneration score.

In the present study, by using our histological score, the punctured IVD showed significant degeneration irrespective of the punctured region. However, in the MRI analysis, there was no significant degenerative IVD change between the ventrally punctured and the non-punctured control groups. We also found that the ventral site of AF is thicker than the dorsal site. Thus, the biomechanical effects of needle puncture on IVD degeneration is thought to be less severe.

Furthermore, the center of NP was deviated dorsally in IVD. NP plays central role in the biological reaction in the IVD [1,17]. Due to these anatomical characteristics and subsequent biomechanical/biological reasons, the degenerative change in the IVDs punctured through the ventral region was significantly milder compared to those of the IVDs punctured through the central or the dorsal region. To expand the versatility of the evaluation for IVD degenerative change to the MRI analysis, we recommend that the central or dorsal region be punctured.

Based on previous reports [14,27], we established the needle sizes as 35G and 33G. According to Elliot et al. [14], the ratio of the needle diameter to the punctured IVD height needed to exceed 0.4 to induce significant degeneration. Thus, in order to not destroy the IVD by a single puncture and induce subsequent degeneration, 35G (ratio 0.5) and 33G (ratio 0.87) were considered as reasonable diameters. Considering the severity of IVD degeneration, we recommend the use of the 35G model for the study of the IVD degeneration adjustment and the 33G model for the study of the IVD regeneration.

The present results also showed that the "time point" was not a predictive variable of the degenerative outcomes. Accordingly, the differences in Pfirrmann grades, the MRI indexes, and our histological classification scores among the 1-, 2-, 4-, 8-, and 12-week points were not significant. Therefore, we concluded that the mouse IVD degeneration induced by needle puncture progressed drastically in one week and then plateaued. This result suggests that one to two weeks of follow-up is sufficient for evaluating the degenerative outcome of the punctured IVD.

In conclusion, this study investigated the IVD region by puncturing with a needle with micro-CT scanning and the severity of the degeneration. Puncturing through the ventral region may not induce efficient degeneration. To induce significant degeneration in the lumbar IVD, the central or dorsal region should be punctured. In any case, our classification can detect the gradual progression of the degenerative changes. Based on the present results, researchers may replace the micro-CT scanning with high-resolution fluoroscopy for assistance in puncturing the central or dorsal region.

Author Contributions

Conceived and designed the experiments: TO HS.

Performed the experiments: TO HS.

Analyzed the data: TO HS KI TT YMI NI.

Contributed reagents/materials/analysis tools: HS.

Wrote the paper: TO HS.

References

1. Yamada K, Sudo H, Iwasaki K, Sasaki N, Higashi H, Kameda Y, et al. Caspase 3 silencing inhibits biomechanical overload-induced intervertebral disk degeneration. *Am J Pathol* 2014; 184: 753–764. doi: 10.1016/j.ajpath.2013.11.010 PMID: 24389166
2. Zhao CQ, Jiang LS, Dai LY. Programmed cell death in intervertebral disc degeneration. *Apoptosis* 2006; 11: 2079–2088. PMID: 17051327
3. Dower A, Chatterji R, Swart A, Winder MJ. Surgical management of recurrent lumbar disc herniation and the role of fusion. *J Clin Neurosci*. 2016; 23: 44–50. doi: 10.1016/j.jocn.2015.04.024 PMID: 26282154
4. Key JA, Ford LT. Experimental intervertebral-disc lesions. *J Bone Joint Surg Am* 1948; 30A: 621–630. PMID: 18099522
5. Rousseau MA, Ulrich JA, Bass EC, Rodriguez AG, Liu JJ, Lotz JC Stab incision for inducing intervertebral disc degeneration in the rat. *Spine (Phila Pa 1976)* 2007; 32: 17–24.

6. Osti OL, Vernon-Roberts B, Fraser RD. 1990 Volvo Award in experimental studies. Annulus tears and intervertebral disc degeneration. An experimental study using an animal model. *Spine (Phila Pa 1976)*. 1990; 15: 762–767.
7. Martin JT, Gorth DJ, Beattie EE, Harfe BD, Smith LJ, Elliott DM. Needle puncture injury causes acute and long-term mechanical deficiency in a mouse model of intervertebral disc degeneration. *J Orthop Res*. 2013; 31: 1276–1282. doi: 10.1002/jor.22355 PMID: 23553925
8. Issy AC, Castania V, Castania M, Salmon CE, Nogueira-Barbosa MH, Bel ED, et al. Experimental model of Intervertebral disc degeneration by needle puncture in Wistar rats. *Braz J Med Biol Res*. 2013; 46: 235–244. PMID: 23532265
9. Yang F, Leung VY, Luk KD, Chan D, Cheung KM. Mesenchymal stem cells arrest intervertebral disc degeneration through chondrocytic differentiation and stimulation of endogenous cells. *Mol Ther*. 2009; 17: 1959–1966. doi: 10.1038/mt.2009.146 PMID: 19584814
10. Hsieh AH, Hwang D, Ryan DA, Freeman AK, Kim H Degenerative anular changes induced by puncture are associated with insufficiency of disc biomechanical function. *Spine (Phila Pa 1976)*. 2009; 34: 998–1005.
11. Masuda K, Aota Y, Muehleman C, Imai Y, Okuma M, Thonar EJ, et al. A novel rabbit model of mild, reproducible disc degeneration by an annulus needle puncture: correlation between the degree of disc injury and radiological and histological appearances of disc degeneration. *Spine (Phila Pa 1976)*. 2005; 30: 5–14.
12. Sobajima S, Kempel JF, Kim JS, Wallach CJ, Robertson DD, Vogt MT, et al. A slowly progressive and reproducible animal model of intervertebral disc degeneration characterized by MRI, X-ray, and histology. *Spine (Phila Pa 1976)*. 2005; 30: 15–24.
13. Masuda K, Imai Y, Okuma M, Muehleman C, Nakagawa K, Akeda K, et al. Osteogenic protein-1 injection into a degenerated disc induces the restoration of disc height and structural changes in the rabbit annular puncture model. *Spine (Phila Pa 1976)*. 2006; 31: 742–754.
14. Elliott DM, Yerramalli CS, Beckstein JC, Boxberger JJ, Johannessen W, Vresilovic EJ The effect of relative needle diameter in puncture and sham injection animal models of degeneration. *Spine (Phila Pa 1976)*. 2008; 33: 588–596.
15. Seki S, Asanuma-Abe Y, Masuda K, Kawaguchi Y, Asanuma K, Muehleman C, et al. Effect of small interference RNA (siRNA) for ADAMTS5 on intervertebral disc degeneration in the rabbit annular needle-puncture model. *Arthritis Res Ther*. 2009; 11: R166. doi: 10.1186/ar2851 PMID: 19889209
16. Sudo H, Minami A Regulation of apoptosis in nucleus pulposus cells by optimized exogenous Bcl-2 overexpression. *J Orthop Res*. 2010; 28: 1608–1613. doi: 10.1002/jor.21185 PMID: 20589931
17. Sudo H, Minami A Caspase 3 as a therapeutic target for regulation of intervertebral disc degeneration in rabbits. *Arthritis Rheum*. 2011; 63: 1648–1657. doi: 10.1002/art.30251 PMID: 21305515
18. Sudo H, Yamada K, Iwasaki K, Higashi H, Ito M, Minami A, et al. Global identification of genes related to nutrient deficiency in intervertebral disc cells in an experimental nutrient deprivation model. *PLoS One* 2013; 8: e58806. doi: 10.1371/journal.pone.0058806 PMID: 23520533
19. Seki S, Tsumaki N, Motomura H, Nogami M, Kawaguchi Y, Hori T, et al. Cartilage intermediate layer protein promotes lumbar disc degeneration. *Biochem Biophys Res Commun*. 2014; 446: 876–881. doi: 10.1016/j.bbrc.2014.03.025 PMID: 24631904
20. Iwasaki K, Sudo H, Yamada K, Higashi H, Ohnishi T, Tsujimoto T, et al. Effects of single injection of local anesthetic agents on intervertebral disc degeneration: ex vivo and long-term in vivo experimental study. *PLoS One* 2014; 9: e109851. doi: 10.1371/journal.pone.0109851 PMID: 25286407
21. Pfirrmann CW, Metzendorf A, Zanetti M, Hodler J, Boos N Magnetic resonance classification of lumbar intervertebral disc degeneration. *Spine (Phila Pa 1976)*. 2001; 26: 1873–1878.
22. Nishimura K, Mochida J Percutaneous reinsertion of the nucleus pulposus. An experimental study. *Spine (Phila Pa 1976)*. 1998; 23: 1531–1538; discussion 1539.
23. Zheng TS, Hunot S, Kuida K, Momoi T, Srinivasan A, Nicholson DW, et al. Deficiency in caspase-9 or caspase-3 induces compensatory caspase activation. *Nat Med*. 2000; 6: 1241–1247. PMID: 11062535
24. Chien WM, Garrison K, Caufield E, Orthel J, Dill J, Fero ML Differential gene expression of p27Kip1 and Rb knockout pituitary tumors associated with altered growth and angiogenesis. *Cell Cycle* 2007; 6: 750–757. PMID: 17361101
25. Elliott DM, Sarver JJ Young Investigator award winner: validation of the mouse and rat disc as mechanical models of the human lumbar disc. *Spine (Phila Pa 1976)*. 2004; 29: 713–722.
26. Smit TH. The use of a quadruped as an in vivo model for the study of the spine—biomechanical considerations. *Eur Spine J*. 2002; 11: 137–144. PMID: 11956920
27. Liang H, Ma SY, Feng G, Shen FH, Joshua Li X Therapeutic effects of adenovirus-mediated growth and differentiation factor-5 in a mice disc degeneration model induced by annulus needle puncture. *Spine J*. 2010; 10: 32–41. doi: 10.1016/j.spinee.2009.10.006 PMID: 19926342

Clinical Study

Correlation analysis between change in thoracic kyphosis and multilevel facetectomy and screw density in main thoracic adolescent idiopathic scoliosis surgery

Hideki Sudo, MD^{a,*}, Yuichiro Abe, MD^b, Terufumi Kokabu, MD^a, Manabu Ito, MD^c,
Kuniyoshi Abumi, MD^d, Yoichi M. Ito, PhD^c, Norimasa Iwasaki, MD^a

^aDepartment of Orthopaedic Surgery, Hokkaido University Hospital, North-15, West-7, Kita-ku, Sapporo, Hokkaido 060-8638, Japan

^bDepartment of Orthopaedic Surgery, Eniwa Hospital, Koganemachi 2-1, Eniwa, Hokkaido 061-1449, Japan

^cDepartment of Spine and Spinal Cord Disorders, Hokkaido Medical Center, Yamanote 5-7, Sapporo, Hokkaido 063-0005, Japan

^dDepartment of Orthopaedic Surgery, Sapporo Orthopaedic Hospital, Hassamu 13-4, Sapporo, Hokkaido 063-0833, Japan

^eDepartment of Biostatistics, Hokkaido University Graduate School of Medicine, North-15, West-7, Kita-ku, Sapporo, Hokkaido 060-8638, Japan

Received 18 September 2015; revised 17 February 2016; accepted 19 April 2016

Abstract

BACKGROUND CONTEXT: Controversy exists regarding the effects of multilevel facetectomy and screw density on deformity correction, especially thoracic kyphosis (TK) restoration in adolescent idiopathic scoliosis (AIS) surgery.

PURPOSE: This study aimed to evaluate the effects of multilevel facetectomy and screw density on sagittal plane correction in patients with main thoracic (MT) AIS curve.

STUDY DESIGN: A retrospective correlation and comparative analysis of prospectively collected, consecutive, non-randomized series of patients at a single institution was undertaken.

PATIENT SAMPLE: Sixty-four consecutive patients with Lenke type 1 AIS treated with posterior correction and fusion surgery using simultaneous double-rod rotation technique were included.

OUTCOME MEASURES: Patient demographics and preoperative and 2-year postoperative radiographic measurements were the outcome measures for this study.

METHODS: Multiple stepwise linear regression analysis was conducted between change in TK (T5–T12) and the following factors: age at surgery, Risser sign, number of facetectomy level, screw density, preoperative main thoracic curve, flexibility in main thoracic curve, coronal correction rate, preoperative TK, and preoperative lumbar lordosis. Patients were classified into two groups: TK<15° group defined by preoperative TK below the mean degree of TK for the entire cohort (<15°) and the TK≥15° group, defined by preoperative TK above the mean degree of kyphosis (≥15°). Independent sample *t* tests were used to compare demographic data as well as radiographic outcomes between the two groups. There were no study-specific biases related to conflicts of interest.

RESULTS: The average preoperative TK was 14.0°, which improved significantly to 23.1° (*p*<.0001) at the 2-year final follow-up. Greater change in TK was predicted by a low preoperative TK (*p*<.0001). The TK<15° group showed significant correlation between change in TK and number of facetectomy level (*r*=0.492, *p*=.002). Similarly, significant correlation was found between change in TK and screw density (*r*=0.333, *p*=.047). Conversely, in the TK≥15° group, correlation was found neither between change in TK and number of facetectomy level (*r*=0.047, *p*=.812), nor with screw density (*r*=0.030, *p*=.880). Furthermore, in patients with preoperative TK<15°, change in TK was significantly correlated with screw density at the concave side (*r*=0.351, *p*=.036) but not at the convex side (*r*=0.144, *p*=.402).

FDA device/drug status: Approved (USS II Polyaxial).

Author disclosures: *HS*: Nothing to disclose. *YA*: Nothing to disclose.

TK: Nothing to disclose. *MI*: Nothing to disclose. *KA*: Nothing to disclose. *YMI*: Nothing to disclose. *NI*: Nothing to disclose.

* Corresponding author. Department of Advanced Medicine for Spine and Spinal Cord Disorders, Hokkaido University Graduate School of Medicine, North-15, West-7, Kita-ku, Sapporo, Hokkaido 060-8638, Japan. Tel.: +81 11 706 5934; fax: +81 11 706 6054.

E-mail address: hidekisudo@yahoo.co.jp (H. Sudo)

CONCLUSIONS: In patients with hypokyphotic thoracic spine, significant positive correlation was found between change in TK and multilevel facetectomy or screw density at the concave side. This indicates that in patients with AIS who have thoracic hypokyphosis as part of their deformity, the abovementioned factors must be considered in preoperative planning to correct hypokyphosis. © 2016 Elsevier Inc. All rights reserved.

Keywords: Adolescent idiopathic scoliosis; Facetectomy; Lenke type 1 scoliosis; Posterior spinal correction and fusion; Screw density; Thoracic kyphosis

Introduction

Posterior spinal correction and fusion with segmental pedicle screw (PS) instrumentation is currently used for the correction of many types of scoliosis. Patients with a primary thoracic adolescent idiopathic scoliosis (AIS) are typically hypokyphotic relative to non-scoliosis patients [1]; therefore, restoration and maintenance of normal sagittal contour as well as satisfactory coronal correction of the main thoracic (MT) curve have been receiving increased attention of late [1–4]. Thoracic hypokyphosis of less than 20° has been correlated with decreased pulmonary function [5]. However, recent studies have reported that PS constructs to maximize scoliosis correction cause further lordosis of the thoracic spine [4,6,7]. These patients would not only demonstrate further decrease of pulmonary function but also show a flat back leading to progressive decompensation and sagittal imbalance [1,8]. Preservation of thoracic kyphosis (TK) is critical to maintain lumbar lordosis after surgical treatment of AIS [1]. To overcome these issues, Ito et al. [9] and Sudo et al. [10,11] recently developed a very simple surgical technique called the simultaneous double-rod rotation technique (SDRRT) for correcting AIS. In this technique, two rods are connected to the screw heads and are simply rotated simultaneously to correct the scoliosis, while TK is maintained or improved. Moreover, hypokyphotic rod deformation is prevented with dual-rod derotation compared with that with single-rod derotation [9–11].

Posterior distraction at each concave-side spinal segment is important for optimal correction in both coronal and sagittal planes [10,11]. In addition, some studies investigated the correlation between scoliosis curve correction and destabilization procedures, such as multilevel facetectomy [12], or scoliosis correction and the number of fixation anchors, such as PS density [13–16]. However, controversy exists regarding the effects of facetectomy and screw density on deformity correction, especially TK restoration in AIS surgery [16]. The purpose of this study is to evaluate the effects of multilevel facetectomy or screw density on sagittal plane correction in patients with MT AIS curve treated with SDRRT.

Materials and methods

After institutional review board approval, data from 64 consecutive patients (7 males, 57 females) with Lenke type 1 AIS curves were retrospectively evaluated; the patients under-

went posterior MT curve correction using SDRRT with a minimum 2-year follow-up from June 2008 to September 2015 at our institution. Exclusion criteria included syndromic (n=14), neuromuscular (n=6), and congenital scoliosis (n=14), and the presence of other thoracic scoliosis curves such as Lenke type 2 double thoracic curves (n=25). No case was lost to follow-up. The average age and Risser sign at surgery were 14.8 (range, 10–20) and 3.6 (range, 0–5) years, respectively (Table 1).

Standing long-cassette posteroanterior and lateral radiographs were evaluated for multiple parameters before surgery and at the 2-year follow-up. Main thoracic curve flexibility was evaluated using preoperative supine bending radiographs. Coronal and sagittal Cobb measurements of MT curves were obtained. The end vertebrae levels were determined on preoperative radiographs and measured on subsequent radiographs to maintain consistency for statistical comparisons [10,11]. Sagittal measurements included TK (T5–T12) and lumbar lordosis (L1–S1) [10,11].

The number of facetectomy levels was counted, and screw density was expressed as the number of screws per level instrumented for each patient.

Surgical technique

Fusion level selection was based on both standing and bending films, and instrumentation levels were determined from end-to-end vertebrae on standing films in most cases. Vertebrae without rotation on bending films were selected as the lowest instrumented vertebra [10]. Surgeries were performed as described previously [9–11]. In brief, after exposure of the posterior spinal elements, side-loading polyaxial PSs (USS II Polyaxial, DePuy Synthes, Raynham, MA, USA) were placed. If PS placement was difficult at the most cephalad vertebra because of its narrowness, a transverse process hook was used. After a multilevel facetectomy, two rods measuring 6 mm in diameter were bent to the anticipated TK. After connecting the two rods to all screw heads, the rod on the concave side should be rotated gently with two rod holders. The convex rod will automatically rotate following the rotation of the concave rod in flexible curves. However, for rigid curves, the assisting surgeons should rotate the rod on the convex side simultaneously to make rod rotation smoother and safer. After 90° rod rotation, several screw heads were tightened to lock the rods. Distraction force was first applied

EVIDENCE & METHODS

Context

The authors sought to evaluate the effect of multilevel facetectomy and screw density on sagittal plane correction in 64 consecutive patients with main thoracic AIS curves.

Contribution

The authors performed a multivariable analysis evaluating a number of potential explanatory factors. When adjusting for other variables, multilevel facetectomy and screw density were found to be significantly correlated with correction.

Implications

This study has a limited number of patients in the sample, albeit consecutive in nature. Given the number of variables included in the model, the authors would have required about 200 patients to ensure the model is not overfit. Given that they have only 64, there is the potential for spurious statistical findings to be present. This along with differences in demographic composition between these patients and those treated at other centers should be considered prior to attempted translation of this study's findings to clinical practice. Given these limitations, the study presents Level IV evidence.

—The Editors

on each screw head on the concave side of the thoracic curve, such that not only scoliosis but also TK could be corrected more effectively by lengthening the posterior column. Then, compression force was applied segmentally on the convex curve. An in situ rod-bending maneuver was not conducted during the surgery. Local bone grafting followed decortication of the laminae. A brace was not required in any patient.

Table 1
Demographic characteristics and clinical features of the subjects

	Mean±standard deviation	Range
Age at surgery (y)	14.8±2.3	10 to 20
Risser sign (grade)	3.6±1.4	0 to 5
No. vertebrae in fusion	10.2±1.5	7 to 13
Screw density (no. of screws/level instrumented)	1.7±0.2	0.7 to 2
Preoperative main thoracic Cobb (°)	62.0±10.0	45 to 90
Flexibility in main thoracic curve (%)	61.3±13.8	31 to 93
Postoperative main thoracic Cobb (°)	17.2±6.2	4 to 31
Coronal correction rate (%)	72.3±9.0	55 to 92
Preoperative thoracic kyphosis (T5–T12) (°)	14.0±9.6	–4 to 55
Postoperative thoracic kyphosis (T5–T12) (°)	23.1±5.3	13 to 30
Change in thoracic kyphosis (T5–T12) (°)	9.1±8.9	–31 to 24
Preoperative lumbar lordosis (L1–S1) (°)	51.5±11.7	19 to 75
Postoperative lumbar lordosis (L1–S1) (°)	53.2±9.3	24 to 70
Change in lumbar lordosis (L1–S1) (°)	1.3±8.9	–20 to 32

Statistical analysis

All data are expressed as mean±standard deviation. Multiple stepwise linear regression analysis was applied to control possible confounding variables and to identify variables independently predictive of change in TK (at 2-year follow-up, preoperative measurements). The following covariates were tested in the multivariate regression analysis: age at surgery, Risser sign, number of facetectomy level, screw density, preoperative MT curve, flexibility in MT curve, coronal correction rate, preoperative TK, and preoperative lumbar lordosis. Significant multivariate predictors of change in TK are reported with their respective predictive equations, including the intercept and regression coefficients (β). Model fit was assessed by the goodness-of-fit F test and R^2 statistic. Independent sample *t* tests were used to compare between-group differences in demographic data. Pearson correlation coefficient and Spearman correlation coefficient analysis were used to assess relationships between change in TK and number of facetectomy level or screw density. Data analyses were performed using JMP statistical software for Windows (version 12; SAS, Inc., Cary, NC, USA). $p < .05$ was considered statistically significant.

Results

Demographic data are summarized in Table 1. On average, 10.2 vertebrae were instrumented in the 64 patients. The average screw density was 1.7. The average preoperative MT curve was 62.0°. The average preoperative MT curve flexibility on bending radiographs was 61.3% (range, 31%–93%). Postoperative radiographs showed an average MT curve of 17.2°. The average MT curve correction rate was 72.3% (range, 55%–92%). Sagittal plane analysis revealed that the average preoperative TK was 14.0° (range, from –4° to 55°), which improved significantly to 23.1° (range, 13°–30°; $p < .0001$) at the 2-year final follow-up. The average change in TK was 9.1° (range, from –31° to 24°). Other data regarding lumbar lordosis are also presented in Table 1.

Multiple stepwise linear regression analysis indicated that two variables were independently predictive of change in TK: number of facetectomy level and preoperative TK. The model fit the data well (goodness-of-fit F test=27.010, $R^2=0.871$, $p < .0001$), indicating that approximately 87% of the variation in change in TK was explained by the two significant independent predictors. Specifically, greater change in TK was predicted by a low preoperative TK ($p < .0001$) (Table 2).

Subgroup analysis

The cohort was then divided into two groups on the basis of preoperative TK. The preoperative TK<15° group was defined by preoperative TK below the mean degree of the kyphosis for the entire cohort (<15°). The preoperative TK≥15° group was defined by preoperative TK above the mean degree of the kyphosis (≥15°). The TK<15° group consisted of 36 patients, whereas the TK≥15° group had 28 patients. Both

Table 2

Associations between various factors and change in thoracic kyphosis (°) using multiple stepwise linear regression analysis

	Regression coefficient	Standard error	95% Confidence interval	t	Standardized β	p
Constant	17.431	12.550	(-7.933, 42.794)	1.39	—	.173
Age at surgery (y)	-0.104	0.509	(-1.132, 0.924)	-0.20	-0.023	.839
Risser sign (grade)	-0.193	0.676	(-1.560, 1.173)	-0.29	-0.028	.7763
Number of facetectomy level (no.)	0.668	0.212	(0.239, 1.097)	3.15	0.2116	.003
Screw density (no. of screws/level instrumented)	-2.120	3.349	(-8.888, 4.649)	-0.63	-0.043	.530
Preoperative main thoracic Cobb (°)	-0.067	0.071	(-0.2111, 0.077)	-0.94	-0.076	.351
Flexibility in main thoracic curve (%)	7.620	4.13	(-0.731, 15.971)	1.84	0.118	.073
Coronal correction rate (%)	0.033	0.025	(-0.018, 0.085)	1.32	0.087	.193
Preoperative thoracic kyphosis (T5–T12) (°)	-0.789	0.066	(-0.922, -0.656)	-12.00	-0.841	<.0001
Preoperative lumbar lordosis (L1–S1) (°)	-0.048	0.087	(-0.224, 0.128)	-0.55	-0.061	.586

groups were similar at baseline with respect to the following parameters: age, Risser sign, preoperative MT Cobb angle, flexibility of MT curve, and correction rate of MT Cobb angle. In addition, no difference was found between the groups regarding number of facetectomy level and screw density. Conversely, significant difference was observed between the groups regarding change in TK ($p<.001$) and preoperative lumbar lordosis ($p=.018$) (Table 3).

The TK<15° group showed significant correlation between change in TK and number of facetectomy level (Pearson:

$r=0.492$, $p=.002$; Spearman: $r_s=0.541$, $p=.007$). Similarly, significant correlation was found between change in TK and screw density (Pearson: $r=0.333$, $p=.047$; Spearman: $r_s=0.397$, $p=.016$). Conversely, in the TK \geq 15° group, correlation was found neither between change in TK and number of facetectomy level (Pearson: $r=0.047$, $p=.812$; Spearman: $r_s=0.155$, $p=.431$), nor with screw density (Pearson: $r=0.030$, $p=.880$; Spearman: $r_s=0.110$, $p=.576$) (Table 4).

Finally, correlation analysis was conducted between change in TK and screw density in the TK<15° group. Change in TK was significantly correlated with screw density at the concave side (Pearson: $r=0.351$, $p=.036$; Spearman: $r_s=0.318$, $p=.058$), whereas no correlation was found between change in TK and screw density at the convex side (Pearson: $r=0.144$, $p=.402$; Spearman: $r_s=0.122$, $p=.480$) (Table 5).

Table 3

Comparison of two groups

	Preop thoracic kyphosis <15° (n=36)	Preop thoracic kyphosis \geq 15° (n=28)	p
Age at surgery	14.9 \pm 2.2	14.7 \pm 2.5	.689
Risser sign	3.8 \pm 1.2	3.3 \pm 1.7	.182
Preoperative Cobb angle	60.3 \pm 8.9	64.1 \pm 11.0	.129
Flexibility of thoracic curve (%)	63.6 \pm 12.9	58.2 \pm 14.4	.119
Correction rate of Cobb angle (%)	73.2 \pm 9.7	71.1 \pm 8.1	.378
Change in thoracic kyphosis	13.7 \pm 6.1	3.3 \pm 8.5	<.001
Preoperative lumbar lordosis	48.4 \pm 11.4	55.4 \pm 11.3	.018
Postoperative lumbar lordosis	53.0 \pm 9.6	53.0 \pm 9.0	.998
Number of facetectomy level	5.0 \pm 2.9	5.3 \pm 2.8	.756
Screw density	1.8 \pm 0.3	1.7 \pm 0.2	.060

Discussion

Given that thoracic AIS is often associated with a preexisting reduction in TK, ideal surgical correction should address this deformity [1]. However, posterior spinal correction and fusion using segmental PS has decreased ability to restore kyphosis in hypokyphotic thoracic cases [4,6,17]. Lowenstein et al. [4] reported that the PS system decreased TK by an average of 10°, whereas Kim et al. [6] reported an average decrease of 9°. In addition, when using the direct vertebral rotation technique to decrease rotational deformity around the

Table 4

Correlation analysis between change in thoracic kyphosis (°) and variable

Variable	Mean±SD	Range	Pearson correlation coefficients			Spearman correlation coefficient		
			Correlation coefficient	95% CI	Statistical significance	Correlation coefficient	95% CI	Statistical significance
Preoperative thoracic kyphosis <15°								
Number of facetectomy level (no.)	5.0±2.9	3–11	r=0.492	(0.196, 0.707)	p=.002	r _s =0.541	(0.287, 0.752)	p=.007
Screw density (no. of screws/level instrumented)	1.8±0.3	0.7–2	r=0.333	(0.048, 0.596)	p=.047	r _s =0.397	(0.088, 0.647)	p=.016
Preoperative thoracic kyphosis ≥15°								
Number of facetectomy level (no.)	5.3±2.8	3–10	r=0.047	(-0.332, 0.413)	p=.812	r _s =0.155	(-0.194, 0.528)	p=.431
Screw density (no. of screws/level instrumented)	1.7±0.2	1.2–2	r=0.030	(-0.347, 0.399)	p=.880	r _s =0.110	(-0.336, 0.409)	p=.576

SD indicates standard deviation; CI, confidence interval.

Table 5

Correlation analysis between change in thoracic kyphosis (°) and screw density in patients with preoperative thoracic kyphosis <15°

Variable	Mean±SD	Range	Pearson correlation coefficients			Spearman correlation coefficient		
			Correlation coefficient	95% CI	Statistical significance	Correlation coefficient	95% CI	Statistical significance
Concave side screw density (no. of screws/level instrumented)	0.9±0.2	0.3–1	r=0.351	(0.026, 0.610)	p=.036	r _s =0.318	(0.049, 0.624)	p=.058
Convex side screw density (no. of screws/level instrumented)	0.9±0.1	0.5–1	r=0.144	(−0.193, 0.452)	p=.402	r _s =0.122	(−0.239, 0.413)	p=.480

SD, standard deviation; CI, confidence interval.

apex of the thoracic curve, the major applied force pushes the thoracic hump downward to decrease vertebral rotation deformity, which eventually causes dekyphosis of the thoracic spine [10].

Conversely, in SDRRT, once the two rods are connected to the screw heads, they are simply rotated simultaneously, resulting in correction of spinal deformity in the coronal and the sagittal planes without using the in situ rod-bending technique [9–11]. Two contoured rods carry the tips of the two screw heads upward and medially to the concave side of the curve, which does not exert any downward force on the vertebral body [9,10]. Both polyaxial screw head and simultaneous double-rod rotation are key to the current technique. Frictional force at the screw–rod interface is decreased, and there is little chance of screw cutout laterally. This technique provided derotation of the apical vertebra as well as restoration of thoracic kyphosis leading to rib hump correction without additional costoplasty. The present study showed that a preoperative TK of 14° increased significantly to 23° at the 2-year follow-up.

Removing the facets and soft tissues between the posterior elements has been indicated to allow greater distraction abilities along the length of the posterior column; however, it is still unclear whether these posterior releases positively affect the sagittal profile of a hypokyphotic thoracic spine [1]. Halanski and Cassidy [12] documented that no significant difference was observed between multilevel facetectomy and coronal or sagittal correction in thoracic AIS surgery. However, they also indicated that under certain circumstances, such as an extremely stiff curve or kyphoscoliotic deformity, the osteotomy may prove to be very useful [12]. Using three-dimensional-finite element analysis, Abe et al. [18] also reported that mobilization of spinal segment by releasing soft tissue or facet joint could be more important than using a stronger correction maneuver with a rigid implant. In the present study, the number of facetectomy level was an independent predictor of change in TK. In addition, in patients with hypokyphotic thoracic spine <15°, significant correlation was found between change in TK and number of facetectomy level. The present results indicate that multilevel facetectomy is an important factor to restore TK in patients with hypokyphotic thoracic spine.

Another possible factor to optimize correction may be screw density. Larson et al. [14] documented that improved per-

centage correction of the major coronal curve was noted in the high-screw density cohort. Conversely, some authors have demonstrated successful results with low-density instrumentation for the treatment of scoliosis [13,19–21]. In addition, Clements et al. [22] reported an advantage in lumbar and thoracic coronal curves on using screws, compared with hooks, although the absolute number of screws used did not correlate with correction. In our study, there was significant correlation between MT coronal curve correction and screw density ($r=0.296$, $p=.018$). In addition, significant correlation was observed between MT coronal curve correction and screw density at the concave side ($r=0.495$, $p<.001$). However, no significant correlation was observed between MT coronal curve correction and screw density at the convex side ($r=-0.150$, $p=.237$). Recently, similar results were reported that only instrumentation at the concave side, particularly at the apical region, was associated with coronal curve correction [15].

As for TK, the effect of implant density on sagittal plane correction and TK restoration has been reported in only a few studies, and the results have been controversial [3,14,16]. Lonner et al. [3] reported that a greater percentage of screws in the construct was related to decreasing kyphosis at 2 years postoperatively ($r=-0.18$, $p=.03$). Larson et al. [14] also revealed that decreased TK was found with increased screw density for Lenke type 1 and 2 curves. Conversely, Liu et al. [16] documented that higher screw density provided better TK restoration than low screw density. In the present study, in patients with preoperative TK<15°, significant positive correlation was found between change in TK and screw density, whereas no correlation was found in patients with TK≥15°, suggesting that screw density had a positive effect on TK restoration in patients with hypokyphotic thoracic spine.

In the current study, in patients with preoperative TK<15°, change in TK was significantly correlated with screw density at the concave side, whereas no correlation was found with the screw density at the convex side. Liu et al. [16] also reported similar results although they did not perform correlation analysis between change in TK and screw density. Salmingo et al. [23] recently analyzed the changes of the implant rod's angle curvature during AIS surgery and showed that implant rod curvature greatly influences sagittal curve correction. In addition, they revealed that the implant rods at the concave side of deformity were significantly deformed after surgery, whereas rods at the convex side did not have significant

deformation, suggesting that corrective forces acting on that side are greater than those on the convex side [23]. From a mechanical point of view, the translational and rotational displacement required for correction at the concave side is always greater than at the convex side, which also results to greater corrective forces at that side [23]. If this corrective force is stronger than the resistant force from the spine and greater than the pullout force from the screw–bone interaction, the spine would follow the shape of the rod [16]. Increased friction at the screw–rod interface that occurs with higher screw density at the concave side would prevent flattening of the contoured rod in the sagittal plane after rod rotation [16]. Due to the aforementioned reasons, the present study indicates that concave-side, rather than convex-side, screw density had an impact on not only scoliosis correction but also TK restoration.

There are some limitations to this study that should be addressed. First, we did not analyze the relationship between rod deformation during surgery and multilevel osteotomy and screw density. We are now collecting pre-bent and postoperative rod geometries from intraoperative tracing of the rod geometry and postoperative three dimensional-computed tomography images, respectively. Second, the relationships between multilevel osteotomy and screw density and clinical symptoms remain unclear.

Conclusions

In the patients with hypokyphotic thoracic spine, significant positive correlation was found between change in TK and multilevel facetectomy or screw density at the concave side. The results indicated that in patients with AIS who have thoracic hypokyphosis as part of their deformity, these factors must be taken into account in the preoperative planning to correct hypokyphosis.

References

- [1] Newton PO, Yaszay B, Upasani VV, Pawelek JB, Bastrom TP, Lenke LG, et al. Preservation of thoracic kyphosis is critical to maintain lumbar lordosis in the surgical treatment of adolescent idiopathic scoliosis. *Spine* 2010;35:1365–70.
- [2] Suk SI, Kim WJ, Kim JH, Lee SM. Restoration of thoracic kyphosis in the hypokyphotic spine: a comparison between multiple-hook and segmental pedicle screw fixation in adolescent idiopathic scoliosis. *J Spinal Disord* 1999;12:489–95.
- [3] Lonner BS, Lazar-Antman MA, Sponseller PD, Shah SA, Newton PO, Betz R, et al. Multivariate analysis of factors associated with kyphosis maintenance in adolescent idiopathic scoliosis. *Spine* 2012;37:1297–302.
- [4] Lowenstein JE, Matsumoto H, Vitale MG, Weidenbaum M, Gomez JA, Lee FY, et al. Coronal and sagittal plane correction in adolescent idiopathic scoliosis: a comparison between all pedicle screw versus hybrid thoracic hook lumbar screw constructs. *Spine* 2007;32:448–52.
- [5] Winter RB, Lovell WW, Moe JH. Excessive thoracic lordosis and loss of pulmonary function in patients with idiopathic scoliosis. *J Bone Joint Surg Am* 1975;57:972–7.
- [6] Kim YJ, Lenke LG, Kim J, Bridwell KH, Cho SK, Cheh G, et al. Comparative analysis of pedicle screw versus hybrid instrumentation in posterior spinal fusion of adolescent idiopathic scoliosis. *Spine* 2006;31:291–8.
- [7] Sucato DJ, Agrawal S, O'Brien MF, Lowe TG, Richards SB, Lenke L, et al. Restoration of thoracic kyphosis after operative treatment of adolescent idiopathic scoliosis: a multicenter comparison of three surgical approaches. *Spine* 2008;33:2630–6.
- [8] Roussouly P, Nnadi C. Sagittal plane deformity: an overview of interpretation and management. *Eur Spine J* 2010;19:1824–36.
- [9] Ito M, Abumi K, Kotani Y, Takahata M, Sudo H, Hojo Y, et al. Simultaneous double-rod rotation technique in posterior instrumentation surgery for correction of adolescent idiopathic scoliosis. *J Neurosurg Spine* 2010;12:293–300.
- [10] Sudo H, Ito M, Abe Y, Abumi K, Takahata M, Nagahama K, et al. Surgical treatment of Lenke 1 thoracic adolescent idiopathic scoliosis with maintenance of kyphosis using the simultaneous double-rod rotation technique. *Spine* 2014;39:1163–9.
- [11] Sudo H, Abe Y, Abumi K, Iwasaki N, Ito M. Surgical treatment of double thoracic adolescent idiopathic scoliosis with a rigid proximal thoracic curve. *Eur Spine J* 2016;25:569–77.
- [12] Halanski MA, Cassidy JA. Do multilevel Ponte osteotomies in thoracic idiopathic scoliosis surgery improve curve correction and restore thoracic kyphosis? *J Spinal Disord Tech* 2013;26:252–5.
- [13] Bharucha NJ, Lonner BS, Auerbach JD, Kean KE, Trobisch PD. Low-density versus high-density thoracic pedicle screw constructs in adolescent idiopathic scoliosis: do more screws lead to a better outcome? *Spine J* 2013;13:375–81.
- [14] Larson AN, Polly DW Jr, Diamond B, Ledonio C, Richards BS 3rd, Emans JB, et al. Does higher anchor density result in increased curve correction and improved clinical outcomes in adolescent idiopathic scoliosis? *Spine* 2014;39:571–8.
- [15] Le Navéaux F, Aubin CE, Larson AN, Polly DW Jr, Baghdadi YM, Labelle H. Implant distribution in surgically instrumented Lenke 1 adolescent idiopathic scoliosis: does it affect curve correction? *Spine* 2015;40:462–8.
- [16] Liu H, Li Z, Li S, Zhang K, Yang H, Wang J, et al. Main thoracic curve adolescent idiopathic scoliosis: association of higher rod stiffness and concave-side pedicle screw density with improvement in sagittal thoracic kyphosis restoration. *J Neurosurg Spine* 2015;22:259–66.
- [17] Newton PO, Marks MC, Bastrom TP, Betz R, Clements D, Lonner B, et al. Surgical treatment of Lenke 1 main thoracic idiopathic scoliosis: results of a prospective, multicenter study. *Spine* 2013;38:328–38.
- [18] Abe Y, Ito M, Abumi K, Sudo H, Salmingo R, Tadano S. Scoliosis corrective force estimation from the implanted rod deformation using 3D-FEM analysis. *Scoliosis* 2015;10(Suppl. 2):S2.
- [19] Hwang CJ, Lee CK, Chang BS, Kim MS, Yeom JS, Choi JM. Minimum 5-year follow-up results of skipped pedicle screw fixation for flexible idiopathic scoliosis. *J Neurosurg Spine* 2011;15:146–50.
- [20] Min K, Sdzuy C, Farshad M. Posterior correction of thoracic adolescent idiopathic scoliosis with pedicle screw instrumentation: results of 48 patients with minimal 10-year follow-up. *Eur Spine J* 2013;22:345–54.
- [21] Takahashi J, Ikegami S, Kuraishi S, Shimizu M, Futatsugi T, Kato H. Skip pedicle screw fixation combined with Ponte osteotomy for adolescent idiopathic scoliosis. *Eur Spine J* 2014;23:2689–95.
- [22] Clements DH, Betz RR, Newton PO, Rohmiller M, Marks MC, Bastrom T. Correlation of scoliosis curve correction with the number and type of fixation anchors. *Spine* 2009;34:2147–50.
- [23] Salmingo RA, Tadano S, Abe Y, Ito M. Influence of implant rod curvature on sagittal correction of scoliosis deformity. *Spine J* 2014;14:1432–9.

北海道における低侵襲脊椎外科 一現状と課題一

最小侵襲脊椎安定術 (MIS_t) の現状と課題
～mini-open TLIFの臨床成績から～

小松 幹, 須田 浩太

北海道せき損センター

はじめに

高齢化が進行し、合併症を多く抱えるハイリスク患者が増加するなかで、脊椎外科領域も低侵襲手術の必要性が高まっている。脊椎外科においては鏡視下手術による腰椎椎間板ヘルニアや脊柱管狭窄症に対する手術を皮切りとして最小侵襲脊椎手術 (Minimally invasive spine surgery: MISS) は普及してきたが、2009年にMISSの一分野として、最小侵襲脊椎安定術 (Minimally invasive spine Stabilization: MIS_t) が提唱され、注目されている¹ (表1)。

当院では以前から不安定性のある症例に対し、transforaminal lumbar interbody fusion (TLIF) を行ってきたが、さらに2005年以降は、より低侵襲化を目指して傍脊柱筋間アプローチを併用したmini-open TLIF (以下、mini TLIF) を開発導入しており²、その有用性を検討した。

Mini TLIFの手術方法

L4 / 5 単椎間固定を例に説明する。皮膚切開はL4 棘突起上端からL5 棘突起下端までの正中縦切開のみで全て行われる。L4 棘突起から傍脊柱筋付着部をメスで切開し、コブエレベーターで症状優位側の椎間関節外側まで展開する。対側の脊柱管狭窄を合併して

除圧が必要な場合には反対側も椎間関節部分まで展開しておく。

次に両側ともに筋間アプローチにて多裂筋の外側から椎間関節外側を展開する³。すなわち、傍脊柱筋の棘突起付着部にて腰筋膜と脊柱起立筋腱膜の間を外側に向かって剥離し、棘突起付着部から約3 cm外側で脊柱起立筋腱膜をメスで縦割する。内側に多裂筋筋膜をみながら、多裂筋と最長筋の筋間を指で鈍的に分けて椎間関節外側からL4 およびL5 横突起まで展開する (図1)。このとき症状優位側のL4 / 5 椎間関節は正中アプローチにてすでに展開されているためメルクマールとなる。適当な開創器にて外側開創部を保持する。筆者らは、頭尾側方向はトリムラインを、左右方向はゲルビー鉤を用いることが多い。

外側開創部から両側の椎弓根スクリューを刺入する。椎間関節外側、横突起、副突起を骨膜下に展開し、付着していた筋肉を除去すると、スクリュー刺入点でより正確になるが、侵襲は大きくなる。X線イメージを用いることで軟部組織の上からの刺入が可能となる。

続いて、脊柱管内から椎間孔の除圧を正中アプローチにて行う。L4 下関節突起ならびにL5 上関節突起は基部より全切除し、椎間板上縁ならびに下縁を確認する。L4 神経根は椎体後壁に沿って神経べらを椎弓根方向に滑らせると確認できる。必要に応じてL

表1

最少侵襲脊椎安定術: MIS _t	
・ MIS-TLIF/PLIF	・ Mini-open TLIF/ PLIF
・ MIS-long fixation	・ XLIF, OLIF/DLIF
・ Balloon kyphoplasty (BKP)	・ Interspinous process motion-sparing implant (X-stop)
・ Cortical bone trajectory (CBT)	・ 人工椎間関節
・ 最少侵襲腰仙椎腸骨固定術 (S2 AIなど)	・ Cervical artificial disc
・ 腰仙椎間関節安定術 (SI)	・ VATS, etc

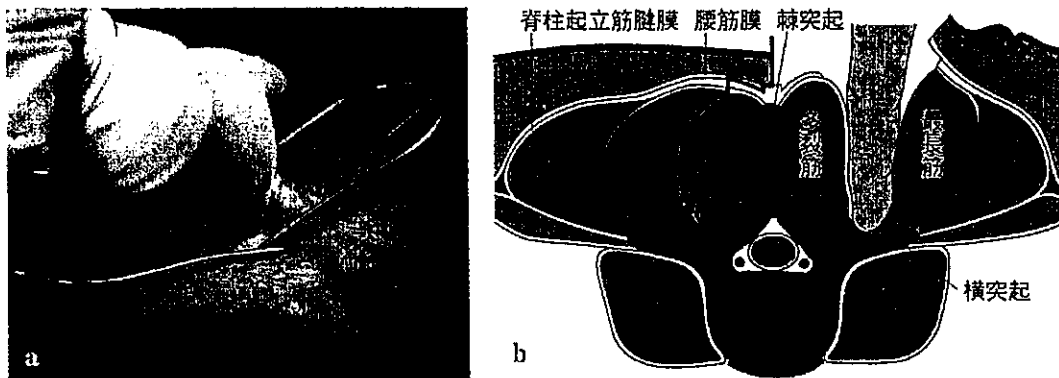


図1 傍脊柱筋間アプローチ (文献3より転載)

棘突起付着部から約3 cm外側で、脊柱起立筋腱膜をメスで縦割し、内側に多裂筋筋膜をみながら、多裂筋と最長筋の筋間を指で鈍的に分けて、椎間関節外側に到達する

4 下関節突起を椎弓根の方向に頭側に切除を加えて、脊柱管から椎間孔内外へのL4神経根走行を確認する。脊柱管狭窄合併例では、両側の内側椎間関節切除にて脊柱管内除圧を行い、L5神経根を確認する。

椎間関節全切除を行った症状優位側から片側進入TLIFを行う (図2)。L4ならびにL5神経根走行に干渉しない部位に椎間板操作のポータルを作成し、棘突起スプレッターで椎間板腔を広げながらキュレットを用いて椎間板切除を行う。筆者らは、2個のボックス型の椎体間ケージを設置しているが、反対側のできるだけ遠い位置にケージを設置する際は外側開創部から、進入側手前に設置する際は正中アプローチからと、ケージの設置位置によって使い分けている。

その後、外側開創部から、両側のロッドを設置してインストルメンテーションを完成させる。椎間関節の残っている反対側に、必要に応じて後側方固定の追加が可能である。

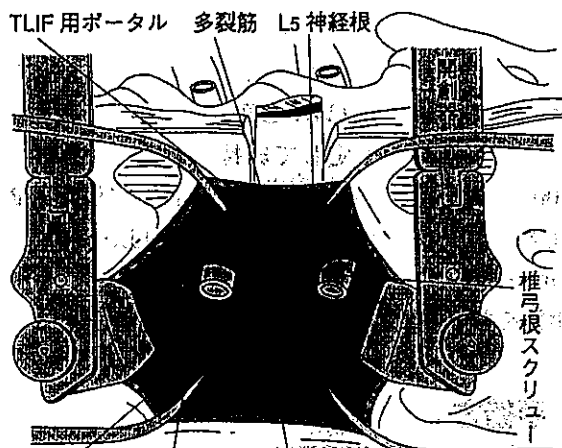


図2 傍脊柱筋間アプローチからの椎体間操作 (文献3より転載)

外側開創部から椎弓根スクリューを刺入する。椎間関節全切除を行った症状側から片側進入TLIFを行う。

手術成績

1) 対象と方法

2005年4月～2015年3月に、変性すべり症、分離すべり症、変性後側弯症などの不安定性を伴う腰椎疾患に対し、1椎間のmini TLIFを施行した32例 (以下mini TLIF群) と従来型TLIFを施行した46例 (以下TLIF群) を対象とした。mini TLIF群は男性15例、女性17例、平均年齢61.4歳で、TLIF群は男性30例、女性16例、平均年齢66.0歳であった。手術椎間は、mini TLIF群においてL3/4が6例、L4/5が18例、L5/Sが8例でTLIF群ではL2/3が1例、L3/4が5例、L4/5が36例、L5/Sが4例であった。平均経過観察期間はmini TLIF群が62.5ヶ月、TLIF群が41.7ヶ月であった (表2)。

手術時間、出血量、術前および術後6ヶ月、1年時のRoland Morris Questionnaire (RDQ)、Oswestry Disability Index (ODI)、骨癒合率、合併症、入院期間、隣接椎間障害に対する追加手術の有無を調査した。

表2

		mini TLIF	TLIF
年齢 (歳)	平均	61.4	66.0
性別	男性	15	30
	女性	17	16
手術椎間	L2/3	0	1
	L3/4	6	5
	L4/5	18	36
	L5/S	8	4
入院期間 (日)	平均	50.9	46.3
経過観察期間 (月)	平均	62.5	41.7

2) 結果

入院期間はmini TLIF群が50.9日, TLIF群が46.3日で有意差は無かった。手術時間はmini TLIF群が127-437分 (平均249分), TLIF群が53-375分 (平均123分) でmini TLIF群で優位に長く, それに比例して平均出血量はmini TLIF群が457ml, TLIF群が230mlとmini TLIF群で多かった (表3)。ODIはmini TLIF群が46%-26%-27%, TLIF群が47%-21%-22%で, 術後はすべて術前より有意に改善したが両群間に有意差は無かった。一方でRDQの臨床成績はmini TLIF群が12.1-7.0-7.1, TLIF群が11.2-6.9-4.3であり, 術後1年ではむしろTLIF群の方が経過良好であった。それぞれ1例の無症候性の偽関節を認め, 骨癒合率はmini TLIF群が96.9%, TLIF群が97.8%であった。神経障害や深部感染などの重篤な合併症はなかった。隣接椎間障害に対し手術追加を要した症例はmini TLIF群で3例 (9.1%), TLIF群で1例 (2.2%) であった。

考 察

mini TLIFでは手術手技が従来のTLIFと比べ手順が多いため, いかに術式に慣れようとも手術時間がより長くなる傾向が明らかとなった。それに比例して術中出血量も多くなる。また, これまでの報告³とは異なり臨床成績は術後1年の時点では従来式のTLIFの方が優れている可能性も示唆された。

表3

	mini TLIF	TLIF
手術時間 (分)	127-437 (平均249)	53-375 (平均123)
平均出血量 (ml)	457	230

近年経皮的椎弓根スクリューを用いたMIS-TLIFやMIS-long fixationが脚光を浴び, その低侵襲性^{2,6}, 低い術後感染率⁴, 早期離床⁵などが注目されているが, 従来式TLIFに将来完全にとって代わる術式であるかどうかは疑問である。従来式TLIFの適応がなかった全身状態の悪い患者や超高齢者においては一定の恩恵があるのは間違いないが, 従来式TLIFの手術手技の重要性が失われることはないと感じている。若手脊椎外科医がMISSに傾倒しすぎるあまり, あるいは指導施設で従来式の手術手技に触れる機会が少ない為に, 従来式手術手技の習熟度が全体として下がり, 応用の効かない脊椎外科医が増えてしまうのではないかという危惧の念さえ抱く。MISSが発展することは患者にとって大いに喜ばしいことで, さらなる進化を期待もするが, 今こそ基本的な手術手技の重要性を再確認したい。

参考文献

1. 石井賢, 松本守雄. 【最小侵襲脊椎安定術 (MIS_t) の実際】 MIS_t手技とPPS (経皮的椎弓根スクリュー) システムの現状と未来. 脊椎脊髄ジャーナル28, 442-448 (2015).
2. 石井賢, 戸山芳昭, 千葉一裕, 他. 【運動器疾患に対する最小侵襲手術】 脊椎手術 矯正・再建術 腰椎変性すべり症と腰椎変性 (後) 側彎症に対する最小侵襲椎間孔腰椎椎体間固定術の手術手技. 別冊整形外科, 124-132 (2011).
3. 森平泰, 須田浩太, 梶野知道他. 【腰椎椎間孔狭窄】 腰椎椎間孔狭窄に対する傍脊柱筋間アプローチを用いたmini-open TLIF. 脊椎脊髄ジャーナル23, 533-538 (2010).
4. O'Toole, J.E., Eichholz, K.M. & Fessler, R.G. Surgical site infection rates after minimally invasive spinal

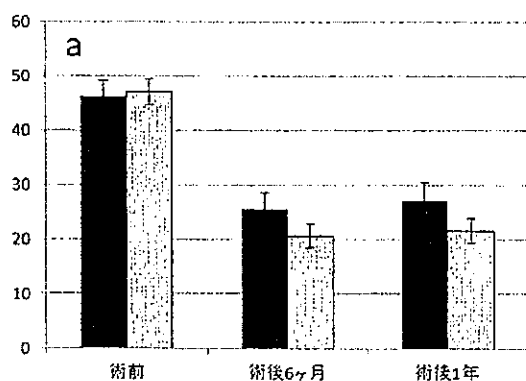
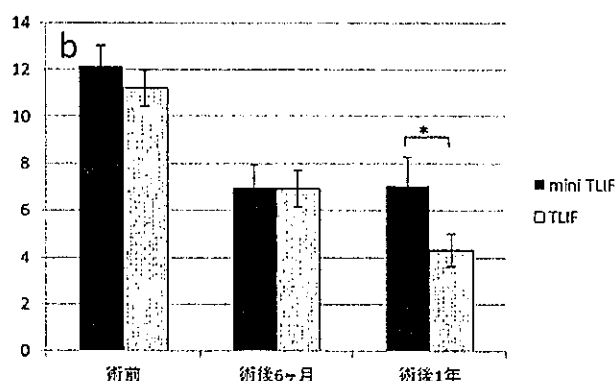


図3 臨床成績

A: ODI B: RDQ * : p<0.05



surgery. Journal of neurosurgery. Spine 11, 471-476 (2009).

5. 佐藤公治, 安藤智洋, 稲生秀文, 他. X-tubeとSEXTANTによるPLIFは低侵襲脊椎手術か MIS-PLIFは従来法より筋侵襲は少ない. 中部日本整形外科災害外科学会雑誌 50, 1019 - 1020 (2007).
6. 種市洋, 北川知明, 稲見聡, 他. mini-open TLIFによる多裂筋障害パターンの分析 MRIを用いた前向き研究. 日本最小侵襲整形外科学会誌 8, 37 (2008).
7. 種市洋, 須田浩太, 楫野知道他. 傍脊柱筋間アプローチと正中アプローチの併用によるMini-open TLIF. 日本整形外科学会雑誌 80, S540 (2006)

手術困難なために遅発性麻痺を生じた びまん性特発性骨増殖症 (DISH) 脊椎骨折の 1 例

木田 博朗, 須田 浩太, 松本 聡子, 小松 幹, 牛久智加良,
山根 淳一, 遠藤 努, 東條 泰明, 神谷 行宣, 三浪 明男

北海道中央労災病院 セキ損センター

要 旨

遅発性麻痺を生じたDISH (Diffuse idiopathic skeletal hyperostosis) に伴う脊椎骨折の 1 例を経験した。

症例は86歳女性, 転倒後に腰背部痛が出現し, Th 12椎体高位でのReverse Chance型骨折と診断された。全身状態不良のため早期手術を断念し保存加療を行ったところ, 受傷7日目にFrankel Cの対麻痺が出現した。CTでは骨折部の転位を認めた。手術可能な状態まで全身状態が回復したため後方固定術を施行したが, 麻痺の改善は見られなかった。

DISHに伴う脊椎骨折では, 骨折部に応力が集中し骨癒合が得られにくく, 転位をきたしやすい。高齢者では全身状態が悪く骨脆弱性が著しい症例が多いため, 手術困難例や術後合併症例が増加しておりこの傾向はますます強まるものと推察する。警鐘を鳴らす意味で本例を報告する。

緒 言

DISHは脊椎を中心とした全身の骨格系における素因的な骨過形成症であり, 高齢男性に比較的多い。DISHに伴う脊椎骨折は不安定性が強く, 急速な麻痺の出現や偽関節がしばしば問題になる。高齢化が進むとともにDISHの脊椎骨折例は増加傾向にあるが, 高齢者であるが故に手術限界例も散発しており, 今後は全身状態や骨脆弱性のために手術不能な例も増加する可能性が高い。

上記の如く手術困難なため遅発性麻痺を生じたDISHを経験したため文献的考察を加えて報告する。

症 例

86才女性

主訴: 腰背部痛。

現病歴: 自宅で転倒後, 腰背部痛のため立位困難となり当院に救急搬送された。

初診時所見: 高度な腰背部痛があったが, 下肢痛や神経学的異常はなく介助歩行可能であった。単純X線写真, CTでは上位胸椎から腰椎にかけての連続した前縦靱帯骨化, 椎体間骨性架橋, 棘上・棘間靱帯骨化を認めた。さらにTh12椎体前壁から後方要素に至る骨折と椎体前方の開大を認め, リバースチャンス骨折 (Reverse Chance型骨折) と診断した。MRIでは同部位での明らかな脊髄の圧迫を認めなかった (図1A-C)。

経過: 早急な固定術が必要と判断したが, 発熱, 炎症反応高値, 低栄養状態, 胸水貯留など全身状態が不良であったため早期手術を断念した。

全身管理を行いながら, 硬性装具を装着し床上安静による慎重な保存加療を行ったが, 受傷7日目にFrankel Cの対麻痺 (MMT: 両腸腰筋以下2) と両L1領域以下の感覚鈍麻と膀胱直腸障害が発生した。CTでは骨折部上位が後方に転位し, 同高位での脊髄圧迫を示唆し (図2A, B), 翌日にはMMT: 両腸腰筋以下0~1まで麻痺が進行した。

麻痺出現2日後において全身状態はわずかに改善傾向を示していたため, リスクを同意の上でTh9からL3までの後方固定術を施行した (図3A, B)。椎骨は紙のように柔らかく, 椎弓根スクリュー刺入時の抵抗を感じなかった。また椎弓は指で触っているだけで折れてしまうほど脆弱であったため, ケーブルやフックの有効なアンカーを確保することを断念した。さらに本症例は低蛋白血症, 低アルブミン血症を伴う低栄養状態であり, 手術創治癒が得られない可能性が高く, インストゥルメンテーションは最小限にとどめるべきとの判断で頭尾側とも3椎体のみのアンカーとした。

術後麻痺の改善はみられなかった。手術創の治癒に

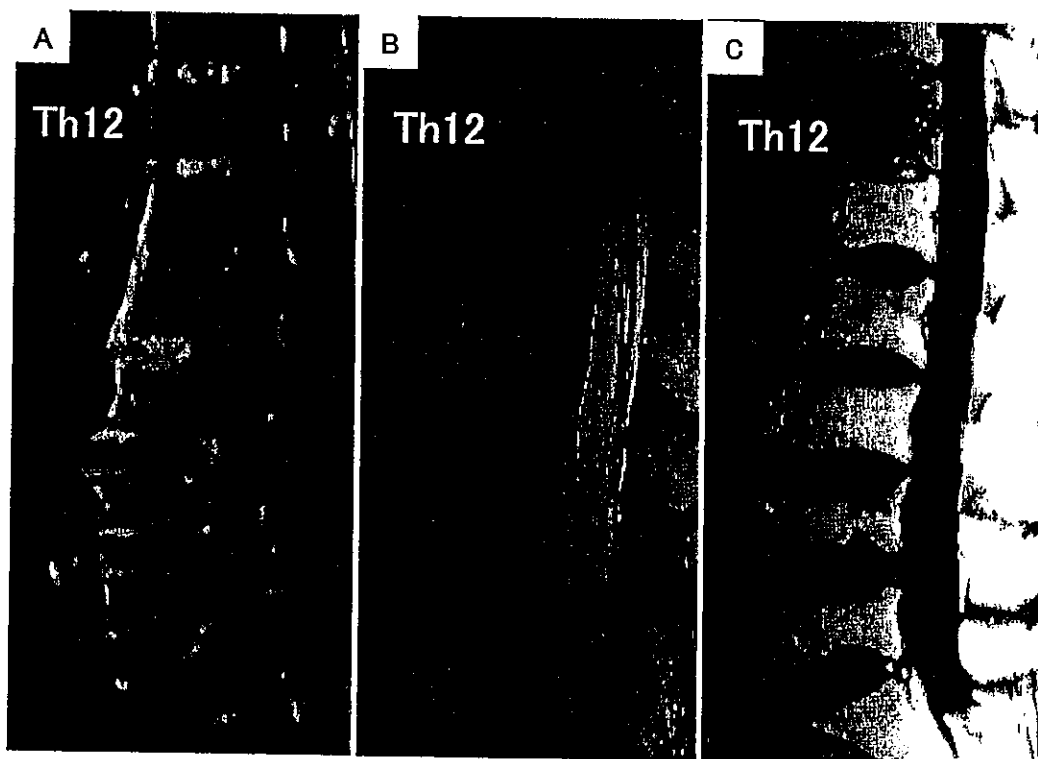


図1：初診時CT, MRI（矢状断像）

CT (A) ではTh12椎体前方はやや開大している。MRI (B：T2WI, C：T1WI) では同部位での明らかな脊髄の圧迫を認めない。

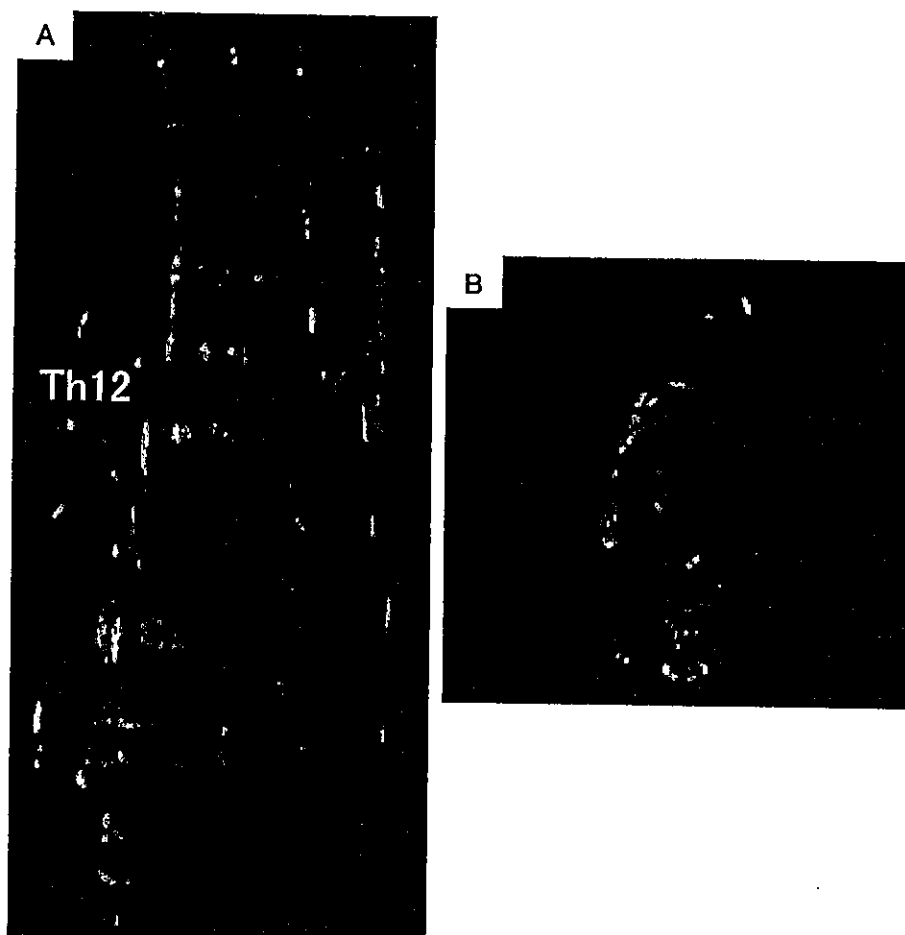


図2：受傷7日目CT (A：矢状断像, B：Th12高位横断像)
骨折部上位が後方に転位し、同高位での脊髄圧迫を示唆する。

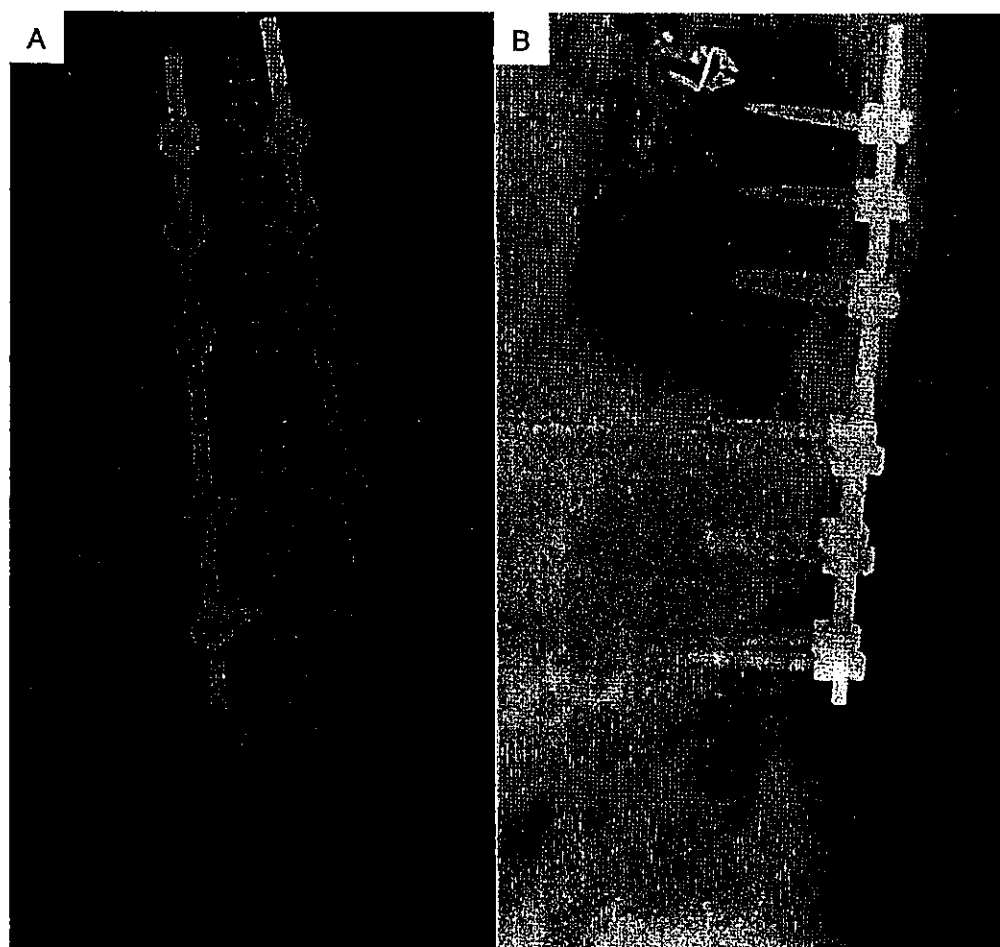


図3：T9—L3後方固定術後単純X線写真
A：正面像，B：側面像。

は8週間を要し、創傷開を繰り返すたびに縫合を追加した。本例ではインストルメンテーションによる固定力には限界があったため、3カ月間を床上安静とした。

考 察

DISHは脊椎を中心とした特徴的な骨増殖を呈する疾患で、主に60才以上の男性にみられる。

1950年にForestierが脊柱の前縦靱帯骨化を中心とする脊柱靱帯骨化により脊椎強直をきたす疾患を強直性脊椎骨増殖症 (ASH) として報告し²⁾、後にResnickら³⁾によりDISHと提唱されるようになった。

de Perettiら¹⁾はDISHおよび強直性脊椎炎に伴う脊椎損傷を4つの型 (①open-wedge anterior fracture; 62.5%, ②sawtooth fracture; 8.4%, ③occult or radiologically invisible fracture; 16.6%, ④non-specific fractures; 12.5%) に分類し、椎体前方開大型の骨折が最も頻度が高いと報告した。この骨折はReverse Chance型骨折と呼ばれ、本症例もこのタイプに属していた。

DISHの患者では、椎間の骨性癒合により可動性が損なわれ、生理的荷重が加わらないため椎体は脆弱化する。また、多椎間にわたり癒合した脊椎は長管骨と同様であり可動性がない。すなわち、骨脆弱な長管骨と同じ状態であり軽度の外力でも骨折を起こしやすい。

また、ひとたび骨折するとレバーアームが長いために骨折部に応力が集中し転位や麻痺を生じやすい。

過去の報告では、DISHに伴う脊椎骨折に対し保存療法を行った28例中16例 (57.1%) に遅発性麻痺が生じている⁴⁾。特に骨粗鬆症が重度で骨脆弱性が強い症例では骨折部の破壊が進行しやすく、転位や遅発性麻痺のリスクが高まると考えられる。こういった症例では早期手術が重要となるが、超高齢者で全身状態が悪く手術が限界の症例は増加傾向にある。また、手術が可能だったとしても骨脆弱性のために十分な固定性を得られない場合も少なくないため、治療に難渋することが予想される。

転倒予防、骨粗鬆症治療、骨脆弱例に対する固定法など課題は山積している。

結 語

遅発性麻痺を生じたDISHに伴う脊椎骨折の1例を経験した。

本骨折は保存療法に抵抗性であり、特に高齢者で骨粗鬆症を伴う症例では骨折部の転位や遅発性麻痺のリスクが高く早期手術が望ましい。手術限界例が増加傾向にあり課題は多い。

キーワード：Diffuse idiopathic skeletal hyperostosis (DISH：びまん性特発性骨増殖症)，Chance fracture (Chance型骨折)，delayed paralysis (遅発性麻痺)

文 献

- 1) de Peretti F, Sane JC, Dran G et al : Ankylosed spine fractures with spondylitis or diffuse idiopathic skeletal hyperostosis : diagnosis and complications. Rev Chir Orthop Reparatrice Appar Mot, 90 : 456-465, 2004.
- 2) Forestier J, Rotes-Querol J : Senile ankylosing hyperostosis of the spine. Ann Rheum Dis, 9 : 321-330, 1950.
- 3) Resnick D, Shaul SR, Robins JM : Diffuse idiopathic skeletal hyperostosis (DISH) : Forestier's disease with extraspinal manifestations. Radiology, 115 : 513-524, 1975.
- 4) 堀内陽介, 奥山邦昌, 有井大典他 : 外傷後に遅発性麻痺を生じた強直脊椎の2例. 臨床整形外科, 47 : 1019-1024, 2012.

頸椎脱臼骨折の初期治療 私の治療戦略

須田浩太 Kota Suda

北海道せき損センター副院長
〒072-0015 北海道美幌市東4条南1丁目3-1

小松 幹 Miki Komatsu

北海道せき損センター整形外科部長

牛久智加良 Chikara Ushiku

北海道せき損センター整形外科部長

校條祐輔 Yusuke Menjo

北海道せき損センター整形外科副部長

松本聡子 Satoko Matsumoto

北海道せき損センター整形外科部長

初期治療におけるポイント

時間との勝負！—完全麻痺でも回復することはある

完全麻痺でも歩行可能なレベルまで回復する例は存在する。脱臼骨折では①受傷時の初期脊髄損傷と②脱臼部位における脊髄絞扼+不安定性による続発脊髄損傷によって麻痺が決定される。なかには完全横断損傷を免れている例があり、迅速な整復により麻痺が改善する。いかなる症例も麻痺回復の可能性があると考えて行動すべきである。

施設と術者

脊髄損傷では迅速かつ適切な初期治療が予後を左右する。一般病院で対応するのは困難であり脊損専門施設があれば手術を含めて依頼するのがベストである。脊損専門施設がない場合は脊椎外科医が常在する救急病院へ依頼する。誰が手術するかで患者の一生が左右されるため、然るべき術者が執刀するか、立ち会ってもらふこと。

移送・受け入れ

患部の固定をしっかりと搬送する。長距離移送ならば航空機やヘリコプターがベターであり麻痺増悪例が少ない。受け入れ施設では複数のスタ

ッフで対応するが、頸椎保護の責任者を決め、その指示に全員が従う。多くの脱臼骨折では伸展位で脊髄絞扼が悪化するため、中間位から軽度屈曲位を保つ。特に胸椎後弯が強い症例では枕を高くする必要がある。

治療戦略

迅速で適格な診断を—まずCTから

短時間で病態を把握するためCTがベストである。バイタルチェック、神経チェック、採血が終わり次第、CTを撮像し損傷形態を把握する。AO分類やSLICスコアなど多くの分類があるが、著者はAllen分類を愛用しており、代表的な5つを紹介する(表1)¹⁾。またDF2(図1)、CE4(図2)、CF4(図3)、VC3(図4)について症例を提示する。

整復が先？手術が先？—時間を考えて臨機応変に

CTの次は短時間で整復できる方法を選ぶ。当センターは30～60分で手術室まで搬入できる体制が整っており、頭蓋直達牽引の準備や整復までの時間と同等である。MRIなど残りの検査を進め手術まで一気に仕上げる。しかし、通常の施設でこ

表1 Allen分類

Distractive-Flexion (DF) = 伸延力+屈曲位	
DF1:	後方靱帯複合体損傷、亜脱臼か自然整復されたものを含む
DF2:	片側椎間関節脱臼、棘突起骨折や椎弓根骨折を伴うこともある
DF3:	両側椎間関節脱臼、転位が50%まで
DF4:	両側椎間関節脱臼、転位が50%以上、極めて不安定
Compressive-Extension (CE) = 圧縮力+伸展位	
CE1:	片側後方要素損傷
CE2:	両側椎弓根骨折
CE3:	CES2以外の両側後方要素損傷
CE4:	不完全転位
CE5:	完全転位
Compressive-Flexion (CF) = 圧縮力+屈曲位	
CF1:	軽度の椎体楔状圧迫骨折（椎体前縁の鈍化）
CF2:	中程度の椎体楔状圧迫骨折（前方椎体高の減少）
CF3:	明らかな椎体骨折（骨折線が生じ、遊離骨片を形成）
CF4:	3mm未満の後方すべり
CF5:	3mm以上の後方すべり
Vertical-Compression (VC) = 圧縮力+中間位	
VC1:	上下の椎体終板のうち片方のみの終板骨折
VC2:	上下両側の椎体終板骨折（骨片転位が少ない）
VC3:	上下両側の椎体終板骨折（骨片転位が明らかな）
Distractive-Extension (DE) = 伸延力+伸展位	
DE1:	前方靱帯断裂・椎間板損傷・椎体横骨折
DE2:	DES1に後方靱帯群損傷を合併（椎体は後方転位）

のスピードは困難であり、麻痺が明らかな症例では頭蓋直達牽引を優先したほうが良い。ただしCEは牽引を緩めると再脱臼する。CFやVCは整復できないと考えたほうが良い。DEやDF4は牽引で悪化する。整復が適しているのはDF2、DF3である。

椎骨動脈とWillis動脈輪

椎骨動脈とWillis動脈輪の後交通動脈（PcomA）によって脳幹部の血流は維持されている。頸椎脱臼骨折では約17%で椎骨動脈閉塞、健常人でも約

15%に椎骨動脈低形成が存在する。また、Willis動脈輪が完全に保たれているのは健常人の約半数であり、椎骨動脈とPcomAの評価は必須である²⁾（図5、図6）。椎骨動脈損傷の回避は当然であるが、致死的风险がある側の椎弓根スクリューは勧めない。例えば両側PcomAが欠損し、右側椎骨動脈が閉塞している症例では左側椎骨動脈のみが脳幹部血流を維持している。この症例に対して左側に椎弓根スクリューを入れるのは良策とは言えない。

気管切開の要否

C5 AIS A以上の麻痺と脱臼骨折が混在した場合、呼吸障害により気切管理となる確率が高い。気管切開が予測される場合、感染を避けるため前方プレートやケージを使用しないほうが無難である。前方インプラントを使用する場合、1週間おいてから気管切開する³⁾。

手術手技

椎体破裂型と関節脱臼型

頸椎脱臼骨折は椎体破裂型（CF、VC）と関節脱臼型（DF、CE、DE）に大別できる。椎体破裂型では前方再建を、関節脱臼型では後方再建を基本に考える。ただし、近年では椎弓根スクリューの登場により椎体破裂型でも後方単独再建が可能となった⁴⁾。

椎体破裂型の手術（表2）

CF1、CF2、VC1は保存治療が基本。CF3、VC2は脊髄圧迫・後弯変形・不安定性により手術。CF4、CF5、VC3では前方除圧+整復固定を行うのが基本。気管切開が予想される場合は術後感染を避ける意味で前方インプラントを避け、後方インストゥルメンテーションを追加する。破裂椎体

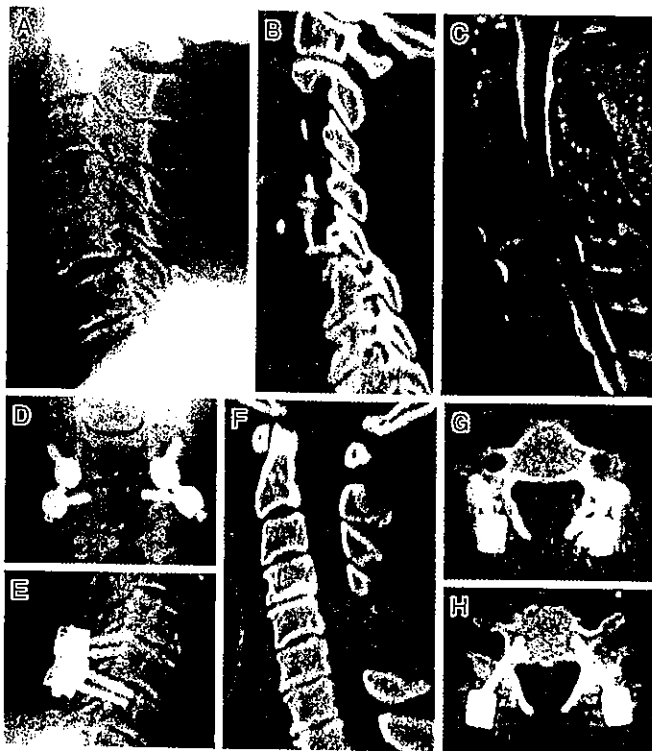


図1 Distractive-flexion injury stage II (DF2) の症例

- ・整復時には屈曲損傷だからといって伸展させるのではなく、屈曲位にしなければ嵌合した関節を整復できないことがある。その場合イメージで安全を確認しながら行うべきである。
- ・骨質が良好であれば外側塊スクリューでも十分な固定性が得られる。骨が脆弱な場合には片側の椎弓根スクリューを要するが、いずれにしても原則一椎間固定で十分である (D-H)。
- ・通常、脱臼が整復されれば除圧の必要はなく椎弓は移植骨母床として利用できるが、椎間板ヘルニアを伴う場合には椎弓形成術を併用する。

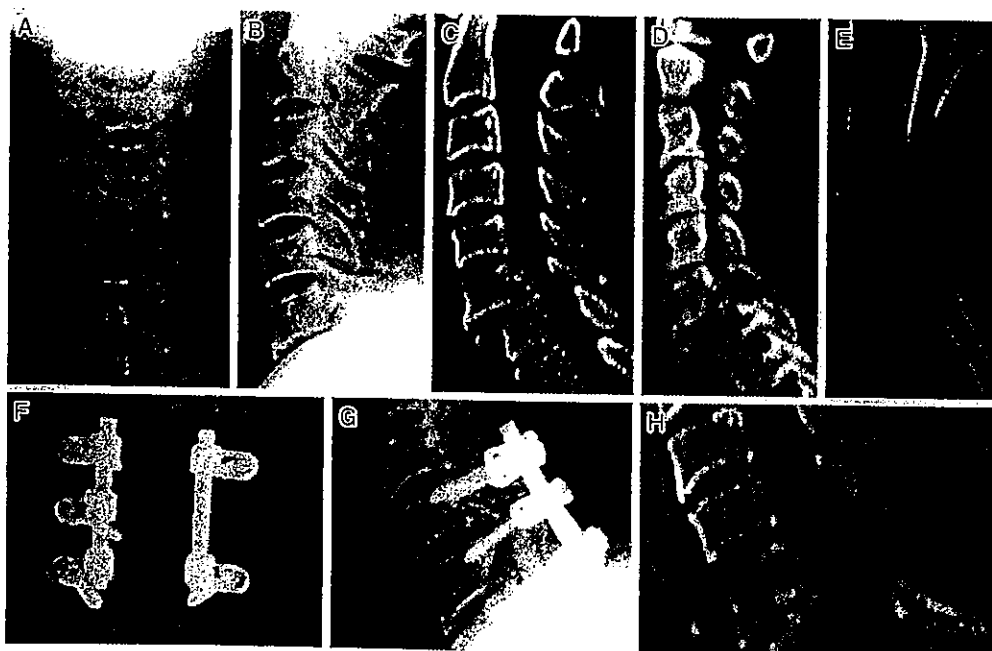


図2 Compressive-extension injury stage IV (CE4) の症例

- ・下位頸椎に発症しやすく、単純X線のみでは見落とされやすい損傷の一つである (A-E)。
- ・損傷2椎以上にまたがり多椎間固定を要する 경우가少なくない (F-H)。
- ・椎弓が完全に floating している場合には椎弓を摘出する場合もあるが必須ではなく、移植骨母床として利用できる場合もある。
- ・外側塊や棘突起が損傷されている場合が多く、外側塊スクリューやワイヤリングがアンカーとして選択できない場合も多い。

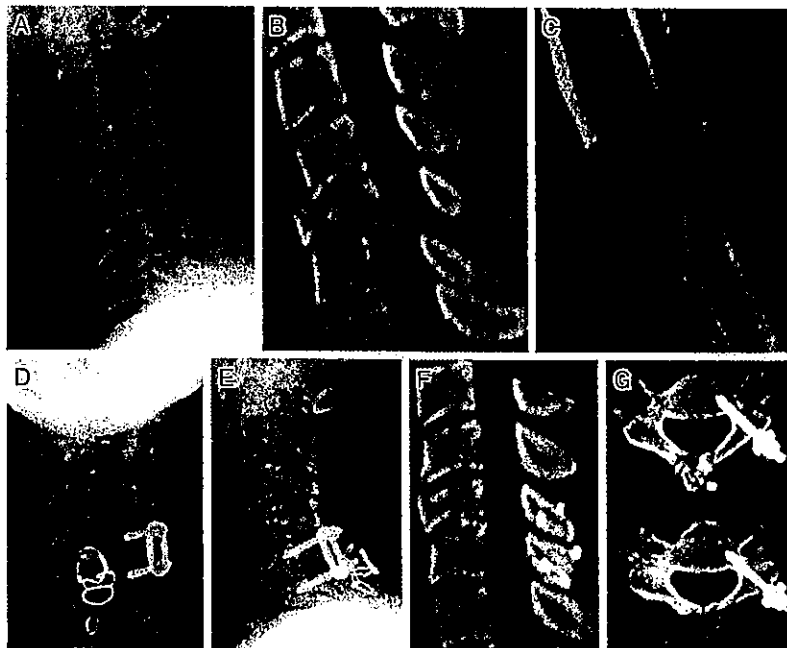


図3 Compressive-flexion injury stage IV (CF4) の症例

- 前方除圧+整復固定術が基本である。
- 椎体破裂の程度が軽度の場合はコンストレインタイプの椎弓根スクリューを用いて後方1椎間固定のみで一期的に治療できる症例もある。

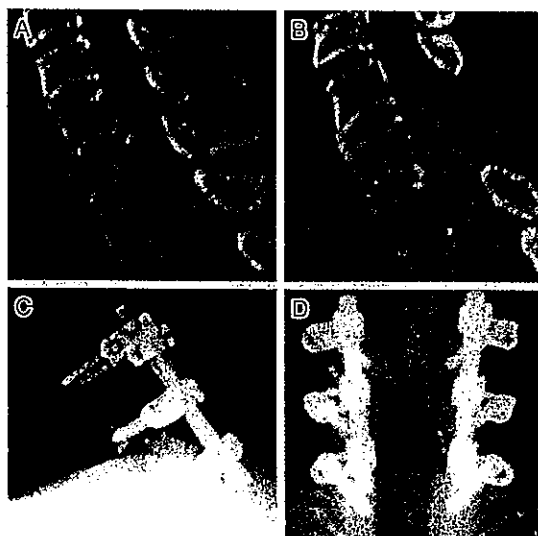


図4 Vertical-compression injury stage III (VC3) の症例

- 椎体破壊が著しい場合には2椎間固定が必要となるが、これもコンストレインタイプの椎弓根スクリューであれば整復位を保持することが可能で一期的な後方整復固定術での治療が可能となった。

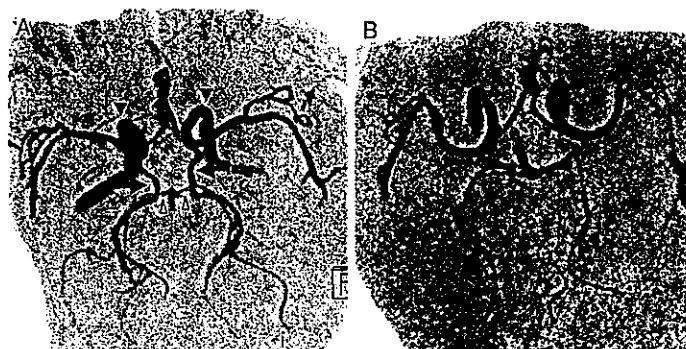


図5

- A: MRAによる後交通動脈 (PcomA) 像 (黒矢印)。左右の椎骨動脈は延髄上縁で合流し脳底動脈となった後、2本の後大脳動脈に分岐する (白矢頭)。PcomAは内頸動脈 (黒矢頭) と椎骨動脈由来の血流を連絡する経路である。
B: PcomAの両側欠損例。椎弓根スクリュー刺入時には椎骨動脈開存の確認が必須である。



図6

- A: MRAによる椎骨動脈像 (矢印)。両側とも血流が保たれている。
B: 右椎骨動脈は途絶している。
C: 造影CT。右横突孔内で椎骨動脈が造影されず (矢印)、血流の途絶または椎骨動脈低形成を疑う。PcomAが欠損していた場合、左側への椎弓根スクリュー刺入は良策とはいえない。

表2 椎体破裂型の手術

		前方 AF (Plate)	後方 Wiring	LMS	CPS
椎体骨折 (+)	CF3	○*	×	×	○*
	CF4・5	○**	×	×	○**
	VC2	○*	×	×	○*
	VC3	○**	×	×	○**

*不安定性や神経障害の程度による

**症例に応じて前方か後方を追加

表3 関節脱臼型の手術

		前方 AF (Plate)	後方 Wiring	LMS	CPS
椎体骨折 (-)	DF2・3	△	○*	○	○
	DF4	×	△	△	○
	CE1	○	○	○	○
	CE2・3	△	△	○	○
	CE4・5	×	×	△	○
	DE2	○	△	△	○

*椎間板ヘルニアでは前方除圧固定

が椎弓根と外側塊に連続し第三骨片を伴わないことがある。このような症例では後方で整復固定が可能である。これらの骨折では通常は2椎間固定となるが、中間椎（骨折椎）にもスクリューを刺入し前方へ押して矯正力をかけると整復位を得られる⁵⁾。逆に上下のスクリューに伸延力をかけすぎると弛みや破損につながる。

関節脱臼型の手術（表3）

DF1, DE1は神経障害がなければ保存治療とする。DF2, DF3で早期手術が不可能な場合は、頭蓋直達牽引による整復を行うが椎間板ヘルニアが生じることがあるので留意する。手術で整復する場合、上関節突起を切除すると脱臼椎を椎間板に対し平行に後方牽引して整復することになり、椎間板ヘルニアの危険性が増す。また、ワイヤリングの際は椎間圧縮力がかからない方法を選択する。ヘルニア合併例でも後方除圧で対応可能であるが、術後MRIで脊髄圧迫が顕著であれば前方除圧を即座に追加する。DF4は非常に不安定で、頭蓋直達牽引は適さない。椎弓根スクリュー、ワイヤー、外側塊スクリューを利用して固定性を担保する。固定性が悪ければ多椎間固定とする。

CE1の不安定性は軽度であり、後方ワイヤリン

グ、前方プレートのどちらでも問題はない。まれに剪断損傷があり強固な固定を要する。CE2, CE3では両側後方要素損傷が伴っておりワイヤリングでは固定できない。外側塊スクリューか椎弓根スクリューを要するが椎弓根骨折や外側塊遊離骨折がある場合は2椎間固定となる。CE4, CE5では後方要素と椎体が分離しており椎弓根スクリューが適している。ワイヤリング・外側塊スクリューの場合は多椎間固定を要する。

DE2は前方固定でも後方固定でも良い。OPLLや脊柱管狭窄など多椎間除圧を必要とする場合は後方除圧固定が容易である。

後療法・予後

脱臼を強固に固定することによって、術直後から体動制限を減じ、体交、排痰措置、看護が容易となる。骨癒合が進む1～3ヵ月間はカラー固定を行うが固定性が良ければ省略する。翌日から車椅子を許可し積極的な呼吸機能訓練、筋力増強訓練、関節可動域訓練、ADL訓練を開始する。初期には坐位によって窒息することがあり、スタッフが常に付き添う。血圧と酸素飽和度（サチュレーション）

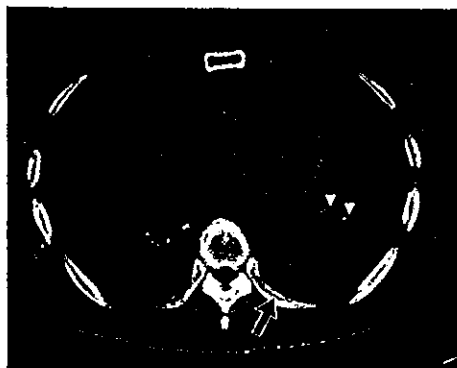


図7

胸水貯留（黒矢印）と無気肺（白矢頭）。特に高位頸損や高齢者では呼吸器合併症の発生が多い。術翌日の超早期から積極的に離床・車椅子移乗などリハビリテーションを行う。急激な酸素飽和度低下時には肺梗塞も疑い、造影CTを実施し評価する。

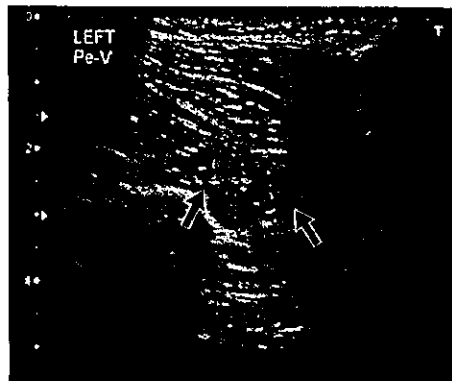


図8

下肢血管エコーによる深部静脈血栓像（黒矢印）。腓骨静脈、中央ヒラメ静脈に血栓が形成されている。麻痺高度例では、高率にかつ受傷超早期から血栓が形成される。検出にエコーが最適であるが、早期からの検出には検者の熟練度に影響される。膝窩部より中枢で血栓がある場合、MR Venographyや造影CTによる肺静脈血栓症の有無も評価する。

ン）をモニターしながら臥位や肺理学療法を行う。肺炎、無気肺（図7）、尿路感染、膀胱炎、深部静脈血栓（図8）、イレウス、消化管出血は頻発するので留意する。

文 献

- 1) Allen BL Jr. et al. A mechanistic classification of closed, indirect fractures and dislocations of the lower cervical spine. Spine (Phila Pa 1976). 1982, 7 (1), 1-27.
- 2) Taneichi H. et al. Traumatically induced vertebral artery occlusion associated with cervical spine injuries: prospective study using magnetic resonance angiography. Spine (Phila Pa 1976). 30 (17), 2005, 1955-62.
- 3) O'Keeffe J. et al, Tracheostomy after anterior cervical spine fixation. J Trauma. 2004, 57 (4), 855-60.
- 4) 錢邦芳. 脊椎脊髓損傷 診断・治療・リハビリテーションの最前線. 損傷脊椎・脊髄に対する治療: 頸椎・頸髓損傷の手術療法・後方再建. 脊椎脊髓ジャーナル. 16, 2003, 360-6.
- 5) 須田浩太ほか. 頸椎インストルメンテーション. 頸椎損傷. 関節外科. 27 (7), 2008, 930-6.

迅速な整復固定の重要性を示唆した頸椎脱臼骨折の1例

「例え運動完全麻痺であっても超早期手術により下肢筋力は完全回復する可能性がある」

福井 隆史¹⁾, 須田 浩太¹⁾, 遠藤 努¹⁾, 松本 聡子¹⁾, 小松 幹¹⁾, 牛久智加良¹⁾,
山根 淳一¹⁾, 東條 泰明¹⁾, 神谷 行宣¹⁾, 三浪 明男¹⁾, 高畑 雅彦²⁾, 岩崎 倫政²⁾

1) 北海道中央労災病院せき損センター

2) 北海道大学大学院医学研究科機能再生医学講座整形外科科学分野

要 旨

今回我々は頸椎脱臼骨折後に四肢運動完全麻痺まで悪化したが、超早期手術により独歩可能まで回復した1例を経験した。症例は65歳男性、自動車運転中の事故にてC5/6レベルの頸椎脱臼骨折を受傷し、当院到着時は改良Frankel B1の完全運動麻痺であった。受傷後約6時間で観血的脱臼整復および頸椎後方固定(C5/6)を施行した。術直後から四肢の自動運動が可能となり、術後14日で独歩可能となった。さらに術後20日の時点で下肢筋力が完全回復した。

受傷後超急性期に観血的脱臼整復および一期的な内固定を施行したことが、下肢運動完全麻痺が完全回復にまで至った要因の一つと考えた。

緒 言

脊髄損傷に対する急性期治療の目的は、1) 神経機能回復の阻害因子(神経圧迫因子)の除、2) 早期離床を可能とする脊椎安定性の獲得、3) 脊髄二次損傷の予防の3点である。すなわち、脊髄麻痺を伴う頸椎脱臼骨折では可及的早期の整復固定が望ましい。しかしながら、運動完全麻痺例において早期脱臼整復固定による麻痺改善効果のエビデンスは乏しい。本稿では頸椎脱臼骨折後に徐々に麻痺が進行し、四肢運動完全麻痺(改良Frankel B1)¹⁾まで悪化したが、超早期手術により手術直後に四肢自発運動が可能となり、術後14日で独歩可能までV字回復を示した症例を紹介し、脊髄損傷に対する急性期治療を一考する。

症 例

症例: 65歳男性、自動車運転中に自損事故にて受傷し前医へ救急搬送された。C5/6レベルにて脱臼骨折

(Allen-Ferguson分類: Distractive-Flexion injury stage IV) を認めた。前医搬入時は改良Frankel Dの麻痺であったが、当院へ搬送前には改良Frankel Cまで悪化し、当院到着時は改良Frankel B1の完全運動麻痺となっていた。すなわち、四肢運動完全麻痺で肛門知覚のみが残存している状態まで悪化していた。

当院到着から54分で手術室へ入室し、到着から1時間20分(受傷から5時間54分)で手術を開始した。手術開始後、約10分で脱臼を整復し(受傷から約6時間5分)、椎弓根スクリューシステムによりC5/6後方固定術を施行し55分で手術が終了した。麻酔覚醒直後に完全麻痺だった四肢の自動運動が可能となり翌日にかけて急速に回復した。手術後3時間30分の時点で触覚・痛覚は完全に改善していた。術後14日で独歩可能となり、術後20日では下肢筋力が完全回復した。

考 察

頸髄損傷に対する早期手術の是非に関しては未だに結論を見ない。Vaccaroらによって受傷後72時間をカットオフ値とした比較研究がなされたが、これにおいては早期手術の有効性は示されなかった²⁾。上記を踏まえFehlingsらによって、脊髄損傷後24時間をカットオフとした多施設前向きコホート研究が行われ、早期手術群ではASIA機能障害スケールが2段階以上改善した症例が有意に多いことが証明された³⁾。さらにNewtonらによって、ラグビーによる頸椎脱臼に対し、受傷後4時間以内に非観血的脱臼整復を施行することで、初診時Frankel AとBの症例を合わせた12例中7例でFrankel E(下肢筋力完全回復)まで改善したことが報告された⁴⁾。一方で受傷後9時間以降の非観血的脱臼整復群では完全回復に至った例はなかった³⁾。またビーグル犬を用いたRabinowitzらの動物実験にお

図1A

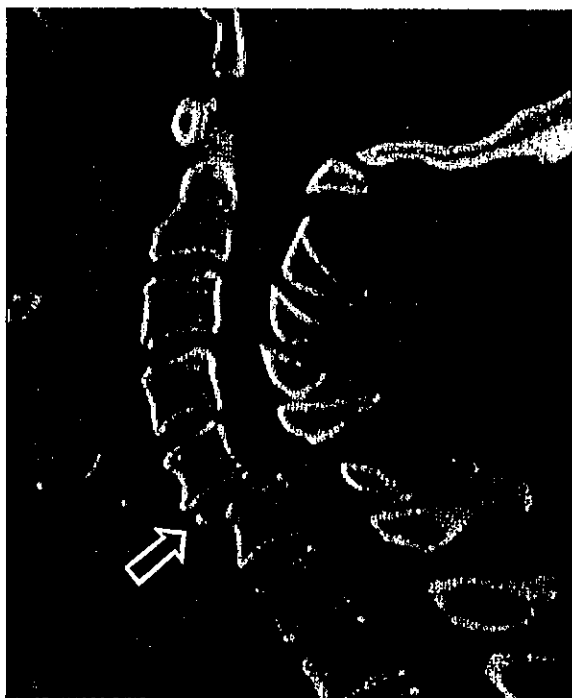


図1B

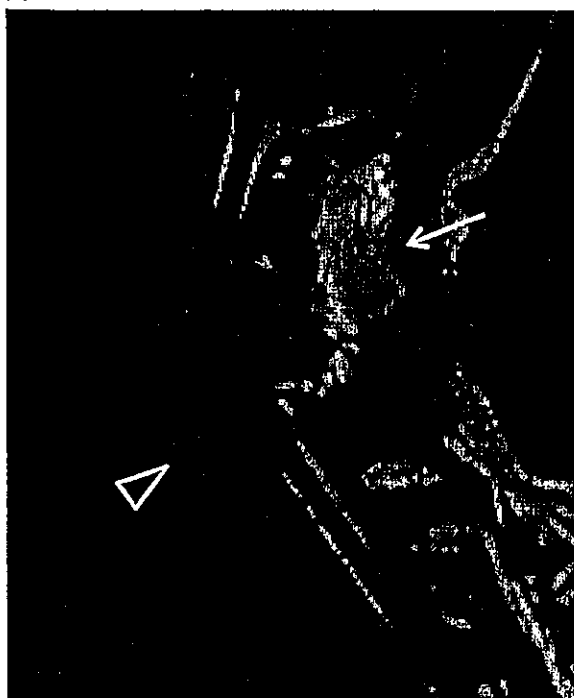


図1 当院搬送時CT画像と前医MRI画像。

(A) 頸椎脱臼 (C5/6) とそれに伴う剥離骨片 (⇨)。

(B) 椎間板の破綻所見 (△) と後方要素の破綻所見 (⇨)。

図2

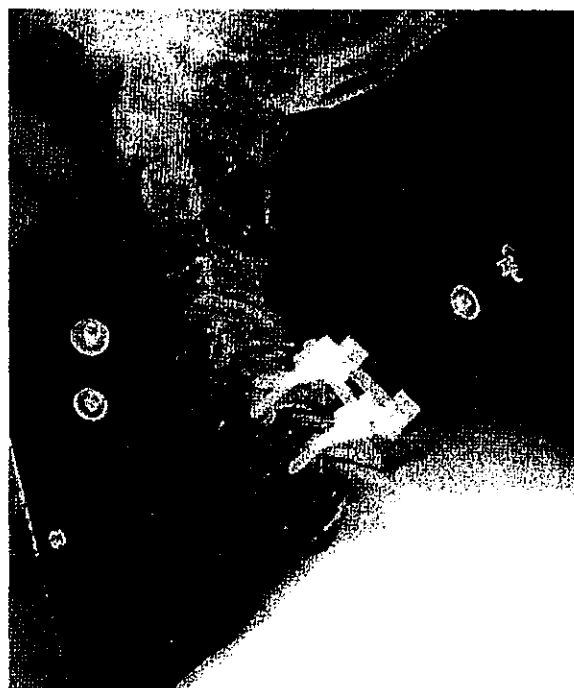
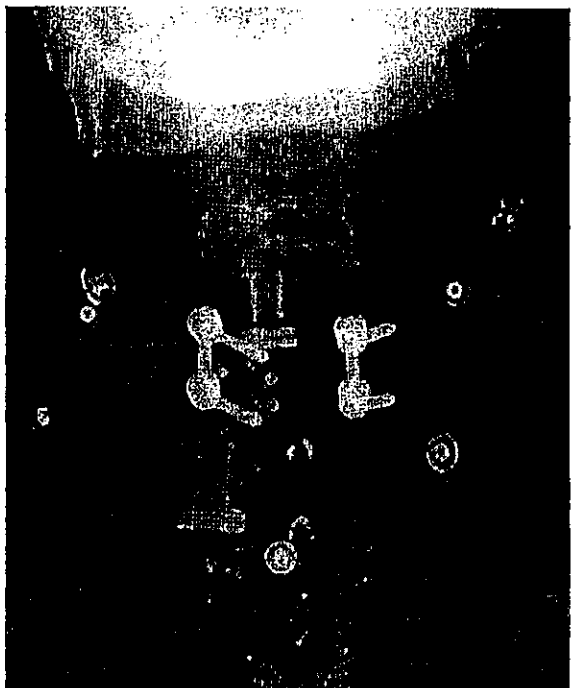


図2 術後単純X線画像

- ・手術開始後、約10分(受傷から約6時間5分)で観血的脱臼整復を施行した。
- ・C5/6 頸椎後方固定術(S-shot)を施行した。
- (右: 椎弓根スクリュー, 左: 外側塊スクリュー, 時間55分, 出血102ml)
- ・術直後から両下肢の麻痺は改善した。

いては、脊髓損傷後6時間以内の観血的神経除圧により神経症状が改善したことが報告されており⁹⁾、頸椎損傷が完治し得るタイムリミットは受傷後6-8時間

ではないかと予想する。無論、仮にタイムリミットを過ぎていても、脊髓の減圧は早ければ早いほど望ましいことに変わりはない。

表 1 初診時から術後経過における身体所見の経時的変化
徒手筋力テスト (MMT: (右/左)) を 0-5 で示した。

	前医 初診時	受傷後 5 H (搬送時)	術後 3 H30M	術後 18H	術後 29H	術後 4 日	術後 7 日	術後 28日
肘関節屈曲	MMT 4/4	MMT 0/4	MMT 3/4	MMT 4/4	MMT 4/4	MMT 4/4	MMT 4/4	MMT 4/4
手関節伸展	MMT 4/4	MMT 0/2	MMT 2/2	MMT 4/3	MMT 4/3	MMT 4/4	MMT 4/4	MMT 4/4
肘関節伸展	MMT 4/4	MMT 0/1	MMT 1/2	MMT 2/3	MMT 3/3	MMT 4/3	MMT 4/3	MMT 4/3
手指屈曲	MMT 4/4	MMT 0/0	MMT 2/2	MMT 3/4	MMT 4/4	MMT 5/5	MMT 5/5	MMT 5/5
手指外転	MMT 4/4	MMT 0/0	MMT 2/2	MMT 2/3	MMT 4/4	MMT 4/4	MMT 4/4	MMT 4/4
股関節屈曲	MMT 4/5	MMT 0/0	MMT 1/2	MMT 4/5	MMT 4/5	MMT 5/5	MMT 5/5	MMT 5/5
膝関節伸展	MMT 4/5	MMT 0/0	MMT 1/3	MMT 4/5	MMT 4/5	MMT 5/5	MMT 5/5	MMT 5/5
足関節背屈	MMT 4/5	MMT 0/0	MMT 1/3	MMT 5/5	MMT 5/5	MMT 5/5	MMT 5/5	MMT 5/5
母趾伸展	MMT 4/5	MMT 0/0	MMT 1/3	MMT 5/5	MMT 5/5	MMT 5/5	MMT 5/5	MMT 5/5
足関節底屈	MMT 4/5	MMT 0/0	MMT 2/3	MMT 5/5	MMT 5/5	MMT 5/5	MMT 5/5	MMT 5/5

Newtonらの報告は、脱臼整復のタイミングのみならず脊髄損傷の不可逆性についても示唆している⁴⁾。交通事故とは異なり、ラグビーのような低エネルギー外傷に伴う頸椎脱臼骨折では脊髄の不可逆的損傷を免れている可能性が高い。すなわち彼らの報告は、1) 低エネルギーで生じた脱臼骨折では脊髄が不可逆性変化を免れている可能性が高いこと、2) 短時間で整復されれば、二次損傷を回避し麻痺改善の可能性が高まることを示している。

本症例において特筆すべきは、超急性期に脱臼整復が可能だったという時間的要素のみならず、それが迅速な観血手術で施行され、更に一期的内固定までを完遂し得た点である。このことが、術後20日という速さで下肢運動麻痺が完全回復まで至った要因と考えてよいだろう。非観血的整復ではHalo ring等を用いた直達牽引により行うため、脱臼整復率は平均74%程度とされ⁶⁾、整復不能例では麻痺を悪化させるリスクもある^{6,7)}。また整復後にHalo vestで外固定を施行する場合には脊椎安定性に不安が残る⁸⁾。一方、観血的整復+内固定術は確実に脱臼整復が可能であり、一期的に強固な内固定を行える利点がある。ただし、極めて迅速に検査から手術まで行える環境、迅速かつ確実な手術が必須条件となる。

低エネルギー外傷ではなくても、脊髄が不可逆損傷を免れている可能性は否定できない。どれほど検査技術が上がったとしても100%の鑑別は不可能である。すなわち、例え完全麻痺例であっても迅速な非観血的整復、あるいは観血的整復固定を旨とし、最善を尽くす姿勢が望まれる。逆に整復や手術が遅れることにより回復不能な状態、すなわち「手遅れ」にしてしまうことがあり得ることを肝に銘じるべきである。

結 語

今回、自動車事故に伴う頸髄損傷に対し、受傷後約6時間で手術を開始し、観血的整復および固定術を施行することにより、麻痺が術後14日で改良Frankel B 1から下肢筋力完全回復まで改善した1例を経験した。完全運動麻痺であっても早期の減圧により神経機能回復の可能性がある。脊髄損傷の急性期医療は脊椎外科医や救急医だけでは不十分なことがあり、体制の整った施設への迅速な搬送が肝要である。

【キーワード】

脊髄損傷 (spinal cord injury), 運動完全麻痺 (complete motor paralysis), 超早期手術 (super-urgent surgery), 完全回復 (complete recovery)

参 考 文 献

1. Matsushita A, Maeda T, Mori E, *et al.*: Subacute T1-low intensity area reflects neurological prognosis for patients with cervical spinal cord injury without major bone injury. *Spinal cord*, 54: 24-28, 2016.
2. Vaccaro AR, Daugherty RJ, Sheehan TP, *et al.*: Neurologic outcome of early versus late surgery for cervical spinal cord injury. *Spine*, 22: 2609-2613, 1997.
3. Fehlings MG, Vaccaro A, Wilson JR, *et al.*: Early versus delayed decompression for traumatic cervical spinal cord injury: Results of the surgical timing in acute spinal cord injury study (STASCIS). *PLoS One*, 7: 1-8, 2012.
4. Newton D, England M, Doll H, Gardner BP.: The case for early treatment of dislocations of the cervical spine with cord involvement sustained playing

- rugby. J Bone Joint Surg Br, 93 : 1646-1652, 2011.
5. Rabinowitz RS, Eck JC, Harper CM Jr, *et al.* : Urgent surgical decompression compared to methylprednisolone for the treatment of acute spinal cord injury : a randomized prospective study in beagle dogs. Spine, 33 : 2260-2268, 2008.
 6. Gelb DE, Hadley MN, Aarabi B, *et al.* : Initial closed reduction of cervical spinal fracture-dislocation injuries. Neurosurgery, 72 (Suppl 2) : 73-83, 2013.
 7. Mahale YJ, Silver JR, Henderson NJ. : Neurological complications of the reduction of cervical spine dislocation. J Bone Joint Surg Br, 75 : 403-409, 1993.
 8. Koch R, Nickel VL. : The halo vest : An evaluation of motion and forces across the neck. Spine, 3 : 103-107, 1978.